USGS
science for a changing world

Simulation of Salinity Intrusion Along the Georgia and South Carolina Coasts Using Climate-Change Scenarios

Prepared in cooperation with the Beaufort-Jasper Water and Sewer Authority

Scientific Investigations Report 2013–5036

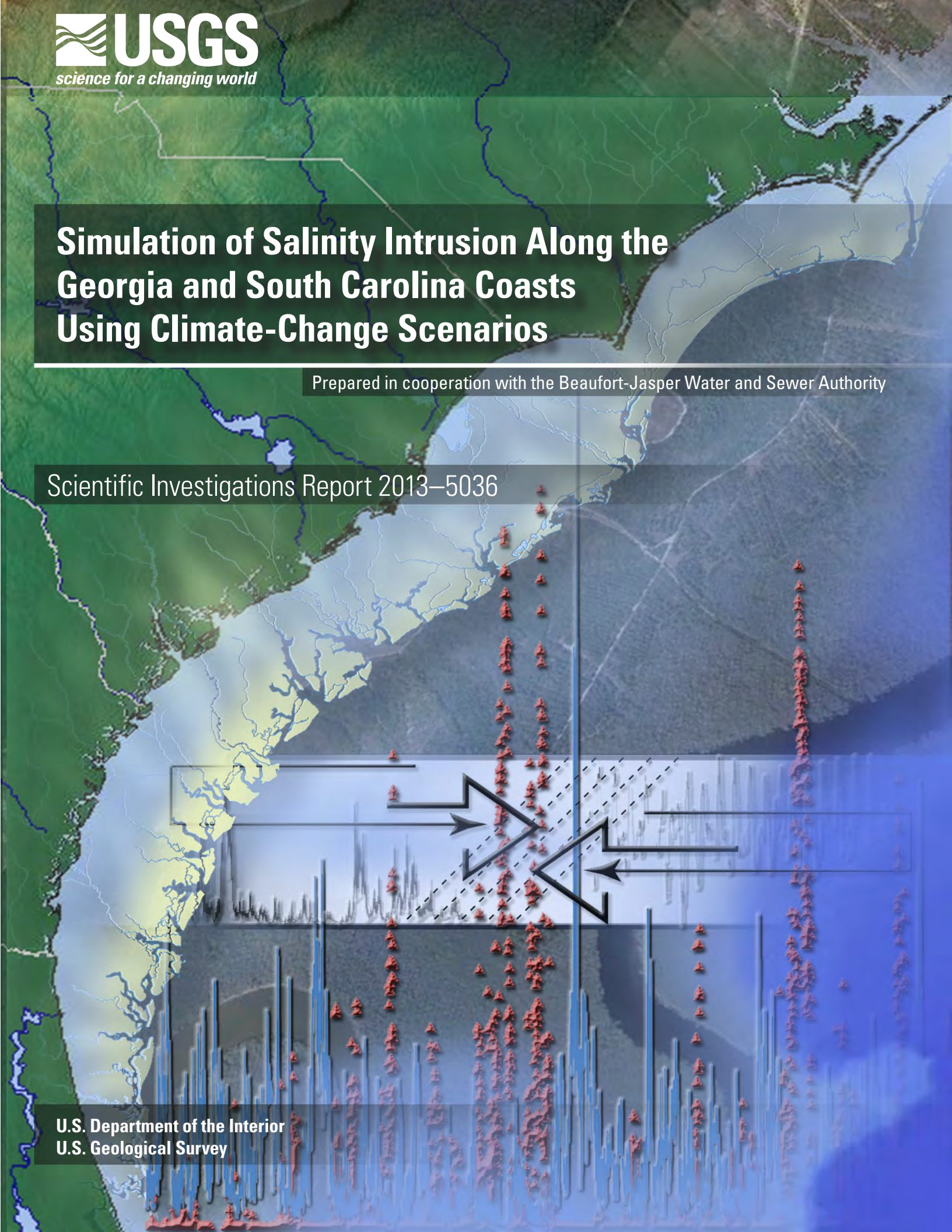

U.S. Department of the Interior
U.S. Geological Survey

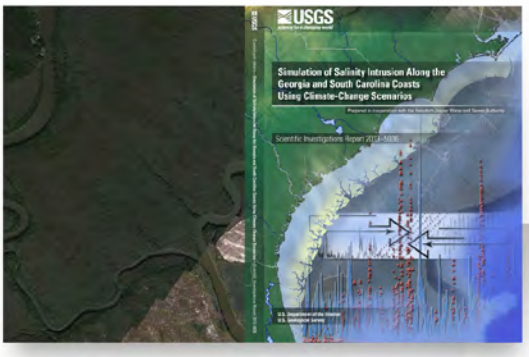

Cover. Images from the freshwater-saltwater interface diagram and graph (see report figures 22 and 23, respectively).

Simulation of Salinity Intrusion Along the Georgia and South Carolina Coasts Using Climate-Change Scenarios

By Paul A. Conrads, Edwin A. Roehl, Jr., Ruby C. Daamen, and John B. Cook

Prepared in cooperation with the Beaufort-Jasper Water and Sewer Authority

Scientific Investigations Report 2013–5036

U.S. Department of the Interior
U.S. Geological Survey

U.S. Department of the Interior
KEN SALAZAR, Secretary

U.S. Geological Survey
Suzette M. Kimball, Acting Director

U.S. Geological Survey, Reston, Virginia: 2013

Suggested citation:
Conrads, P.A., Roehl, E.A., Jr., Daamen, R.C., and Cook, J.B., 2013, Simulation of salinity intrusion along the Georgia and South Carolina coasts using climate-change scenarios: U.S. Geological Survey Scientific Investigations Report 2013–5036, 92 p. + 5 apps.
(http://pubs.usgs.gov/sir/2013/5036/)

Acknowledgments

The authors thank Mr. Charles Sexton, Director of Engineering with Beaufort-Jasper Water and Sewer Authority, and Dr. Kenan Ozekin, Senior Account Manager with the Water Research Foundation (WaterRF), for their technical assistance and coordination.

Contents

Figures

Tables

Conversion Factors and Datums

Inch/Pound to SI

Multiply	By	To obtain
	Length	
foot (ft)	0.3048	meter (m)
mile (mi)	1.609	kilometer (km)
	Area	
acre	0.004047	square kilometer (km^2)
square mile (mi^2)	2.590	square kilometer (km^2)
	Flow rate	
cubic foot per second (ft^3/s)	0.02832	cubic meter per second (m^3/s)

Vertical coordinate information is referenced to the National Geodetic Vertical Datum of 1929 (NGVD 29).

Horizontal coordinate information is referenced to either the North American Datum of 1927 (NAD 27) or the North American Datum of 1983 (NAD 83).

Elevation, as used in this report, refers to distance above the vertical datum.

Specific conductance is given in microsiemens per centimeter at 25 degrees Celsius (µS/cm at 25 °C).

Abbreviations*

ADMi	Advanced Data Mining International
AI	Artificial Intelligence
AIW	Atlantic Intracoastal Waterway
ANN	Artificial Neural Network
BASINS	Better Assessment Science Integrating Point and Non-Point Sources
BEP	back error propagation
BJWSA	Beaufort-Jasper Water and Sewer Authority
CRADA	Cooperative Research and Development Agreement
DSS	decision support system
ECHO	The ECHO GCM is a hybrid coupled ocean-atmosphere GCM of the Hamburg version of the European Center atmospheric GCM (ECHAM) and the Hamburg Primitive Equation ocean GCM (HOPE)
ECHO-HSPF	linked ECHO GCM output with the HSPF watershed model
EFDC	Environmental Fluid Dynamics Code
EIS	Environmental Impact Statement
FCFWRU	Florida Cooperative Fish and Wildlife Research Unit
GCM	Global Circulation Model
GPA	Georgia Ports Authority
GUI	graphical user interface
HSPF	Hydrologic Simulation Program-FORTRAN watershed model
I-95	Interstate 95
ME	mean error
MLP	multi-layer perceptron
MSM	marsh succession model
M2M	Model-to-Marsh Decision Support System
M2M-2	Updated Model-to-Marsh Decision Support System
N.C.	North Carolina
NOAA	National Oceanic and Atmospheric Administration
NRC	National Resource Council
NWIS	National Water Information System
OLS	ordinary least squares
PME	percent model error
PRISM	Pee Dee River and Atlantic Intracoastal Waterway Salinity Intrusion Model
PRISM-2	Updated Pee Dee River and Atlantic Intracoastal Waterway Salinity Intrusion Model
psu	practical salinity units
Q	streamflow input
RMSE	root mean square error
R2	coefficient of determination
SARP	Sectoral Applications Research Program
S.C.	South Carolina
SC	specific conductance
SCDHEC	South Carolina Department of Health and Environmental Control
SNWR	Savannah National Wildlife Refuge
SSR	state space reconstruction
TMDL	total maximum daily load
USACE	U.S. Army Corps of Engineers
USC	University of South Carolina
USEPA	U.S. Environmental Protection Agency
USGS	U.S. Geological Survey
WL	water level
XWL	tidal range
1D	one dimensional
2D	two dimensional
3D	three dimensional
3DVis	three-dimensional visualization

*Model variables are provided in table 7 and appendixes 1 and 3.

Simulation of Salinity Intrusion Along the Georgia and South Carolina Coasts Using Climate-Change Scenarios

By Paul A. Conrads,[1] Edwin A. Roehl, Jr.,[2] Ruby C. Daamen,[2] and John B. Cook[2]

Abstract

Potential changes in climate could alter interactions between environmental and societal systems and adversely affect the availability of water resources in many coastal communities. Changes in streamflow patterns in conjunction with sea-level rise may change the salinity-intrusion dynamics of coastal rivers. Several municipal water-supply intakes are located along the Georgia and South Carolina coast that are proximal to the present day saltwater-freshwater interface of tidal rivers. Increases in the extent of salinity intrusion resulting from climate change could threaten the availability of freshwater supplies in the vicinity of these intakes. To effectively manage these supplies, water-resource managers need estimates of potential changes in the frequency, duration, and magnitude of salinity intrusion near their water-supply intakes that may occur as a result of climate change. This study examines potential effects of climate change, including altered streamflow and sea-level rise, on the dynamics of saltwater intrusion near municipal water-supply intakes in two coastal areas. One area consists of the Atlantic Intracoastal Waterway (AIW) and the Waccamaw River near Myrtle Beach along the Grand Strand of the South Carolina Coast, and the second area is on or near the lower Savannah River near Savannah, Georgia. The study evaluated how future sea-level rise and a reduction in streamflows can potentially affect salinity intrusion and threaten municipal water supplies and the biodiversity of freshwater tidal marshes in these two areas.

Salinity intrusion occurs as a result of the interaction between three principal forces—streamflow, mean coastal water levels, and tidal range. To analyze and simulate salinity dynamics at critical coastal gaging stations near four municipal water-supply intakes, various data-mining techniques, including artificial neural network (ANN) models, were used to evaluate hourly streamflow, salinity, and coastal water-level data collected over a period exceeding 10 years. The ANN models were trained (calibrated) to learn the specific interactions that cause salinity intrusions, and resulting models were able to accurately simulate historical salinity dynamics in both study areas.

Changes in sea level and streamflow quantity and timing can be simulated by the salinity intrusion models to evaluate various climate-change scenarios. The salinity intrusion models for the study areas are deployed in a decision support system to facilitate the use of the models for management decisions by coastal water-resource managers. The report describes the use of the salinity-intrusion models decision support system to evaluate salinity-intrusion dynamics for various climate-change scenarios, including incremental increases in sea level in combination with incremental decreases in streamflow. Operation of municipal water-treatment plants is problematic when the specific-conductance values for source water are greater than 1,000 to 2,000 microsiemens per centimeter (µS/cm). High specific-conductance values contribute to taste problems that require treatment. Data from a gage downstream from a municipal water intake indicate specific conductance exceeded 1,000 µS/cm about 5.4 percent of the time over the 14-year period from August 1995 to August 2008. Simulations of specific conductance at this gaging station that incorporates sea-level rises resulted in a doubling of the exceedances to 11.0 percent for a 1-foot increase and 17.6 percent for a 2-foot increase. The frequency of intrusion of water with specific conductance values of 1,000 µS/cm was less sensitive to incremental reductions in streamflow than to incremental increases in sea level. Simulations of conditions associated with a 10-percent reduction in streamflow, in combination with a 1-foot rise in sea level, increased the percentage of time specific conductance exceeded 1,000 µS/cm at this site from 11.0 to 13.3 percent, and a 20-percent reduction in streamflow increased the percentage of time to 16.6 percent.

Precipitation and temperature data from a global circulation model were used, after scale adjustments, as input to a watershed model of the Yadkin-Pee Dee River basin, which flows into the Waccamaw River and Atlantic Intracoastal Waterway study area in South Carolina. The simulated streamflow for historical conditions and projected climate change in the future was used as input for the ANN model in decision support system. Results of simulations incorporating climate-change projections for alterations in streamflow indicate an increase in the frequency of salinity-intrusion events and a shift in the seasonal occurrence of the intrusion events from the summer to the fall.

[1]U.S. Geological Survey.

[2]Advanced Data Mining, LLC, Greenville, South Carolina.

Introduction

Adapting to future climatic change will likely present numerous challenges to water-resource managers in coastal regions of the world. The east coast of the United States falls into this category, given the large number of people living along the Atlantic seaboard and the added strain on resources as populations grows, particularly in the Southeast. Increased temperatures, changes in regional precipitation regimes, and rises in sea level may have a large effect on existing hydrological systems in coastal regions. Many of the major municipal water-supply intakes along the southeastern coast of the United States are considered to be vulnerable to anticipated changes in climate (fig. 1; Furlow and others, 2002). Four of the municipal intakes in figure 1 are along the South Carolina and Georgia coast and were analyzed for this report. Two intakes are in the Waccamaw River–Atlantic Intracoastal Waterway (AIW) area, and two are in the lower Savannah River estuary along the South Carolina and Georgia border.

The balance between streamflow conditions within a coastal drainage basin and sea levels governs the characteristics and frequency of salinity intrusion into coastal rivers. Salinity intrusion into freshwater coastal rivers has been, and continues to be, one of the most important global challenges for coastal water-resource managers, industries, and agriculture (Bear and others, 1999). Major economic and environmental consequences of saltwater intrusion include the degradation of natural ecosystems and the contamination of municipal, industrial, and agricultural water supplies (Bear and others, 1999). Coastal communities need to find approaches for the sustainability of freshwater supplies while minimizing the impact on natural systems. Increases in the frequency, magnitude, and duration of salinity intrusion into the coastal rivers near the surface-water intakes could increase the vulnerability and threaten the potability of water at the four freshwater municipal intakes, as well as the biodiversity of nearby freshwater tidal marshes.

Waccamaw River, AIW, and lower Savannah River, as with many major estuarine systems, supply many local and regional water-resource needs. The tidal parts of these systems supply water to the growing coastal communities along the South Carolina and Georgia coasts, provide assimilative capacity for municipal wastewater discharges, and offer recreational opportunities along the coast (figs. 2, 3). With increases in industrial and residential development along the South Carolina and Georgia coasts, there are competing, and often conflicting, demands on coastal water resources.

Coastal water-resource managers need planning tools that will provide estimates of the change in the magnitude, frequency, and duration of salinity intrusion events near water intakes projected to occur in response to anticipated changes in climate. Changes in climate could affect precipitation patterns and result in changing patterns of streamflow to the coast. Climate change also could affect the rate of sea-level rise. Concerns associated with sea-level rise are not limited to the flooding of low-lying coastal areas but include effects of altered salinity-intrusion dynamics on the availability of freshwater supplies along the coast. For municipalities with water-supply intakes in tidally affected waters proximal to the freshwater-saltwater interface, the convergence of changes in hydrologic regime and sea-level rise associated with potential climate change could have a dramatic effect on salinity intrusion and freshwater availability. Fortunately, there have been extensive data collection and salinity modeling efforts for areas near water-supply intakes in the two study areas, Waccamaw River and AIW, South Carolina, and lower Savannah River, Georgia. These monitoring and modeling efforts were initiated to address various coastal water-resources issues. Although these efforts did not directly address the effects of salinity intrusion resulting from potential climate change, the data and models (with modifications) can be used by interested parties to evaluate climate-change effects.

Figure 1. Vulnerability ratings for potential salinity intrusion at selected major municipal water-supply intakes along the coast of the Gulf of Mexico and the Atlantic Ocean (modified from Furlow and others, 2002).

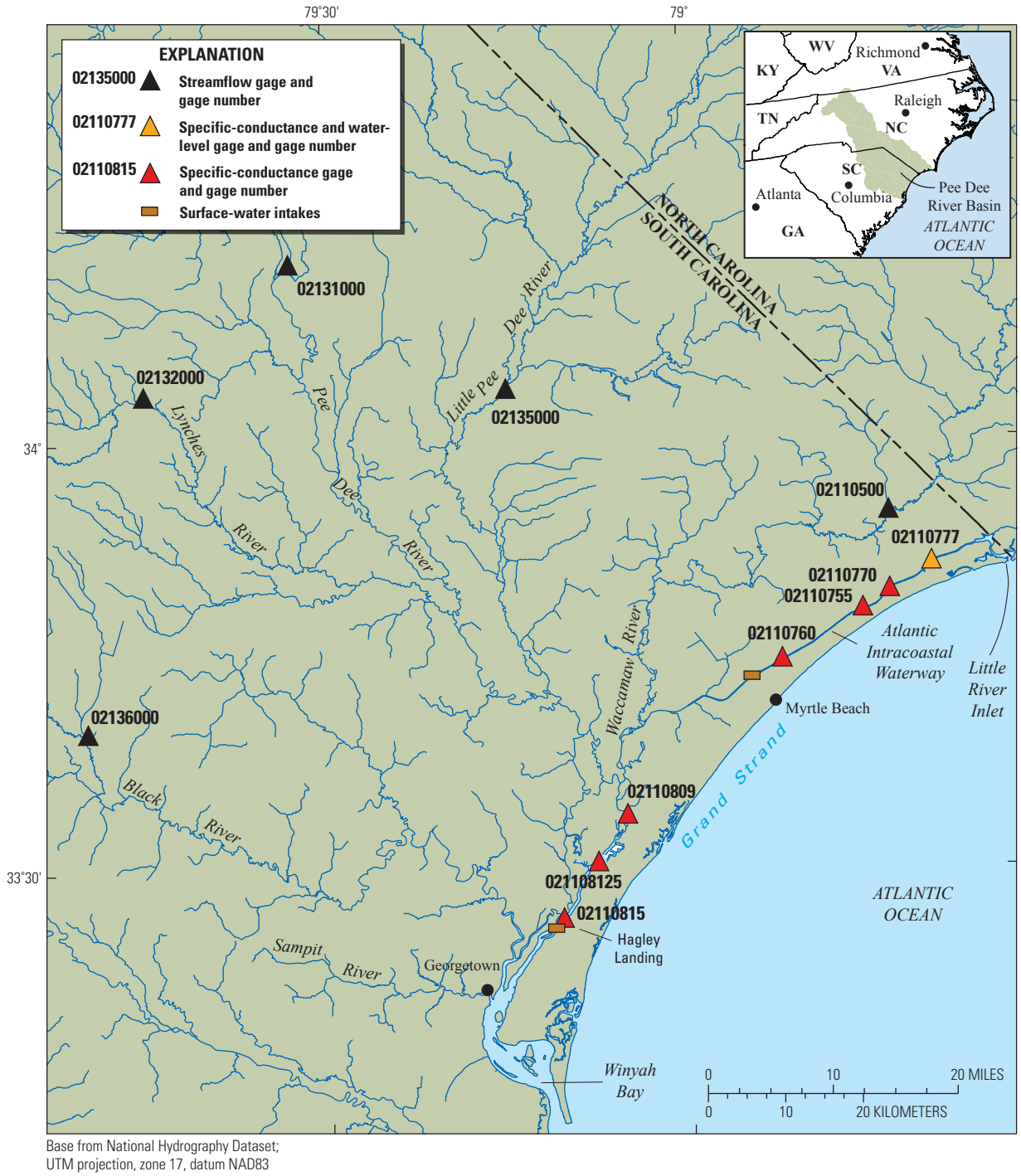

Base from National Hydrography Dataset;
UTM projection, zone 17, datum NAD83

Figure 2. Location of the Waccamaw River and Atlantic Intracoastal Waterway study area and selected gages in the Pee Dee River Basin, South Carolina.

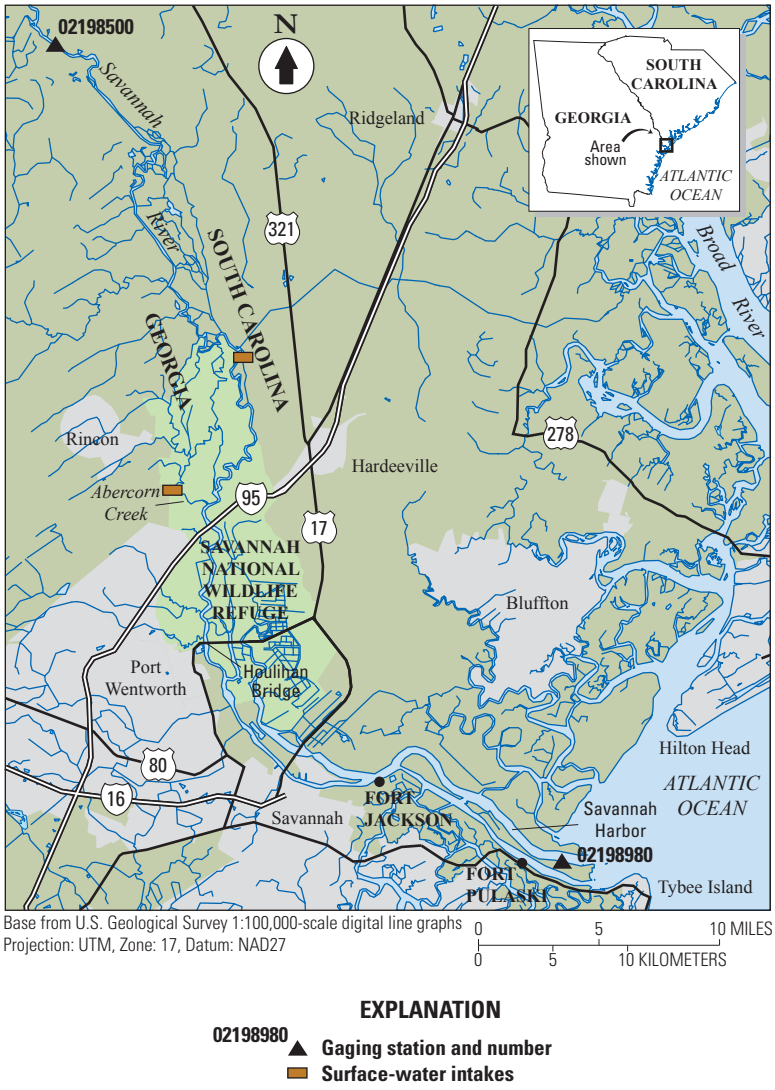

Figure 3. Location of the lower Savannah River study area, including the Savannah National Wildlife Refuge and coastal South Carolina and Georgia.

The U.S. Geological Survey (USGS), in cooperation with the Beaufort-Jasper Water and Sewer Authority (BJWSA), initiated a study to (1) modify existing decision support systems (DSS) with embedded empirical salinity intrusion models to evaluate sea-level rise and changes in streamflow patterns, (2) collaborate with researchers at the University of South Carolina on the simulation of streamflow hydrographs using a watershed model and downscaled rainfall and temperature inputs from regional and global climate models, and (3) document the DSSs and selected climate-change scenarios. To meet the objectives of this study, the USGS entered into a Cooperative Research and Development Agreement (CRADA) with Advanced Data Mining International (ADMi) in 2002 to collaborate on applying data mining and artificial neural network (ANN) models to water-resources investigations. This study was done in collaboration with the University of South Carolina (USC) and South Carolina Sea Grant Consortium (Sea Grant) (Whitehead and others, 2011). The USC and Sea Grant effort was funded through a National Oceanic and Atmospheric Administration (NOAA) Sectoral Applications Research Program (SARP; Funding# OAR-CPO-2008-2000994, CFDA# 11.431, Competition# 2074474).

The USGS, a non-regulatory Federal science agency with national scope and responsibilities, is uniquely positioned to serve the Nation's needs in understanding and responding to global climate change (Burkett and other, 2011). The USGS Global Change Science Strategy recognizes core USGS strengths and applies them to address key societal problems. This study addresses two of the six programmatic goals for the USGS to improve understanding of (1) droughts, streamflows, and water availability under changing land use and climate, and (2) coastal response to sea-level rise, climate hazards, and human development.

Purpose and Scope

This report presents the results of a study in which the effects of changes in streamflow and tidal water-level conditions on salinity intrusion in the Waccamaw River and AIW and the lower Savannah River were simulated using a modified **P**ee Dee **R**iver and Atlantic **I**ntracoastal Waterway **S**alinity Intrusion **M**odel **D**ecision **S**upport **S**ystem (PRISM DSS) (Conrads and Roehl, 2007) and the lower Savannah River estuary **M**odel-**to**-**M**arsh **D**ecision **S**upport **S**ystem (M2M DSS) (Conrads and others, 2006). Modifications made to these DSSs to enable evaluation of potential effects of climate change are documented in this report. In addition, examples of model scenarios from these DSSs are provided for their respective study areas. The development and application of the PRISM DSS and M2M DSS were documented in earlier reports. Sections of those reports have been updated for this report.

An important part of the USGS mission is to provide scientific information for the effective water-resources management of the Nation. To assess the quantity and quality of the Nation's surface water, the USGS collects hydrologic and water-quality data from rivers, lakes, and estuaries using standardized methods and maintains the data from these stations in a national database. Often these databases are under-utilized and under-interpreted for addressing contemporary hydrologic issues. The techniques presented in this report demonstrate the manner in which valuable information can be extracted from existing USGS databases to assist local, state and Federal agencies. The application of data-mining techniques, including ANN models, to the Waccamaw River, AIW, and the lower Savannah River estuary, demonstrates how empirical models of complex hydrologic systems can be developed, disparate databases and models can be integrated, and study results can be easily disseminated to meet the needs of a broad range of end users.

Description of the Study Areas

The Waccamaw River and AIW, and the lower Savannah River, study areas are the coastal parts of two major watersheds in the Carolinas and Georgia (fig. 4). The Yadkin-Pee Dee River and Savannah River watersheds are large drainage basins (18,500 and 9,850 square miles (mi^2), respectively) that drain into the Coastal Plain of the Southeast. Both watersheds have large reservoirs that regulate streamflow in major parts of the watersheds and supply water to major coastal communities. During low-flow and drought periods, it is not unusual for regulated streamflows to compose more than 80 percent of the inflow to the coast. A general description of each watershed and study area follows.

Base From ESRI® Data & Maps, 2009
Hydrologic Unit Boundaries From US Department of Agriculture, 2009, 1:24,000
Universal Transverse Mercator projection, NAD 83, Zone 17

Figure 4. Locations of the Yadkin-Pee Dee River, Savannah River, and selected basins in North Carolina, South Carolina, and Georgia.

Waccamaw River and Atlantic Intracoastal Waterway Study Area

The Waccamaw River and AIW study area is located in the Grand Strand of South Carolina, an area of rapidly growing coastal communities from Little River Inlet in the north to Winyah Bay in the south (fig. 2). Often the reach of the AIW near Little River Inlet is referred to as the "North End" and the reach of the Waccamaw River near Hagley Landing is referred to as the "South End." The Pee Dee River basin, including the Waccamaw River tributary, supplies freshwater to the Grand Strand of South Carolina. The headwaters of the Pee Dee River are in the Blue Ridge Province of North Carolina and Virginia and drain 6,800 mi² in North Carolina above Blewett Falls Lake (fig. 5) before flowing through South Carolina to the Atlantic Ocean (Seaber and others, 1994).

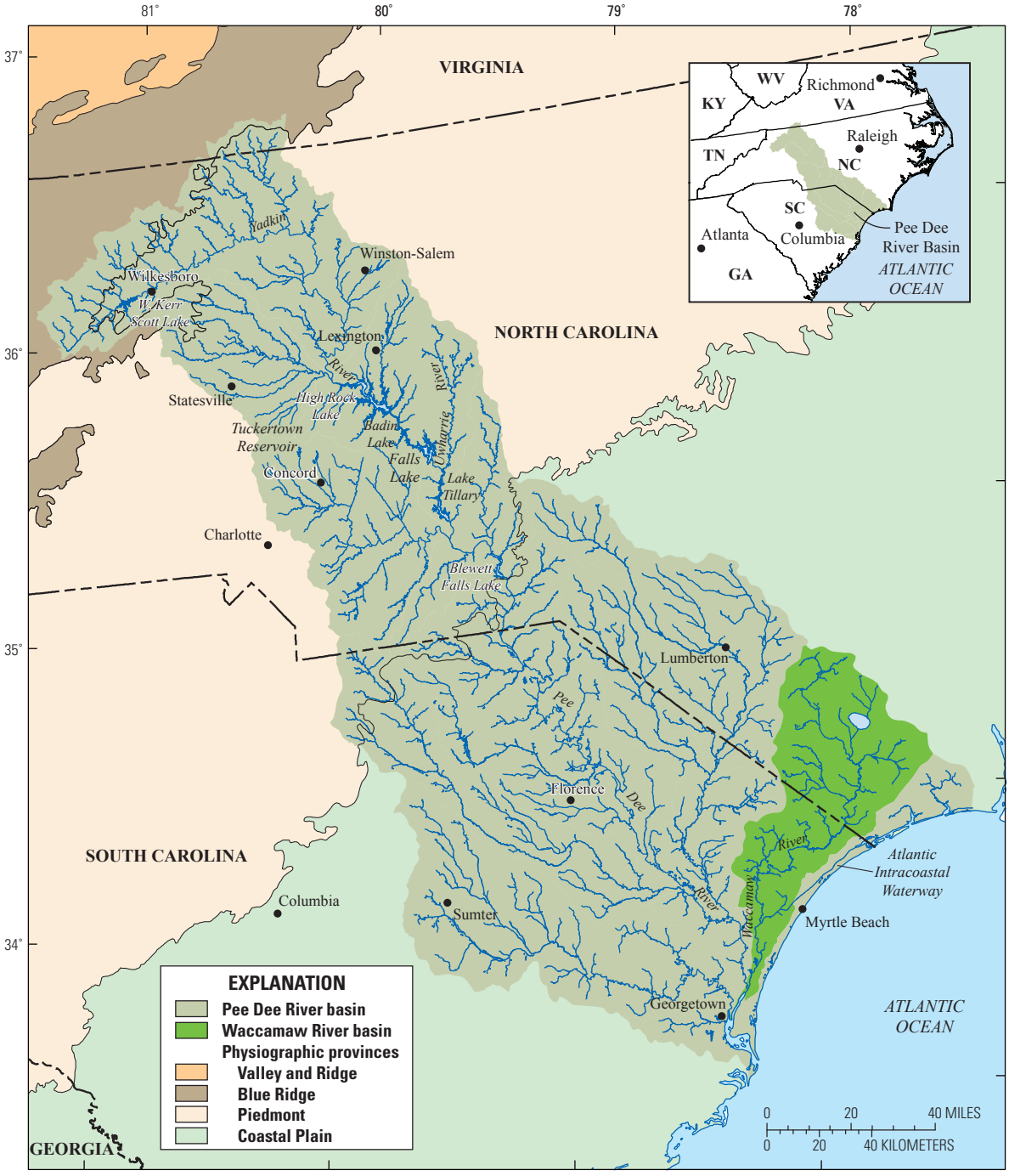

Base from 1:100,000-scale National Hydrography Dataset.
Albers Equal Area projection; central meridian-96 00 00; datum NAD83.

Figure 5. Physiographic provinces and location of surface-water bodies in the drainage basin of the Waccamaw River and Atlantic Intracoastal Waterway study area in North and South Carolina.

Above the confluence with the Uwharrie River, the stream is known as the Yadkin River, and below as the Pee Dee River, or Great Pee Dee River (U.S. Geological Survey, 1986). The Pee Dee River flows through seven impoundments in North Carolina. The first impoundment is the W. Kerr Scott Lake, a reservoir west of Wilkesboro, N.C. Downstream, a chain of five reservoirs impounds 50 miles of the river; these are High Rock Lake, Tuckertown Reservoir, Badin Lake, Falls Lake, and Lake Tillery (North Carolina Department of Environment and Natural Resources, 2001). The seventh impoundment is Blewett Falls Lake, located approximately 15 miles upstream from the South Carolina State line (table 1). There are no impoundments or regulation of the Pee Dee streamflow in South Carolina.

The Pee Dee River below Blewett Falls Lake drains approximately 11,700 mi^2 and has five major tributaries: the Little Pee Dee, the Lynches, the Black, the Waccamaw, and the Sampit Rivers (Seaber and others, 1994) (figs. 2 and 5). The Little Pee Dee, Lynches, Black, and Waccamaw River tributaries are unregulated, undeveloped, and drain rural areas. Downstream from U.S. Highway 701, the Pee Dee River branches successively into Bull, Thoroughfare, and Schooner Creeks (fig. 6). These three creeks eventually flow into the Waccamaw River and Winyah Bay. Most of the freshwater streamflow to the AIW from the Pee Dee River basin is carried by Bull Creek to the Waccamaw River.

Table 1. Description of seven reservoirs on the Yadkin-Pee Dee River, North Carolina.

[From North Carolina Department of Environment and Natural Resources, Division of Water Quality, 1998]

Reservoir	Surface area, acres	Owner
W. Kerr Scott Lake	1,480	U.S. Army Corps of Engineers
High Rock Lake	12,200	Alcoa Power Generation, Inc.
Tuckertown Reservoir	2,550	Alcoa Power Generation, Inc.
Badin Lake	5,350	Alcoa Power Generation, Inc.
Falls Lake	203	Alcoa Power Generation, Inc.
Lake Tillery	5,260	Carolina Power and Light
Blewett Falls Lake	2,570	Carolina Power and Light

Figure 6. Locations of selected water-quality monitoring stations and water-supply intakes in the Waccamaw River and Atlantic Intracoastal Waterway study area, Grand Strand, South Carolina.

The Waccamaw River (drainage area of 1,440 square miles) originates in North Carolina and enters the AIW about 10 miles north of the mouth of Bull Creek. Prior to the 1930s, the Waccamaw River flowed southward toward Winyah Bay. In the 1930s, the U.S. Army Corps of Engineers constructed a canal to form the waterway from Enterprise Landing to the Little River Inlet, which enables a large portion of the freshwater in the Waccamaw River to flow northward through the AIW into the Atlantic Ocean through Little River Inlet (Drewes and Conrads, 1995). The Waccamaw River drains extensive cypress and hardwood swamps (U.S. Geological Survey, 1986). There are seven USGS gaging stations on the Pee Dee River and its major tributaries (table 2).

Table 2. Description of U.S. Geological Survey gaging stations on the Pee Dee River and its major tributaries, North and South Carolina.

[mi², square mile; SC, South Carolina]

Station name (fig. 2)	Station number	Period of record	Drainage area, in mi²	River mile
Waccamaw River near Longs, S.C.[1]	02110500	1950 to 2013	1,110	185.4
Pee Dee River near Rockingham, N.C.[2]	02129000	1906 to 2013	6,863	1,192
Pee Dee River near Bennettsville, S.C.[2]	02130561	1990 to 2013	7,600	1,153
Pee Dee River at Pee Dee, S.C.[1]	02131000	1938 to 2013	8,830	2,100.2
Lynches River at Effingham, S.C.[1]	02132000	1929 to 2013	1,030	243.4
Little Pee Dee River at Galivants Ferry, S.C.[1]	02135000	1942 to 2013	2,790	241.7
Black River at Kingstree, S.C.[1]	02136000	1929 to 2013	1,252	286.7

[1]Station used for streamflow input to artificial neural network models.

[2]Not shown in figure 2.

The reach of the AIW from just south of Little River Inlet to just north of Hagley Landing provides freshwater for the coastal communities of the Grand Strand (fig. 6). In the 1980s, major water purveyors switched from groundwater to surface-water sources to avoid taste and odor problems associated with the groundwater supplies (Carswell and others, 1988). Three municipal surface-water intakes are in the tidal, freshwater portions of the AIW, Waccamaw River, and Bull Creek (fig. 6). During the drought of 1998 to 2002, salinity intrusion forced a municipal water supplier to temporarily suspend withdrawals until the freshwater-saltwater interface moved downstream from the intake.

Lower Savannah River Study Area

The lower Savannah River estuary extends from the Interstate 95 bridge to confluence with the Atlantic Ocean (fig. 3). The headwaters of the Savannah River originates in the Blue Ridge physiographic province, at the confluence of the Seneca and Tugaloo Rivers, near Hartwell, Ga. The Savannah River forms the State boundary between South Carolina and Georgia to the divergence of the Little Back River near the coast (figs. 7, 8). The Keowee River flows through Lakes Jocassee and Keowee into Lake Hartwell. From Lake Hartwell, the Savannah River flows through the Piedmont and the Coastal Plain physiographic provinces (fig. 7). The city of Augusta, Ga., is on the Fall Line, which separates these two provinces. The slope of the river ranges from an average of about 3 feet per mile in the Piedmont to less than 1 foot per mile in the Coastal Plain. Upstream from the Fall Line, three large Federal multi-purpose dams (Lake Hartwell, Richard B. Russell Lake, and J. Strom Thurmond Lake) provide hydropower, water supply, recreational facilities, and a limited degree of flood control. Thurmond Dam controls most of the streamflow regulation that affects the Savannah River at Augusta (Sanders and others, 1990). A list of the reservoirs in the Savannah River basin with surface areas greater than 1,000 acres is presented in table 3.

The lower Savannah River is a deltaic system that branches into a series of interconnected distributary channels, including the Little Back, Middle, Back, and Front Rivers (fig. 8). The hydrology of the system is dependent upon precipitation, runoff, channel configuration, streamflow, and seasonal and daily tidal fluctuations (Latham, 1990; Pearlstine and others, 1990). As is typical of coastal rivers in Georgia and South Carolina, the shallow, deltaic branches of the Savannah River did not provide natural features for a harbor, such as deep embayments or natural scouring of deep channels. Historically, the Back River had the larger channel and the larger proportion of streamflow compared with those of the Front River (Barber and Gann, 1989). The Savannah Harbor was developed along the lower 21 miles of the Savannah River during the mid-1800s to the present (2012). The Savannah Harbor has a history of channel deepening, widening, creation of turning and sedimentation basins, and maintenance dredging and disposal, as the harbor was changed from a natural river system with a controlling depth of 10 feet (ft) at low tide to a modified river with a currently (2013) maintained depth of 42 ft at low tide (Barber and Gann, 1989).

Two important entities are located in the Savannah River estuary—the Savannah National Wildlife Refuge (SNWR) and the Georgia Ports Authority (GPA) facilities (fig. 8). The tidal freshwater marsh is an essential part of the 28,000-acre SNWR. Located between river mile 18 and river mile 40, the SNWR is home to a diverse variety of wildlife and plant communities. To the east of the Little Back and Back Rivers, the SNWR contains a 3,000-acre impoundment system that is actively managed for migratory wading birds and waterfowl and is periodically flooded with freshwater from the Little Back River. Neighboring the SNWR, the GPA maintains

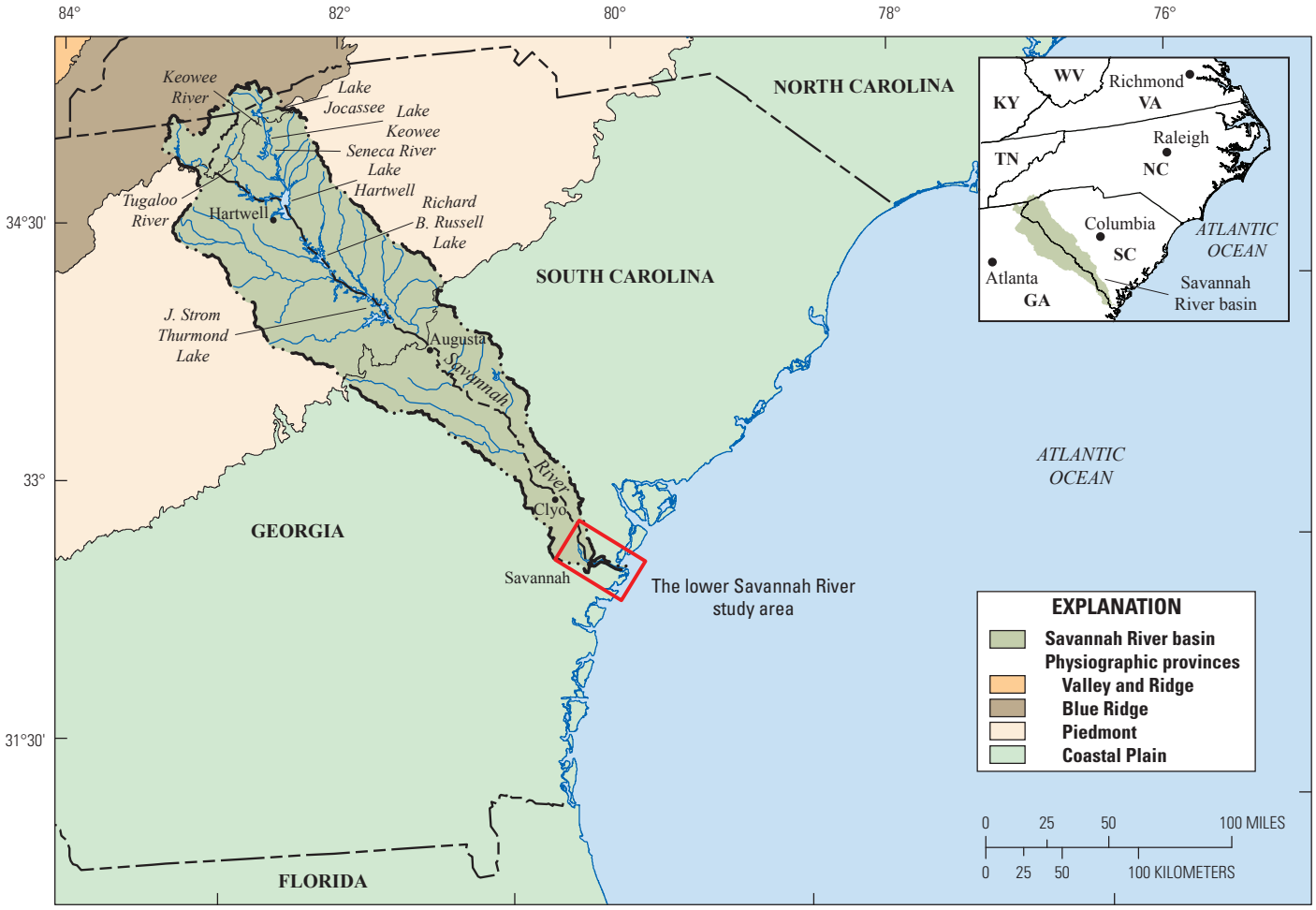

Base from U.S. Geological Survey 1:2,000,000-scale digital line graphs, Projection: Albers
1st standard parallel: 29°30'00", 2nd standard parallel: 45°30'00", Central meridian: -81°00'00"
Latitude of origin: 23°00'00", False easting: 0.0, False northing: 0.0, Datum: NAD83

Figure 7. Location of selected surface-water bodies in the lower Savannah River basin, North Carolina, South Carolina, and Georgia.

Table 3. Description of six reservoirs in South Carolina with greater than 1,000 acres on the Savannah River.

[From South Carolina Water Resources Commision, 1983]

Reservoir	Surface area, acres	Owner
Lake Jocassee	18,372	Duke Energy
Lake Keowee	18,372	Duke Energy
Lake Hartwell	56,000	U.S. Army Corps of Engineers
Richard B. Russell Lake	26,650	U.S. Army Corps of Engineers
J. Strom Thurmond Lake	71,100	U.S. Army Corps of Engineers
Stevens Creek[1]	2,400	South Carolina Electric and Gas

[1]Data from Stringfield, 1995.

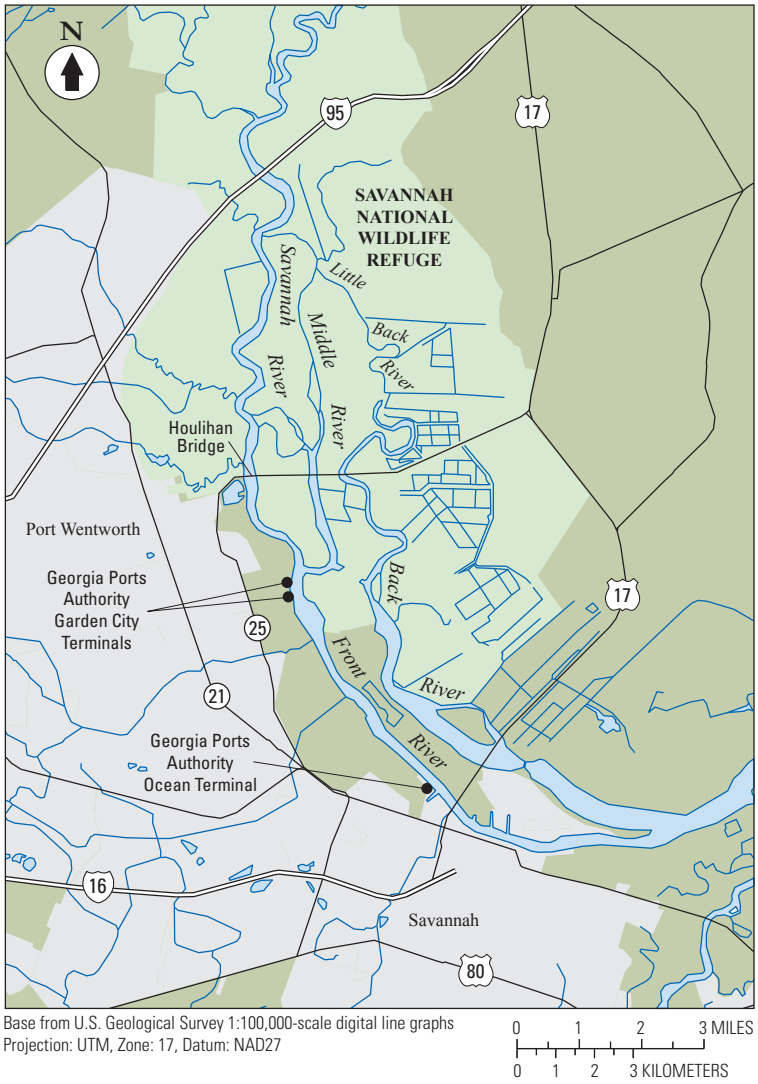

Figure 8. Location of Georgia Ports Authority facilities and the Savannah National Wildlife Refuge in the lower Savannah River basin, South Carolina and Georgia.

two deepwater terminal facilities—Garden City Terminal and Ocean Terminal (fig. 8). To support navigation and the terminal activities of the GPA, the river channel and turning basins are maintained by dredging downstream from the U.S. Highway 17 bridge (Houlihan Bridge) to approximately 20 miles offshore from the harbor entrance.

Substantial modifications made to the Savannah River estuary during the past 30 years include the installation and operation of a tide gate on the Back River in 1977, deepening of the shipping channel to 38 ft (from 34 ft) in 1978, decommissioning of the tide gate in 1991, and deepening of the shipping channel to 42 ft (from 38 ft) in 1994. The cumulative effect of the channel modifications can be seen in the upstream movement of the freshwater-saltwater interface over the past century. The average position of the freshwater-saltwater interface for four historical periods (1875, 1940, 1965, and 1997) and their associated channel depths are shown in figure 9 (E. EuDaly, U.S. Fish and Wildlife Service, written commun., 2005). Data used in figure 9 were obtained from historical sources, as noted in the figure, and provide a qualitative comparison of the position of the freshwater-saltwater interface and the spatial extent of the freshwater marsh.

Two municipal water-supply intakes are located in the freshwater part of the upper estuary. The city of Savannah maintains an intake on Abercorn Creek, a tributary to the Savannah River approximately 1 mile upstream from the Interstate 95 bridge (fig. 3). Abercorn Creek in Georgia, at the location of the intake, experiences reversing streamflow from the connection to the Savannah River but low salinity concentrations (Conrads and others, 2011). The freshwater intake for the Beaufort-Jasper Water and Sewer Authority is located at a canal off of the Savannah River near Hardeeville, S.C. (fig. 3). The water levels are affected by tidal backwater at the intake canal near Hardeeville, but streamflows do not reverse at this location on the Savannah River, and salinity intrusion has not affected the availability of freshwater at this intake.

Previous Studies

Many investigations have been conducted to address the quantity and quality of water resources in the study areas and the use of data-mining techniques to study salinity dynamics in these estuarine systems. Carswell and others (1988) investigated the potential freshwater supply of the AIW as an alternative to groundwater sources and, on the basis of statistical analysis and mechanistic models, determined that the AIW could provide an adequate supply of freshwater. Drewes and Conrads (1995) determined the assimilative capacity of the Waccamaw River and AIW using dynamic one-dimensional streamflow and water-quality models. These assimilative capacity models were subsequently used by the South Carolina Department of Health and Environmental Control (SCDHEC) to determine the total maximum daily load (TMDL) for dissolved oxygen (South Carolina Department of Health and Environmental Control, 1998).

The South Carolina Department of Natural Resources and a consortium of stakeholders entered into a cooperative agreement with the USGS to apply data-mining techniques to the long-term time-series datasets to analyze and simulate salinity dynamics near the freshwater intakes along the Grand Strand of South Carolina. Through that effort, Conrads and Roehl (2007) developed the **P**ee Dee **R**iver and Atlantic **I**ntracoastal Waterway **S**alinity Intrusion **M**odel (PRISM) DSS to evaluate the effects of regulated streamflows of the Pee Dee River on salinity intrusion in the Waccamaw River and AIW.

Many ecological and hydrological studies have been conducted to evaluate the potential effects of the proposed

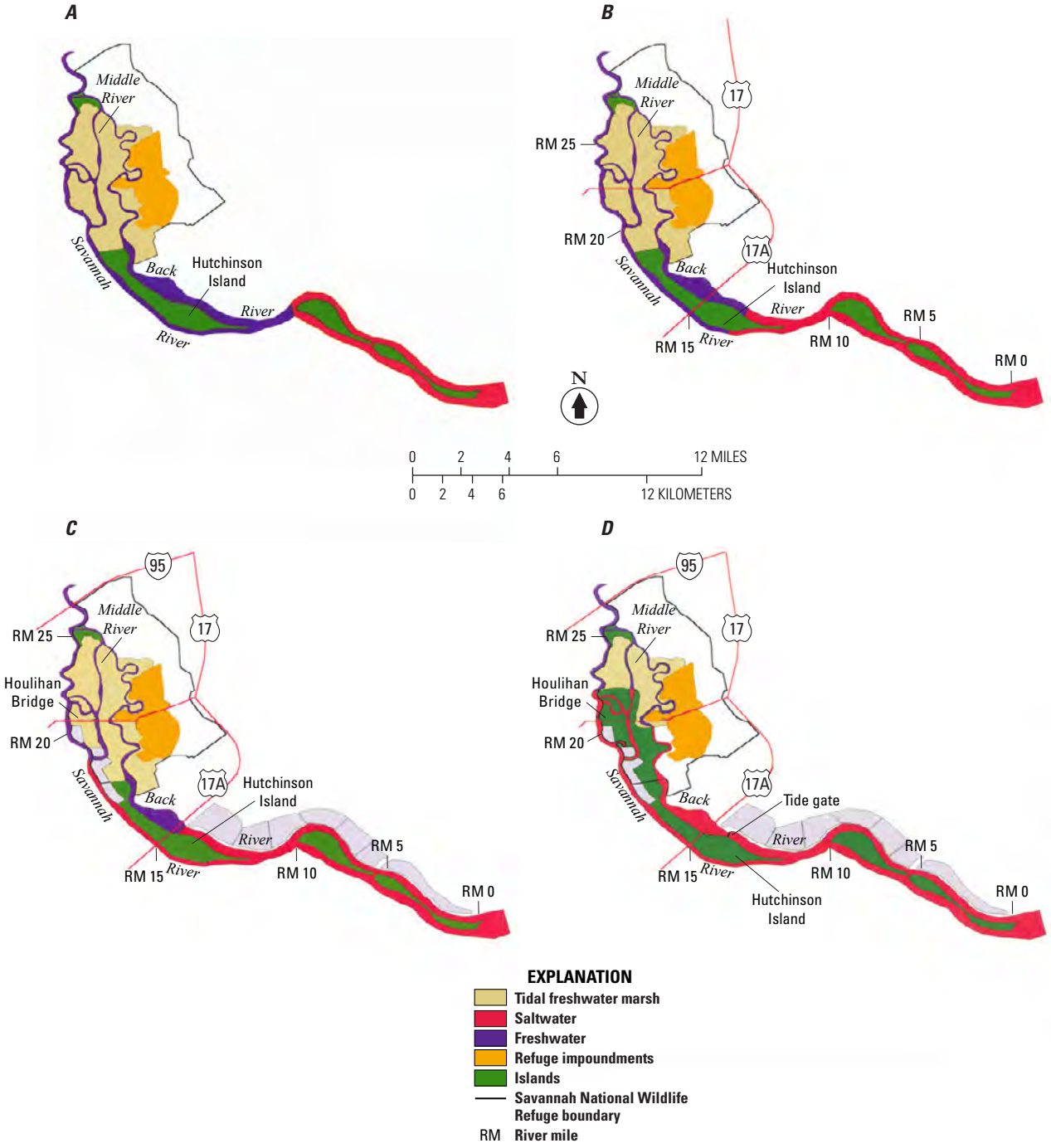

Figure 9. Location of the upstream extent of salinity intrusion along the Savannah and Back Rivers, greater than 0.5 practical salinity unit for four channel depths; (*A*) 13–15 feet in 1875; (*B*) 26–30 feet in 1940; (*C*) 34 feet in 1965; and (*D*) 42 feet in 1997. Maps produced by the U.S. Fish and Wildlife Service, Charleston Field Office. Data references used are (*A*) Granger (1968), (*B*) Lamar (1942), (*C*) U.S. Environmental Protection Agency, STORET Database 1998 (*http://www.epa.gov/STORET/*), and (*D*) Applied Technology and Management, 1998.

deepening of Savannah Harbor (Collins and others, 2001; Will and Jennings, 2001; Conrads and others, 2006; Tetra Tech, 2006; Welch and Kitchens, 2006). The three-dimensional (3D) hydrodynamic model Environmental Fluid Dynamics Code (EFDC) was used to assess the effects of proposed deepening of the harbor on salinity dynamics in the lower Savannah River (Tetra Tech, 2006). These studies were used in the development of the Environmental Impact Statement for the proposed deepening of Savannah Harbor (U.S. Army Corps of Engineers, 2012).

Conrads and others (2006) developed a Model-to-Marsh DSS to integrate hydrodynamic and ecological models being used to evaluate a potential deepening of the Savannah Harbor. The 3D hydrodynamic model, EFDC, and a marsh succession model (MSM) were developed by different scientific teams (Tetra Tech, 2005, 2006; Welsh and Kitchens, 2006) to evaluate the environmental impacts of the harbor deepening. The EFDC model predicts changes in river water levels and salinity in the system in response to potential harbor geometry changes. The MSM predicts plant distribution in the tidal marshes in response to changes in the water-level and salinity conditions in the marsh. To link the riverine predictions of the EFDC to the MSM, a "model to marsh" (M2M) DSS was developed using data-mining techniques that included ANN models, which simulated river and marsh water levels and salinity in the vicinity of the Savannah National Wildlife Refuge for the full range of 11.5 years of data from river and marsh gaging networks. The EFDC, MSM, and M2M were integrated in a DSS for use by various regulatory and scientific stakeholders.

Conrads and others (2011) developed a DSS to evaluate the potential effect of salinity and chloride concentration in Abercorn Creek, the source water for the city of Savannah's water supply, from a proposed deepening of Savannah Harbor. The effects of proposed deepening of Savannah Harbor on salinity intrusion in the upper reaches of the lower Savannah River estuary, including Abercorn Creek, was evaluated using mechanistic and empirical modeling approaches to simulate chloride concentrations at the city's intake. The mechanistic approach modified the 3D EFDC model used for evaluating potential harbor deepening effects for the Environmental Impact Statement (EIS). The empirical approach to simulate chloride concentrations was to develop models directly from the available data using ANN models. The ANN models use streamflow and specific conductance (field measurement for salinity) time series for inputs. The mechanistic and empirical modeling approaches were integrated into a DSS for simulation of salinity dynamics under various harbor-deepening scenarios.

Approach

The emerging field of data mining addresses the issue of extracting information from large databases (Weiss and Indurkhya, 1998). Data mining is a powerful tool for converting large databases into a form usable in solving problems that are otherwise imponderable because of the large numbers of explanatory variables or poorly understood process physics. Data-mining methods come from different technical fields, such as signal processing, statistics, artificial intelligence, and advanced visualization. Data mining employs methods for maximizing the information content of data, determining which variables have the strongest correlations to the problems of interest, and developing models that predict future outcomes. This knowledge encompasses both understanding of cause-effect relations and predicting the consequences of alternative actions. Data mining is used extensively in financial services, banking, advertising, manufacturing, and e-commerce to classify the behaviors of organizations and individuals and to predict future outcomes.

The ultimate goal of this study is to produce a model that effectively predicts salinity intrusion into the freshwater portions of the two study areas for a given set of streamflow, coastal water-level, and tidal-range conditions. The approach taken used all available streamflow, coastal water-level, and specific-conductance measurements from the individual gaging stations since the establishment of the coastal gaging networks in the two study areas. The modeling approach used correlation functions that were synthesized directly from data to predict how the change in specific conductance at each gage location is affected by streamflow and tidal conditions over time. Data-mining techniques, including ANNs, were previously applied to develop DSSs (PRISM and M2M) to predict salinity at gaging stations in the two study areas (Conrads and others, 2006; Conrads and Roehl, 2007). The two DSSs allowed users to simulate changes in salinity resulting from changes in regulated streamflow to the study areas. To evaluate salinity intrusion due to potential climate change, changes in streamflow and sea level need to be simulated separately and in combination. The PRISM and M2M were modified to simulate increases and decreases in sea level and changes in unregulated streamflow into the study areas.

Global circulation models (GCMs) are used in climate-change studies to simulate future precipitation and temperature resulting from different emission scenarios. The GCMs predict global changes in climate on large scales of 100- to 500-square-kilometer (km^2) grids (Daly and others, 2008), but the output cannot be used directly as inputs to watershed models. Downscaling techniques are used to transform the GCM regional output to the scale of local interest. To generate streamflow input to the salinity models, CGMs need to be coupled with watershed-runoff models. Conceptual integration of these models is depicted in figure 10. Global atmospheric circulation models provide large-scale (>250-km^2 grid) estimations of precipitation and temperature conditions under various carbon emission scenarios. To generate regional scale (about 12-km^2 grid) precipitation and temperature estimates, the global circulation model output is either dynamically or statistically downscaled (Wood and others, 2004). These regional precipitation and temperature predictions are then used as inputs to watershed models to predict changes in freshwater streamflow to the study areas.

To generate streamflow values for input to the PRISM DSS, researchers at the University of South Carolina (USC) applied the Hydrologic Simulation Program-Fortran (HSPF) watershed model as part of the BASINS modeling package distributed and support by the U.S. Environmental Protection Agency (USEPA) (*http://www.epa.gov/waterscience/basins/*) to the Yadkin-Pee Dee River watershed (Whitehead and others, 2011). The HSPF watershed model was used for simulation of streamflows at the five long-term USGS gaging

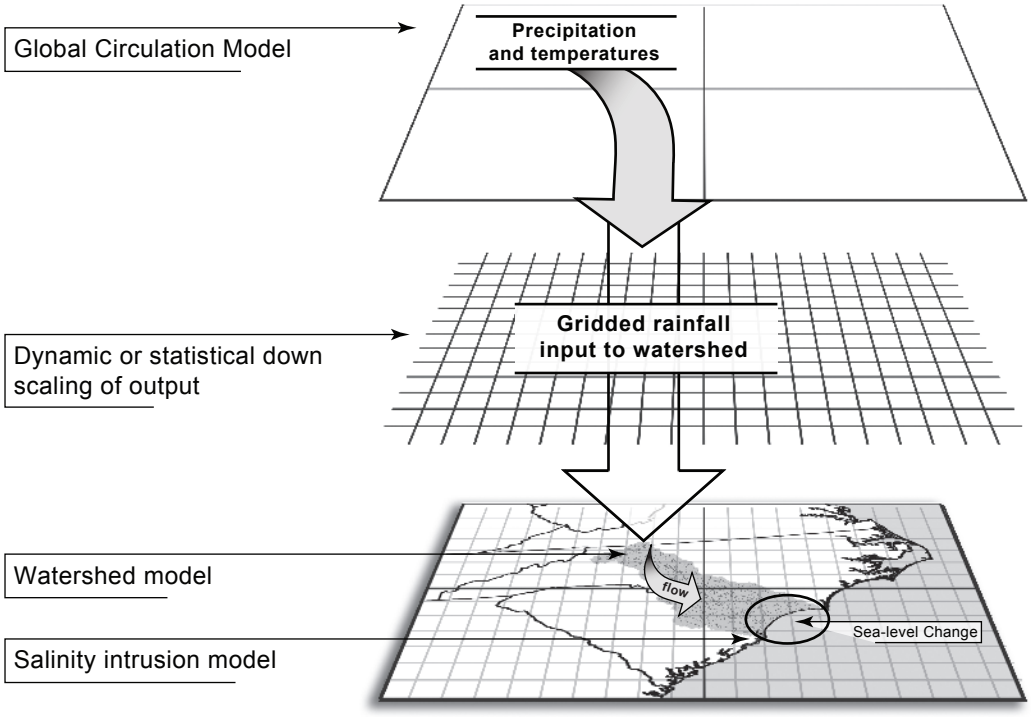

Figure 10. Schematic diagram showing the conceptual modeling approach for evaluation of the effects of climate change on salinity intrusion, North and South Carolina.

stations used for inputs to PRISM (table 2). Streamflows at these locations can be used as streamflow inputs to the PRISM DSS. The USC hydrologic modeling work did not include the application of HSPF to the Savannah River basin. Changes in precipitation and temperature projected by GCMs were evaluated only for the Waccamaw River and AIW study area.

The hydrologic model developed by USC for the Yadkin-Pee Dee River watershed included simulations of the potential effects of climate change on streamflows. Projected streamflow for future climate conditions were simulated by the HSPF model using forecasted regional precipitation and temperature scenarios. The regional precipitation and temperature scenario data were supplied by Dr. Katherine Hayhoe of Texas Tech University under contract with the USGS (Dalton and Jones, 2010). These one-eighth degree daily downscaled datasets include the PCM, CCSM3, GFDL 2.0, GFDL 2.1, HADCM3, BCM2, CGCM3, CNRM, ECHAM5, and ECHO GCMs. Data for each model are available for some or all of the A1FI, A1B, A2, and B1 emission scenarios. Each GCM scenario includes maximum and minimum daily temperature and precipitation values (*http://cida.usgs.gov/climate/gdp/* accessed August 19, 2011).

The USGS activities in the project, in collaboration with ADMi, included modification of the DSSs, retraining of selected ANN models, simulation of climate-change scenarios, coordination with the USC and Sea Grant researchers, and documentation of the study results. The PRISM and M2M DSSs were originally designed to evaluate the effect of changes in regulated streamflows from hydropower facilities on the Yadkin-Pee Dee and Savannah Rivers on the variability of salinity. Users could modify regulated streamflow using three input options—constant streamflow, percent of historical streamflows, or a user-defined hydrograph. Four of the streamflow inputs to the PRISM DSS are for unregulated tributaries to the Pee Dee River. The PRISM DSS was modified to allow users to input user-defined hydrographs for the unregulated tributaries generated from the HSPF watershed model. For the M2M DSS, there is only one regulated streamflow input (Savannah River at Clyo, Ga.), and the DSS did not need to be modified for unregulated streamflow inputs.

The two DSSs also were modified to allow simulations of incremental increases in sea level. Changes in hydrology and sea level can be simulated separately and in combination by modifying streamflow and (or) coastal water-level inputs to the DSSs. Using the user-defined hydrograph streamflow input option, users can simulate changes to salinity dynamics on the basis of altered streamflow patterns to the coast. These streamflow inputs can be determined anecdotally (for example, 10-percent wetter winters and springs and 10-percent drier summers and falls) or using hydrographs simulated from the integrated downscaled GCM and regional watershed models. These input hydrographs can be evaluated in combination with incremental sea-level rise. The updated DSSs are referred to as PRISM-2 and M2M-2.

Data-Collection Networks

Many resource agencies (including the USGS, National Oceanic Atmospheric Administration, USEPA, South Carolina Department of Health and Environmental Control, Georgia Environmental Protection Division, and local colleges and universities) have collected data on the Waccamaw River and AIW, and lower Savannah River estuary. The USGS maintains the National Water Information System (NWIS), a distributed network of computers and file servers for the storage and retrieval of water data collected at approximately 1.5 million sites around the country, as part of the USGS program disseminating water data to the public. Descriptions of the data-collection networks for the two study areas follow.

Waccamaw River and Atlantic Intracoastal Waterway

Data from three networks were used to build, train (calibrate), and test the seven specific-conductance ANN models in the Waccamaw River and AIW study area. One network is the long-term streamflow network in the Pee Dee and Waccamaw River basin, upstream from tidal effects (fig. 2). Data from the long-term streamflow network originated as early as 1906 (table 2), and more than 50 years (1950–2007) of concurrent data are available for four stations on the principal tributaries to the Pee Dee River—the Waccamaw, Lynches, Little Pee Dee, and Black Rivers.

The second network is the coastal network of specific-conductance and water-level[3] gaging stations in the Waccamaw River and AIW study area (fig. 2; table 4). The coastal gaging network does not have the temporal continuity of the streamflow network. Gaging stations often were installed to support special investigations and discontinued upon completion of a particular study. Specific-conductance data, collected at 15-minute intervals from 1983 to 2010, were available for the study with periods of record ranging from 3 to 27 years for 19 stations. Water levels and streamflow were gaged in addition to specific conductance at some of the tidal gaging network sites (table 4). Data obtained from the coastal gaging network during the past 27 years encompass a wide

[3]The water-level data typically refers to elevation of a known vertical datum. Gage height is the measurement of water-level elevation above an arbitrary datum. For the Waccamaw River and AIW study area, the data are gage heights. Water level is used when a datum correction to the National Geodetic Vertical Datum of 1929 has been applied to the data. For the lower Savannah River study area, the water-level data were collected to NGVD 29.

Table 4. Description of U.S. Geological Survey coastal gaging network in the Waccamaw River-Atlantic Intracoastal Waterway study area of South Carolina.

[S.C., South Carolina; WL, water level; Q, flow; SC, specific conductance; AIW, Atlantic Intracoastal Waterway. Artificial neural network models were developed for stations shown in bold text]

Station name	Station number	Name used in this report	Characteristics measured	Period of record
Waccamaw River at Conway Marina at Conway, S.C.	02110704	Conway Marina	WL, Q, SC	1991–2013
Waccamaw River at Pitch Landing, S.C.	02110707		WL, SC	1986–1989
Waccamaw River at Peachtree Landing, S.C.	02110715		SC	1990–1991
AIW at S.C. Highway 544 at Socastee, S.C.	02110725	Highway 544	WL, SC	1986–1992
AIW at Vereens Marina at North Myrtle Beach, S.C.	02110730		WL, SC	1983–1991
AIW at Briarcliffe Acres, S.C.	**02110755**	**Briarcliffe Acres**	**SC**	**1983–2013**
AIW at Myrtlewood Golf Course, S.C.	**02110760**	**Myrtlewood**	**SC**	**1986–1989, 1994–2013**
AIW at Grand Strand Airport at North Myrtle Beach, S.C.	**02110770**	**Grandstrand Airport**	**SC**	**1987–2013**
AIW at S.C. Highway 9 at Nixons Crossroads, S.C.	**02110777**	**Little River Inlet**	**WL, Q, SC**	**1986–2013**
Waccamaw River at Bucksport, S.C.	02110802		WL, Q, SC	1983–1995
Waccamaw River at Wachesaw Landing, S.C.	**02110809**	**Wachesaw**	**SC**	**1986–1989, 2002–2013**
Waccamaw River at Mt. Rena Landing near Murrells Inlet, S.C.	02110812		SC	1986–1989
Waccamaw River near Pawleys Island, S.C.	**021108125**	**Pawleys Island**	**WL, SC**	**2002–2013**
Thoroughfare Creek at Berlin near Pawleys Island, S.C.	021108135		WL, SC	1989
Waccamaw River at Hagley Landing, S.C.	**02110815**	**Hagley Landing**	**WL, SC**	**1986–2013**
Waccamaw River at U.S. Highway 17 at Georgetown, S.C.[1]	02110850		SC	1985–1989
Pee Dee River at U.S. Highway 701, S.C.	02135200	Highway 701	SC	1986–1994
Pee Dee River at Arundel Plantation near Jackson, S.C.	02135225		WL, SC	1989
Winyah Bay at Mouth near Georgetown, S.C.[1]	02136390		SC	1986–1989

[1]Station not shown in figure 6.

range of meteorological conditions, including large rainfalls in a 24-hour period, major hurricanes, and drought conditions. In addition to data from the USGS networks, wind speed and direction data from the National Weather Service meteorological network were obtained from the Charleston Harbor gage of the Southeast Climate Center.

Lower Savannah River

For the lower Savannah River study area, data from two networks were used to develop and test five river specific-conductance and seven marsh ANN models of the lower Savannah River estuary. The first network consists of USGS gaging stations (table 5; fig. 11*A*). Streamflow records collected at an hourly interval are available for the gage on the Savannah River near Clyo, Ga. (station 02198500; fig. 3), which was established in 1929. The USGS has maintained data-collection network stations on the Little Back River near the SNWR and in the lower Savannah River since the late 1980s. These stations collect water-level and (or) specific-conductance data at 15-minute intervals (fig. 11*A*). Locations of gaging stations that measure specific conductance, water level, and streamflow in the study are listed in table 5 and shown in figures 3 and 11*A*.

The second network is the USGS marsh network, which consists of seven sites established in the tidal freshwater marshes to evaluate potential effects of deepening the Savannah Harbor on plant communities (Welch and Kitchens, 2006). The Florida Cooperative Fish and Wildlife Research Unit (FCFWRU) of the USGS collected water-level and near-surface pore-water specific-conductance time-series data from the marsh network from June 1999 to March 2007. The USGS marsh network consists of four sites on the Little Back and Back Rivers, two on the Middle River, and one on the Front River (fig. 11*B*). The marsh monitoring sites consist of a pressure transducer and a specific-conductance probe just below the surface of the marsh, approximately 6 inches. The locations of the USGS continuous marsh gaging stations correspond to locations where the FCFWRU has conducted plant studies since the 1980s.

Table 5. Description of U.S. Geological Survey continuous river and marsh gaging networks used in the lower Savannah River study area.

[NAD 83, North American Datum of 1983; Q, flow; WL, water level; SC, specific conductance; USFW, U.S. Fish and Wildlife Service; PSC, pore-water specific conductance. Artificial neural network models were developed for stations shown in bold text]

Station number	Station location and name used in this report	Characteristics measured	Period of record	Longitude (decimal degrees, NAD 83)	Latitude (decimal degrees, NAD 83)
U.S. Geological Survey River Gaging Network (figs. 3 and 11*A*)					
02198500	Savannah River near Clyo	Q	October 1929–2013	–81.269	32.528
02198840	**Savannah River at I-95 Bridge**	**WL, SC**	**June 1987–2013**	**–81.151**	**32.236**
02198920	**Front River at Houlihan Bridge**	**WL, SC**	**October 1987–2013**	**–81.151**	**32.166**
02198977	Front River at Broad Street	WL	October 1987–2013	–81.096	32.184
021989784	**Little Back River at Lucknow Canal**	**SC**	**May 1990–2013**	**–81.118**	**32.171**
02198979	Little Back River near Limehouse	WL	June 1987–2013	–81.117	32.185
021989791	**Little Back River at USFW Dock**	**SC**	**October 1989–2013**	**–81.118**	**32.186**
02198980	Savannah River at Fort Pulaski	WL	October 1987–2013	–80.903	32.034
U.S. Geological Survey Marsh Network (fig. 11*B*)					
B1	**Little Back River marsh**	**WL, PSC**	**June 1999–December 2006**	**–81.128**	**32.192**
B2	**Little Back River marsh**	**WL, PSC**	**June 1999–March 2007**	**–81.127**	**32.173**
B3	**Back River marsh**	**WL, PSC**	**June 1999–December 2006**	**–81.126**	**32.154**
B4	**Back River marsh**	**WL, PSC**	**June 1999–December 2006**	**–81.109**	**32.131**
F1	**Front River marsh**	**WL, PSC**	**June 1999–April 2006**	**–81.148**	**32.187**
M1	**Middle River marsh**	**WL, PSC**	**June 1999–June 2006**	**–81.135**	**32.192**
M2	**Middle River marsh**	**WL, PSC**	**June 1999–December 2006**	**–81.133**	**32.184**

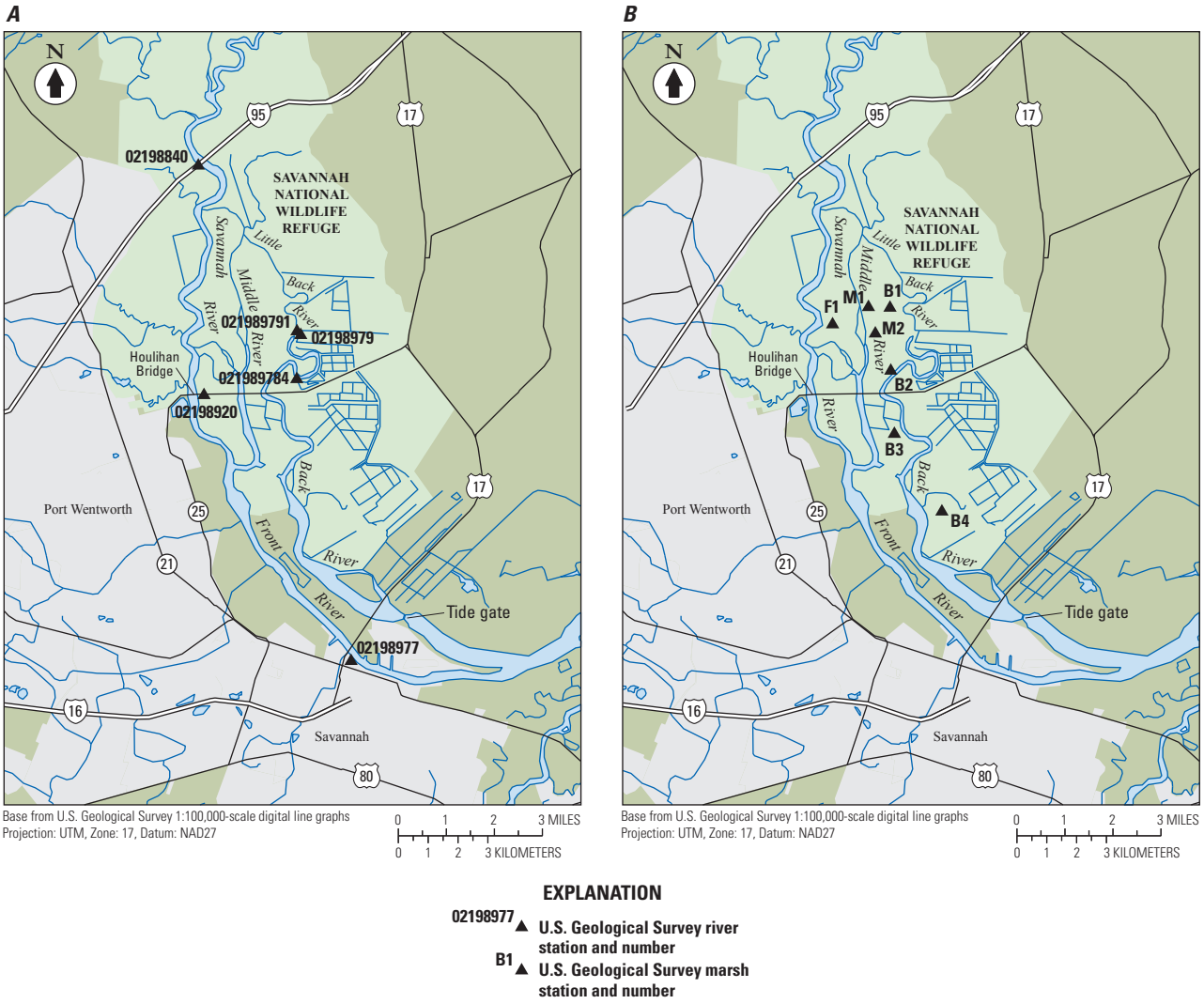

Figure 11. Location of U.S. Geological Survey (*A*) river gaging stations and (*B*) marsh gaging stations in the vicinity of the Savannah National Wildlife Refuge, South Carolina and Georgia (modified from Conrads and others, 2006).

Characterization of Historical Streamflow, Water Level, and Specific Conductance Dynamics

Estuarine systems are complex systems that are constantly responding to changing hydrologic, tidal, and meteorological conditions. Dyer (1997) states that the challenge of studying estuaries is "… that river flow, tidal range, and sediment distribution are continually changing and this is exacerbated by the continually changing weather influences. Consequently, some estuaries may never really be steady-state systems; they may be trying to reach a balance they never achieve." The estuarine portions of the AIW, Waccamaw River, and Savannah River are constantly integrating the changing streamflow of the Pee Dee River and Savannah River basins; the changing tidal conditions of the Atlantic Ocean; and the changing meteorological conditions, including wind direction and speed, rainfall, low- and high-pressure systems, and hurricanes. In the following sections, historical streamflow and tidal water levels and their effects on salinity intrusion are characterized.

Characterization of Historical Pee Dee River Streamflow

Streamflow in the Waccamaw River and AIW study area is regulated by releases from Blewett Falls Lake near Rockingham, N.C. Daily duration hydrographs, based on 82 years of data, are shown in figure 12. Daily duration hydrographs characterize the state of a stream with respect to time. For example, suppose daily streamflow data for a 78-year period are available for a station and the 75th-percentile streamflow is 10,000 cubic feet per second (ft^3/s) for a particular day of

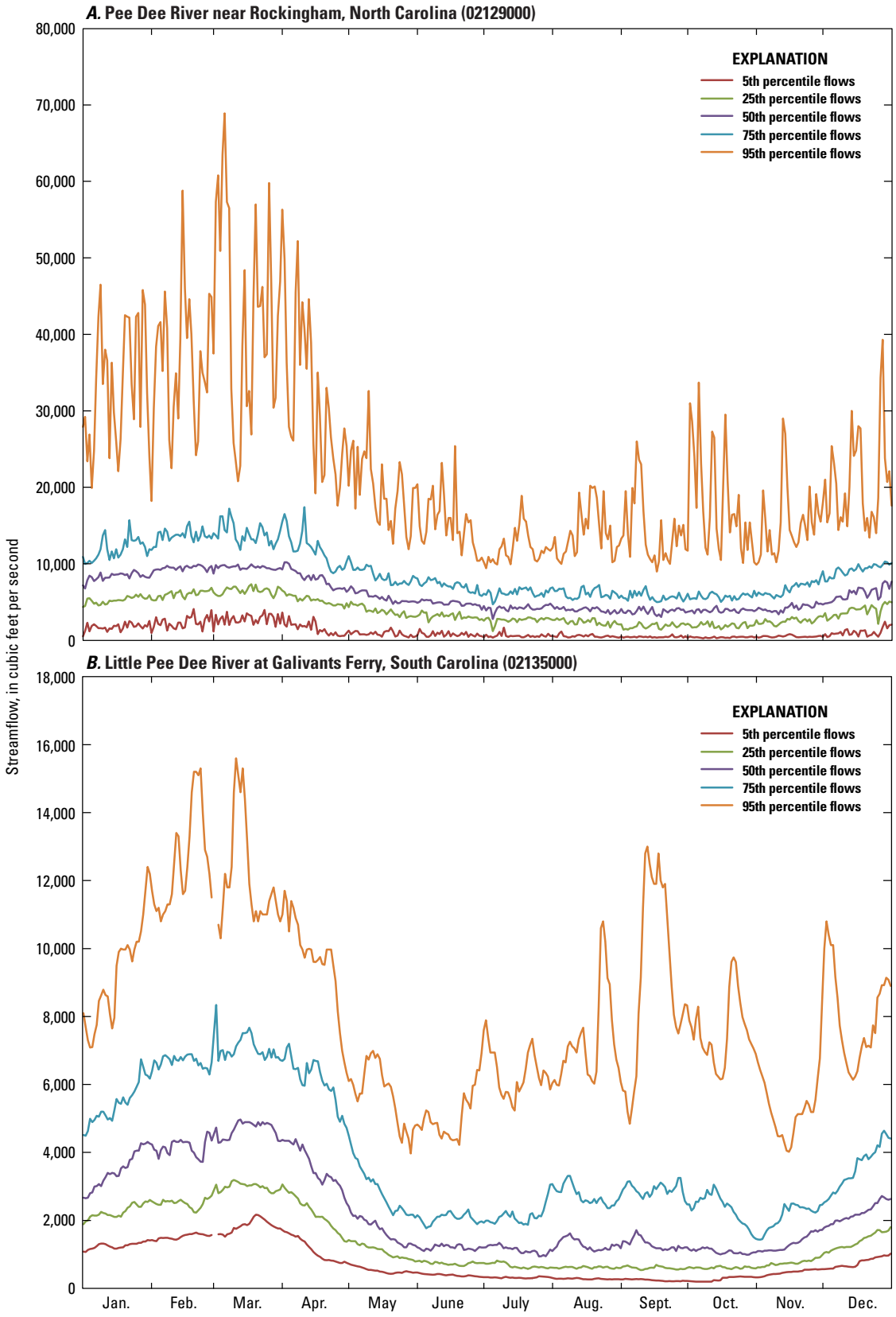

Figure 12. Streamflow duration hydrographs for (*A*) Pee Dee River near Rockingham, North Carolina (station 02129000), 1928–2010, and (*B*) Little Pee Dee River at Galivants Ferry, South Carolina (station 02135000) 1942–2010.

the year, say January 3, then 75 percent of all streamflows that occurred on January 3 of each of the 78 years of data were equal to or less than 10,000 ft^3/s. Streamflows from the 0 to 10th percentile typically occur during very dry conditions, and streamflows from the 90th to 100th percentile typically occur during very wet conditions. It is assumed that streamflows from the 25th to 75th percentile occur during normal hydrologic conditions. Streamflow at station 02129000, Pee Dee River near Rockingham, N.C., ranged from a minimum of less than 500 ft^3/s during periods of low streamflow to greater than 60,000 ft^3/s during periods of high streamflow (fig. 12*A*). Seasonally, the highest streamflows occur in late winter and early spring (February through March), and the lowest streamflows occur in late summer and early fall (July through October).

The large variation in the percentile streamflows, especially in the 95th-percentile streamflows, is a result of the regulated streamflow and large variation in releases from the Blewett Falls Lake. The Little Pee Dee River, which is the largest tributary to the Pee Dee River, and the other tributaries are unregulated, and the large variation in the duration hydrographs is not as pronounced as those of regulated streams, as illustrated by the duration hydrograph for the Little Pee Dee River at Galivants Ferry, S.C. (station 02135000; fig. 12*B*). The regulated streamflows decrease the range of the low and medium percentile streamflows, compared to unregulated streams. For the Little Pee Dee River, there is a larger distribution from the 5th to the 75th percentile streamflows, compared to the same percentiles for the Pee Dee River near Rockingham, N.C. (station 02129000; fig. 12).

Although regulation affects the natural streamflow regime over short-term (hours to days) periods, streamflow over longer term periods (weeks to months) generally is similar to that of unregulated streams. For example, the hourly streamflow values shown in figure 13*A* for the regulated Pee Dee River at Pee Dee (station 02131000) have a greater difference from the unregulated Lynches, Little Pee Dee, and Black Rivers (stations 02132000, 02135000, 02136000, respectively) than the 7-day average streamflow values for the same period shown in figure 13*B*.

Characterization of Historical Lower Savannah River Streamflow

Streamflow at Savannah River near Clyo, Ga. (station 02198500), is regulated by releases from Lake Thurmond Dam near Augusta, Ga. From 1930 to 2010, the 5th- and 95th-percentile streamflows ranged from a minimum of 4,000 ft^3/s to more than 50,000 ft^3/s (fig. 14). Seasonally, the highest streamflows occur in late winter and early spring (February through March), and the lowest streamflows occur in late summer and early fall (August through October).

During the 11-year period from 1994 to 2005 (the period of record used to develop the M2M-2 DSS), the Savannah River experienced extreme streamflow conditions. During the winter and spring of 1998, floods from above-normal rainfall during El Niño conditions resulted in streamflows of greater than 50,000 ft^3/s (fig. 15), which exceeded the 95th-percentile daily streamflow for the period of record. Following the El Niño, the southeastern United States experienced drought from 1998 to 2002, inclusive, and the Savannah River at Clyo, Ga., experienced minimum streamflows of 4,500 ft^3/s. Streamflows during the drought generally ranged from the 5th percentile to the historical minimum for the period of record.

Characterization of Historical Waccamaw River and Atlantic Intracoastal Waterway Water Levels

The AIW and Waccamaw River experience semi-diurnal tides consisting of two high tides and two low tides in a 24.8-hour period. A 14-day periodic tidal cycle also occurs, resulting in spring and neap tides. Spring tides are periods of increased tidal range that occur during the time of full and new moons. Neap tides are periods of decreased tidal range that occur around the onset of waxing and waning moons. There are also seasonal and annual cycles to tides. The mean and spring tidal ranges for Little River Inlet are 4.63 and 5.56 ft, respectively, and for Winyah Bay are 4.60 and 5.40 ft, respectively (table 6; National Oceanic and Atmospheric Administration, 2010). As the tidal wave propagates upstream, the tidal range decreases with the increased freshwater streamflow of the Pee Dee and Waccamaw Rivers and energy losses due to channel geometry. In the AIW, the mean tidal range decreases to 2.08 ft at the S.C. Highway 544 bridge at Socastee (table 6). In the Waccamaw River, the mean tidal range decreases to 1.24 ft at Conway. An approximate 3- to 4-hour lag of the tide occurs from Nixons Crossroad at S.C. Highway 9 (station 02110777) to Socastee at S.C. Highway 544 (station 02110725) on the AIW, and an approximate 5-hour lag occurs between Hagley Landing (station 02110815) and Conway Marina (02110704) on the Waccamaw River.

The tidal range, the difference in height between consecutive high and low water levels, at the AIW at S.C. Highway 9 gaging station (02110777) for the period July 1994 to June 1996 clearly shows the 14- and 28-day spring-neap tidal cycles, along with seasonal and semi-annual cycles (fig. 16). For example, a high spring tide (tidal range greater than 4.5 ft) is followed 14 days later by a low spring tide (tidal range less than 4.5 ft). A similar 28-day pattern is apparent in the neap tides where a low neap tide (tidal range less than 3.5 ft) is followed 14 days later by a high neap tide (tidal range greater than 3.5 ft). The biggest differences in spring and neap tides occur in spring (March and April) and fall (October and November) of the year. Minimum differences between the spring and neap tides occur in the summer (June and July) and in the winter (December and January).

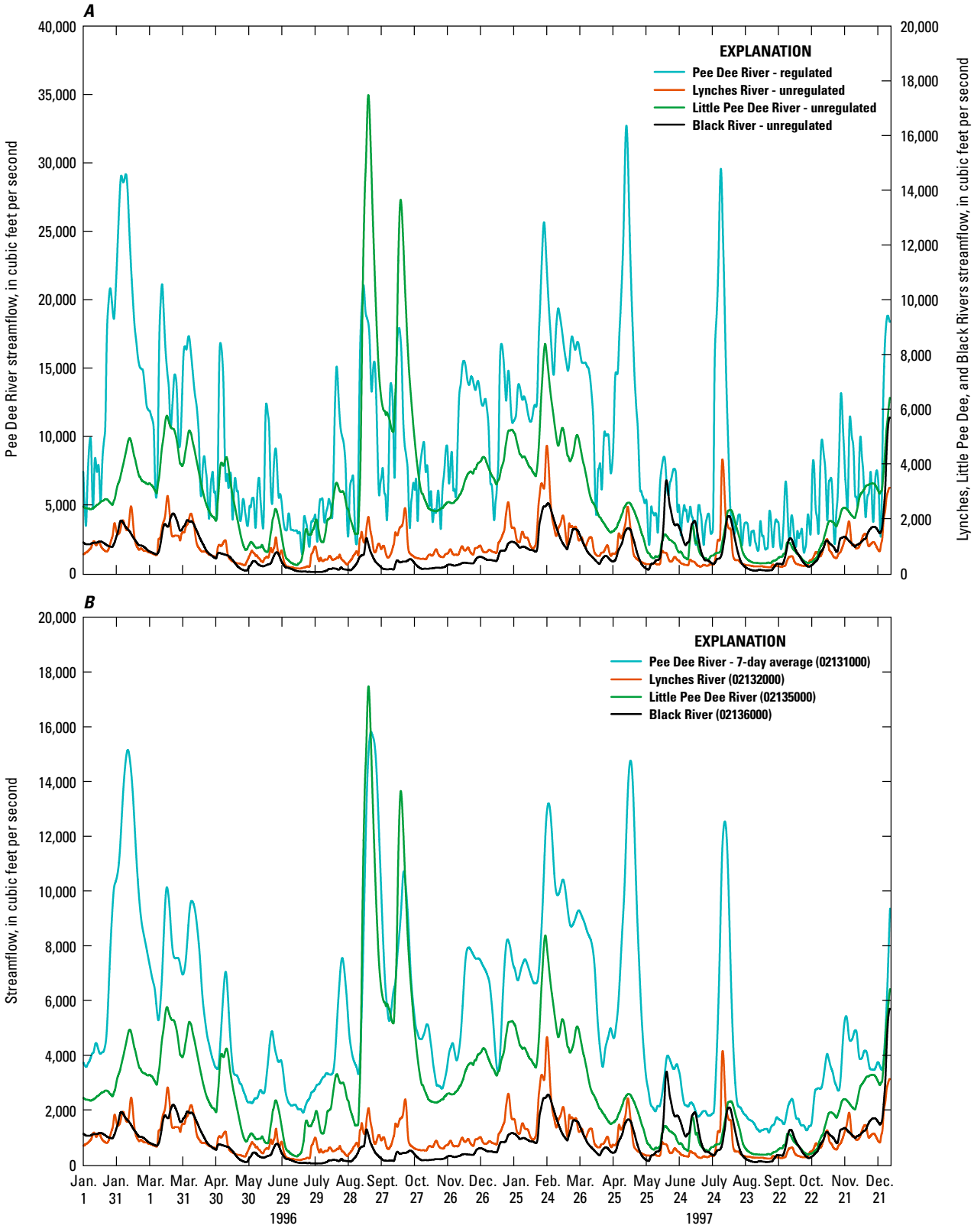

Figure 13. Hourly streamflow for (*A*) the Pee Dee (02131000), Lynches (02132000), Little Pee Dee (02135000), and Black Rivers (02136000) and (*B*) 7-day average flow for the Pee Dee River and hourly streamflow for the Lynches, Little Pee Dee, and Black Rivers, January 1, 1996–December 31, 1997. Locations of gages are shown in figure 2.

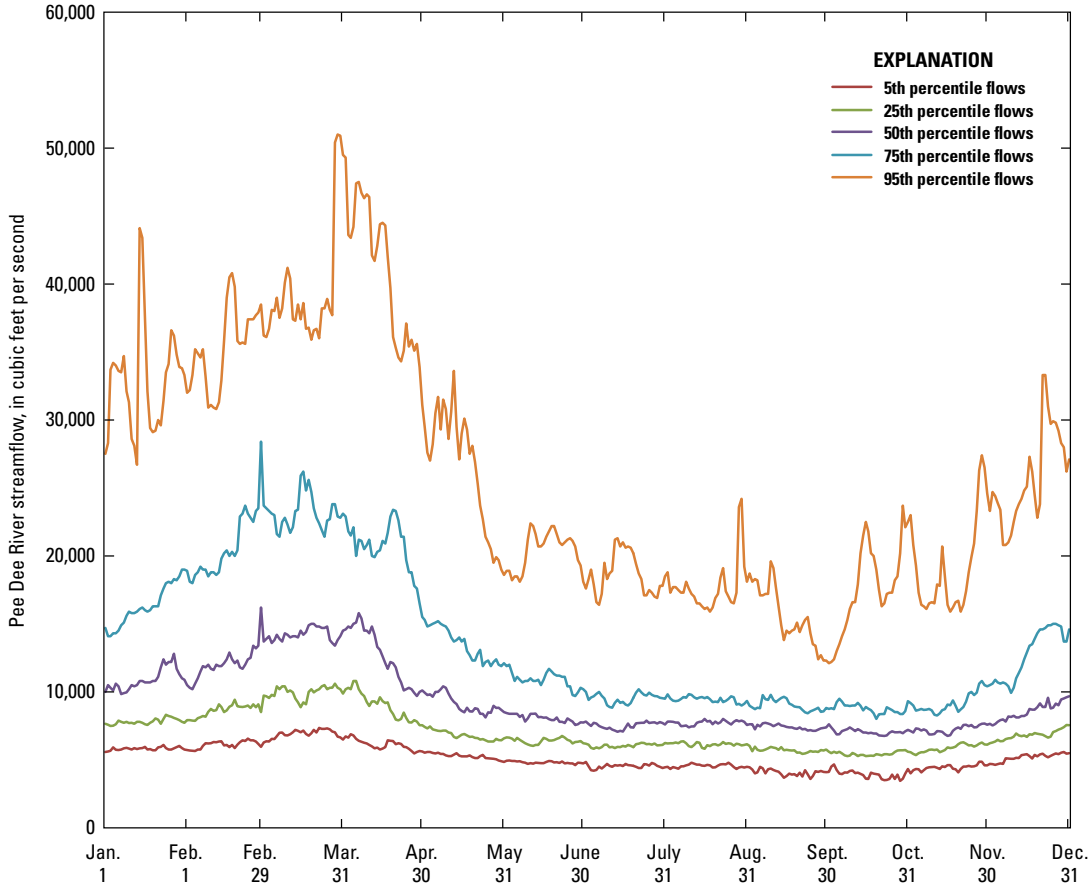

Figure 14. Streamflow duration hydrographs for Savannah River near Clyo, Georgia (station 02198500), 1930–2010.

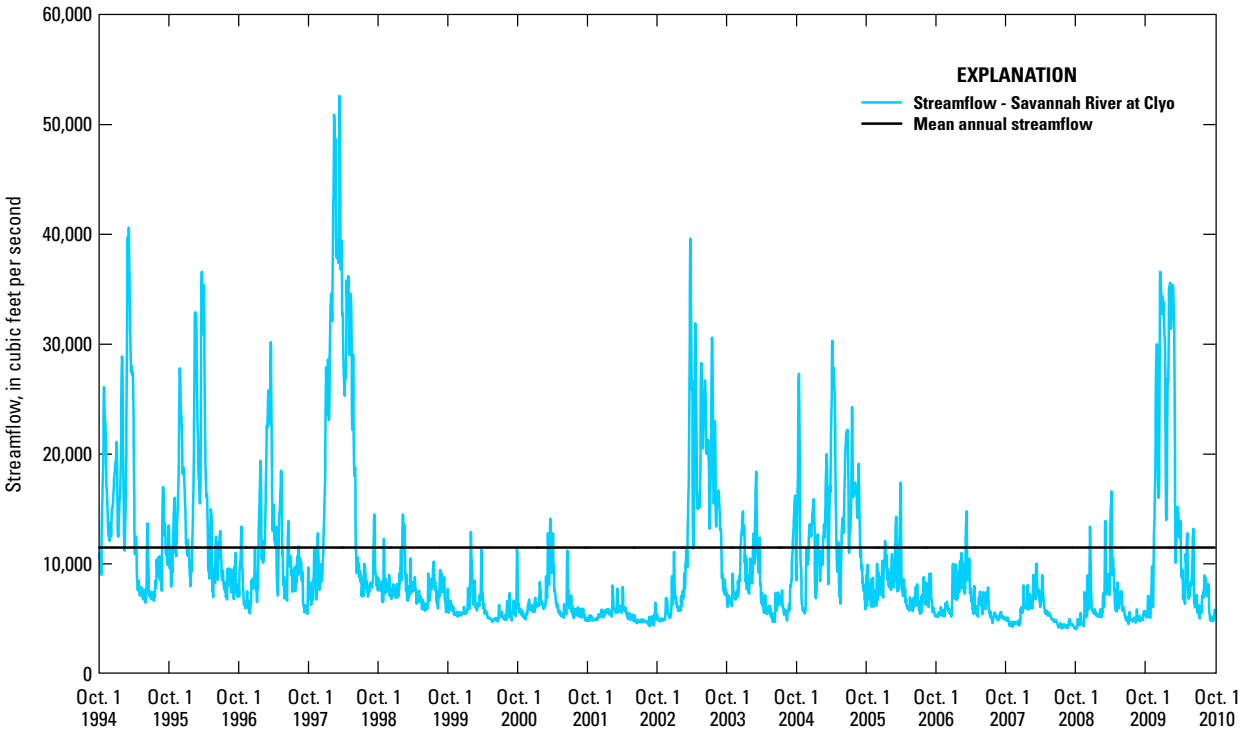

Figure 15. Daily streamflow and mean annual streamflow for Savannah River near Clyo, Georgia, October 1, 1994–September 30, 2010.

Table 6. Mean tide range, spring tide range, and mean tide levels for selected locations on the Atlantic Intracoastal Waterway and Waccamaw River, South Carolina.

[Data from National Oceanic and Atmospheric Administration, 2010]

Location	Mean tide range, in feet	Spring tide range, in feet	Mean tide level, in feet[1]
Atlantic Intracoastal Waterway (fig. 6)			
Little River	4.63	5.56	2.47
Nixons Crossroads	4.10	4.55	2.18
Myrtle Beach Airport	2.88	3.34	1.60
North Myrtle Beach	1.78	2.10	1.25
Socastee Bridge (S.C. Highway 544)	2.08	2.45	1.18
Winyah Bay and Waccamaw River (fig. 6)			
Winyah Bay Entrance[2]	4.60	5.40	2.50
Waccamaw River Entrance[2]	3.60	4.24	1.91
Hagley Landing	3.47	3.99	1.88
Thoroughfare Creek	3.34	3.94	1.84
Wachesaw Landing	2.74	3.18	1.53
Bull Creek Entrance	2.46	2.85	1.38
Bucksport	2.16	2.48	1.25
Enterprise Landing	2.00	2.40	1.10
Waccamaw River at Conway	1.24	1.44	0.76
Savannah River (fig. 3)			
Fort Pulaski	6.92	8.03	3.60
Fort Jackson	8.10	8.70	3.67
Port Wentworth	8.14	9.12	4.28
U.S. Highway 17	7.63	8.55	4.06
Seaboard Coast Line Railroad Bridge (Interstate 95 bridge)	6.20	7.20	3.30

[1]The arithmetic mean of high and low tides. The mean tide level is listed relative to the mean lower low water datum.

[2]Not shown in figure 6.

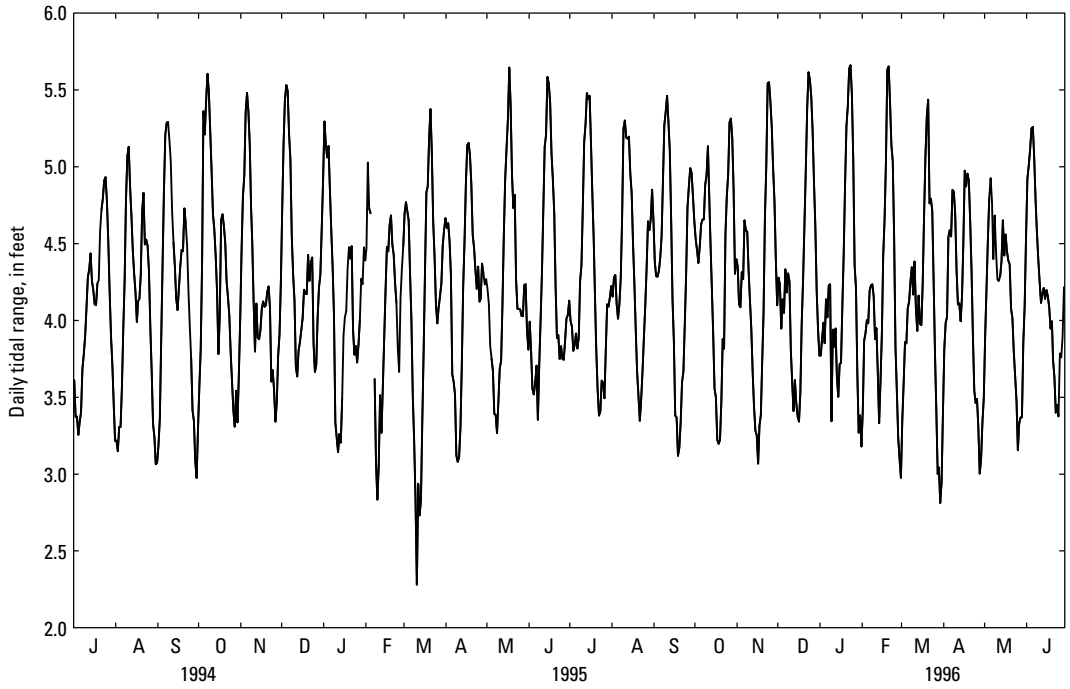

Figure 16. Daily tidal range at Atlantic Intracoastal Waterway at South Carolina Highway 9 (station 02110777), July 1994–June 1996.

The water levels at four stations on the AIW and the Pee Dee and Waccamaw Rivers during a 17-day period in October 1998 are shown in figure 17*A*. The spring-tide period, characterized by the large amplitude in tidal range, occurred around October 7; the neap-tide period, characterized by the relatively small amplitude in tidal range, occurred around October 14. During periods of medium and high streamflow, the tidal signals at Waccamaw River at Conway Marina and Pee Dee River at S.C. Highway 701 are overwhelmed by streamflow. Water levels for the same four stations on the AIW and Pee Dee and Waccamaw Rivers are shown during a 45-day period of high streamflow during January and February 1999 in figure 17*B*. Streamflow at Pee Dee River at Pee Dee, S.C., (station 02131000) peaked at 22,400 ft^3/s on January 29, and streamflow at Waccamaw River near Longs, S.C., (station 02110500, fig. 2) peaked at 7,280 ft^3/s on February 7 (not shown in fig. 17*B*). The tidal signal was negligible at water levels greater than 6 ft at the gaging station Pee Dee River at U.S. Highway 701 and at water levels greater than 4 ft at the Waccamaw River at Conway Marina. Water levels are expressed relative to the National Geodetic Vertical Datum of 1929 (NGVD 29).

Characterization of Historical Lower Savannah River and Marsh Water Levels

Semi-diurnal tides also occur in the lower Savannah River study area. The tidal range increases along the South Carolina coast from north to south. The NOAA network of subordinate tide stations reports that a mean tidal range of 6.92 ft at Fort Pulaski (*http://Co-ops.nos.noaa.gov/tides10*), whereas it reports a mean tide range of 4.63 ft at Little River Inlet. The tidal ranges of the lower Savannah River can increase relative to that at the harbor as the tidal wave propagates upstream and the volume of water moves into small channel geometry. For example, the mean tidal ranges at Fort Jackson (near the confluence of the Back and Front Rivers) and Port Wentworth were 8.10, and 8.14, respectively (table 6). Farther upstream at the U.S. Highway 17 bridge and Interstate 95 bridge, the tidal range decreased to 7.63 and 6.2 ft, respectively, with the increased effects of the freshwater streamflow of the Savannah River and decrease in channel size. There is an approximately 1-hour lag of the tide from Fort Pulaski to the Little Back and Back Rivers at the U.S. Highway 17 bridge.

Figure 18 shows the water levels at three USGS gaging stations on the Savannah River during October 2002. The neap tidal period, characterized by the relatively small amplitude in tidal range, occurred around October 14 and 28, and the spring tidal period, characterized by the larger amplitude in tidal range, occurred around October 7 and 21. During the spring tide early in the month, the highest water levels occurred at the Broad Street gage (station 02198977; fig. 11) and were greater than the downstream water levels at Fort Pulaski (station 02198980; fig. 3). As the tidal range diminished during October, the highest water levels were experienced at the most upstream gaging station at the Interstate 95 bridge (station 02198840; fig. 11*A*) where the high water is affected by streamflow.

The tidal range for the Fort Pulaski gage (station 02198980) is shown in figure 19 for the period June 2001 to May 2003; the 14-day spring-neap tidal range is clearly illustrated. For example, a high spring tide (tidal range greater than 8 ft) is followed by a low spring tide (tidal range less than 8 ft). A similar pattern is apparent in the neap tides where a low neap tide (tidal range less than 5.5 ft) is followed by a high neap tide (tidal range greater than 5.5 ft). Seasonal and semi-annual cycles of minimum and maximum tidal ranges can also be seen in figure 19.

Water-level dynamics in the tidal marshes are dependent on the height of the water, the surface elevation of the marsh, and inertial effects. Tidal fluctuations in marsh water levels are greatest during the spring tides and least during neap tides. Water levels at USGS gaging stations on the Little Back, Middle, and Front Rivers in the SNWR marsh are shown in figures 20 and 21. In figure 20, hourly water levels in the Little Back River near Limehouse (station 02188979, left y-axis) are shown with marsh water levels (right y-axis). The Little Back River water-level time series shows the periods of spring tides. Multi-day periods of substantial tidal fluctuations at the four marsh sites along the Little Back and Back Rivers occur during spring tides beginning around December 15 and 29, 2001, and January 28, 2002. In figure 21, similar water-level responses are seen for the marsh sites along the Middle River and Front River. Multi-day periods of substantial tidal fluctuations for the three marsh sites coincide with spring tides beginning around November 10, November 29, December 10, and December 29, 2001.

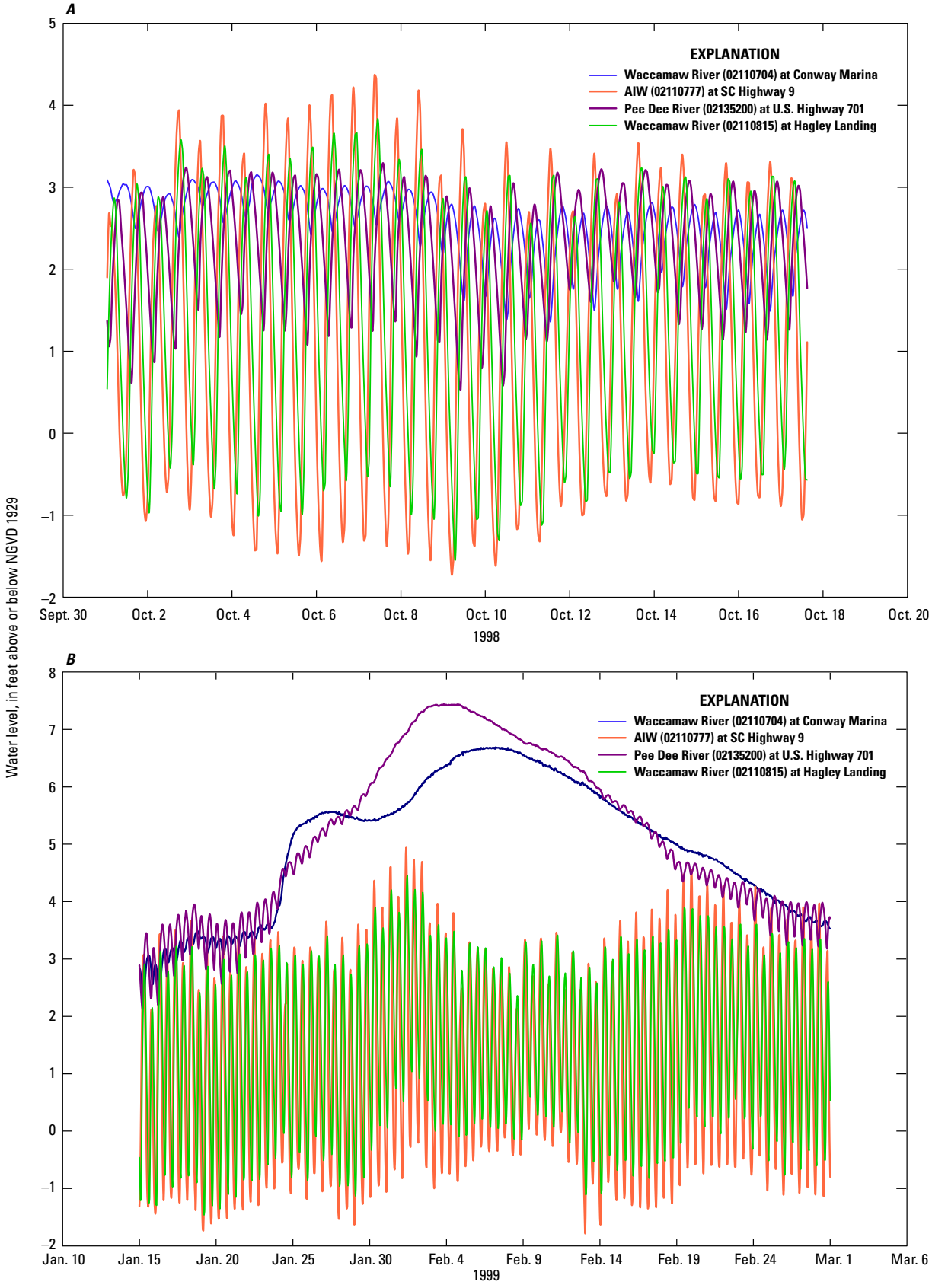

Figure 17. Hourly water levels at four gaging stations on the Pee Dee and Waccamaw Rivers and the Atlantic Intracoastal Waterway (AIW), South Carolina, for (*A*) a low-flow period October 1–17, 1998, and (*B*) a high-flow period January 15–March 1, 1999.

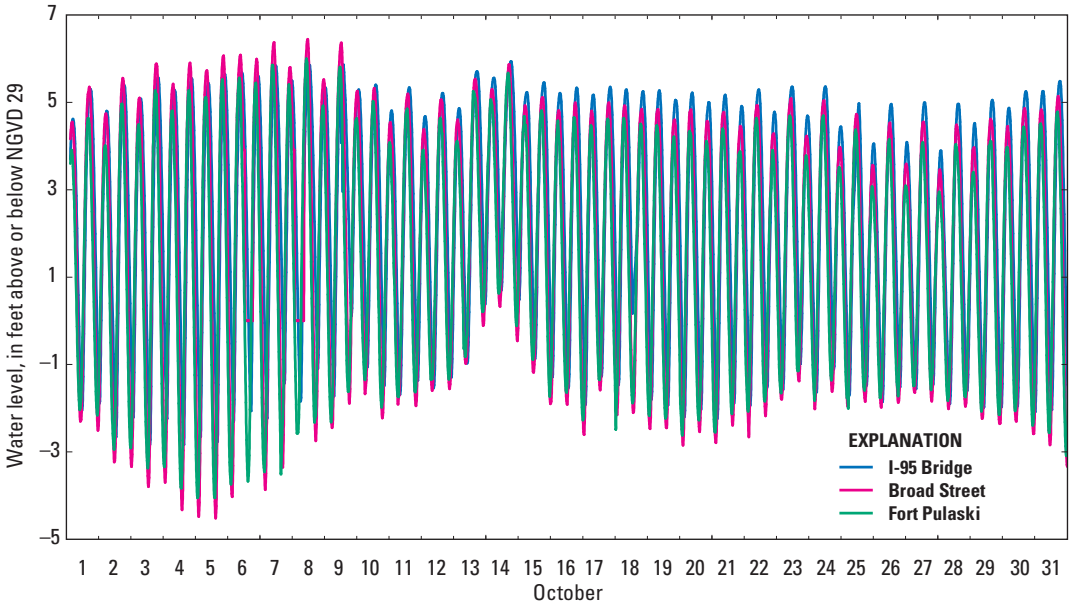

Figure 18. Hourly water levels at three gaging stations on the Savannah River, Georgia, October 1–31, 2002.

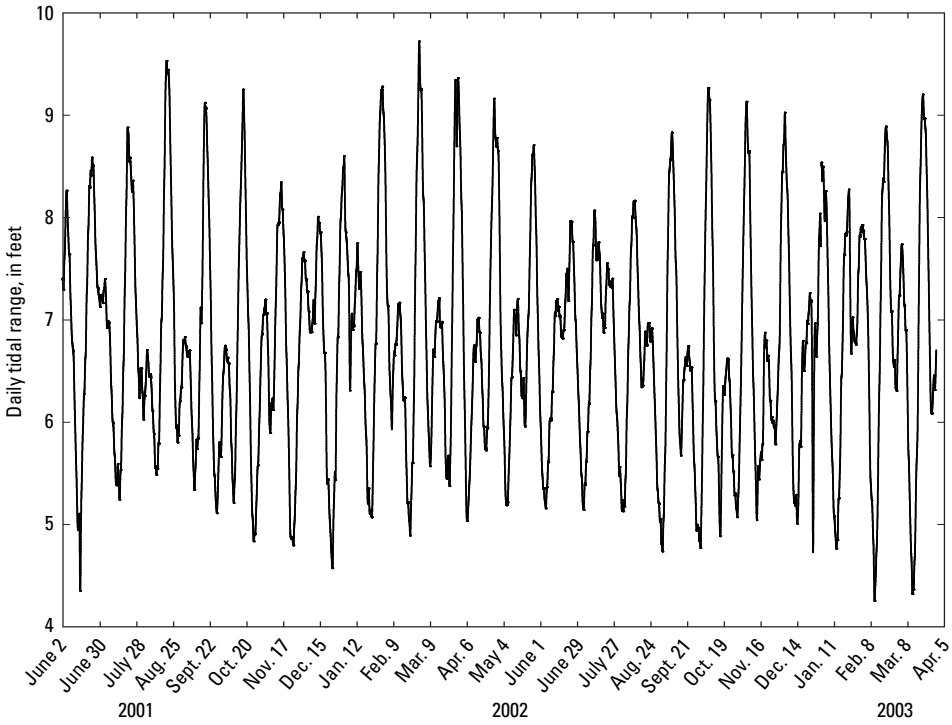

Figure 19. Daily tidal range at Savannah River at Fort Pulaski (02198980), Georgia, June 2001–April 2003.

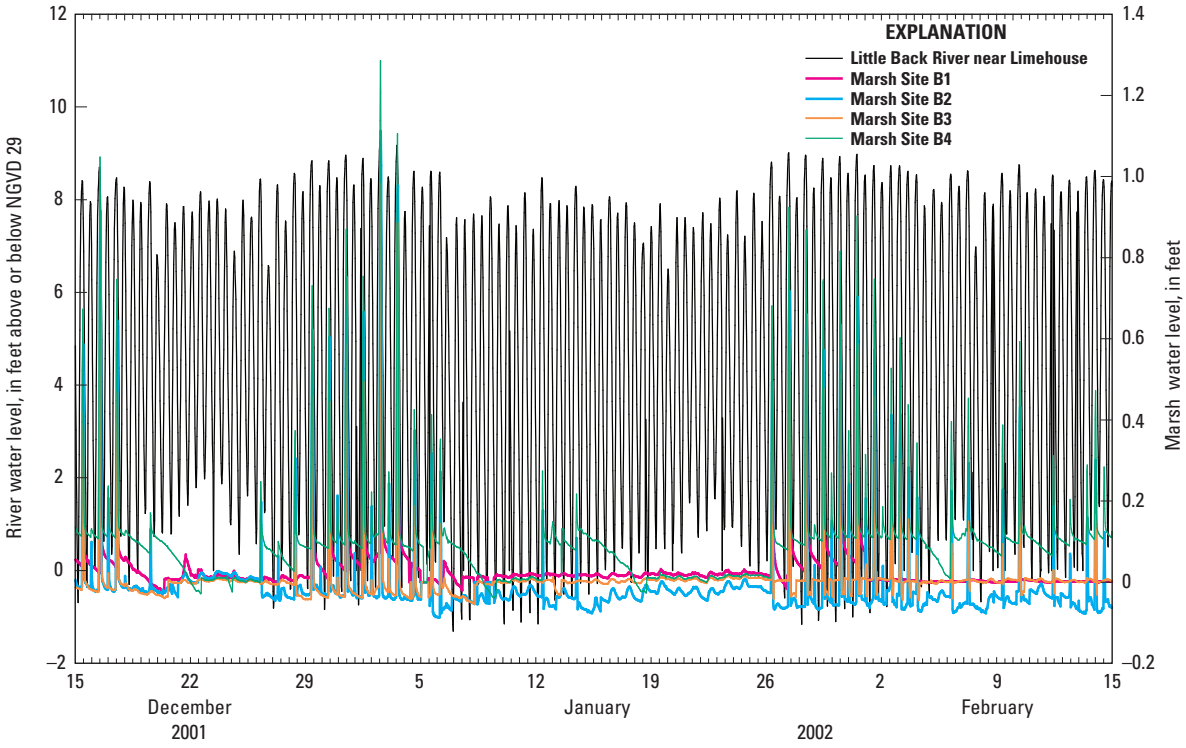

Figure 20. Hourly water-level data for the four Back River marsh gaging stations and Little Back River gaging stations for the period December 15, 2001–February 15, 2002.

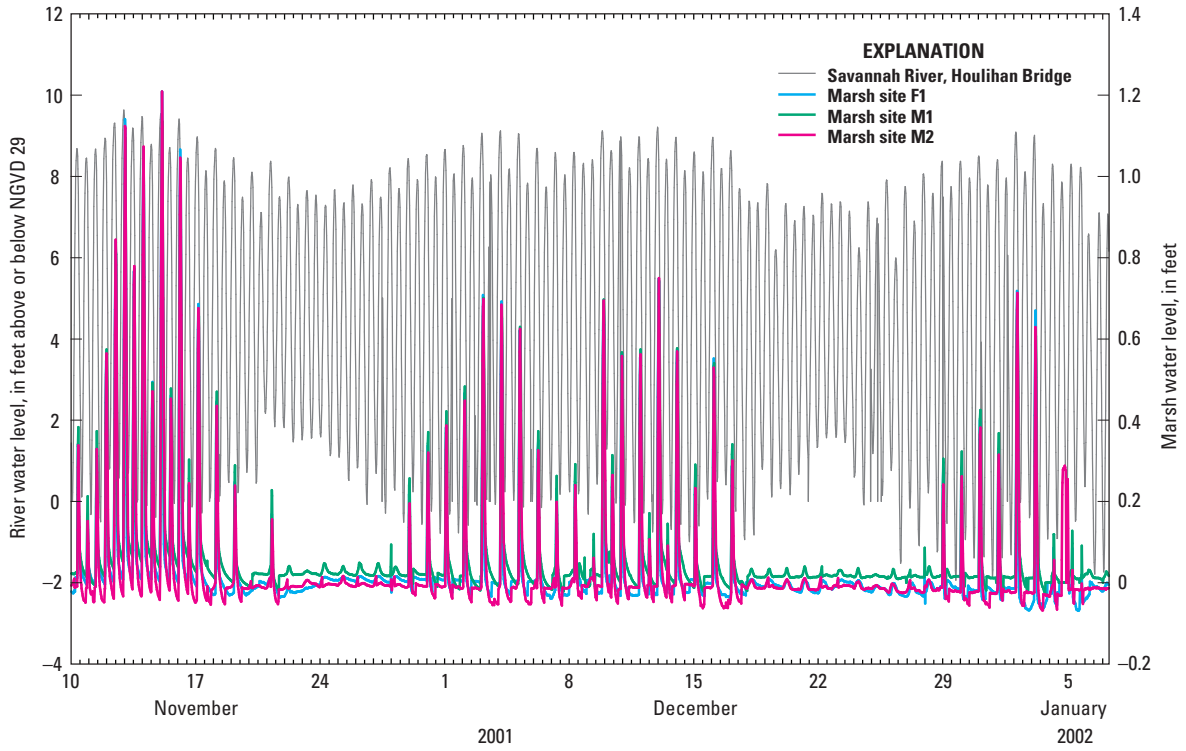

Figure 21. Hourly water-level data for three marsh gaging stations along the Middle and Front Rivers, and Savannah River water level at Houlihan Bridge (station 02198920), Georgia, November 10, 2001–January 7, 2002.

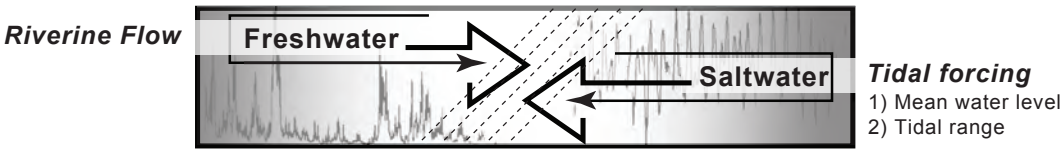

Figure 22. Conceptual model of the major factors controlling the position of the freshwater-saltwater interface.

Characterization of Historical Specific Conductance

Specific conductance, a measure of the ability of water to conduct electrical current, is commonly used to compute salinity (Miller and others, 1988). In this report, specific conductance and salinity are used interchangeably. Salinity in study areas is constantly responding to changing streamflow and tidal conditions. The location of the saltwater-freshwater interface is balanced between upstream freshwater river streamflows and downstream tidal forcing (fig. 22). During periods of high streamflow, it is difficult for salinity to intrude upstream, and the saltwater-freshwater interface moves downstream toward the ocean. During periods of low streamflow, the saltwater-freshwater interface is moved upstream by tidal forcing, by an increase in mean water level, a change in tidal range, or a combination of the two.

Waccamaw River and Atlantic Intracoastal Waterway

The location of the saltwater-freshwater interface in the Waccamaw River and Atlantic Intracoastal Waterway is affected by streamflow from the Pee Dee and Waccamaw Rivers. The daily mean specific conductance for the Waccamaw River at Hagley Landing (station 02110815) and the daily mean streamflow for the Pee Dee River at Pee Dee, S.C. (station 02131000) for the October 1994 to September 2010 are shown in figure 23. The period encompasses streamflow conditions ranging from the high streamflows of the El Niños in 1998 and 2003 to the low streamflows of the extended droughts from 1998 to 2002 and 2007 to 2008. During periods of medium and high streamflows (streamflow greater than 5,000 ft^3/s), the specific conductance is generally low. (For plotting purposes, streamflow was multiplied by 0.1, and 9 ft was subtracted from the gage height.) During periods of low streamflow (streamflow less than 5,000 ft^3/s), specific-conductance values increase representing periods of salinity intrusion. During the low-flow periods prior to the high streamflows measured during the El Niño of 1998, salinity intrusions associated with specific-conductance values of 3,000 to 5,000 microsiemens per centimeter at 25 degrees Celsius (µS/cm) were common. During droughts, such as after the high streamflow in 1998, extended periods of low streamflow occurred. The low streamflow contributed to increases in salinity, with daily mean specific-conductance values often greater than 15,000 µS/cm and occasional values greater than 20,000 µS/cm (fig. 23). A specific conductance of 20,000 µS/cm is equal to a salinity of 11.9 practical salinity units (psu).

A similar relation between low streamflow and high salinity can be seen in the mean specific conductance for the North End of the AIW at Grand Strand Airport (station 02110770) and the daily mean streamflow for the Waccamaw River at Longs, S.C. (station 02110500) for the period from October 1, 1994, to September 30, 2011 (fig. 24). The extended low-flow periods after 1999 are apparent; streamflows rarely reached 6,000 ft^3/s. During the low-flow periods prior to the El Niño of 1998, salinity intrusion with specific-conductance values of 6,000 to 15,000 µS/cm were common; in contrast, salinity intrusions exceeding 15,000 µS/cm were common during the extended droughts after 1998.

Although salinity levels at the North End of the AIW and the South End of the Waccamaw River respond similarly to reduced streamflow, the response to changes in tidal conditions is very different. The primary tidal forces counteracting the river streamflows are the mean coastal water levels and tidal range (fig. 22). For the Pawleys Island gage (station 021108125; fig. 2) at the South End, salinity intrusions occur when the streamflow of the Pee Dee River is less than about 5,000 ft^3/s and the mean water levels are high. Figure 25 depicts two salinity intrusion events in 2007. The streamflow in the Pee Dee River (station 02131000) decreased from 20,000 ft^3/s in late April 2007 to less than 5,000 ft^3/s in early May (note that streamflow and gage height were adjusted on figure 25 for plotting purposes). Note that the intrusion events coincide with high mean water level, as indicated by the Little River Inlet gage heights, rather than spring tides. On May 13, 2007, gage height exceeded 4.5 ft. Soon after, the streamflow exceeded 5,000 ft^3/s and specific conductance decreased. The increase in mean water levels increased the volume of higher salinity ocean water in Winyah Bay and the lower Waccamaw River. Small decreases in streamflow allow the salinity to move farther upstream. Although streamflows were low, less than 5,000 ft^3/s in mid-May, the next intrusion did not occur until the Little River Inlet gage height increased to 4.5 ft on June 4, 2007.

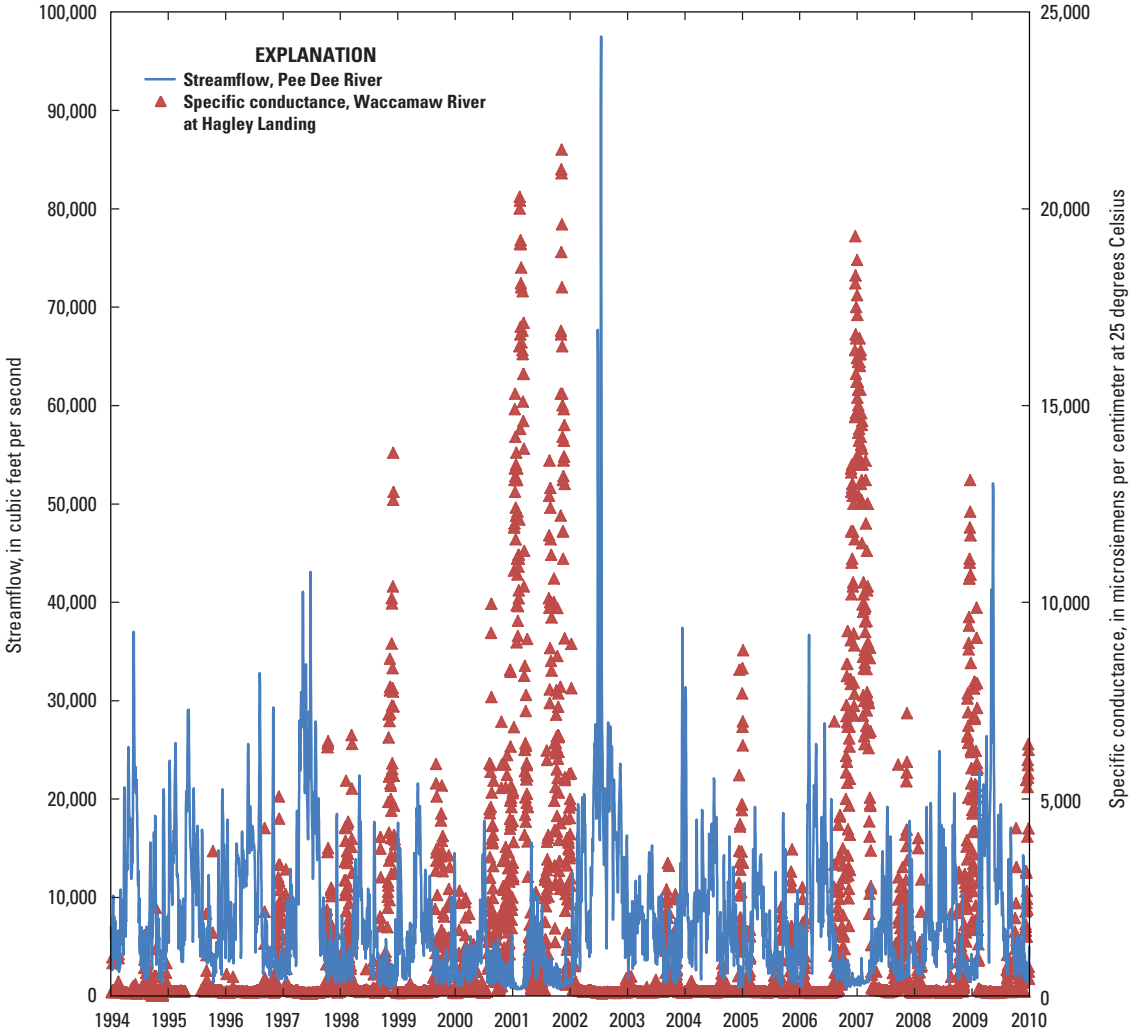

Figure 23. Daily mean specific conductance at Waccamaw River at Hagley Landing, South Carolina (02110815), and daily mean streamflow at Pee Dee River at Pee Dee, South Carolina (02131000), October 1, 1994–September 30, 2010.

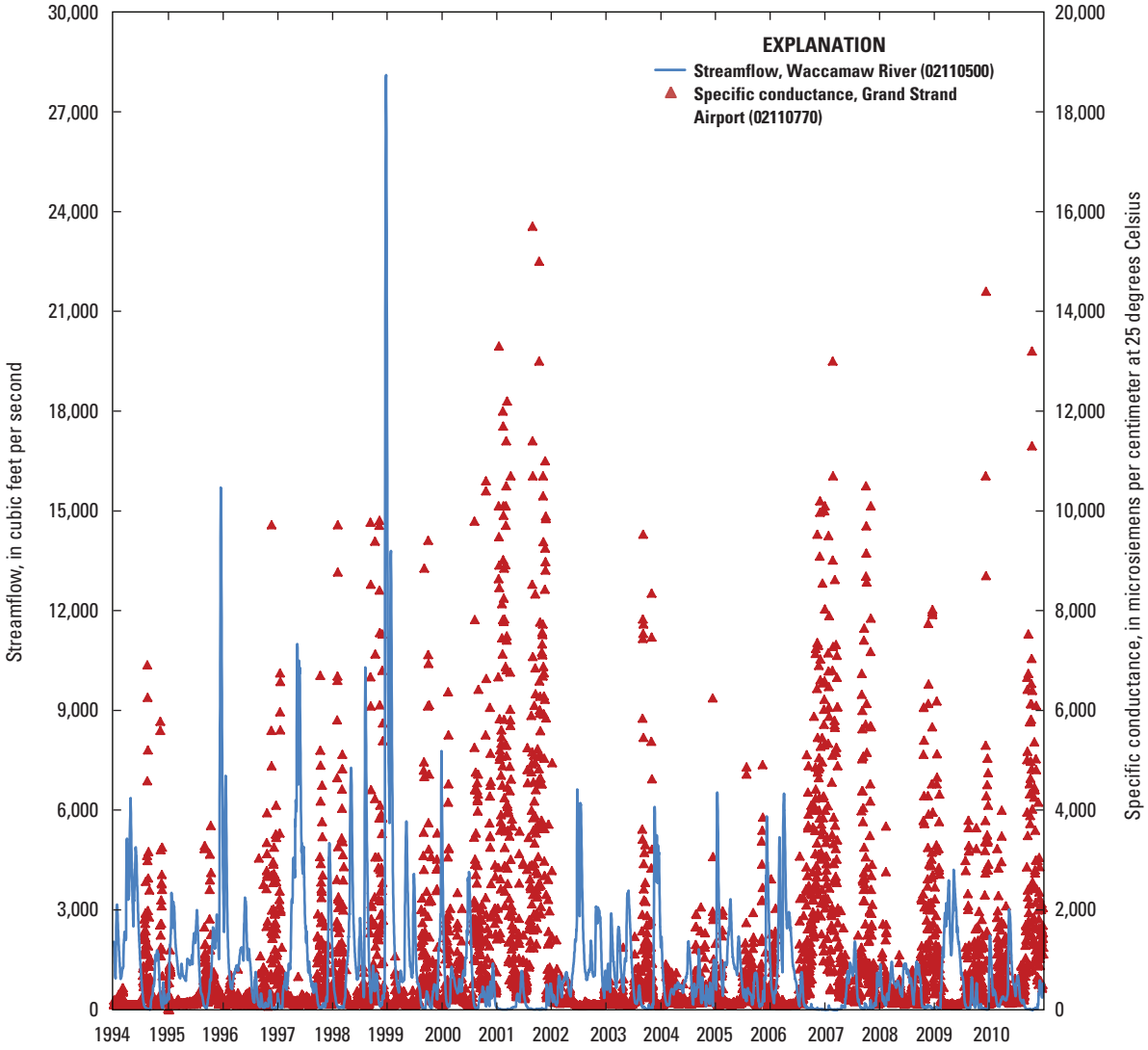

Figure 24. Daily mean specific conductance at Atlantic Intracoastal Waterway at Grand Strand Airport, South Carolina, and daily mean streamflow at Waccamaw River at Longs, South Carolina, October 1, 1994–September 30, 2010.

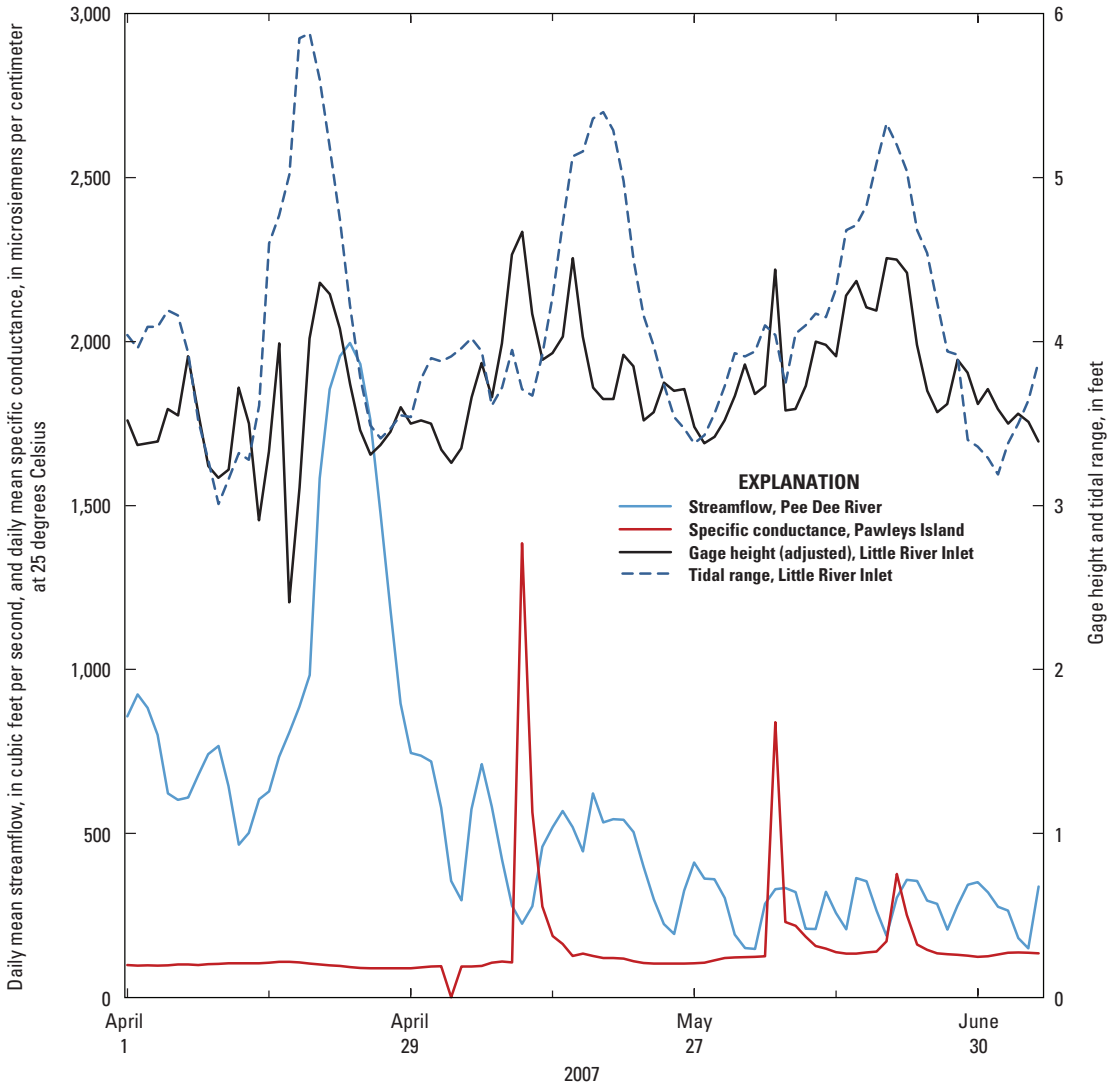

Figure 25. Daily mean specific conductance at Waccamaw River at Pawleys Island (station 021108125), daily mean streamflow at Pee Dee River (station 02131000), and daily mean gage height and daily mean tidal range at Little River Inlet (station 02110777), South Carolina, April 1, 2007–June 30, 2007. Note: For plotting purposes, the Pee Dee River streamflow was multiplied by 0.1, and 9 feet was subtracted from the Little River Inlet gage height.

At the North End of the AIW, salinity increased in response to the tidal range rather than the mean coastal water levels. A series of salinity intrusion events at the Briarcliffe Acres gage (station 02110755; fig. 2) on the AIW in July and August 2008 are shown using specific conductance in figure 26. (For plotting purposes, streamflow was multiplied by 0.1, and 9 ft was subtracted from the gage height.) Soon after the Pee Dee River and Waccamaw River streamflows dropped below approximately 3,000 and 200 ft^3/s, respectively. In early June 2008, the salinity intruded until the streamflows increased in early September 2008. The peaks of the specific conductance coincide with the spring tides, as seen in the maximum tidal range values during June to September 2007. Although there is a 14-day spring-neap tide cycle along the South Carolina coast, three of the four intrusion events shown in figure 26 occurred during the high spring tide, which occurs on a 28-day cycle. The event on June 19, 2008, not associated with the spring tide, occurred during the lowest Waccamaw River and Pee Dee River streamflows.

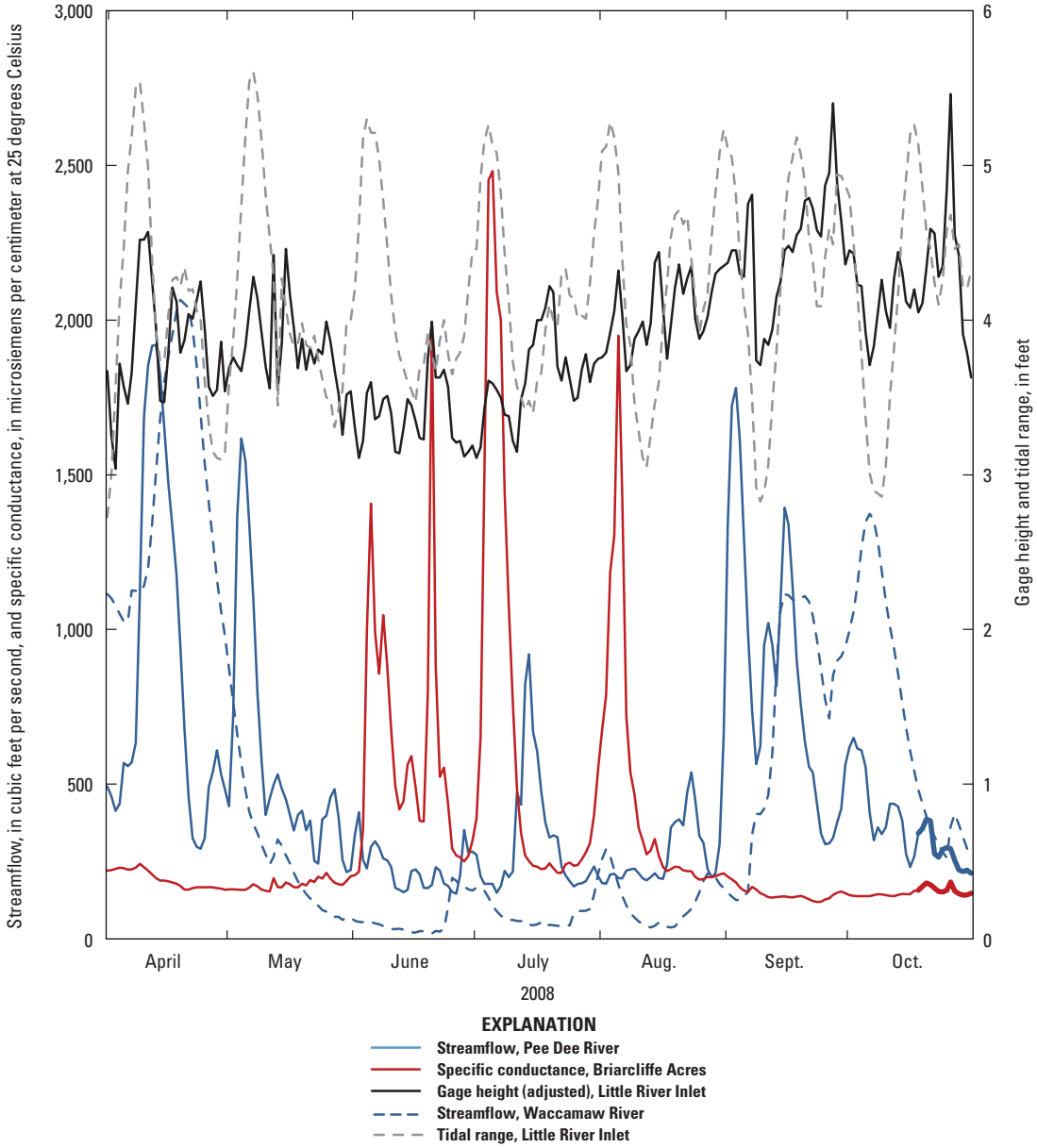

Figure 26. Daily mean specific conductance at Waccamaw River at Briarcliffe Acres (station 02110755), Pee Dee River streamflow (station 02131000), and gage height and tidal range at Little River Inlet (station 02110777), April 1, 2008–October 31, 2008. Note: For plotting purposes, Pee Dee River streamflow was multiplied by 0.1, and 9 feet was subtracted from the Little River Inlet gage height.

Lower Savannah River

Historically, daily mean streamflows at the Savannah River near Clyo, Ga., (station 02198500) ranged from about 5,000 to about 50,000 ft^3/s (U.S. Geological Survey, 2012). Streamflow at the Clyo gage and specific conductance at the Interstate 95 gage (02198840) from October 1994 to September 2010 are shown in figure 27. As with the Grand Strand in the Waccamaw River and AIW study area (figs. 23 and 24), periods of high specific conductance coincided with periods of low streamflow. During extended low-flow periods the daily maximum specific conductance commonly exceeded 1,000 µS/cm at the Savannah River Interstate 95 gage. Like the North and South Ends of the Grand Strand, there is a convergence of conditions needed for the elevated specific conductance: Savannah River streamflow must be less than 6,000 ft^3/s at the occurrence of spring tide of the new moon. The daily maximum specific conductance at the Interstate 95 gage, the daily mean streamflow for the Clyo gage, and the dates of the new moon for the summer 2009 are shown in figure 28. During the new moon, tidal ranges are greatest because the gravitational attraction between the sun and moon are aligned. The increased tidal energy under these conditions typically leads to a salinity-intrusion event. Meteorological conditions, such as tropical storms and high winds, may exacerbate salinity intrusion.

The Savannah River estuary is considered a partially stratified system. A conceptual diagram of the primary factors that affect stratification and the position of the freshwater-saltwater interface in the Savannah River are shown in figure 29. During spring tides (tides with the largest tidal range), there is increased energy in the system and more mixing of the less dense freshwater of the river with the denser saltwater of the harbor, which results in smaller variation

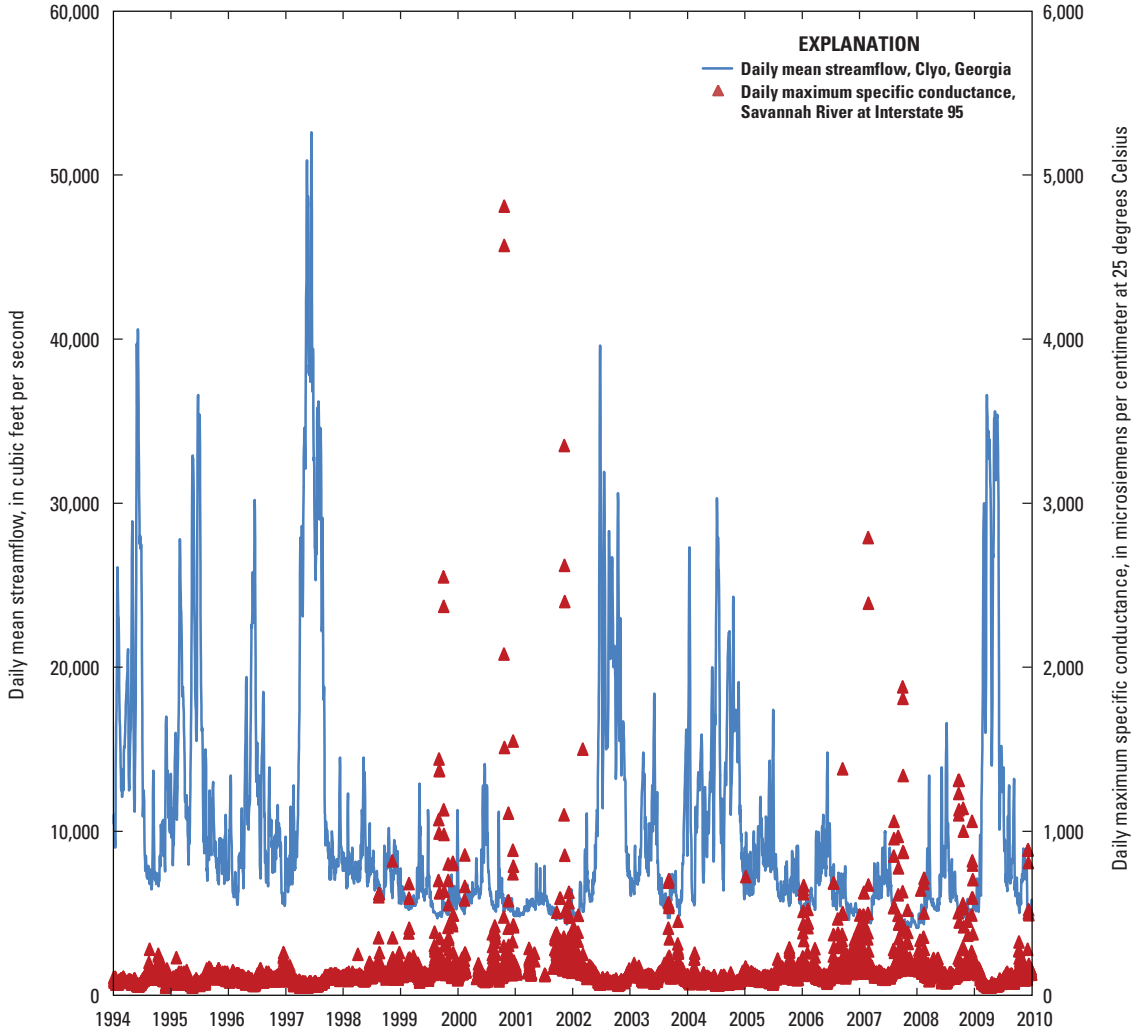

Figure 27. Maximum daily specific conductance at Savannah River near Port Wentworth, Georgia (station 02198840, I-95 Bridge), and streamflow at Savannah River near Clyo, Georgia (station 02198500), January 1, 1994–September 30, 2010.

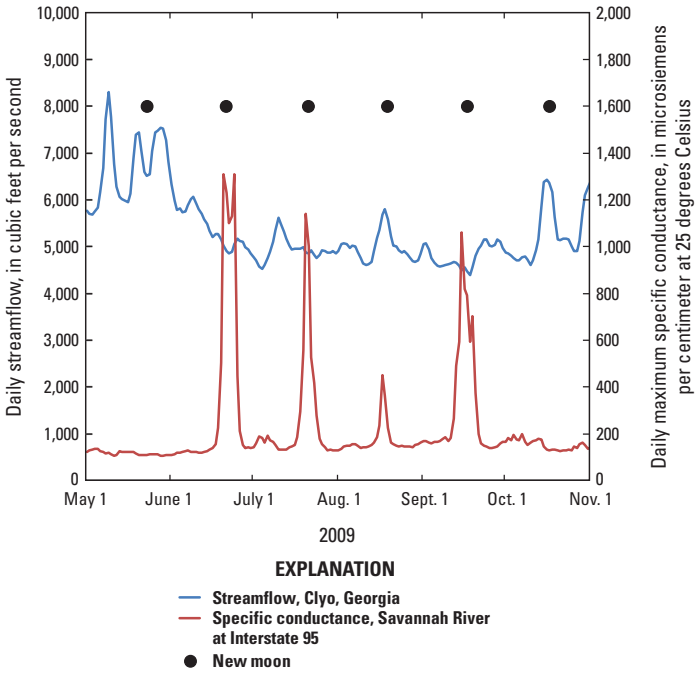

Figure 28. Daily streamflow at Savannah River near Clyo, Georgia (station 02198500), and daily specific conductance at the Savannah River near Port Wentworth, Georgia (station 02198840), I-95 Bridge, May–October 2009, including occurrences of the new moon.

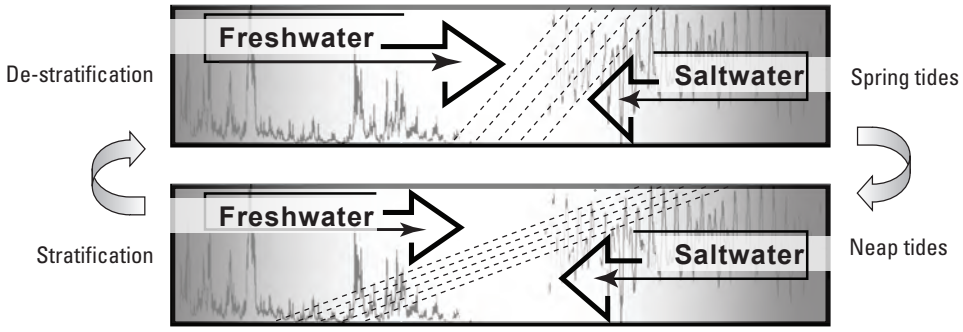

Figure 29. Conceptual model of the location of the freshwater-saltwater interface and salinity stratification–de-stratification cycle in estuarine rivers.

in vertical salinity concentrations. During neap tides (tides with the smallest tidal range), there is decreased energy in the system and less mixing between the freshwater and saltwater which allows freshwater to flow downstream over the saltwater intruding upstream. The decrease in mixing results in an increased stratification and increased salinity intrusion upstream. The stratification and de-stratification of salinity at station GPA 4 (a specific-conductance gaging station maintained by Georgia Ports Authority near the USGS station 02198977; fig. 11*A*) for 2 months during summer 1997 is shown in figure 30. During the neap tides around Julian day 225 (August 12), there is approximately a 15-psu difference in salinity between the bottom and surface of the channel. During the spring tides around Julian days 205 and 235, the system de-stratifies, and the differences between the bottom and surface salinities are only 3 to 5 psu.

Tidal marshes are constantly integrating the changing river conditions in their water levels (frequency and duration

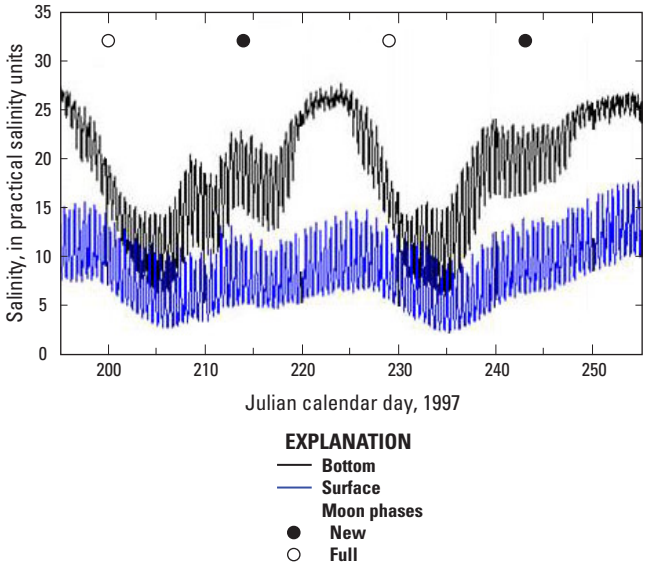

Figure 30. Hourly surface and bottom salinities for station GPA 4, Georgia, and occurrences of the moon phase, July 15–September 13, 1997 (modified from Tetra Tech, 2005). The plot shows the de-stratification of the Savannah River on about Julian days 205 and 235 and the stratification on about Julian day 225.

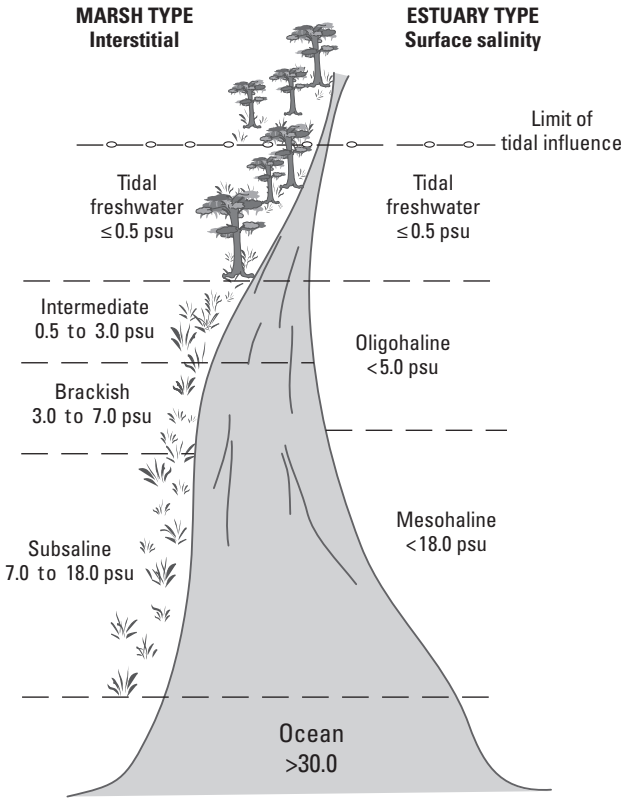

Figure 31. Tidal marsh types classified by interstitial salinity (Pearlstine and others, 1990) and average estuary surface salinities (Cowardin and others, 1979; modified from Odum and others, 1984). [<, less than; ≤, less than or equal to; psu, pratical salinity units]

of inundations), and the salinity concentration in the interstitial pore water of the root zone varies accordingly. Plant community distributions in the marshes are affected by interstitial salinities (fig. 31). The marsh sites do not exhibit the semi-diurnal variability in salinity shown by the river (fig. 32) but depend on the frequency and magnitude of the flooding of river water on the marsh. The connection between interstitial salinities of the marshes and water-column salinities occurs when riverine salinity intrusions are concurrent with the spring-tide water levels. The specific-conductance time series of the four marsh gaging stations along the Little Back and Back Rivers, and the specific conductance for the Front River at Houlihan Bridge (station 02198920), are shown in figure 32. The four marsh sites show a distinct gradient of increasing specific-conductance values from upstream (Site B1) to downstream (Site B4). Increased specific conductance in the marsh generally occurs following increased specific conductance in the river when water levels are high enough to flood the marsh. The pore-water specific-conductance time series of three marsh streamgaging stations along the Middle and Front Rivers and specific conductance for the Front River at the Houlihan Bridge water-level gage (station 02198920) are shown in figure 33.

Simulation of Specific Conductance

Models generally fall into one of two categories: mechanistic, also referred to as deterministic models, and empirical. Mechanistic models are created from first-principles equations, whereas empirical models adapt generalized mathematical functions to fit a line or surface through data from one or more variables. Simulating the specific conductance of estuarine systems typically is done using dynamic mechanistic models that incorporate the mathematical descriptions of the coastal hydrodynamics. These 1D, 2D, or 3D models often require extensive data collection and are time consuming to apply to complex coastal systems with satisfactory results. Often mechanistic model calibration for estuaries is particularly difficult because of low watershed gradients, poorly defined drainage areas, tidal complexities, and a lack of understanding of watershed and marsh processes (Conrads and Roehl, 2005). Although mechanistic models have been the state of the practice for regulatory evaluations of anthropogenic effects on estuarine systems, developments in the field of advanced statistics, machine learning, and data mining offer opportunities to develop empirical ANN models that often are more

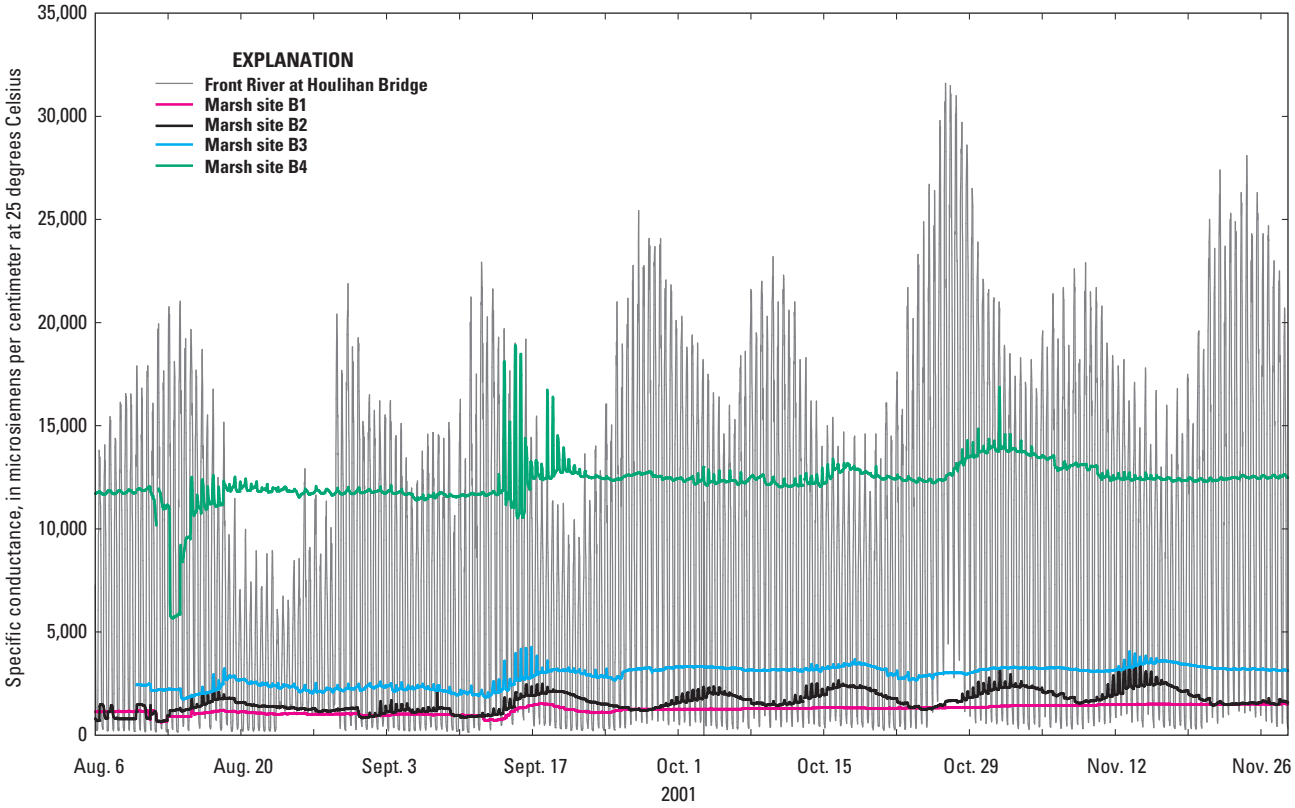

Figure 32. Hourly specific conductance at four marsh gaging stations along the Little Back and Back Rivers and hourly specific conductance at Houlihan Bridge on the Front River (02198920), Georgia, August 6–November 30, 2001.

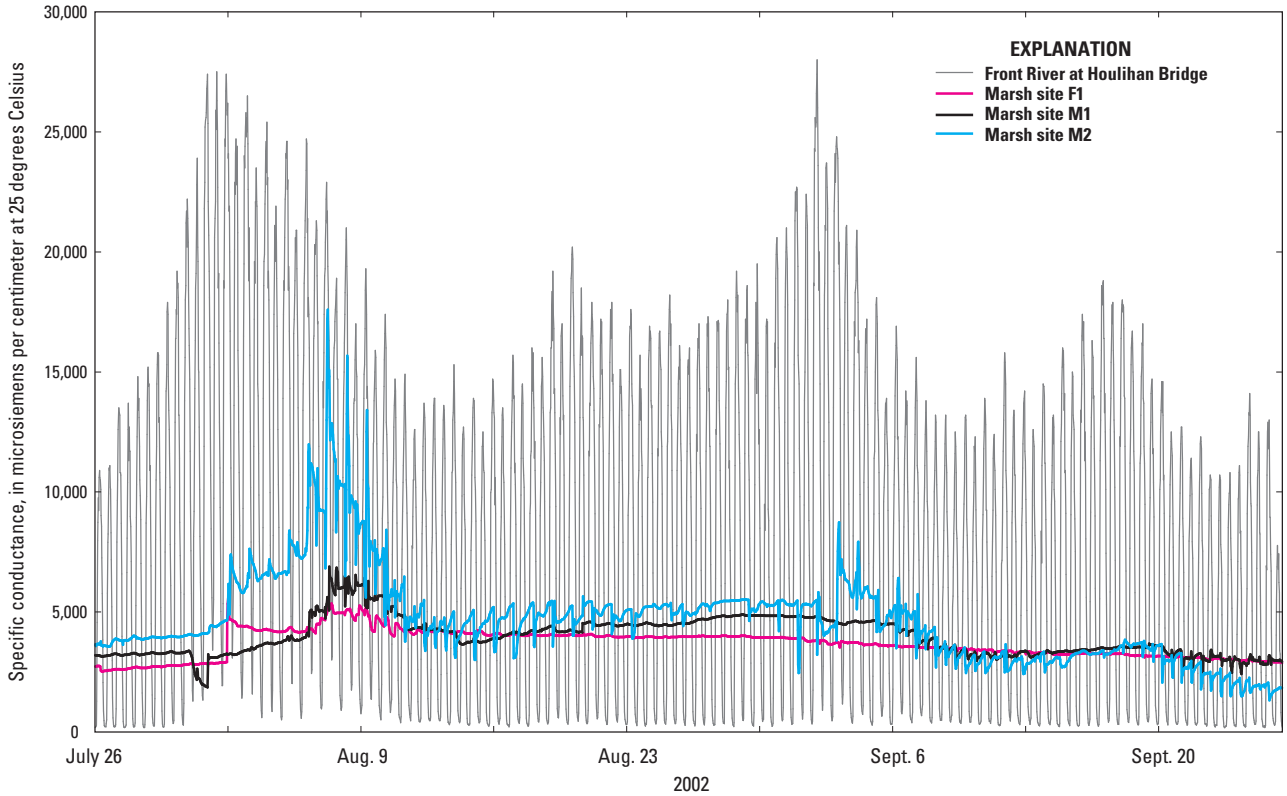

Figure 33. Hourly pore-water specific conductance for two marsh gaging stations on the Middle River, one marsh gaging station on the Front River, and one river gaging station at Houlihan Bridge on the Front River (02198920), Georgia, July 26–September 27, 2002.

accurate. Conrads and Roehl (1999) compared the application of a mechanistic model and an ANN model to simulate dissolved oxygen concentrations for the tidally affected Cooper River in South Carolina. They found that the ANN models offer some important advantages, including faster development time, utilization of larger amounts of data, the incorporation of optimization routines, and model dissemination in spreadsheet applications.

Artificial Neural Network Models

ANN models are empirical models that are developed directly from data. The most common empirical modeling approach is ordinary least squares (OLS), which relates variables using straight lines, planes, or hyper-planes, whether the actual relations are linear or not. Calibration of either type of model attempts to optimally synthesize a line or surface through the measured data. Calibration of models is difficult when data have substantial measurement error or are incomplete, or when the variables for which data are available provide only a partial explanation of the sources of variability. The principal advantages of empirical models, such as ANN models, over mechanistic models are that they can be developed faster and are more accurate provided that the modeled systems are well characterized by data. Empirical models, however, are prone to problems when poorly applied. Overfitting and multicollinearity caused by correlated input variables can lead to invalid mappings, or relations, between input and output variables (Roehl and others, 2003).

An ANN model is a flexible mathematical structure capable of describing complex nonlinear relations between input and output datasets. The structure of ANN models is loosely based on the biological nervous system with interconnections of neurons and synapses (Hinton, 1992). Although numerous types of ANN models exist, the most commonly used type of ANN model is the multi-layer perceptron (Rosenblatt, 1958), which is used in this study and described in detail by Jensen (1994). Multi-layer perceptron ANNs can synthesize functions to fit multi-dimensional, nonlinear data. Devine and Roehl (2003) and Roehl and Conrads (1999) describe the application of the multi-layer perceptron (MLP) ANN to model and control combined manmade and natural systems, including disinfection byproduct formation, industrial air emissions monitoring, and surface-water systems affected by point- and nonpoint-source pollution.

Multi-layer perceptron ANNs are constructed from layers of interconnected processing elements called neurons that execute a simple "transfer function" (fig. 34). All input layer neurons are connected to all hidden layer neurons, and all hidden layer neurons are connected to all output layer neurons. Multiple hidden layers are possible, but a single layer is sufficient for most problems.

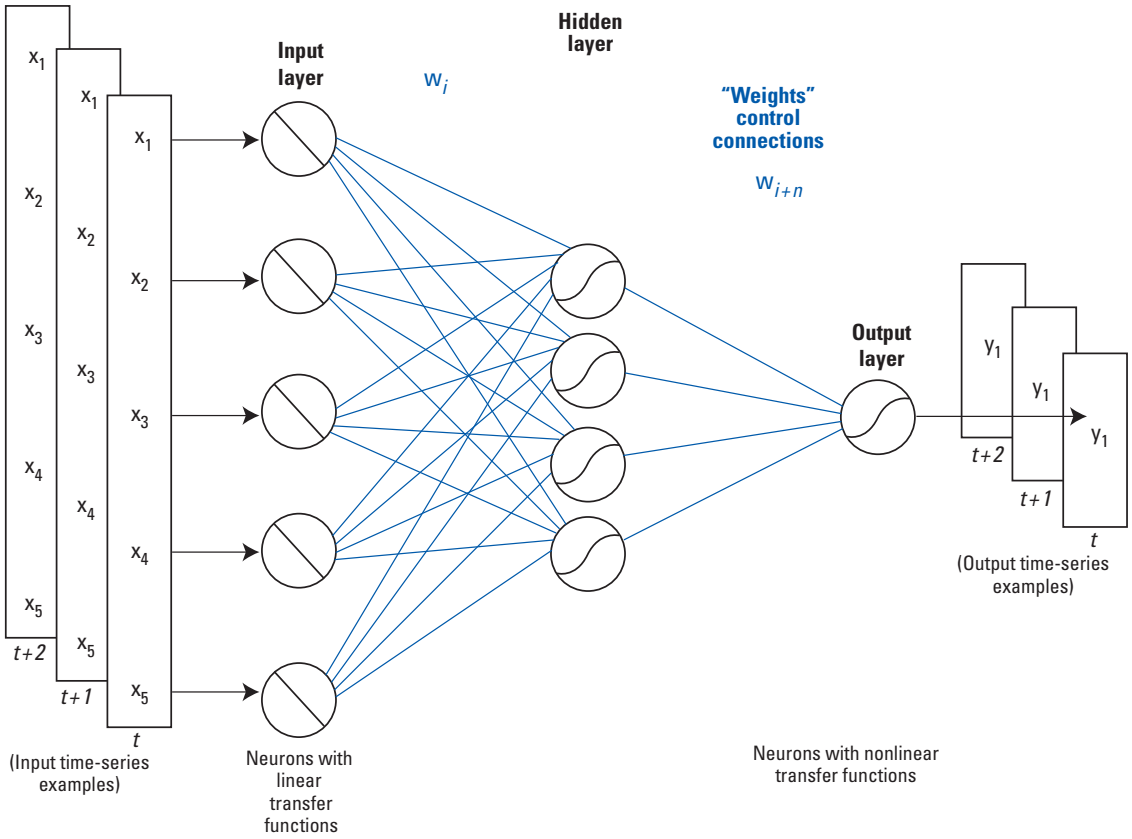

Figure 34. Multi-layer perceptron artificial neural network architecture (from Conrads and Roehl, 2007).

Typically, linear transfer functions are used to scale input values from the input layer to the hidden layer and generally fall within the range that corresponds to the most linear part of the s-shaped sigmoid transfer functions used from the hidden layer to the output layer (fig. 34). Each connection has a weight, w_i, associated with it, which scales the output received by a neuron from a neuron in an antecedent layer. The output of a neuron is a simple combination of the values it receives through its input connections and the associated weights, as well as the neuron's transfer function.

An ANN is "trained" by iteratively adjusting its weights to minimize the error by which it maps inputs to outputs for a dataset composed of input/output vector pairs. Prediction accuracy during and after training can be measured by a number of metrics, including coefficient of determination (R^2) and root mean square error (RMSE). An algorithm that is commonly used to train multi-layer perceptron ANNs is the back error propagation (BEP) training algorithm (Rumelhart and others, 1986). The algorithm optimally minimizes the error in the objective function by adjusting the weights into and out of the hidden layer of the model (fig. 34).

Experimentation with various ANN model architectural and training parameters is a typical part of the modeling process. For correlation analysis or predictive modeling applications, a number of potential ANN models are trained and evaluated for their statistical accuracy and their representation of dynamics of the system. Interactions between combinations of variables are considered, in addition to the selection of the training dataset from the overall dataset. In developing ANN models, it is customary to set aside a subset of the data to provide an independent evaluation of model performance. Typically, datasets are bifurcated into "training" and "testing" datasets. There are many strategies for partitioning data into training and test datasets, but the most common is random selection of a specified percentage of the total population of measurements.

The models were calibrated using the training dataset and evaluated with the testing dataset. For models with a large dataset with good representation over the range of historical behaviors, a small percentage of the dataset (10–25 percent) may be selected for the training dataset. For models with limited data, a larger percentage (75–100 percent) may be used in the training dataset. To mitigate the extrapolation and sparseness issues, the ANN models were conservatively trained using a method referred to as "stop training" to both fit the data and extrapolate in a minimally nonlinear and, therefore, predictable fashion. Stop training simply means stopping the training process before the ANN has fit the data to the maximum extent possible. Architectural and training parameters allow the modeler to control the geometric complexity of the surface that the ANN fits to the data. The data-mining software used for this application writes R^2 and RMSE to the graphical user interface (GUI) during training, and an inflection in the rate of change in these parameters indicates a transition from a generally linear, multivariate surface fit to a progressively nonlinear fit. This inflection point was used to trigger stop training.

In general, a high-quality predictive model can be obtained when

- the data ranges are well distributed throughout the state space of variables describing the physical system of interest,
- the input variables selected by the modeler share mutual information about the output variables, and
- the functional form "prescribed" or "synthesized" by the model to "map" (correlate) input variables to output variables is a good one. Machine-learning techniques, like ANN models, synthesize a best fit to the data. Techniques such as ordinary least squares and finite-difference models prescribe the functional form of the model's fit to the calibration data.

Subdividing a complex modeling problem into subproblems and then addressing each is an effective means of achieving the optimal results. A collection of sub-models whose calculations are coordinated by a computer program constitutes a "super-model." For the Waccamaw River-AIW and lower Savannah River studies, daily ANN models (sub-models) were developed for specific conductance at a particular gaging station. These sub-models were then incorporated into a super-model application that integrated the model controls, model database, and model outputs. The super-models for the project are the **P**ee Dee **Ri**ver and Atlantic **I**ntracoastal Waterway **S**alinity Intrusion **M**odel (Version **2**) **D**ecision **S**upport **S**ystem (PRISM-2 DSS) and the Savannah **M**odel-**to**-**M**arsh (Version **2**) **D**ecision **S**upport **S**ystem (M2M-2 DSS). The ANN models described in Conrads and others (2006), Conrads and Roehl (2007), and in this report were developed using the iQuest™ data-mining software[4] (Version 2.03C DM Rev31). The ANN models were deployed in the DSSs using the Visual Basic run-time library of the iQuest R/T™ software.

Data-Mining Techniques

Data mining extracts information from large databases using a variety of techniques from various disciplines. For estuarine systems such as the Waccamaw River and AIW, and the lower Savannah River study areas, most of the large databases consist of 15-minute time-series data of streamflows, water levels, and specific conductance values. The behavior, or dynamics, of a natural system results from interactions between multiple physical forces. For example, the specific conductance at a fixed location is subject to daily, seasonal, and annual streamflow conditions and semi-diurnal, fortnight, seasonal, and annual tidal conditions. The data-mining

[4]The iQuest™ software is exclusively distributed by Advanced Data Mining, LLC, 3620 Pelham Road, PMB 351, Greenville, SC 29615–5044, Phone (864) 201–8679, email *info@advdatamining.com*, *http://www.advdmi.com*.

exercise characterizes the principal physical forces by extracting their response from time-series data.

Signals, or time-series data, manifest three types of behavior: periodic, noise, or chaotic. Periodic behavior is perfectly predictable. Examples of periodic behavior are the diurnal sunlight and temperature patterns caused by the rising and setting sun or tidal water levels resulting from orbital mechanics. Noise refers to random components, usually attributed to measurement error, and is unpredictable. Chaotic behavior is neither totally periodic nor noise and always has a physical cause. Weather provides an example of chaotic behavior. Chaotic behavior is somewhat predictable, especially for small time frames and prediction horizons.

For the application of the ANN models to coastal rivers in South Carolina and Georgia, data-mining techniques were applied to maximize the information content in time-series data while diminishing the influence of poor or missing measurements. Methods used to develop the salinity models, including signal decomposition, spectral analysis, state-space reconstruction, signal decorrelation, and correlation and sensitivity analysis are described below.

Signal Decomposition

Signal decomposition involves splitting a signal into subsignals called components that are independently attributable to different physical forces. To analyze and model these time series, the periodic and chaotic components of the signals need to be separated. Signal decomposition can be accomplished through various techniques, such as digital filtering and the use of time derivatives, and time delays. As previously discussed, digital filtering techniques can be used to remove or isolate the chaotic component in the tidal water-level, or gage height, time series. Digital filtering also can diminish the effect of noise in a signal to improve the amount of useful information that it contains. Computation of the tidal range time series from the water-level time series isolates the periodic components of the water-level time series. An example of 61 days of hourly gage-height data and filtered gage-height data for the Little River Inlet is shown in figure 35. The filtered gage heights represent the chaotic component of the tidal gage-height signal.

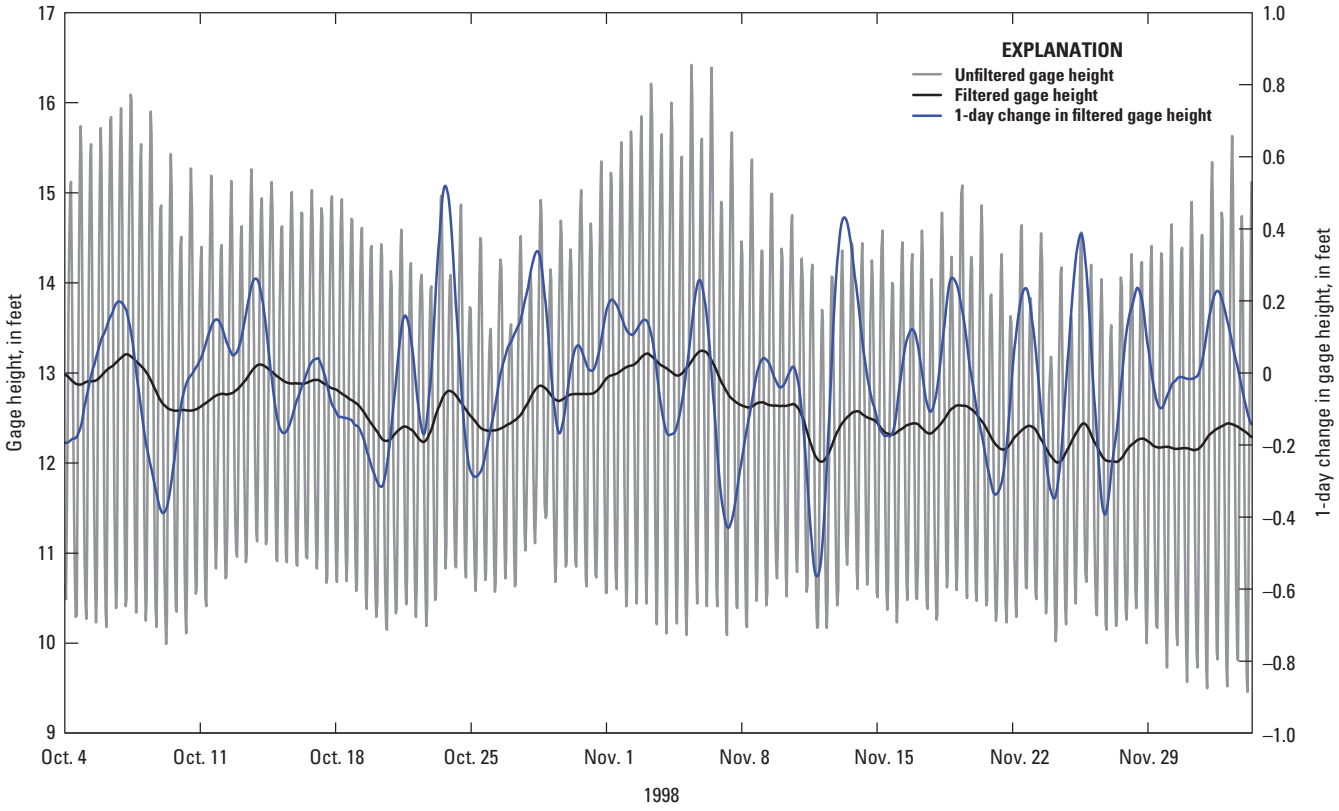

Figure 35. Hourly gage heights at Atlantic Intracoastal Waterway at South Carolina, Highway 9 (Little River Inlet station 02110777), filtered gage heights for tidal influence, and 1-day change in filtered gage heights for the 60-day period October 4–December 4, 1998.

The use of time derivatives is a common analytical method for analysis of the dynamics of a system. Time derivatives (the change in a parameter or a period of time) were computed from the measured, computed, and filtered variables for the Waccamaw River and AIW, and lower Savannah River, study areas to further understand the dynamics of the system. The 1-day change of the filtered water-level time series for a 60-day period was plotted with the original time series and the filtered data (fig. 35). The 1-day derivatives show the rate of change of the chaotic component of the water-level time series. For the 60-day period, the daily change in filtered gage height ranged from –0.5 ft to 0.5 ft.

Often time delays, or lags, occur between when an event is measured and the time that the response is observed in a system. Modeling a system is more complicated when two events of interest, a cause and an effect, do not occur simultaneously. For example, it takes approximately 2 day for the measured streamflow at the Clyo, Ga., gage on the Savannah River (station 02198500) to have an effect on downstream specific conductance at the Interstate 95 gage on the Savannah River (station 02198840). The time between cause and effect is called the time delay or lags. Each input variable of a model has its own delay. Determining the correct time delays for pulses and system response is critical to accurately simulate a dynamic system. For the Waccamaw River and the AIW, there are time delays between the measured streamflow at the Pee Dee River at Pee Dee, S.C., (station 02131000) and the response in specific conductance at the gaging stations in the Waccamaw River and the AIW. Time delays also occur among measured streamflow values for the four tributaries to the Pee Dee River. Time delays from the point when the streamflow enters the system to the point when the river responds to the streamflow were determined for each gage.

Spectral Analysis

A signal decomposition technique that was effectively used for the models in the Waccamaw River and AIW study area is spectral component analysis. Spectral analysis provides a means of splitting a raw signal, in this case a set of monitoring data, into different frequency components that represent various lengths of time from daily to annual. These signals are then used as potential inputs to the ANN models. Signals representing different spectral frequencies were computed by generating various sizes of moving-window averages to capture temporal variability in the signal, such as daily, weekly, monthly, seasonal, intra-annual, and annual averages. The differences between a moving-window average and the next larger window-sized moving-window average are also calculated, and the resulting signal is a spectral component of the original signal for that particular averaging interval. This approach is analogous to band-pass spectral filtering in that it decomposes a raw signal into different spectral components. This approach also systematically decorrelates each spectral component signal. For example, the total inflow to the AIW and Waccamaw River was computed, and moving-window averages for 3-, 7-, 14, 30, and 60-day periods were computed. The difference between subsequent moving-window averages, such as 3-day and 7-day, were computed. No differences are computed for the largest moving-window average. The 14-day and 30-day moving-window averages of total inflow and the difference between the 14-day and 30-day moving-window averages for 1995 to 2009 are shown in figure 36.

State-Space Reconstruction

Chaos Theory provides a conceptual framework referred to as "state space reconstruction" (SSR) for representing dynamic relations (Abarbanel, 1996). Data collected at a point in time can be organized as a vector of measurements; for example, element one of the vector might be the water level, element two the streamflow, and so on. Engineers will say that a process evolves from one state to another in time, and that a vector of measurements, also referred to as a "state vector," represents the process state at the moment the measurements were made. A sequence of state vectors represents a state history. Mathematicians will say that the state vector is a point in a "state space" having a number of dimensions equal to the number of elements in the vector. For example, eight vector elements equate to eight dimensions. Empirical modeling is the fitting of a multidimensional surface to the points arrayed in state space.

Chaos Theory proposes that a process can be optimally represented (reconstructed) by a collection of state vectors, Y(t), using an optimal number of measurements x, equal to local dimension, d_L, that are spaced in time, t, by integer multiples of an optimal time delay, τ_d (Abarbanel, 1996)[5] For a multivariate process of k independent variables, Y(t) is expressed as

$$Y(t) = \{[x_1(t), x_1(t-\tau_{d1}),\ldots, x_1(t-(d_{L1}-1)\tau_{d1})],\ldots, [x_k(t), x_k(t-\tau_{dk}),\ldots, x_k(t-(d_{Lk}-1)\tau_{dk})]\}\ , \quad (1)$$

where each $x(t,\tau_{di})$ represents a different dimension in state space and, therefore, a different element in a state vector. Values of d_{L1} and τ_{d1} are estimated analytically or experimentally from the data. The mathematical formulations for models are derived from those for state vectors. A dependent variable of interest, y(t), can be predicted from prior measurements (also known as forecasting) of k independent variables (Roehl and Conrads, 2006) and expressed as

$$y(t) = F\{[x_1(t-\tau_{p1}), x_1(t-\tau_{p1}-\tau_{d1}),\ldots, x_1(t-\tau_{p1}-(d_{M1}-1)\tau_{d1})],\ldots, [x_k(t-\tau_{pk}), x_k(t-\tau_{pk}-\tau_{dk}),\ldots, x_k(t-\tau_{pk}-(d_{Mk}-1)\tau_{dk})]\}\ , \quad (2)$$

where F is an empirical function, such as an ANN, each $x(t,\tau_{pi},\tau_{di})$ is a different input to F, and τ_{pi} is yet another time delay. For each variable, τ_{pi} is constrained to the time delay at which an input variable becomes uncorrelated to all other

[5]In Chaos Theory, d_L and τ_d are called dynamical invariants, and are analogous to the amplitude, frequency, and phase angle of periodic time series.

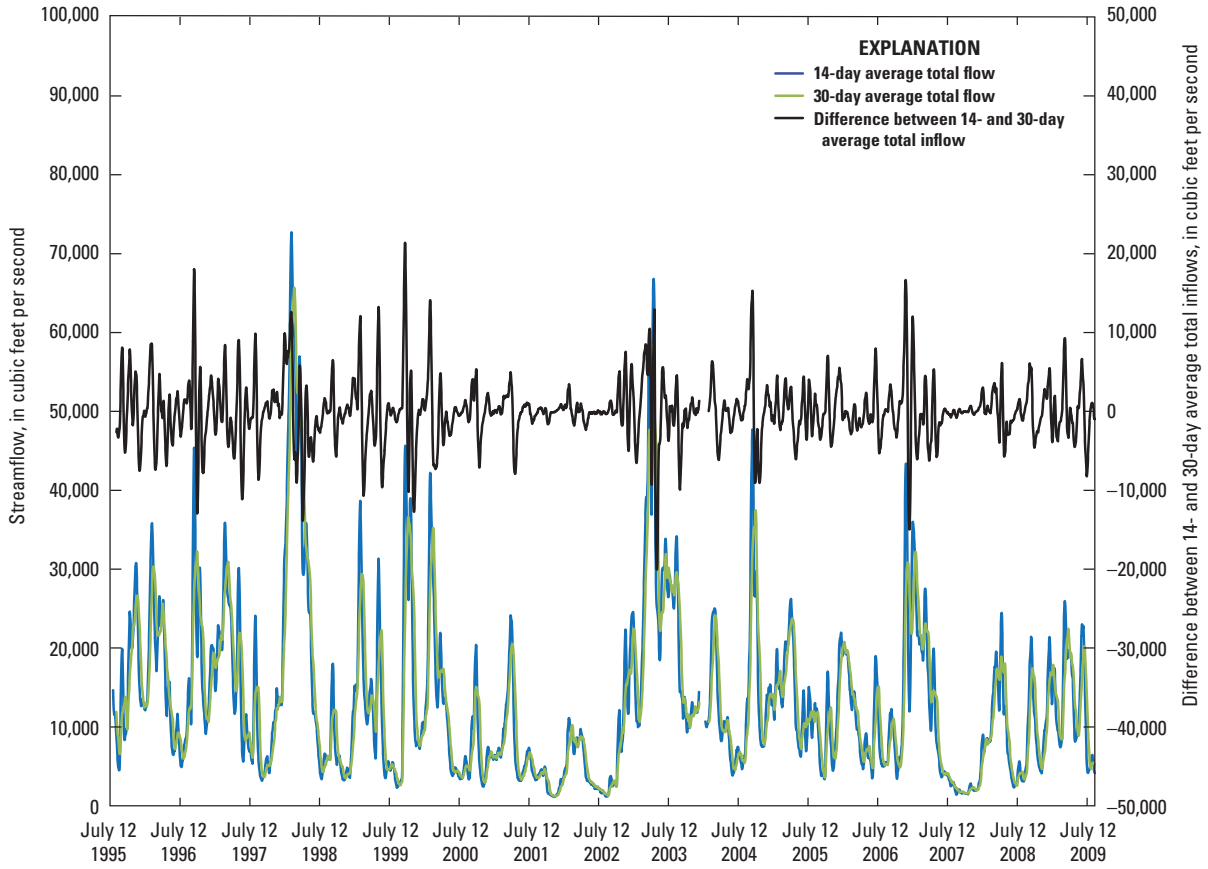

Figure 36. Fourteen-day and 30-day moving-window averages of total inflow to the Waccamaw River and Atlantic Intracoastal Waterway study area, South Carolina, and the difference between the 14-day and 30-day moving-window averages, 1995–2009. Total flow is the sum of the flow from the Pee Dee (station 02131000), Lynches (station 02132000), Little Pee Dee (station 02135000), Black (station 02136000), and Waccamaw Rivers (station 02110500).

inputs but can still provide useful information about y(t), or is constrained to the time delay of the most recent available measurement of x_i, or is constrained to the time delay at which an input variable is most highly correlated to y(t). In equation 2, the state space local dimension d_{Lk} of equation 1 is replaced with an empirically determined model input variable dimension d_{Mk}, less than or equal to d_{Lk}. The empirically derived input variable dimension parameter d_{Mk} tends to decrease with an increasing number of independent variables.

Signal Decorrelation

Explanatory variables typically have a strong relation to the behavior of a response variable. When using multiple explanatory variables, it is difficult, if not impossible, to understand the individual effects of variables (sometimes referred to as "confounded or correlated variables") on a response variable. Empirical models, such as the ANNs of this study, are not based on physical processes that govern the nature of interrelations between input variables. To be able to clearly analyze the effects of confounded variables, the unique informational content of each variable must be determined by decorrelating the confounded variables. For example, although the water-level signal at Little River Inlet (station 02110777; figs. 2, 35, and 37) is dominated by the tidal signal, it also responds to the total inflow signal (computed streamflow to the AIW and Waccamaw River). Although the coefficient of determination between the water level and streamflow signal is relatively low, 0.082, it is important to be able to determine the effect of total streamflow on water levels. During high-flow periods, such as spring of 1998 and 2003, the higher streamflow contributes to an increase in the minimum water levels in the Little River Inlet (fig. 37).

The water-level signal at Little River Inlet was decorrelated from the total inflow by using a Single Input Single Output (SISO) ANN model; the total inflow signal, as

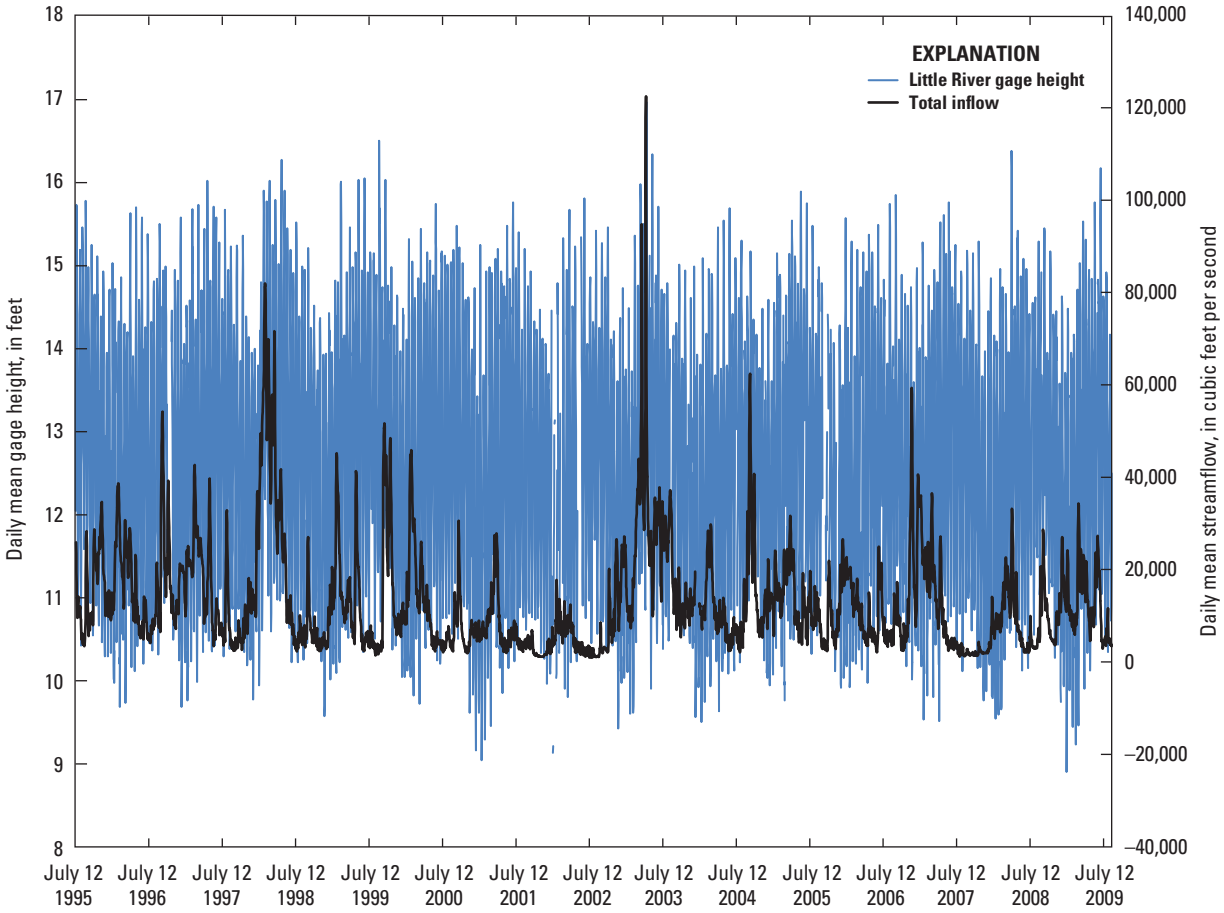

Figure 37. Daily mean gage height at Little River Inlet (station 02110777) and daily mean total inflow to the Waccamaw River and Atlantic Intracoastal Waterway study area, South Carolina, 1995–2009. Total inflow is the sum of the flow from the Pee Dee (station 02131000), Lynches (station 02132000), Little Pee Dee (station 02135000), Black (station 02136000), and Waccamaw Rivers (station 02110500).

described above, was the input variable, and the water level at the Little River Inlet gage was the output variable (fig. 38). The residual error (the difference between predicted and measured values) is the unshared information between the two signals and is the decorrelated signal for water levels at Little River Inlet. Figure 39 shows the measured and predicted water levels, as well as the residual error, from the decorrelation model. The SISO model simulated the low-frequency portion of the measured time series well but did not capture the higher frequencies as seen in the spikes in the measured time series. The SISO model did simulate the effect of the high-flow events on 1998 and 2003 gage heights.

Correlation and Sensitivity Analysis

The relations between the many variables and their decomposed components are ascertained through correlation analyses to provide an additional understanding of system dynamics. Sensitivity analysis quantifies the relations between a dependent variable of interest and causal variables. For example, salinity intrusion is dependent on streamflow and tides. Computing sensitivities requires defining the relations among variables through modeling. The ANN computer program systematically correlates factors that most affect parameters of interest (for example, specific conductance) to determine combinations of controlled and uncontrolled variables (for example, regulated streamflow and tidal conditions).

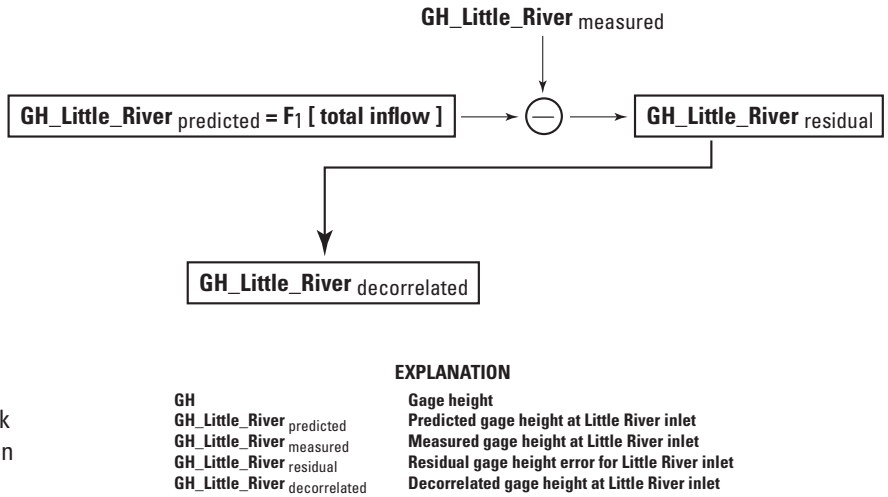

Figure 38. Schematic diagram showing the gage height decorrelation model. F1 is a Single Input Single Output Artificial Neural Network model (SISO ANN). The residual error from the SISO ANN is computed by subtracting the GH_Little_River predicted values from the measured values. (Total inflow is the sum of the flow from the Pee Dee (station 02131000), Lynches (station 02132000), Little Pee Dee (station 02135000), Black (station 02136000), and Waccamaw Rivers (station 02110500)).

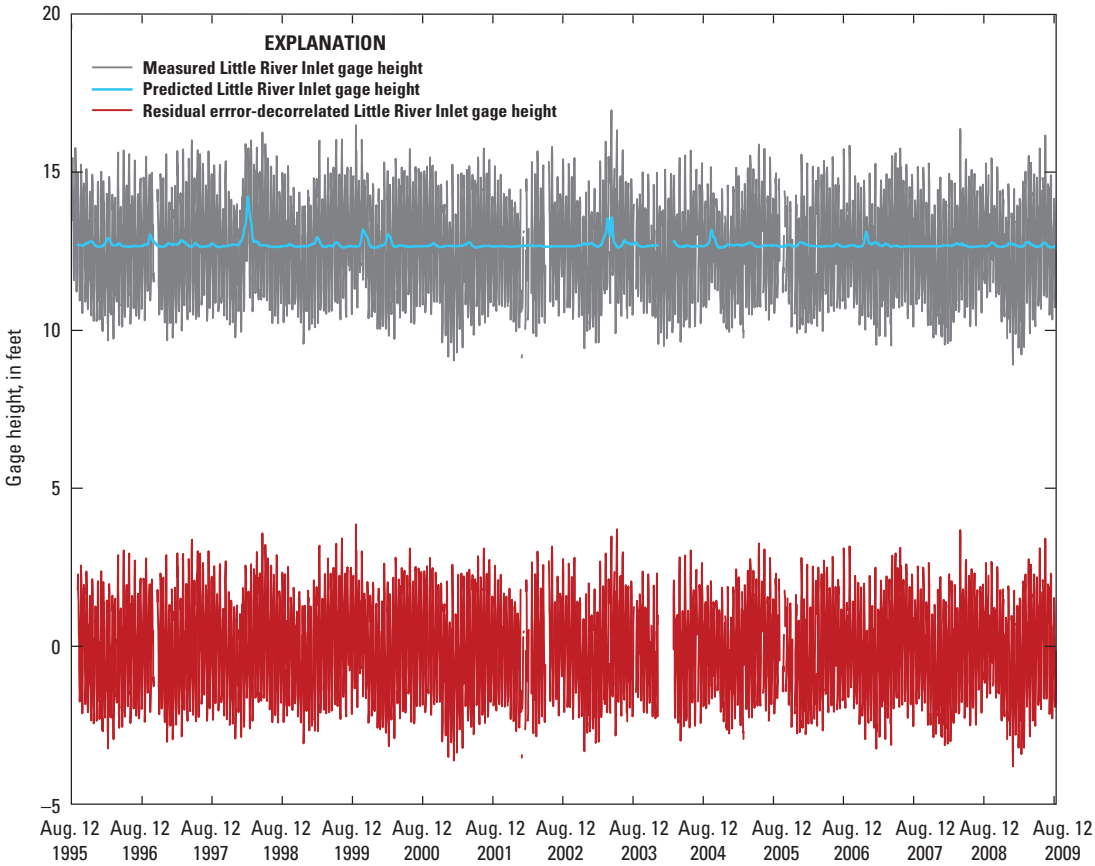

Figure 39. Measured, predicted, and residual error from the Single Input Single Output Artificial Neural Network model used to decorrelate gage height at Little River Inlet (station 02110777) from the total flow to the Waccamaw River and Atlantic Intracoastal Waterway study area, South Carolina, August 12, 1995–August 12, 2009. The decorrelated gage height is the residual error time series. The gap in predicted Little River Inlet gage height is due to missing total inflow data.

Limitations of the Historical Datasets

As with any modeling effort, empirical or deterministic, the reliability of the model is dependent on the quality of the data and range of measured conditions used for training or calibrating the model. For accurate simulations, data must encompass the full range of streamflow, water-level, tide-range, and salinity conditions that the ANN model is based on. As noted previously, substantial changes in the salinity response of the system can occur as a result of a small change in streamflow (figs. 23, 24, and 27). Although data are available for the coastal network from the early 1980s, the data were not always of a sufficient quality for use in developing empirical models. Environmental monitoring technology has changed substantially over the past 20 years (1990–2010). One of the most important changes for monitoring in estuarine systems has been improvement in the timers (or clocks) in the recording equipment. For monitoring estuarine environments, it is essential that the correct time of the passing of the tidal wave, and associated physical properties, is recorded. Timing errors are analogous to physically moving the gage upstream or downstream. The timer used for paper-punch recorders in the 1980s and early 1990s often drifted from the true time. The USGS South Carolina Water Science Center started using satellite telemetry in the mid-1980s and instrumented all gaging stations in the coastal network of the Waccamaw River and AIW study area in the mid-1990s. The clocks associated with satellite telemetry are much more accurate than the recorders, and the gage has a limited window (less than 15 seconds) to transmit the recorded data to a satellite. As a result, timing errors are nearly eliminated from the real-time data.

The timing errors of the early data often are not apparent upon inspection of a time series. Prediction errors (differences between measured and simulated values) of preliminary specific- conductance models show larger errors when using the data collected prior to 1995 than when using the data collected after 1995. Because of these timing errors, it was decided that only data collected after 1995 would be used for the development of the ANN models to minimize errors resulting from various instrumentation. In Savannah, the removal of the tide gate in 1991 (fig. 11) and the deepening of the harbor in 1994 from 38 ft to 42 ft had a large effect on the salinity dynamics of the system. As a result, only data collected after the deepening were used to develop the specific-conductance models for the lower Savannah River study area. The datasets for the Waccamaw River and AIW, and the lower Savannah River, study areas cover a large range in hydrologic conditions, including high-flow conditions from the El Niño of 1998, extended droughts, and many hurricanes and tropical storms.

Development and Evaluation of Specific-Conductance Models

The following sections describe the development and evaluation of the specific-conductance (SC) models for selected gaging stations in the Waccamaw River and AIW, and lower Savannah River, study areas. For this study, the models for the PRISM-2 DSS were retrained with additional data collected since their original development; a description and documentation of the retrained PRISM-2 ANN models of the Waccamaw River and AIW study area are presented below. A summary of the PRISM-2 ANN models input and output variables, a description of the variables used in the models, and model performance statistics are listed in tables 7, 8, and 9, respectively. The models for the M2M-2 DSS were not retrained; a detailed description and documentation of those models can be found in Conrads and others (2006). A brief discussion of the models is presented below, and a summary of the M2M-2 ANN models input and output variables, a description of the variables used in the models, and model performance statistics are listed in Appendixes 1, 2, and 3, respectively.

The specific-conductance models for both study areas were developed in two stages. The first stage simulates the daily average specific conductance to capture the long-term dynamics of the system. The second stage simulates the higher frequency hourly specific conductance, using the predicted daily specific conductance as input to the model as a carrier signal. The predicted specific conductance output from the first stage model cascades into the second stage model as a daily specific conductance input. The ANN model architecture for each gage with the use of model predictions from the daily model to the hourly model is shown in figure 40.

Table 7. Summary of model input and output variables used in the Pee Dee River and Atlantic Intracoastal Waterway Salinity Intrusion Model Decision Support System-Version 2 (PRISM-2 DSS).

Model	Input variable	Output variable
	North End	
sc755_cc_f25-final	WL777_RANN_F25, WL777_RANN_D12H, WL777_RANN_F25_D1D, WL777_RANN_F25_D3D, XWL777_RANN_F25, XWL777_RANN_F25_D1D, QTOTAL_A14D, QTOTAL_D7D, QTOTAL_D14D	P_SC755_CC_F25
sc760_cc_f25-final	QTOTAL_A30D, QTOTAL_D7D, QTOTAL_D14D, WL777_RANN_F25, WL777_RANN_D6H, WL777_RANN_D12H, WL777_RANN_F25_D1D, WL777_RANN_F25_D3D, WL777_RANN_F25_D7D	P_SC760_CC_F25
sc770_cc_f25-final	QTOTAL_A7D, QTOTAL_D7D, QTOTAL_D14D, WL777_RANN_F25, WL777_RANN_F25_D1D, WL777_RANN_F25_D3D, XWL777_RANN_F25, XWL777_RANN_F25_D1D	P_SC770_CC_F25
sc777_cc_f25-final	QTOTAL_A7D, QTOTAL_D1D, WL777_RANN_F25, XWL777_RANN_F25, WL777_RANN_F25_D1D, WL777_RANN_F25_D3D, XWL777_RANN_F25_D1D	P_SC777_CC_F25
sc755_cc-final	WL777_RANN_F25_A3D, WL777_RANN_D3H, WL777_RANN_D6H, WL777_RANN_D12H, XWL777_RANN_A12H, P_SC755_CC_F25	P_SC755_CC
sc760_cc-final	WL777_RANN_F25_A3D, WL777_RANN_D3H, WL777_RANN_D6H, WL777_RANN_D12H, WL777_RANN_F25_D1D, XWL777_RANN_A12H, P_SC760_CC_F25	P_SC760_CC
sc770_cc-final	WL777_RANN_D6H, WL777_RANN_D12H, WL777_RANN_F25_D1D, XWL777_RANN_A12H, P_SC770_CC_F25	P_SC770_CC
sc777_cc-final	P_SC777_CC_F25, WL777_RANN_A12H, WL777_RANN_D3H, WL777_RANN_D6H, WL777_RANN_D12H, XWL777_RANN_D12H	P_SC777_CC
	South End	
sc809_cc_f25-final	QTOTAL_A7D, QTOTAL_D1D, WL777_RANN_F25, XWL777_RANN_F25, WL777_RANN_D12H, XWL777_RANN_D6H	P_SC809_CC_F25
sc8125_cc_f25-final	QTOTAL_A7D, WL777_RANN_F25, XWL777_RANN_F25_D1D, WL777_RANN_D12H, XWL777_RANN_D6H, SINE-W0_ID12H, COS-W0_IA7D	P_SC8125_CC_F25
sc815_cc_f25-final	QTOTAL_A7D, QTOTAL_D1D, WL777_RANN_F25, WL777_RANN_D12H, SINE-W0_ID12H, COS-W0_IA7D	P_SC815_CC_F25
sc809_cc-final	P_SC809_CC_F25, WL777_RANN_F25, WL777_RANN_D3H, WL777_RANN_D6H, WL777_RANN_D12H, XWL777_RANN_A12H, XWL777_RANN_D6H	P_SC809_CC
sc8125_cc-final	WL777_RANN_F25, WL777_RANN_D3H, WL777_RANN_D6H, WL777_RANN_D12H, P_SC8125_CC_F25	P_SC8125_CC
sc815_cc-final	WL777_RANN_F25, WL777_RANN_D3H, WL777_RANN_D6H, WL777_RANN_D12H, P_SC815_CC_F25	P_SC815_CC

Table 8. Description of variables used in the Pee Dee River and Atlantic Intracoastal Waterway Salinity Intrusion Model Decision Support System-Version 2 (PRISM-2 DSS) artificial neural network models.

[I, interpolated; Q, streamflow; D, daily; m, measured; F, filled; WL, water level; H, hourly; XWL, tidal range; SC, specific conductance; MWA, moving window average; hr, hour; A24, 24-hour MWA; F25, daily tidally filtered; ANN, artificial neural network model; RANN, residual from ANN; P, predicted]

Variable	Input or output variable	Description
COS-W0_IA7D	Output	Cosine of DIR-W0_IA7D
DIRD	Input	24-hour moving window average wind direction, degrees
DIRH	Input	Hourly wind direction, degree
DIR-W0_I	Output	Wind direction interpolated up to 6 hours to fill missing values, with random values used when wind speed = 0, degrees
DIR-W0_IA12H	Output	12-hr MWA of DIR-W0_I
DIR-W0_IAXD	Output	XX-day MWA of DIR-W0_I
dSCXXXXD(pu-pm)	Input	Difference in SCXXXXDp(u), predicted SC for user specified input, SCXXXXDpm, and predicted SC for measured conditions, SCXXXXDpu, microsiemens per centimeter.
dSCXXXXH(pu-pm)	Input	SCXXXXHp(u) - SCXXXXHpm
FWL777Dm	Input	Filled measured daily water level at gage 02110777, feet
FWL777Hm	Input	Filled measured hourly water level at gage 02110777, feet
IFXWL777Dm	Input	24-hour moving window averaged IFXWL777Hm, feet
IFXWL777Hm	Input	Interpolated filled measured hourly 12.4-hour water level maximum range at gage 02110777, feet
InpOptionXXXX	Input	QxxxxxDu input option for gage XXXX set on Setpoints worksheet. Abreviation XXXX is the unique four-digits for inflow stations.
IQ10500Dm	Input	Interpolated measured daily average Q5000, cubic feet per second
IQ13200Dm	Input	Interpolated measured daily average Q132000, cubic feet per second
IQ13500Dm	Input	Interpolated measured daily average Q135000, cubic feet per second
IQ13600Dm	Input	Interpolated measured daily average Q136000, cubic feet per second
P_SCXXXX_CC_F25	Output	Predicted SCXXXX_CC_F25 by ANN model
P_SCXXXX_F25	Output	Predicted SCXXXX_CC by ANN model
Q10500_A24	Output	24-hr MWA of flow at USGS gage 02110500, cubic feet per second
Q13100_A24	Output	24-hr MWA of flow at USGS gage 02131000, cubic feet per second
Q13100Dm	Input	Interpolated measured daily average Q131000, cubic feet per second
Q13200_A24	Output	24-hr MWA of flow at USGS gage 02132000, cubic feet per second
Q13500_A24	Output	24-hr MWA of flow at USGS gage 02135000, cubic feet per second
Q13600_A24	Output	24-hr MWA of flow at USGS gage 02136000, cubic feet per second
QOTHER_A1D	Output	Sum of measured inflows other than Q13100_A24, = Q10500_A24 + Q13200_A24(t=-48hrs) + Q13500_A24 + Q13600_A24(t=-24hrs).
QOTHER_AXXD	Output	XX-day MWA of QOTHER_A1D. In PRISM XX = 1, 7, 14, 30
QOTHER_DXXD	Output	QOTHER_AXXD - QOTHER_AYYD, where XX and YY indicate successive MWAs, e.g., QOTHER_D14D = QOTHER_A14D - QOTHER_A30D
QotherDm	Input	Sum of measured inflows other than Q13100D: Q5000D + Q13200 (time=-48hrs) + Q13500 + Q13600 (time=-24hrs), cubic feet per second
QTOTAL_A1D	Output	QOTHER_A1D + Q13100_A24(t=-24hrs)
QTOTAL_AXXD	Output	XX-day MWA of QTOTAL_A1D. In PRISM XX = 1, 7, 14, 30
QTOTAL_DXXD	Output	QTOTAL_AXXD - QTOTAL_AYYD, where XX and YY indicate successive MWAs, e.g., QTOTAL_D14D = QTOTAL_A14D - QTOTAL_A30D
QtotalDm	Input	Q13100Dm (time=24hrs) + QotherDm, cubic feet per second
SCXXXX_CC	Output	Hourly specific conductance at indicated gage. The "_CC" denotes that the raw siganl was corrected for errors

Table 8. Description of variables used in the Pee Dee River and Atlantic Intracoastal Waterway Salinity Intrusion Model Decision Support System-Version 2 (PRISM-2 DSS) artificial neural network models.—Continued

[I, interpolated; Q, streamflow; D, daily; m, measured; F, filled; WL, water level; H, hourly; XWL, tidal range; SC, specific conductance; MWA, moving window average; hr, hour; A24, 24-hour MWA; F25, daily tidally filtered; ANN, artificial neural network model; RANN, residual from ANN; P, predicted]

Variable	Input or output variable	Description
SCXXXX_CC_F25	Output	SCXXXX_CC filtered to remove diurnal and semi-diurnal variability. Filtering results from applying a 13-hr and a 25-hr MWA to WL777_RANN in sucession.
SCXXXXDm	Input	Daily measured specific conductance (SC) for gage XXXX, microsiemens per centimeter. "CC" indicated corrected time series. Abreviation XXXX is the unique four-digits for SC stations.
SCXXXXDm/p+dSC	Input	SCXXXXDm + dSCXXXXD(pu-pm) if SCXXXXDm is not missing, else = SCXXXXDpm + dSCXXXXD(pu-pm)
SCXXXXDp(m)	Input	Daily predicted specific conductance (SC) for gage XXXX, microsiemens per centimeter. Abreviation XXXX is the unique four-digits for SC stations.
SCXXXXDp(u)	Input	Daily predicted specific conductance (SC) for gage XXXX using input Q13100Du, microsiemens per centimeter. Abreviation XXXX is the unique four-digits for SC stations.
SCXXXXHm	Input	Hourly measured SC for gage XXXX". CC" indicated twice corrected
SCXXXXHm/p+dSC	Input	SCXXXXHm + dSCXXXXH(pu-pm) if SCXXXXHm is not missing, else = SCXXXXHpm + dSCXXXXH(pu-pm)
SCXXXXHp(m)	Input	Hourly predicted SC for gage XXXX using input Q13100Dm
SCXXXXHp(u)	Input	Hourly predicted SC for gage XXXX using input Q13100Du
SINE-W0_ID12H	Output	Sine of DIR-W0_I
WL777_C	Output	02110777 hourly water level that has been corrected for errors
WL777_RANN	Output	Residual error of ANN model having QOTHER-related inputs to predict WL777_C. This decorrleates the WL boundary condition from the Q-related boundary condition. WL77_RANN is the the parameter used to calculate WL-related inputs to ANN models.
WL777_RANN_AXXH	Output	XX-hr MWA of WL777_RANN. In PRISM XX = 3, 6, 12 hours
WL777_RANN_DXXH	Output	WL777_RANN_AXXH - WL777_RANN_AYYH, where XX and YY indicate successive MWAs, e.g., WL777_RANN_D3H = WL777_RANN_A3H - WL777_RANN_A6H
WL777_RANN_F25	Output	WL777_RANN filtered to remove diurnal and semi-diurnal variability. Filtering results from applying a 13-hr and a 25-hr MWA to WL777_RANN in sucession.
WL777_RANN_F25_AXXD	Output	XX-day MWA of WL777_RANN_F25. In PRISM XX = 3, 7, 14 days
WL777_RANN_F25_DXXD	Output	WL777_RANN_AXXD - WL777_RANN_AYYD, where XX and YY indicate successive MWAs, e.g., WL777_RANN_D3D = WL777_RANN_A3D - WL777_RANN_A7D
XWL777_RANN_AXXH	Output	XX-hr MWA of XWL777_RANN_I. In PRISM XX = 3, 6, 12 hours
XWL777_RANN_DXXH	Output	XWL777_RANN_AXXH - XWL777_RANN_AYYH, where XX and YY indicate successive MWAs, e.g., XWL777_RANN_D6H = XWL777_RANN_A6H - XWL777_RANN_A12H
XWL777_RANN_F25	Output	XWL777_RANN_I filtered to remove diurnal and semi-diurnal variability. Filtering results from applying a 13-hr and a 25-hr MWA to XWL777_RANN_I in sucession.
XWL777_RANN_F25_AXXD	Output	XX-day MWA of XWL777_RANN_I. In PRISM XX = 3 days
XWL777_RANN_F25_DXXD	Output	XWL777_RANN_AXXD - XWL777_RANN_AYYD, where XX and YY indicate successive MWAs, e.g., XWL777_RANN_D1D = XWL777_RANN_A1D - XWL777_RANN_A3D
XWL777_RANN_I	Output	Tidal range calculated as the difference between the maximim and miniumum WL777_RANN values for each semi-diurnal tidal cycle. The "_I" indicates subsequent filling of missing values by linear interpolation.

Table 9. Summary of performance statistics for models used in the Pee Dee River and Atlantic Intracoastal Waterway Salinity Intrusion Model Decision Support System-Version 2 (PRISM-2 DSS).

[HLN, hidden layer neurons; min, minimum; SC, specific conductance; max, maximum; N, number of input vectors; R^2, coefficient of determination; RMSE, root mean square error; MSE, mean square error; PME, percent model error; Test%, percent of dataset used for testing]

Model name	Station number	OUTPUTS	HLN	Training dataset							Testing dataset							
				Range of output variable							Range of output variable							
				Min	Max	N_{train}	R^2_{train}	$RMSE_{train}$	MSE_{train}	PME	Min	Max	N_{test}	Test%	R^2_{test}	$RMSE_{test}$	MSE_{test}	PME
Daily models																		
sc755_cc_f25-final	02110755	P_SC755_CC_F25	2	62	6,220	2,086	0.69	223	49,779	3.6	62	4,380	2,190	51	0.69	189	35,678	4.4
sc760_cc_f25-final	02110760	P_SC760_CC_F25	2	51	282	2,100	0.74	19	366	8.3	50	270	886	30	0.72	20	382	8.9
sc770_cc_f25-final	02110770	P_SC770_CC_F25	2	79	14,700	2,958	0.87	643	413,738	4.4	82	12,600	1,291	30	0.86	625	391,070	5.0
sc777_cc_f25-final	02110777	P_SC777_CC_F25	2	80	36,100	2,853	0.88	2,672	7,137,883	7.4	79	35,500	1,250	30	0.88	2,736	7,483,335	7.7
sc809_cc_f25-final	02110809	P_SC809_CC_F25	3	70	2,430	1,396	0.86	46	2,141	2.0	69	2,810	663	32	0.87	53	2,803	1.9
sc8125_cc_f25-final	021108125	P_SC8125_CC_F25	1	70	12,100	1,485	0.85	544	296,413	4.5	68	13,000	662	31	0.88	441	194,368	3.4
sc815_cc_f25-final	02110815	P_SC815_CC_F25	1	60	21,800	2,825	0.88	1,094	1,197,662	5.0	60	21,400	1,234	30	0.85	1,171	1,370,682	5.5
Hourly models																		
sc755_cc-final	02110755	P_SC755_CC	2	57	13,600	12,822	0.60	694	481,334	5.1	50	13,600	103,525	89	0.58	332	110,115	2.4
sc760_cc-final	02110760	P_SC760_CC	2	50	386	14,690	0.73	20	397	5.9	40	366	58,263	80	0.73	20	388	6.0
sc770_cc-final	02110770	P_SC770_CC	2	0	30,200	20,738	0.85	1,084	1,175,120	3.6	0	32,600	82,426	80	0.84	1,076	1,157,465	3.3
sc777_cc-final	02110777	P_SC777_CC	2	54	46,900	10,367	0.89	2,147	4,607,999	4.6	54	51,500	89,915	90	0.84	4,213	17,750,919	8.2
sc809_cc-final	02110809	P_SC809_CC	3	68	7,490	12,678	0.81	143	20,397	1.9	67	7,490	49,227	80	0.76	91	8,342	1.2
sc8125_cc-final	021108125	P_SC8125_CC	2	66	18,700	6,017	0.81	1,480	2,191,534	7.9	56	18,700	53,857	90	0.77	723	522,132	3.9
sc815_cc-final	02110815	P_SC815_CC	2	60	26,900	15,366	0.84	1,345	1,809,208	5.0	60	28,100	88,512	85	0.83	1,378	1,899,750	4.9

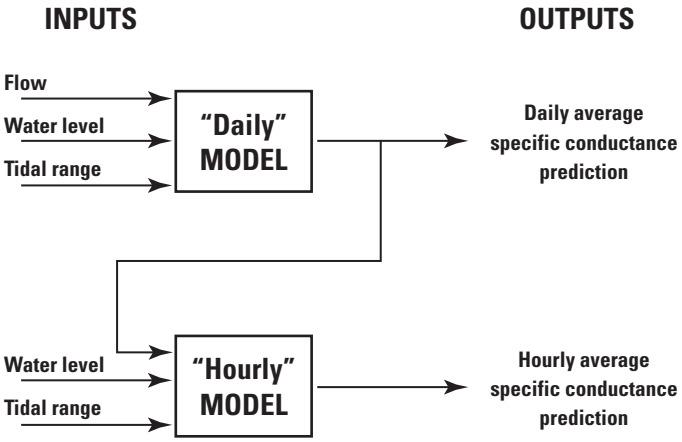

Figure 40. Schematic diagram showing the two-stage model architecture to predict specific conductance at a gaging station. This is an example of a "cascading" model where the output from the first model (daily average specific conductance) is used as an input to the second model.

Statistical Measures of Prediction Accuracy

Statistical measures of prediction accuracy were computed for the specific conductance models. Statistics for the first stage (daily) and second stage (hourly) models provide measures of the performance of individual models in the cascading modeling approach to simulate specific conductance. The statistics for the individual models are not necessarily indicative of the quality of the final estimates, which are based on multiple models. Thus, the specific conductance models are best evaluated using the statistics for the final daily and hourly simulation.

Model accuracy typically is reported in terms of coefficient of determination (R^2) and commonly is interpreted as the "goodness of the fit" of a model. A different interpretation poses the question: How much information does one variable or a group of variables provide about the behavior of another variable? For example, in the first context, an $R^2 = 0.6$ might be disappointing, whereas in the latter, it is merely an accounting of how much information is shared by the variables being used. The mean error (ME) and root mean square error (RMSE) statistics provide a measure of the prediction accuracy of the ANN models. The ME is a measure of the bias of model predictions—whether the model over- or under-predicts the measured data. The ME is presented as the adjustment to the simulated values to equal the measured values; therefore, a negative mean error indicates an over-prediction by the model, and a positive mean error indicates an under-prediction. Mean errors near zero may be misleading because negative and positive discrepancies in the simulations can cancel each other. The RMSE addresses the limitations of mean error by computing the magnitude, rather than the direction (sign), of the discrepancies. The units of the ME and RMSE statistics are the same as the simulated variable of the model.

The accuracy of the models, as given by RMSE, is best evaluated with respect to the measured range of the output variable. The percent model error (PME) is the ratio of the RMSE to the range of the output measured data. A model may have a low RMSE, but if the range of the output variable is small, the model may be accurate only for a narrow range of conditions and the model error may be a relatively large percentage of the model response. For example, if the RMSE for a model is 0.5 ft and the measured range is 0 to 2 ft, the percentage model error would be 25 percent. Likewise, a model may have a large RMSE, but if the range of the output variable is large, the model error may be a relatively small percentage of the total model response. For example, if the RMSE for a model is 2 ft and the measured range is 0 to 20 ft, the percentage model error would be 10 percent.

Waccamaw River and Atlantic Intracoastal Waterway Models

The ANN models developed for the original **P**ee Dee **R**iver and Atlantic **I**ntracoastal Waterway **S**alinity **M**odel (PRISM; Conrads and Roehl, 2007) were trained using data from July 11, 1995, to December 31, 2002. Although there are extensive specific-conductance data for the Waccamaw River and AIW study area, critical gaging stations near the freshwater-saltwater interface—Wachesaw and Pawleys Island gaging stations (stations 02110809 and 021108125; table 4)—were either established or re-established in 2002 and had limited data when the models were first developed. For this study, the database was extended to August 31, 2009, and the previously developed ANN models (Conrads and Roehl, 2007) were retrained using the additional data, which included additional drought periods and tropical storms.

The following sections describe the development of the specific-conductance models for seven sites in the Waccamaw River and AIW study area that experience salinity intrusions. Four of the seven gaging stations are in the north end of the study area near Little River Inlet, and the models are referred to as the "North End models" (stations 02110755, 02110760, 02110770, and 02110777; fig. 2). Three of the seven gaging stations are in the south end of the system near Hagley Landing and Winyah Bay, and the models are referred to as the "South End models" (stations 02110809, 021108125, and 02110815, fig. 2).

The model development incorporated combinations of the decomposed total inflow (summation of the regulated and unregulated streamflows) and water-level (WL) signals that represented different spectral frequencies. For the daily models, the representation of the dynamic input signals is as follows: moving-window averages of 1, 3, 7, 14, and 30 days were calculated for total inflow (QTOTAL), and moving-window averages of 3, 7, and 14 days were computed for the decorrelated water levels (WL777_RANN) and were named

sequentially for the increasing moving-window size. For example, QTOTAL_A3 represented the 3-day moving-window average for rainfall, QTOTAL_A7 represented the 7-day average, QTOTAL_A14 represented the 14-day average, and so on. The moving-window sizes were selected to capture daily, weekly, and monthly variability of the parameters. For each parameter, differences between each moving-window average and the next larger window-sized moving window average were calculated, for example, QTOTAL_D7D = QTOTAL_A7 - QTOTAL_A14, RAIN_D14D = QTOTAL_A14 - QTOTAL_A30, and so on.

The ANN models were developed iteratively by starting with a candidate pool of input variables, training the ANN, and then using prediction accuracy statistics, such as R^2 and input-output sensitivities, to cull the least important input variables. It is left to the ANN to learn which parameters and spectral ranges are the best predictors of behaviors that are manifest in the specific-conductance signal.

Datasets with numerous salinity intrusion events were randomly bifurcated into training and testing datasets. Percentages of the dataset used for testing the daily models ranged from 30 to 51 and, for testing the hourly models, 80 to 90 (table 9). Statistical measures used to evaluate the models—R^2, ME, RMSE, and PME—were computed for the training and testing datasets for each model (table 9). In the following sections, examples of daily and hourly models are described for each group of models in the North and South Ends of the Waccamaw River and AIW study area.

North End Models

The daily specific-conductance model for Briarcliffe Acres (sc755_cc_f25-final, table 7) uses streamflow, water-level, and tidal-range inputs (table 7). The streamflow inputs (Q) are 14-day moving-window average total inflow (QTOTAL_A14D), the difference between the 7- and 14-day moving-window average of total inflow (QTOTAL_D7D), and the difference between the 14- and 30-day moving-window average (QTOTAL_D14D). The water-level data inputs are decorrelated daily tidally filtered water levels from Little River Inlet (WL777_RANN_F25), the difference between the 12- and 25-hour moving-window average of water levels (WL777_RANN_D12H), the difference between the 1- and 3-day moving-window average of daily tidally filtered water levels (WL777_RANN_F25_D1D), and the difference between the 3- and 7-day moving-window average of daily tidally filtered water levels (WL777_RANN_F25_D3D). The tidal range (XWL) inputs are the decorrelated daily filtered tides and the difference between the 1- and 3-day moving-window average of the daily tidal range (XWL777_RANN_F25 and XWL777_RANN_F25_D1D, respectively). For testing and training the daily model, 4,276 data values were available; and about 51 percent (2,090 data points) was used for training (table 9). The R^2 for the training and testing are 0.69 and 0.69, respectively (table 9). The daily model had two hidden-layer neurons.

The hourly specific-conductance model (sc755_cc-final, table 7) uses the simulated daily specific conductance from the daily specific-conductance model and water-level and tidal inputs from the Little River Inlet gage (table 7). The simulated daily specific-conductance input (P_SC755_CC_F25) captures the long-term movement of the specific conductance that is characterized by the streamflow and the chaotic components of the water-level signal. Water-level and tidal-range data are used to capture the semi-diurnal tidal signal. The water-level inputs include the 3-day moving-window average of the daily tidally filtered decorrelated water level at Little River Inlet (WL777_RANN_F25_A3D) and the differences between the 3- and 6- hour, 6- and 12-hour, and 12- and 25-hour moving-window averages of decorrelated water levels (WL777_RANN_D3H, WL777_RANN_D6H, and WL777_RANN_D12H, respectively). Tidal-range input is the 12-hour moving-window average of decorrelated tidal range (XWL777_RANN_A12H). For testing and training the hourly model, 116,347 data values were available; and about 11 percent (12,822 data points) was used for training. The R^2 for the training and testing are 0.60 and 0.58, respectively (table 9). The hourly model had two hidden-layer neurons.

The measured and simulated daily specific-conductance values for the four North End specific-conductance models are shown in figure 41. The daily models effectively simulated the timing and range of the salinity-intrusion events. The measured and simulated hourly specific-conductance values for the four North End models are shown in figure 42. In general, the models were able to simulate the timing of the salinity-intrusion events, although the models do not always capture the peak values of the events.

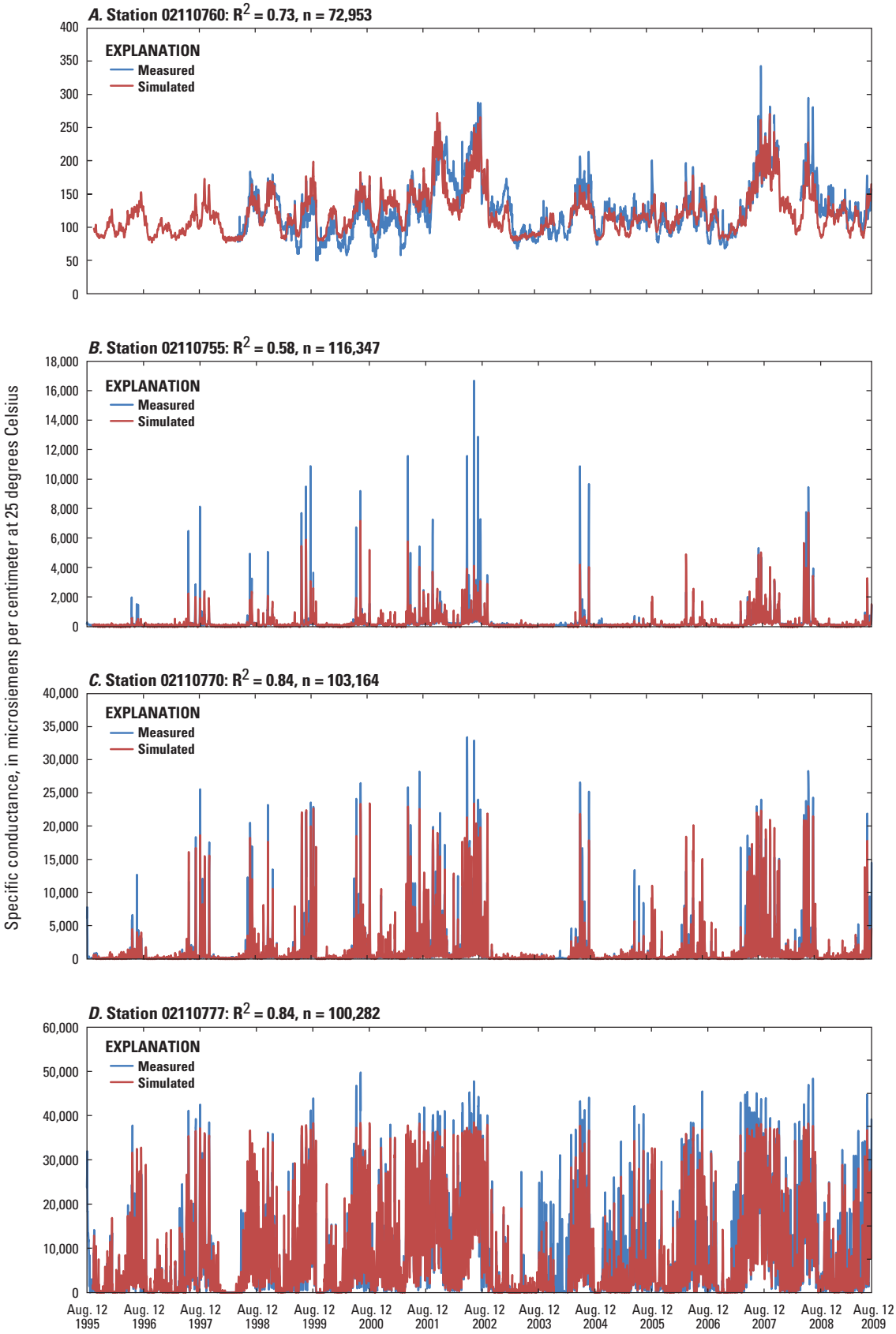

Figure 41. Measured and simulated specific-conductance values from the daily model for four U.S. Geological Survey gages on the North End of the Atlantic Intracoastal Waterway, South Carolina: (*A*) Myrtlewood (station 02110760), (*B*) Briarcliffe Acres (station 02110755), (*C*) Grand Strand Airport (station 02110770), and (*D*) Little River Inlet (station 02110777), August 12, 1995–August 12, 2009.

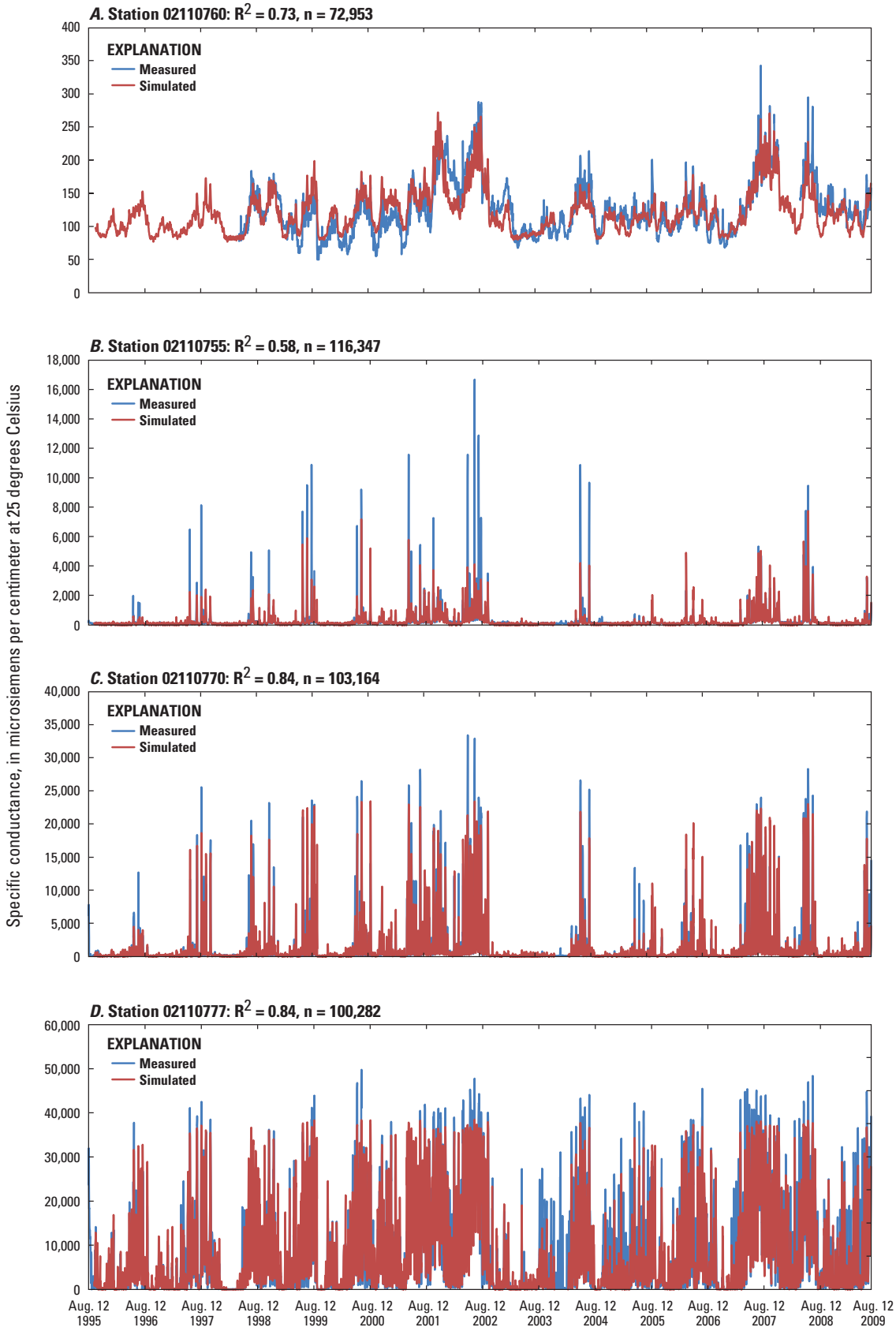

Figure 42. Measured and simulated specific-conductance values from the hourly model for four U.S. Geological Survey gages on the North End of the Atlantic Intracoastal Waterway, South Carolina: (*A*) Myrtlewood (station 02110760), (*B*) Briarcliffe Acres (station 02110755), (*C*) Grand Strand Airport (station 02110770), and (*D*) Little River Inlet (station 02110777), August 12, 1995–August 12, 2009.

South End Models

The daily specific-conductance model (SC8125_cc_f25-final, table 7; fig. 43) for Waccamaw River at Pawleys Island uses streamflow, water-level, and tidal-range inputs. The streamflow input is the 7-day moving-window average of total inflow (QTOTAL_A7D). The water-level inputs include the decorrelated daily tidally filtered water level (WL777_RANN_F25) and the difference between the 12-hour and 25-hour decorrelated water levels (WL777_RANN_D12H). The tidal range inputs are the differences between the 1- and 3-day, and 6- and 12-hour, moving-window averages of decorrelated daily tidal range (XWL777_RANN_F25_D1D and XWL777_RANN_F25_D6H, respectively). For testing and training the daily model, 2,147 data values were available; and about 69 percent (1,485 data points) was used for training (table 9). The coefficients of determination, R^2, for the training and testing are 0.85 and 0.88, respectively (table 9). The daily model had one hidden-layer neuron.

The hourly specific-conductance model (SC8125_cc-final; table 7; fig. 44) uses the simulated daily specific conductance (P_SC8125_CC_F25) from the daily specific-conductance model and water-level inputs from the Little River Inlet gage. The water-level inputs include decorrelated filtered daily water level (WL777_RANN_F25), the difference between the 3-hour and 6-hour moving-window average water level (WL777_RANN_D3H), the difference between the 6-hour and 12-hour moving-window average water level (WL777_RANN_D6H), and the difference between the 12-hour and 25-hour moving-window average water level (WL777_RANN_D12H). For testing and training the hourly model, 59,874 data values were available; and about 10 percent (6,017 data points) was used for training (table 9). The R^2 values for the training and testing are 0.81 and 0.77, respectively (table 9). The hourly model had two hidden-layer neurons.

Lower Savannah River and Marsh Specific-Conductance Models

The ANN models for the Model-to-Marsh Decision Support System (M2M DSS) were not retrained for this study. However, the M2M DSS was updated for this study by limiting the models in the application to the USGS river and marsh specific-conductance gaging network (table 5). The original application included 84 ANN models for water level and specific conductance for river and marsh sites monitored by Georgia Ports Authority (Conrads and others, 2006). The Georgia Ports Authority sites had limited temporal deployments, have much smaller datasets, and did not monitor as large a range of streamflow and tidal conditions as monitored at the USGS river and marsh sites. These models were removed from the updated application. The specific conductance ANN models of the USGS marsh sites include specific-conductance prediction for four GPA sites (GPA 10, GPA11, GPA11R, and GPA12) on the Savannah and Middle Rivers (fig. 45). The models for these four sites were left in the application. A description of the ANN models used in the M2M-2 DSS, descriptions of variables, and a summary of performance statistics used for models in this study can be found in appendixes 1, 2, and 3, respectively. Salinity model inputs and outputs for one of the river models and one of the marsh models are described in the following sections. For the M2M DSS, specific-conductance model output was converted to salinity.

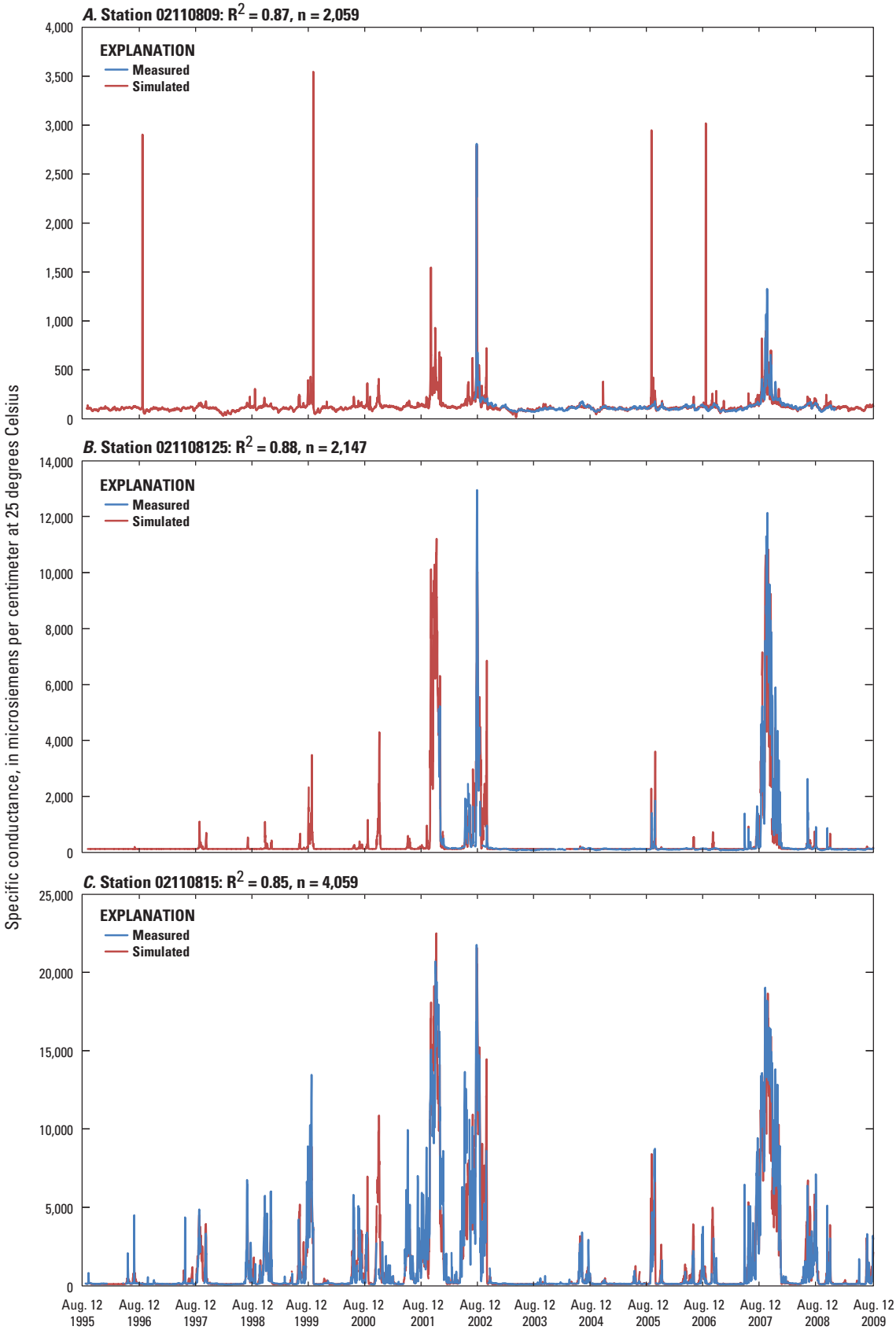

Figure 43. Measured and simulated specific-conductance values from the daily model for three U.S. Geological Survey gages on the Waccamaw River, South Carolina: (*A*) Wachesaw (station 02110809), (*B*) Pawleys Island (station 021108125), and (*C*) Hagley Landing (station 02110815), August 12, 1995–August 12, 2009.

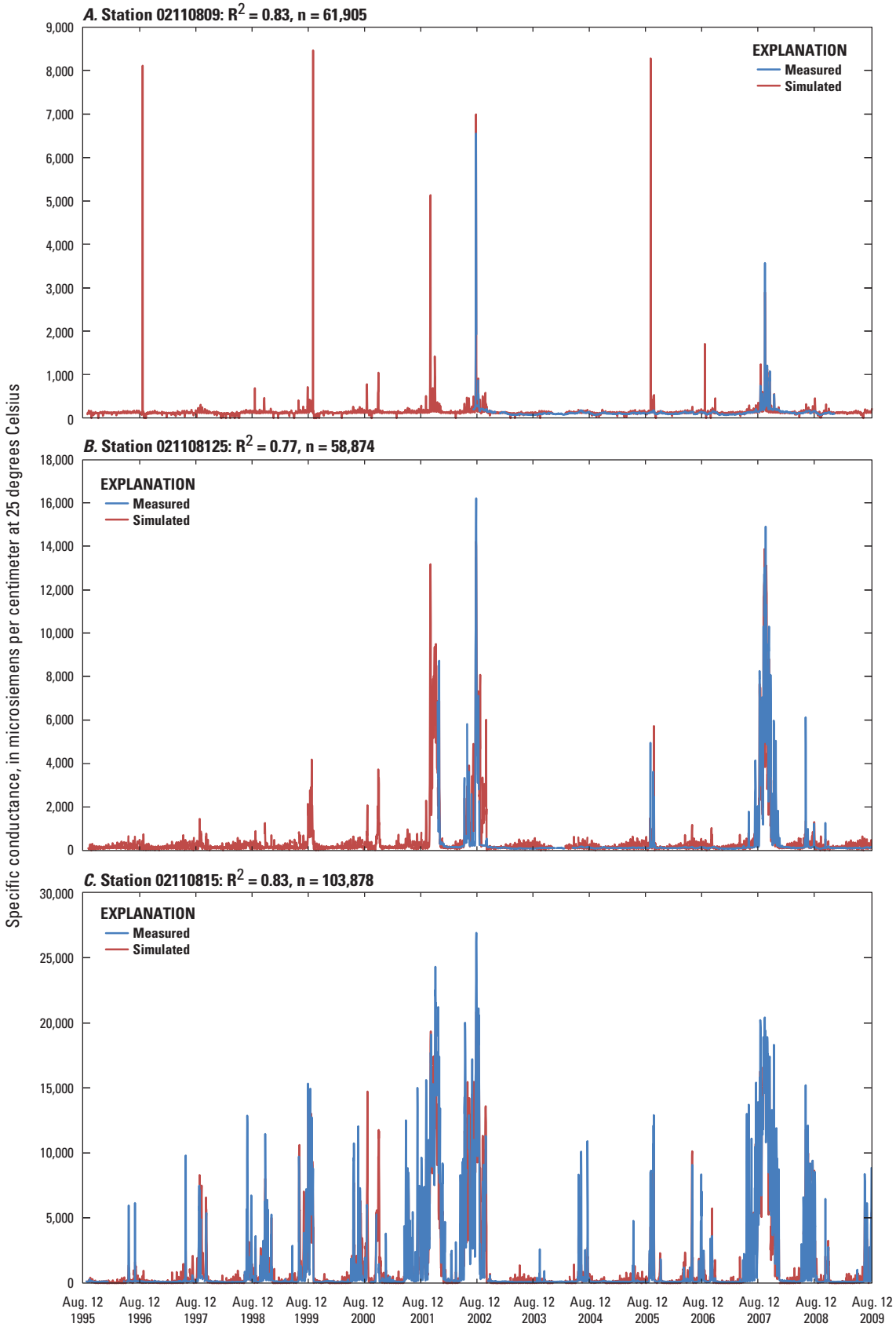

Figure 44. Measured and simulated specific-conductance values from the hourly model for three U.S. Geological Survey gages on the Waccamaw River, South Carolina: (*A*) Wachesaw (station 02110809), (*B*) Pawleys Island (station 021108125), and (*C*) Hagley Landing (station 02110815), August 12, 1995–August 12, 2009.

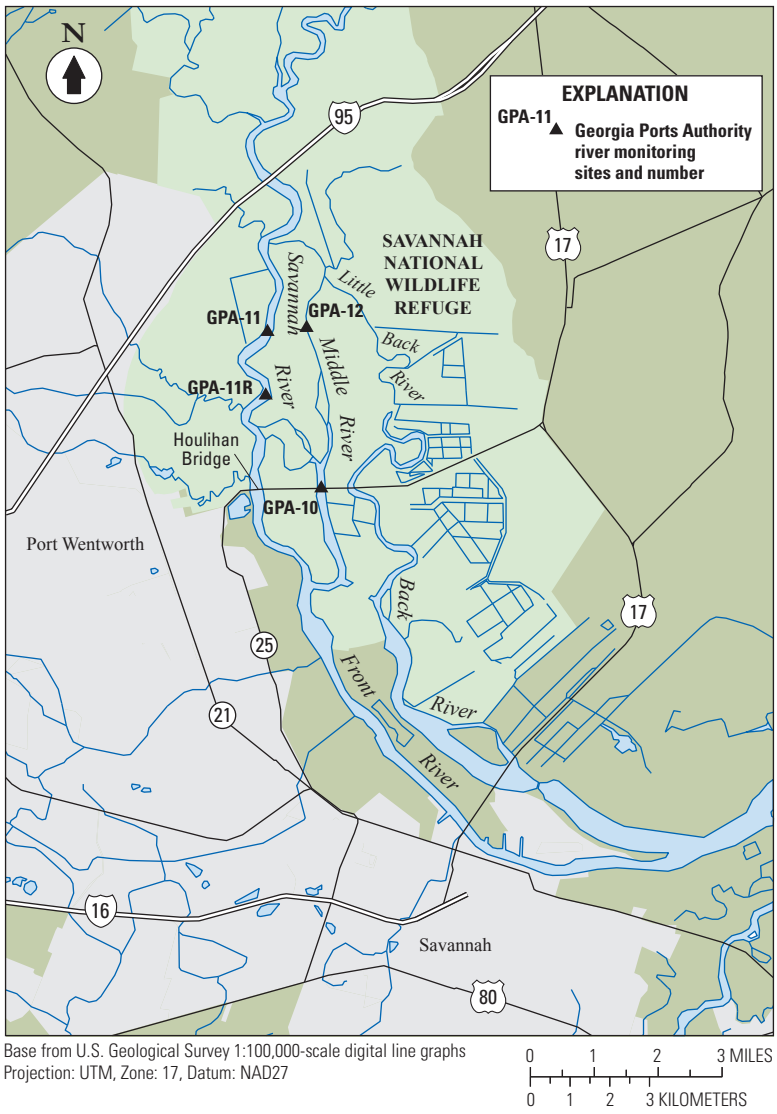

Figure 45. Location of Georgia Ports Authority river monitoring gages, South Carolina and Georgia. Data from these gages were used as inputs to the salinity models of the U.S. Geological Survey marsh sites (fig. 11*B*).

Riverine Specific-Conductance Model for Savannah River at the I-95 Bridge

The daily salinity model (sc8840a-2005-1, appendix 1) for Savannah River at I-95 (station 02198840) uses six streamflow, two water-level, and two tidal-range inputs. A brief description of the variables used in the M2M-2 is provided in appendix 2. The streamflow inputs are daily average streamflow (Q8500A), the 1-day change in streamflow (D8500A), daily streamflow lagged 2 days (LAQ2), the 2-day change in streamflow (the 2-day change in streamflow; DAQ2), the 16-day change in streamflow (DAQ16), and the 30-day change in streamflow (DAQ30). The water-level inputs are the filtered daily water level from the Fort Pulaski gage (FWL8980A) and the 1-day change in tidally filtered daily water level (DWLA). The tidal range daily inputs are daily tidal range (XWL8980A) and the 1-day change in daily tidal range (DXWLA). The daily model had three hidden-layer neurons (appendix 1). For testing and training the daily model, there were 87,365 data values available. Approximately 12 percent of the data was used for training, and 88 percent was used for testing. The R^2 for the training and testing are 0.97 and 0.96, respectively (appendix 3).

The hourly salinity model (sc8840h-2005-1, appendix 1) is based on simulated daily specific-conductance values from the daily model, one tidal-range input, and four water-level inputs. The simulated daily specific-conductance input (PSC8840A) captures the long-term movement of

the specific conductance that is characterized by the streamflow and tidal-range data in the daily model. The tidal-range input is the hourly tidal range (NXWL). The four water-level inputs—LG1NWL, LG1D3NWL, LG4D3NWL, and LG7D3NWL—are the 1-hour lagged water level and the 3-hour change in the water level lagged 1, 4, and 7 hours, respectively. The lagged water-level inputs capture the periodic semi-diurnal tidal cycle signal. For testing and training the hourly model, there were 87,969 data values. Approximately 12 percent of the data was used for training, and 88 percent was used for testing. The R^2 for the training and testing are 0.88 and 0.85, respectively (appendix 3).

The measured and simulated hourly salinities at I-95 (station 02198840) are shown in figure 46 for summer 2002. This period was at the end of the 5-year drought that began in 1998 and had the highest salinity intrusions of that drought period. The model simulations captured the salinity intrusions occurring on 14- and 28-day cycles. The model also was able to simulate the full range of the large salinity intrusion on about August 7, 2002.

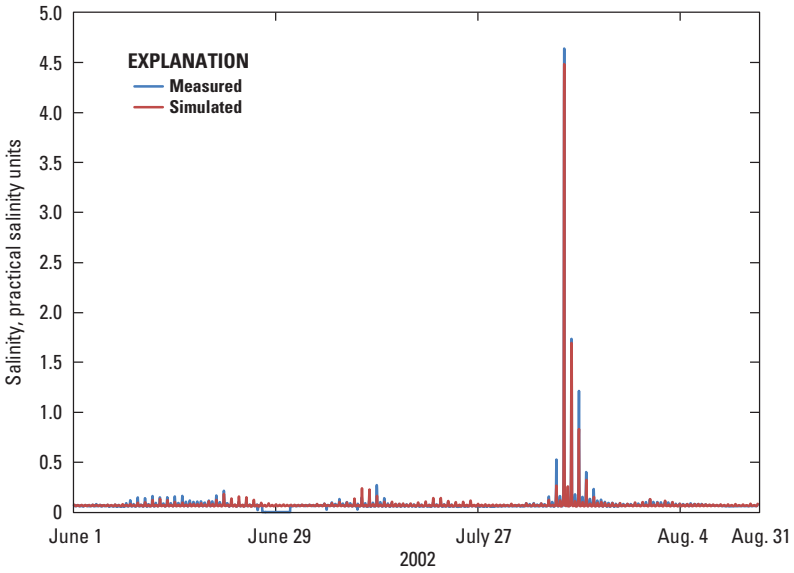

Figure 46. Measured and simulated hourly salinities at Savannah River at Interstate 95 (station 02198840), Georgia, June 1–August 31, 2002.

Marsh Specific-Conductance Model at Site B2

For modeling the USGS marsh sites, simulated data for four of the GPA stations were used as inputs. The models for the four GPA stations were necessary to simulate potential mitigation scenarios to divert additional streamflow to the Middle and Little Back Rivers to mitigate an increase in salinity in the vicinity of the SNWR resulting from a potential deepening of Savannah Harbor (Conrads and others, 2006). One concern with using only the long-term USGS gaging stations to simulate the pore-water salinity in the marsh is that there would not have been any data on the Middle River which could have been important for evaluating mitigation scenarios involving creating or closing channels connecting the Front, Middle, Little Back, and Back Rivers. Data in this area are available from the GPA river network (fig. 45). Although the data from these stations are limited to conditions from either the summer of 1997 or 1999, data from GPA10, GPA11, GPA11R, and GPA12 were used as inputs to the marsh salinity models to address spatial distribution of the river salinity inputs for the marsh salinity models.

There are two technical issues associated with using the short-term GPA data. The first issue is that the GPA data are not concurrent with the USGS marsh data (summers of 1997 and 1999 for GPA gaging stations and 2000 to 2005 for USGS gaging stations). The models for the four GPA stations (fig. 45) were used to simulate the time series of specific conductance for 2000 to 2005. To generate the data for this period, the GPA models were used to make salinity predictions for a range of streamflow conditions much larger than those measured during the summers of 1997 and 1999. The second issue is that the GPA data are highly correlated. To ensure that the data from the GPA sites provide unique information for the marsh models, the data for stations GPA11, GPA11R, and GPA12 were systematically decorrelated from GPA10.

The marsh pore-water salinities were modeled in two stages. For the first stage, USGS river data were used to simulate the marsh salinity. For the second stage, GPA river data were used to determine the residual error (difference between the simulated and measured marsh salinity) from the first-stage model. The final marsh salinity predictions are the sum of the predictions from the two models.

The first stage pore-water salinity model (pb2msc-2005-2, appendix 1) for Little Back River at Site B2 used 10 specific-conductance inputs and differences in specific conductance from two USGS river gaging stations in the vicinity of SNWR. Two inputs are the differences in specific conductance at the Little Back River at U.S. Fish and Wildlife Dock (station 021989791) and Savannah River at Interstate 95 (station 02198840), and the difference between Little Back River at U.S. Fish and Wildlife Dock (station 02198979) and Front River at Houlihan Bridge (station 02198920), variables SCDIF8840A and SCDIF8920A, respectively. There were four moving-window average inputs of 48 hours, and 1, 2, and 4 weeks (variables FSC89791A48, FSC89791D1WK, FSC89791D2WK, FSC89791D4WK) and four time-derivative inputs (variables LG672FSC89791A4WKD4WK, FSC89791DA48, DFSC89791DA48, and LG3DF-SC89791DA48). The model had one hidden-layer neuron (appendix 1). For testing and training the daily model, there were 20,912 data values available (approximately 5 years of hourly data from 1999 to 2005; appendix 2). Ten percent of the data was used for training, and 90 percent was used for testing. The R^2 for the training and testing is 0.83 for each.

The second stage model (prb2msc) simulated the residual error from the first-stage marsh pore-water salinity model. The four inputs used to simulate the residual error are the weekly averages of the decorrelated specific-conductance variable from each GPA site and a 1-week moving-window average of specific conductance at GPA 10 (variables RSC10S_11B_A1WK, RSC10S_11BR_A1WK, RSC10S_12RS_A1WK, and PSCGPA10S_FLR_A1WK, respectively). The final prediction is a summation of the marsh and residual models; the R^2 is 0.92 and the percent model error is 6.5 (appendix 3). The measured and simulated hourly pore-water salinities are shown in figure 47 for summer 2002. This period occurred at the end of the 5-year drought that began in 1998 and had the highest salinity intrusions of the drought period. The model simulated long-term change in salinity but under-simulated the higher salinity changes occurring on 14- and 28-day cycles.

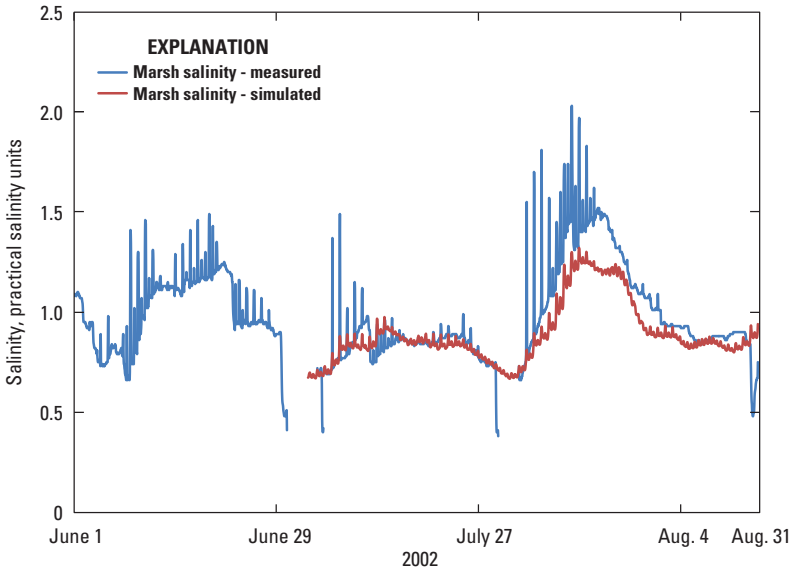

Figure 47. Measured and simulated hourly pore-water salinities at Little Back River at Site B2, Georgia, June 1–August 31, 2002.

Development of the Decision Support Systems

Natural-resource managers and stakeholders face difficult challenges when managing interactions between natural and manmade systems. Even though the collective interests and computer skills of the community of managers, scientists, and other stakeholders are quite varied, equal access to the scientific knowledge is needed for them to make the best possible decisions. Dutta and others (1997) define decision support systems (DSSs) as "systems helping decision makers to solve various semi-structured and unstructured problems involving multiple attributes, objectives, and goals… Historically, the majority of DSSs have been either computer implementations of mathematical models or extensions of database systems and traditional management information systems." Environmental resource managers commonly use complex mathematical (mechanistic) models based on first-principle physical equations to evaluate options for using the resource without damage. Although there appears to be no strict criteria that distinguish a DSS from other types of programs, Dutta and others (1997) suggest that artificial intelligence (AI) is a characteristic of more advanced DSSs: "With the help of AI techniques DSSs have incorporated the heuristic models of decision makers and provided increasingly richer support for decision making. Artificial intelligence systems also have benefited from DSS research as they have scaled down their goal from replacing to supporting decision makers."

The PRISM-2 and M2M-2 DSSs are spreadsheet applications that provide predictive models with real-time databases for ANN model simulation, graphical user interfaces, and displays of results. As spreadsheet applications, the DSSs are easily distributable and immediately usable by all interested parties. The development of the DSSs for the Waccamaw River and AIW, and the lower Savannah River, required a number of steps (described previously), including (1) merging all the data into a single comprehensive database, (2) developing specific-conductance ANN sub-models, and (3) developing a Microsoft Office Excel™ application that integrates the new database and ANN sub-models into a single package that is easy to use and disseminate.

Architecture

The basic architectural elements of the PRISM-2 and M2M-2 DSSs are shown in figures 48 and 49, respectively. The DSSs read and write files for the various run-time options that can be selected by the user through the system's GUI. A historical database is read into the simulator along with the ANN sub-models at the start of a simulation. By using GUI controls, the user can evaluate various streamflow scenarios and sea-level-rise scenarios. The outputs generated by the simulator are written to files for post processing in Microsoft Office Excel™ or other analysis software packages. The PRISM-2 DSS also provides streaming graphics for each gage during simulations and 3D visualization of the specific-conductance response for the North End and South End models. The M2M-2 DSS provides a two-dimensional color-gradient visualization of pore-water salinity concentrations in the tidal marsh near the SNWR.

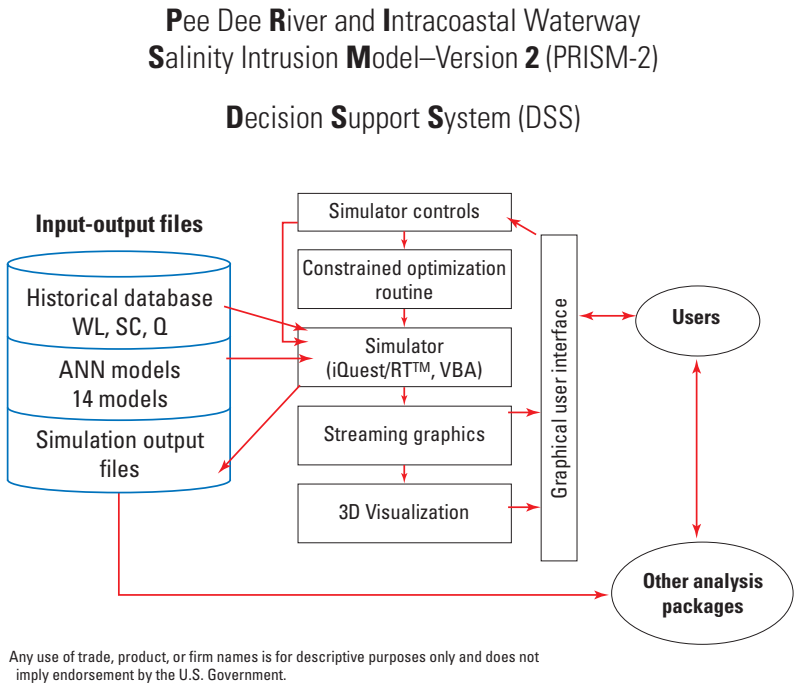

Figure 48. Architecture of the Pee Dee River and Intracoastal Waterway Salinity Intrusion Model-2 Decision Support System (PRISM-2 DSS) (modified from Conrads and Roehl, 2007). [WL, water level; SC, specific conductance; Q, flow; ANN, artificial neural network; VBA, visual basic for applications; RT, run-time]

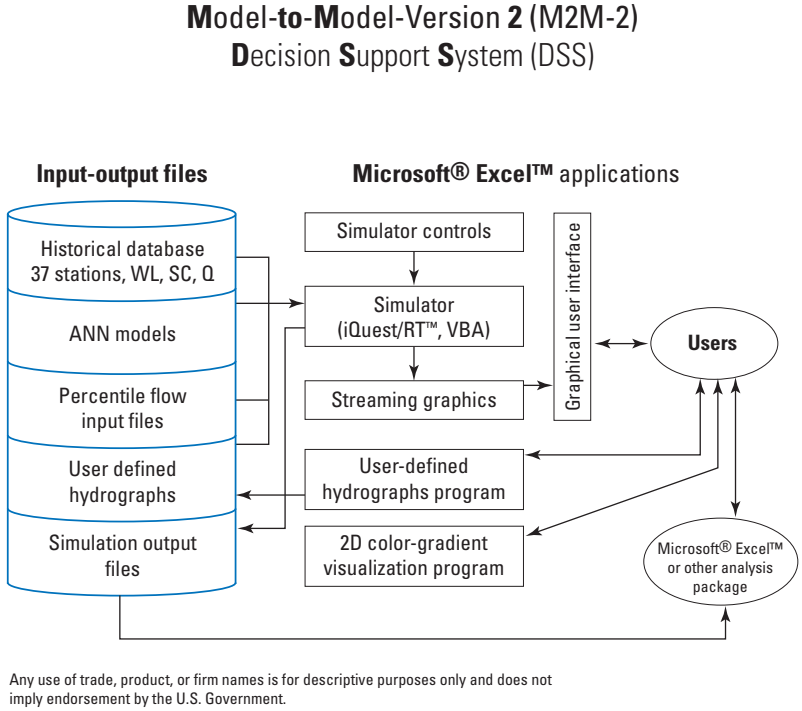

Figure 49. Architecture of the Model-to-Marsh-2 Decision Support System (DSS) (modified from Conrads and others, 2006). [WL, water level; SC, specific conductance; Q, flow; ANN, artificial neural network; VBA, visual basic for applications; RT, real-time]

Historical Databases

Review of the measured data in the historical databases was necessary for quality control because of a variety of problems previously discussed, including erroneous and missing values and timing errors causing phase shifts. For the PRISM-2 DSS, the resulting database comprises 14 years of hourly and daily data for 14 stations. For the M2M-2 DSS, the resulting database comprises 11 years of half-hourly data for 51 stations. The streamgaging stations, characteristics, period of record of the data in the PRISM-2 DSS and M2M-2 DSS databases are listed in tables 10 and 11, respectively.

Table 10. Stations, characteristics, period of record, and time interval of data in the Pee Dee River and Atlantic Intracoastal Waterway Salinity Intrusion Model Decision Support System-Version 2 (PRISM-2 DSS) database.

[Q, streamflow; wl, water level; xwl, tide range; wsp, wind speed; sc, specific conductance; wdir, wind direction; SC, South Carolina]

Station location	Site identifier	Character-istic	Time interval	Start date	End Date	Agency
Waccamaw River near Longs, S.C.	2110500	Q	Hourly	July 1995	August 2009	U.S. Geological Survey
Pee Dee River at Pee Dee, S.C.	2131000	Q	Hourly	July 1995	August 2009	U.S. Geological Survey
Lynches River at Effingham, S.C.	2132000	Q	Hourly	July 1995	August 2009	U.S. Geological Survey
Little Pee Dee River at Galivants Ferry, S.C.	2135000	Q	Hourly	July 1995	August 2009	U.S. Geological Survey
Black River at Kingstree, S.C.	2136000	Q	Hourly	July 1995	August 2009	U.S. Geological Survey
AIW at S.C. Highway 9 at Nixons Crossroads, S.C.	2110777	wl, xwl	Hourly	July 1995	August 2009	U.S. Geological Survey
AIW at Briarcliffe Acres, S.C.	2110755	sc	Hourly	July 1995	August 2009	U.S. Geological Survey
AIW at Myrtlewood Golf Course, S.C.	2110760	sc	Hourly	July 1995	August 2009	U.S. Geological Survey
AIW at Grand Strand Airport at North Myrtle Beach, S.C.	2110770	sc	Hourly	July 1995	August 2009	U.S. Geological Survey
AIW at S.C. Highway 9 at Nixons Crossroads, S.C.	2110777	sc	Hourly	July 1995	August 2009	U.S. Geological Survey
Waccamaw River at Wachesaw Landing, S.C.	2110809	sc	Hourly	July 1995	August 2009	U.S. Geological Survey
Waccamaw River near Pawleys Island, S.C.	21108125	sc	Hourly	July 1995	August 2009	U.S. Geological Survey
Waccamaw River at Hagley Landing, S.C.	2110815	sc	Hourly	July 1995	August 2009	U.S. Geological Survey
Charleston Harbor, Charleston, S.C.		wsp, wdir	Hourly	July 1995	August 2009	National Weather Service

Table 11. Stations, characteristics, period of record, and time interval of data in the Model-to-Marsh Decision Support System-Version 2 (M2M-2 DSS) database.

[Q, streamflow; wl, water level; sc, specific conductance; xwl, tide range; psc, pore-water specific conductance]

Site identifier	Station location	River or marsh site	Charac-teristic	Time interval	Start date	End date	Agency
2198500	Savannah River near Clyo	River	Q	half hourly	January 1994	December 2005	U.S. Geological Survey
2198840	Savannah River at I-95 Bridge	River	wl, sc	half hourly	January 1994	December 2005	U.S. Geological Survey
2198920	Front River at Houlihan Bridge	River	wl, sc	half hourly	January 1994	December 2005	U.S. Geological Survey
2198977	Front River at Broad Street	River	wl	half hourly	January 1994	December 2005	U.S. Geological Survey
21989784	Little Back River at Lucknow Canal	River	sc	half hourly	January 1994	December 2005	U.S. Geological Survey
2198979	Little Back River near Limehouse	River	wl	half hourly	January 1994	December 2005	U.S. Geological Survey
21989791	Little Back River at USFW Dock	River	sc	half hourly	January 1994	December 2005	U.S. Geological Survey
2198980	Savannah River at Fort Pulaski	River	wl, xwl	half hourly	January 1994	December 2005	U.S. Geological Survey
B1	Little Back River marsh	Marsh	wl, psc	half hourly	June 1999	December 2005	U.S. Geological Survey
B2	Little Back River marsh	Marsh	wl, psc	half hourly	June 1999	March 2007	U.S. Geological Survey
B3	Back River marsh	Marsh	wl, psc	half hourly	June 1999	December 2006	U.S. Geological Survey
B4	Back River marsh	Marsh	wl, psc	half hourly	June 1999	December 2006	U.S. Geological Survey
F1	Front River marsh	Marsh	wl, psc	half hourly	June 1999	April 2006	U.S. Geological Survey
M1	Middle River marsh	Marsh	wl, psc	half hourly	June 1999	June 2006	U.S. Geological Survey
M2	Middle River marsh	Marsh	wl, psc	half hourly	June 1999	December 2006	U.S. Geological Survey

Table 11. Stations, characteristics, period of record, and time interval of data in the Model-to-Marsh Decision Support System-Version 2 (M2M-2 DSS) database.—Continued

[Q, streamflow; wl, water level; sc, specific conductance; xwl, tide range; psc, pore-water specific conductance]

Site identifier	Station location	River or marsh site	Charac-teristic	Time interval	Start date	End date	Agency
GPA04	Savannah River near Fort Jackson	River	wl, sc	half hourly	July 1997 July 1999	September 1997 October 1999	Georgia Ports Authority
GPA05	Back River upstream of Tide Gate	River	wl, sc	half hourly	July 1997 July 2000	September 1997 October 1999	Georgia Ports Authority
GPA06	Front River upstream of Broad Street	River	wl, sc	half hourly	July 1997 July 2001	September 1997 October 1999	Georgia Ports Authority
GPA07	Back River downstream of Houlihan Bridge	River	wl, sc	half hourly	July 1997 July 2002	September 1997 October 1999	Georgia Ports Authority
GPA08	Front River downstream of Houlihan Bridge	River	wl, sc	half hourly	July 1997 July 2003	September 1997 October 1999	Georgia Ports Authority
GPA09	Front River at Houlihan Bridge	River	wl, sc	half hourly	July 1997 July 2004	September 1997 October 1999	Georgia Ports Authority
GPA10	Middle River at Houlihan Bridge	River	wl, sc	half hourly	July 1997 July 2005	September 1997 October 1999	Georgia Ports Authority
GPA11	Front River upstream of Houlihan Bridge	River	wl, sc	half hourly	July 1997 July 2006	September 1997 October 1999	Georgia Ports Authority
GPA11R	Front River upstream of Houlihan Bridge	River	wl, sc	half hourly	July 1997 July 2007	September 1997 October 1999	Georgia Ports Authority
GPA12	Middle River upstream of Houlihan Bridge	River	wl, sc	half hourly	July 1997 July 2008	September 1997 October 1999	Georgia Ports Authority
GPA12R	Middle River upstream of Houlihan Bridge	River	wl, sc	half hourly	July 1997 July 2009	September 1997 October 1999	Georgia Ports Authority
GPA13	Little Back River downstream of Union Creek	River	wl, sc	half hourly	July 1997 July 2010	September 1997 October 1999	Georgia Ports Authority
GPA14	Savannah River at I-95 Bridge	River	wl, sc	half hourly	July 1997 July 2011	September 1997 October 1999	Georgia Ports Authority
GPA15	Little Back River at Houlihan Bridge	River	wl, sc	half hourly	July 1997 uly 2012	September 1997 October 1999	Georgia Ports Authority
GPA21	Front River downstream of U.S. Highway 17 Bridge	River	wl, sc	half hourly	July 1997 July 2013	September 1997 October 1999	Georgia Ports Authority
GPA22	Front River downstream of confluence with Middle River	River	wl, sc	half hourly	July 1997 July 2014	September 1997 October 1999	Georgia Ports Authority
Site1 marsh	Front River upstream of Houlihan Bridge	Marsh	wl, psc	half hourly	June 1999	October 2002	Georgia Ports Authority
Site1 canal	Front River upstream of Houlihan Bridge	Marsh	wl, psc	half hourly	June 1999	October 2002	Georgia Ports Authority
Site2 Marsh	Back River	Marsh	wl, psc	half hourly	June 1999	October 2002	Georgia Ports Authority
Site2 Canal	Back River	Marsh	wl, psc	half hourly	June 1999	October 2002	Georgia Ports Authority
Site3 marsh	Back River	Marsh	wl, psc	half hourly	June 1999	October 2002	Georgia Ports Authority
Site3 canal	Back River	Marsh	wl, psc	half hourly	June 1999	October 2002	Georgia Ports Authority
Site4 marsh	Back River	Marsh	wl, psc	half hourly	June 1999	October 2002	Georgia Ports Authority
Site4 canal	Back River	Marsh	wl, psc	half hourly	June 1999	October 2002	Georgia Ports Authority
Site 5 marsh	Middle River upstream of Houlihan Bridge	Marsh	wl, psc	half hourly	June 1999	October 2002	Georgia Ports Authority
Site 5 canal	Middle River upstream of Houlihan Bridge	Marsh	wl, psc	half hourly	June 1999	October 2002	Georgia Ports Authority
Site6 marsh	Middle River upstream of Houlihan Bridge	Marsh	wl, psc	half hourly	June 1999	October 2002	Georgia Ports Authority
Site6 canal	Middle River upstream of Houlihan Bridge	Marsh	wl, psc	half hourly	June 1999	October 2002	Georgia Ports Authority
Site7 marsh	Front River upstream of Houlihan Bridge	Marsh	wl, psc	half hourly	June 1999	October 2002	Georgia Ports Authority
Site7 canal	Front River upstream of Houlihan Bridge	Marsh	wl, psc	half hourly	June 1999	October 2002	Georgia Ports Authority
Site8 marsh	Little Back River	Marsh	wl, psc	half hourly	June 1999	October 2002	Georgia Ports Authority
Site8 canal	Little Back River	Marsh	wl, psc	half hourly	June 1999	October 2002	Georgia Ports Authority
Site9 marsh	Middle River upstream of Houlihan Bridge	Marsh	wl, psc	half hourly	June 1999	October 2002	Georgia Ports Authority
Site9 canal	Middle River upstream of Houlihan Bridge	Marsh	wl, psc	half hourly	June 1999	October 2002	Georgia Ports Authority
Site10 marsh	Middle River downstream of Houlihan Bridge	Marsh	wl, psc	half hourly	June 1999	October 2002	Georgia Ports Authority
Site10 canal	Middle River downstream of Houlihan Bridge	Marsh	wl, psc	half hourly	June 1999	October 2002	Georgia Ports Authority

Decision Support System Visualization Programs

The simulations provided by the DSSs integrate the historical database with the ANN models. The date/time controls on the control panels (fig. 50) enable the user to adjust start and end dates and time-step size for a simulation. The simulator allows the user to run "what-if?" simulations by varying streamflow and sea level from their historical values. There are three major inputs to the ANN models— streamflow, coastal water level, and tidal range. Of these three inputs, the user can adjust streamflow and coastal water levels. The DSSs assume that the tidal range will not be affected by sea-level rise. To evaluate climate-change scenarios, the streamflow and water-level inputs can be manually manipulated by the user, whereas tidal range is set to the historical values. The user can raise or lower sea level using a constant value, and the user has three simulation input variable options for streamflow:

- percentage of historical streamflow to the system,
- user-set streamflow to a constant value, and
- user-defined hydrograph.

Explanations of how to use each of the options in the PRISM-2 and M2M-2 DSSs can be found in the user's manuals in appendixes 4 and 5, respectively.

The PRISM-2 3D visualization (3DVis) worksheet provides graphical longitudinal specific-conductance profiles at the South and North Ends of the Waccamaw River and AIW study area. The visualization worksheet is designed to visualize and animate periods of special interest. Data and the controls for operating the 3DVis worksheet are on the left side of the 3DVis worksheet (fig. 51). The data are a subset of the data displayed on the "Run" worksheet (appendix 4) and are provided for reference while using the 3DVis worksheet.

Two plots for the North End of the study area are shown in figure 51. The left plot shows the specific-conductance profile representing the actual historical data (when available), and the right plot shows the profile predicted by using the user-specified streamflow condition. Note that the predicted profiles are meaningful only if the models are set up to use exactly the same input streamflow condition. For example, the plots shown in figure 51 were created using all models with the Pee Dee River streamflows set at 80 percent of the actual historical streamflows.

To spatially visualize the marsh salinity response, the M2M-2 DSS is distributed with the "2D Color-Gradient Visualization Program" (fig. 52) that interpolates and extrapolates simulator output to fill and color a grid of the study area (appendix 5). The program provides a qualitative view of the large-scale, longitudinal gradients of the marsh parallel to the river, rather than a quantitative view of small-scale lateral gradients in the marsh perpendicular to the river. For the application, the seven USGS marsh gaging stations were used because of the large range of measured hydrologic conditions, especially non-drought conditions, compared with that of the GPA marsh sites.

Although the marsh-data time series provides a temporally detailed description of changing salinity conditions, the seven sites provide information only on large-scale, longitudinal gradients in the system rather than small-scale, lateral variations in the marsh. Ecological interest in marsh salinity response typically is on seasonal and annual time scales rather than the smaller time scales of riverine responses of hours and days. For the color-gradient visualization program, users can select moving-window averages of 1 to 12 months from the M2M-2 DSS simulator results.

Spatial visualization is based on a 100 meter (m; 1,076 square feet) grid of the study area. The 29,000-cell grid covers the tidal marshes from Interstate 95 to the Highway 17

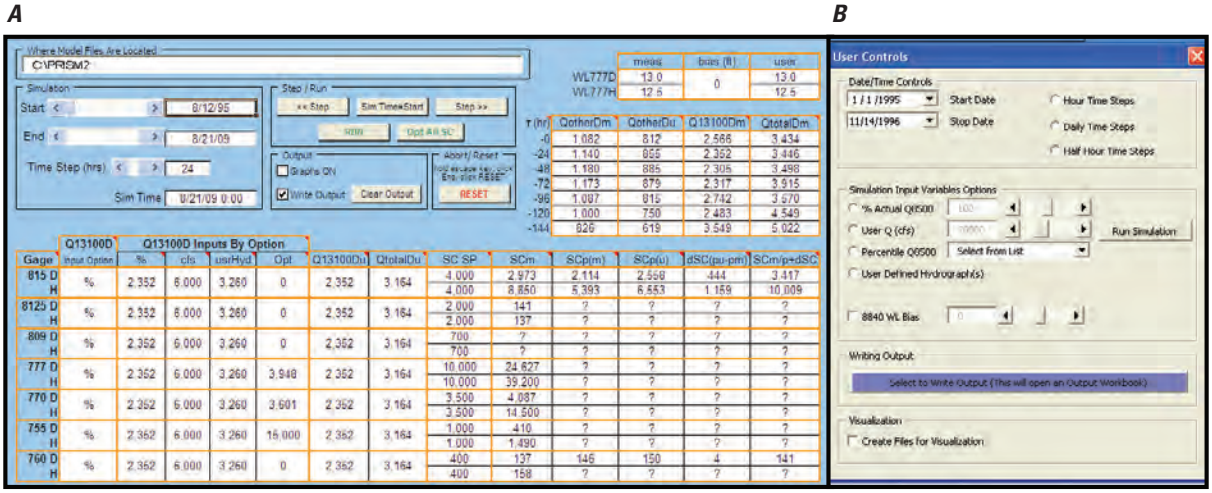

Figure 50. Screen capture of model simulation control panels used to set parameters and run a simulation in the (*A*) Pee Dee River and Intracoastal Waterway Salinity Intrusion Model-2 Decision Support System and the (*B*) Model-to-Marsh-2 Decision Support System.

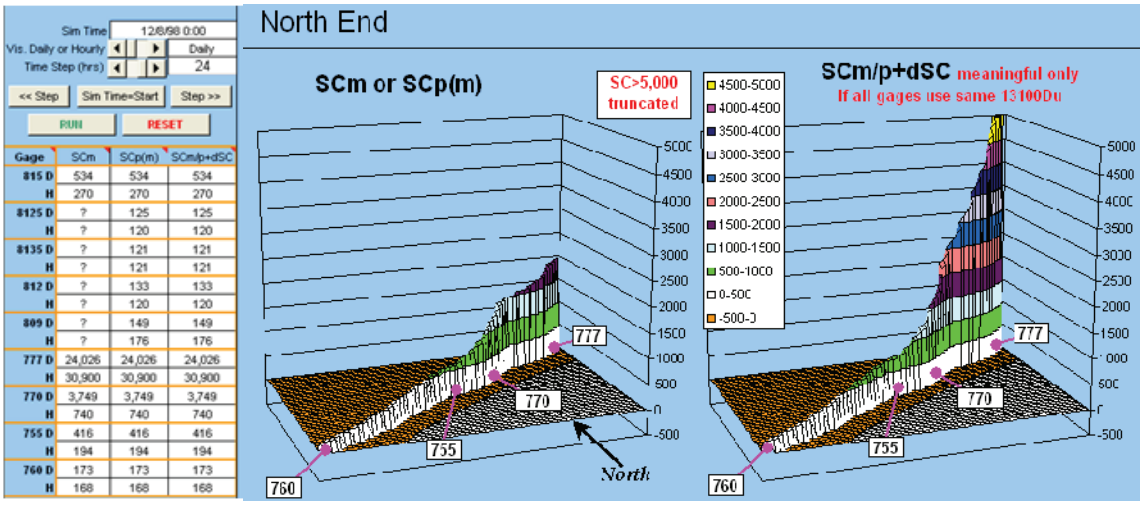

Figure 51. Screen capture of the three-dimensional visualization (3DVis) worksheet showing the specific conductance of salinity intrusion at the North End of the Waccamaw River and Atlantic Intracoastal Waterway study area, South Carolina, for a climate-change scenario (from Conrads and Roehl, 2007). Note: Gage numbers (first column on left) indicate last three or four digits of the eight- or nine-digit station numbers. Pee Dee flow input (131000Du) is set at 80 percent of the historical streamflow.

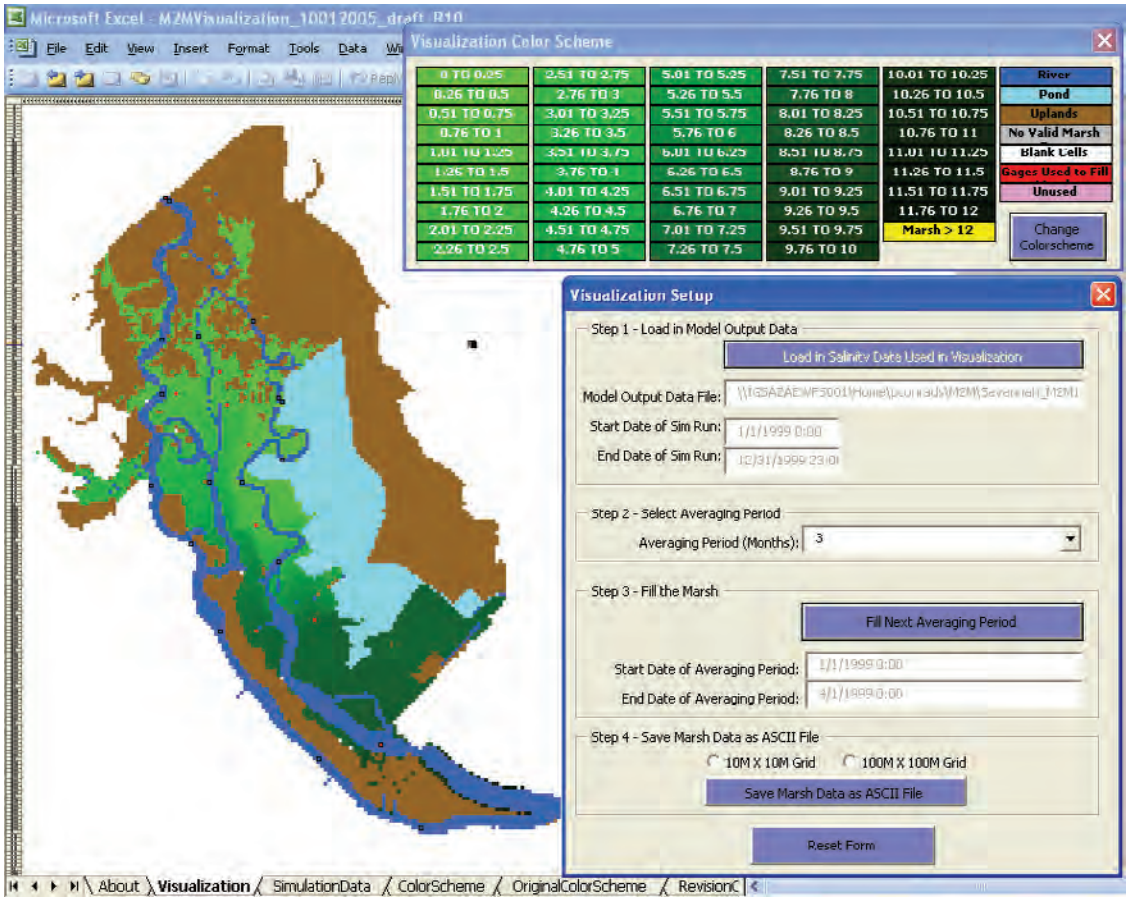

Figure 52. Screen capture of the Two-Dimensional Color-Gradient Visualization Program. Left image shows spatial distribution of marsh salinity based on data from seven U.S. Geological Survey marsh stations. Panel in the upper right of the screen shows the user-specificed color scheme. Panel in the lower right shows the users controls of the visualization program.

bridges on the Back and Front Rivers (fig. 3). Interpolation is performed using a simple ratio of linear distances between the nearest USGS marsh gaging station and the distance from a cell to the nearest gaging station. To enlarge the areal extent of measured marsh data (see USGS marsh network, fig. 11*B*), river gaging stations on the Savannah River at Interstate 95 (station 02198840; fig. 11*B*) and Back River upstream from the tide gate (fig. 11*B*) were added to interpolate and extrapolate cells upstream from sites M1 and M2 and downstream from site B4.

The program allows the user to configure the color scale and export all salinity values and grid parameters—cell size and corner coordinates—as an ASCII file for input into a mapping package such as ArcView™. In addition to the 100-m grid, a 10-m (107.6 square feet) grid (2,900,000 cells) was developed to minimize numerical computation errors when overlaying the grid data and irregular polygons in geographic information system (GIS) applications.

Climate-Change Scenarios and Simulations Using the PRISM-2 and M2M-2 Decision Support Systems

The DSS applications for Waccamaw River and AIW, and the lower Savannah River, study areas provide water-resource managers from State and local agencies a tool for evaluating changes in the timing, magnitude, frequency, and duration of salinity at gaging locations resulting from potential climate change. Prior to the final determination of potential effects near municipal intakes, several issues concerning protection of coastal water intakes need to be addressed. What level of protection is required? What is the maximum specific-conductance value that is acceptable? Is an intake required to stay online 100 percent of the time, or are limited intrusion events acceptable? Can an increase in salinity at the water-supply intake be minimized by increases in regulated streamflow? The DSSs allows users to simulate changes in sea level and streamflow, separately and in combination, and analyze the specific-conductance response at seven river gaging stations along the Grand Strand and the salinity response at five river gaging stations and seven marsh gaging stations in the lower Savannah River. The output can aid users in understanding the complex interaction of sea level, streamflow, and salinity dynamics in these estuarine systems.

The following sections describe the application of the DSSs to evaluate salinity intrusions for various climate-change scenarios, including sea-level rise and changes in streamflow. Examples using PRISM-2 are followed by examples using M2M-2 DSS. Scenarios were selected to demonstrate the capabilities of the DSSs for using changes in coastal water level (sea level) and streamflow. Scenarios include incremental sea-level rise, incremental reductions in historical flows to the study areas, combination of incremental increases in sea-level rise and incremental reductions in flow, and GCM projected flows for 2040–2070 in combination with increment increase in sea level.

The capabilities of the two DSSs are similar, and the scenarios could be simulated with the PRISM-2, the M2M-2 DSS, or both. An example using the simulated output from the Yadkin-Pee Dee watershed model that was run with downscaled precipitation and temperature inputs from a GCM also is provided. The output obtained from simulations of climate-change scenarios is only intended to demonstrate the utility of the DSSs and is not intended to be interpreted as a regulatory application of the DSSs. The results of the scenario simulations are compared to a simulated historical baseline, sometimes referred to as “predicted actual” conditions. On some plots, the measured data are shown and can be compared to the model simulation of “predicted actual” condition for an indication of the model performance. The scenarios used in this study are listed in table 12.

Table 12. Climate-change scenarios used in the Pee Dee River and Atlantic Intracoastal Waterway Salinity Intrusion Model Decision Support System-Version 2 (PRISM-2 DSS) and the Model-to-Marsh Decision Support System-Version 2 (M2M-2 DSS).

[DSS, decision support system; SLR, sea-level rise; PRISM-2 DSS, Pee Dee River and Atlantic Intracoastal Waterway Salinity Intrusion Model Decision Support System-Version 2; M2M-2 DSS, Model-to-Marsh Decision Support System-Version 2; ft, foot; na, not applicable; Q, streamflow; GCM, global circulation model; HSPF, Hydrologic Simulation Program-Fortran]

Scenario	Description	DSS	Report section	Figures	Tables
Changes in sea level					
Incremental sea-level rise	Sea-level rise in 0.5 ft increments from 0 to 3 ft	PRISM-2	Salinity response to sea-level rise: PRISM-2 DSS	56–59	na
	Sea-level rise in 0.5 ft increments from 0 to 3 ft	M2M-2	Salinity response to sea-level rise and reduced streamflow: M2M-2 DSS	70, 71	na
Changes in streamflow					
GCM-HSPF generated flow	GCM projected flows for 2040–2070	PRISM-2	Salinity response to user-defined streamflow hydrographs: PRISM-2	60–64, 66	na
Incremental Reduction in historical Q	Percent reductions in historical flows by 5, 10, 15, 20, and 25 percent	PRISM-2	Percent of historical flow: PRISM-2	67	na
Changes in sea level and streamflow					
GCM-HSPF generated flow	GCM projected flows for 2040–2070 with SLR of 1 ft and 2 ft	PRISM-2	Salinity response to user-defined streamflow hydrographs: PRISM-2	65	na
Incremental SLR and reductions in historical Q	Sea-level rise in 0.5 ft increments from 0 to 3 feet and percent reductions in historical flows by 5, 10, 15, 20, and 25 percent	PRISM-2	Salinity response to percent reductions of historical flow: PRISM-2	67, 68	14
	Sea-level rise in 0.5 ft increments from 0 to 3 feet and percent reductions in historical flows by 5, 10, 15, 20, and 25 percent	M2M-2	Salinity response to sea-level rise and reduced streamflow: M2M-2 DSS	72–74	15
	Two dimensional color-gradient visualization of the pore-water salinity in the tidal marshes a 1 ft sea-level rise and a 20 percent reduction in streamflow	M2M-2	Salinity response to sea-level rise and reduced streamflow on marsh pore-water salinity: M2M-2 DSS	75, 76	na

Sea-Level Rise: PRISM-2 and M2M-2 Decision Support Systems

In the PRISM-2 and M2M-2 DSSs, sea level can be decreased by as much as 1 ft or increased by as much as 3 ft in 0.1- ft increments. To place potential sea-level rise in the context of historical sea-level trends and accelerated sea-level rise resulting from various atmospheric-emission scenarios, a methodology developed by the U.S. Army Corps of Engineers (U.S. Army Corps of Engineers; 2011) was applied to tide data from three NOAA tide gages along the South Carolina and Georgia Coast (fig. 53).

The USACE (2011) recommends that analysts provide a minimum of three rates of sea-level rise. The low rate is based on locally measured rates of sea-level rise. These rates are preferably from tidal stations with a minimum of 40 years of data. Intermediate and high rates of sea-level rise are based on future accelerated rates resulting from various global-emission scenarios. For these rates, the USACE recommends using equations from the National Research Council (National Research Council, 1987) report "Responding to Changes in Sea Level: Engineering Implications" for low, moderate, and high accelerated sea-level-rise rates (NRC curves I, II, and III, respectively). Although the NRC report is more than 20 years old, the USACE recommends the use of the equations in the report because the sea-level rises in the scenarios are greater than those presented in the Intergovernmental Panel on Climate Change report (Intergovernmental Panel on Climate Change, 2007). The IPCC 2007 report did not take into account rapid melting of Antarctica ice, and the sea-level-rise rates are considered to be too low (U.S. Army Corps of Engineers, 2011).

Rates of local sea-level rise for seven NOAA tidal stations along or near the Georgia and South Carolina coasts were obtained from the NOAA website (*http:// tidesandcurrents.noaa.gov/ sltrends/slrmap.html*, table 13). All of the tidal stations had more than 50 years of record. Of the seven sites, the Springmaid Pier site had the highest rate of local sea-level rise, 0.161 inch per year (in/year) or 4.09 millimeters per year (mm/year). Because of their proximity to

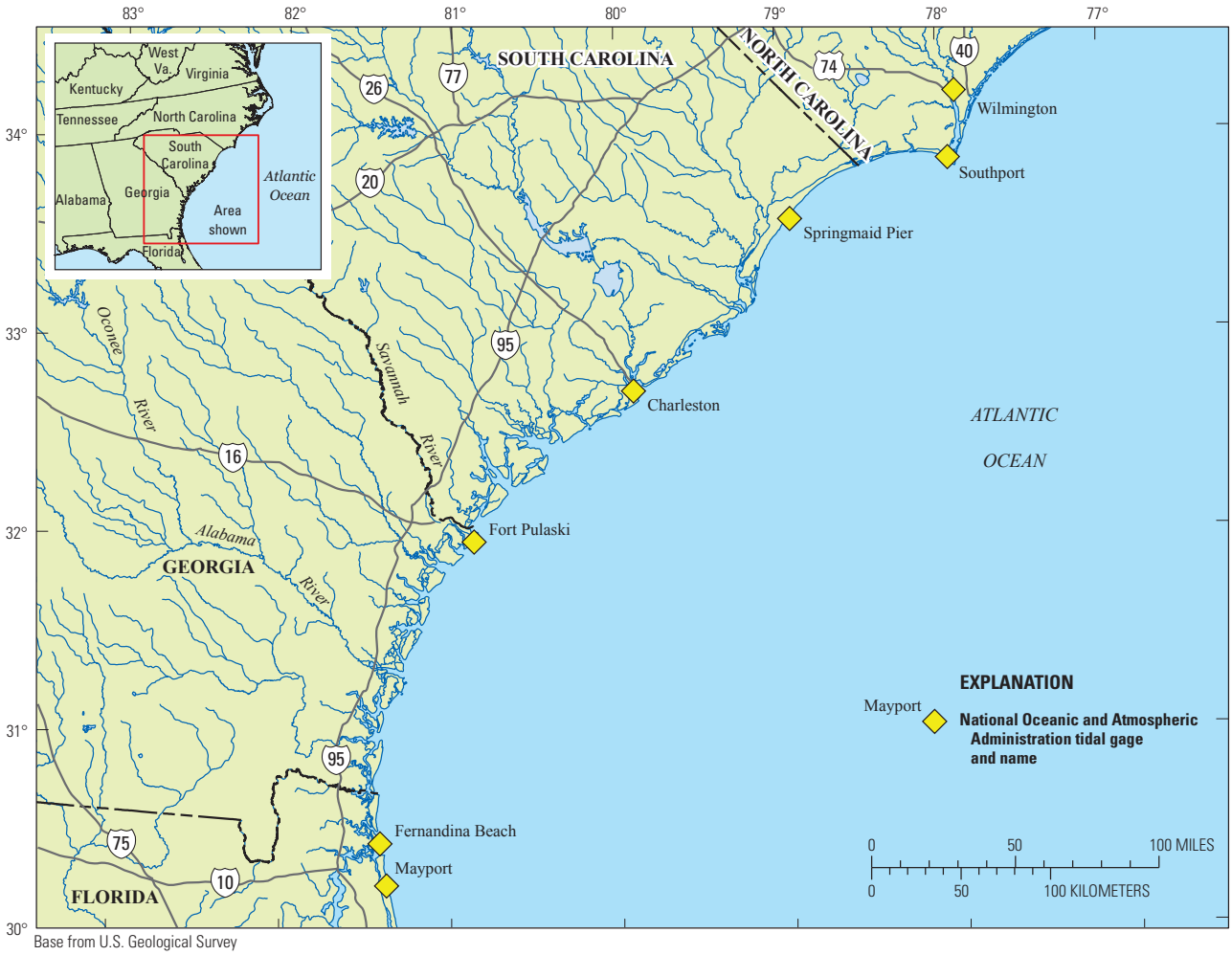

Figure 53. Location of tidal gages along the coast of North Carolina, South Carolina, Georgia, and Florida.

Table 13. Local sea-level rise rates and beginning year of data collection for seven tidal stations along the North and South Carolina, Georgia, and Florida coast.

[mm, millimeter]

Station (fig. 53)	Local sea-level rise rate (mm/year)	Beginning year of data collection
Wilmington, N.C.	2.07	1935
Southport, N.C.	2.08	1933
Springmaid Pier, S.C.	4.09	1957
Charleston, S.C.	3.15	1921
Fort Pulaski, Ga.	2.98	1935
Fernandina Beach, Fla.	2.02	1897
Mayport, Fla.	2.4	1928

the study areas, three of the sites—Fort Pulaski, Charleston, and Springmaid Pier—were selected for use in generating projected rates of sea-level rise using the approach suggested in the USACE circular (2011). For each of the three sites, four sea-level-rise rates were determined; the local historical sea-level-rise trend (table 13) and three NRC curves (I, II, and III) were computed (fig. 54). The NRC curves are adjusted for the local historical sea-level rise trend.

The sea-level-rise curves for the three sites are similar. The differences are the result of the differences in the local sea-level-rise trend. For Springmaid Pier, it is projected that a 1-ft (30.5-centimeter (cm)) rise will take 75 years, based on historical trends, or 40 years with the high accelerated sea-level-rise rate (NRC III) anticipated in response to increased global emission. For Fort Pulaski, a 1-ft sea-level rise will take more than 100 years, based on historical trends. With accelerated sea-level rise based on the NRC curves, a 1-ft rise at the three sites could take from approximately 40 to 70 years, depending on the emission scenario.

To simulate the effects of sea-level rise, the mean coastal water levels were increased in 0.5-ft increments to simulate sea-level rises of up to 3 ft in PRISM-2 and M2M-2. The specific conductance response to a 1-ft and 2-ft sea-level rise at the Pawleys Island gage (station 021108125, fig. 2), just downstream from a municipal freshwater intake, is shown for December 2001 to August 2009 in figure 55*A*. The "predicted actual" is the model simulation result of the measured data for the period. In this simulation, the magnitude and duration of the large intrusion events of 2002 and 2007 are increased with a 1- and 2-ft sea-level rise. The frequency and magnitude of the smaller intrusion events from 2002 to 2007 increase from one event with specific conductance greater than 2,000 µS/cm to four events with specific conductance greater than 2,000 µS/cm for a 1-ft sea-level rise and five events with specific conductance greater than 6,000 µS/cm for a 2-ft sea-level rise.

Simulations also indicate that the duration of salinity-intrusion events would increase with rising sea levels. The salinity intrusion during the droughts in 2002 and 2007 caused the municipal water supply intake upstream from the Pawleys Island gage to be taken offline. Figure 55*B* shows specific conductance values for the drought period of May 2007 to January 2008 and the specific conductance response simulated for 1-ft and 2-ft rises in sea level. During this simulation period, the model with historical sea-level conditions (predicted actual conditions in the figure) predicted 73 days when values were greater than 2,000 µS/cm. In contrast, for a 1-ft rise in sea level, the number of days in which specific conductance exceeded 2000 µS/cm increased to 121 days and for a 2-ft rise to 161 days. For the same period, the number of consecutive days that specific conductance for actual conditions exceeded 2,000 µS/cm was 48 (September 14 to October 31). A 1-ft rise increased the duration of the intrusion to 86 days (August 14 to November 7), and a 2-ft rise increased the duration of the intrusion to 128 days (August 12 to December 17).

Salinity intrusion events also can be viewed with the 3D visualization plots in PRISM-2. Three days of the moderate intrusion event from October 25 to 27, 2008, are shown in figure 56, along with the simulated specific-conductance response to 1-ft and 2-ft sea-level rises. The longitudinal profile of the actual conditions shows the specific conductance increased in the range of 4,500 to 5,000 µS/cm at the Hagley Landing gage (02110815) and 500 to 1,000 µS/cm at the Pawleys Island gage (021108125). A 1-ft and a 2-ft rise in sea level increases the magnitude and duration of salinity intrusions at the Pawleys Island gage and farther upstream at the Wachesaw gage (02110809). (Note that specific conductance values greater than 5,000 µS/cm are truncated in the 3D plot of figure 56.) Under simulated actual conditions, there was one day (October 26, 2008) at the Pawleys Island gage when the daily mean specific-conductance values were greater than 500 µS/cm. Simulations incorporating a 1-ft rise in sea level show that the magnitude of the event increases in the range of 2,500 to 3,000 µS/cm but lasts only 1 day of the 3-day period. For a 2-ft rise, the magnitude increased to greater than 4,000 µS/cm, and there are 3 days with specific conductance greater than 4,000 µS/cm.

For the operators of municipal water-treatment plants, often the concern with the source water is not the magnitude of the salinity intrusion but whether the specific conductance of the source water at the intake exceeds a predetermined threshold level. When the specific-conductance values of source water are greater than 1,000 to 2,000 µS/cm, additional treatment or blending with lower specific-conductance water is required to eliminate taste problems and potential health concerns. Nomographs were generated from six sea-level-rise scenario simulations with PRISM-2. The mean coastal water levels were increased in increments of 0.5 ft to simulate

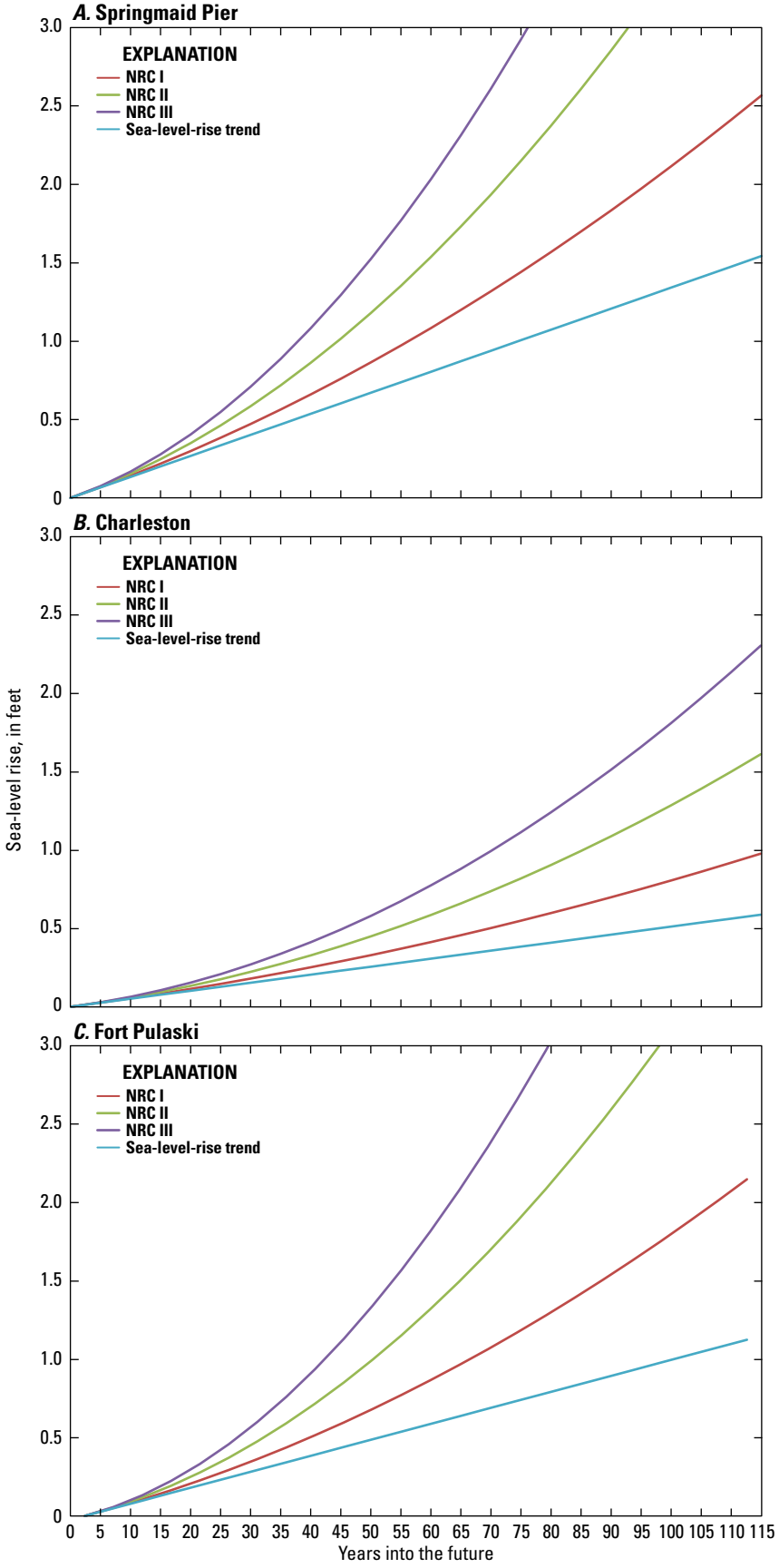

Figure 54. Sea-level rise curves for three sites along the Georgia and South Carolina coast: (*A*) Springmaid Pier, (*B*) Charleston, and (*C*) Fort Pulaski (National Research Council, 1987).

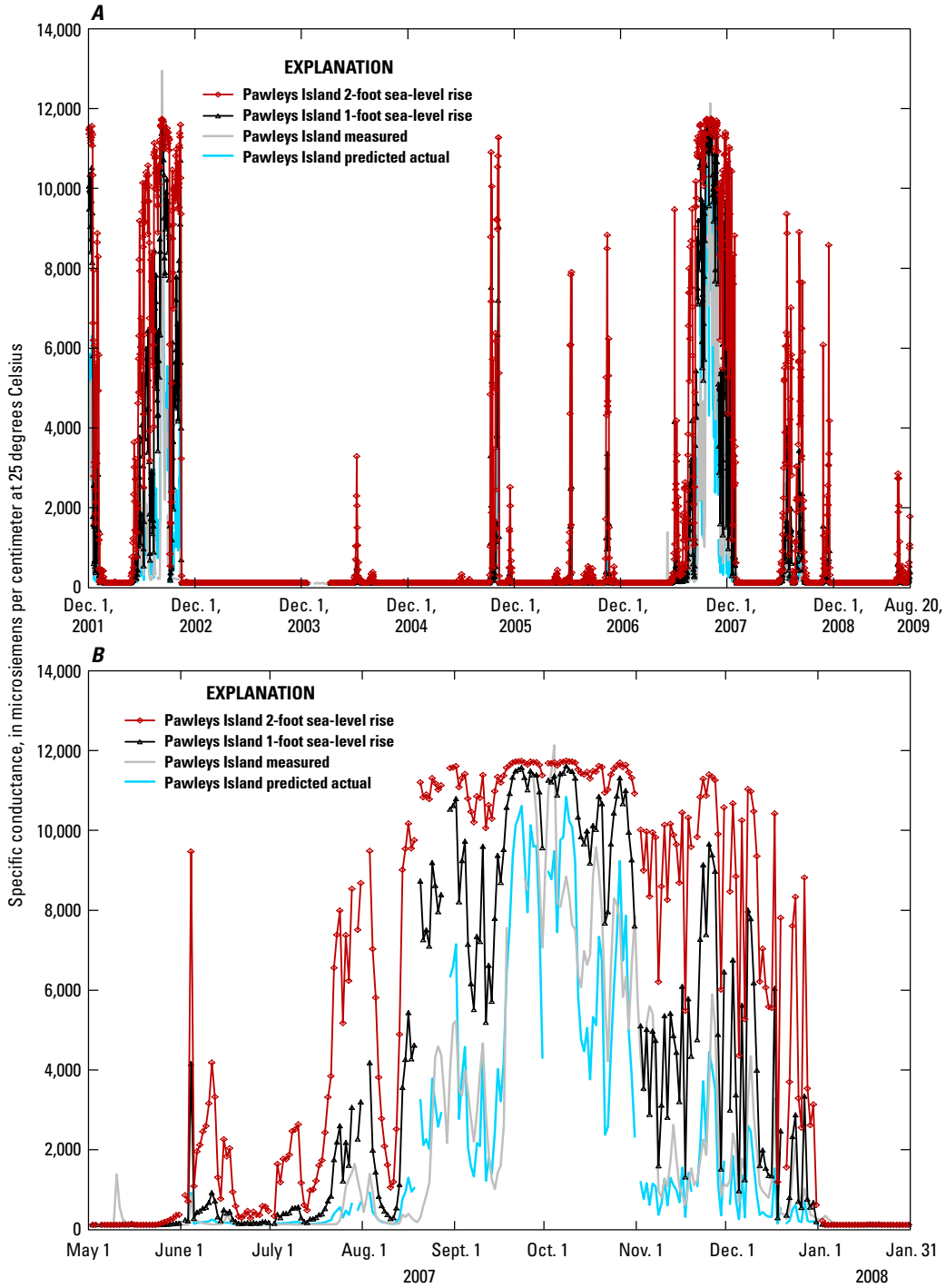

Figure 55. Simulated specific conductance at Pawleys Island gage (021108125) for actual conditions and for a 1-foot and 2-foot sea-level rise for (*A*) December 1, 2001–August 20, 2009, and (*B*) May 1, 2007–January 31, 2008.

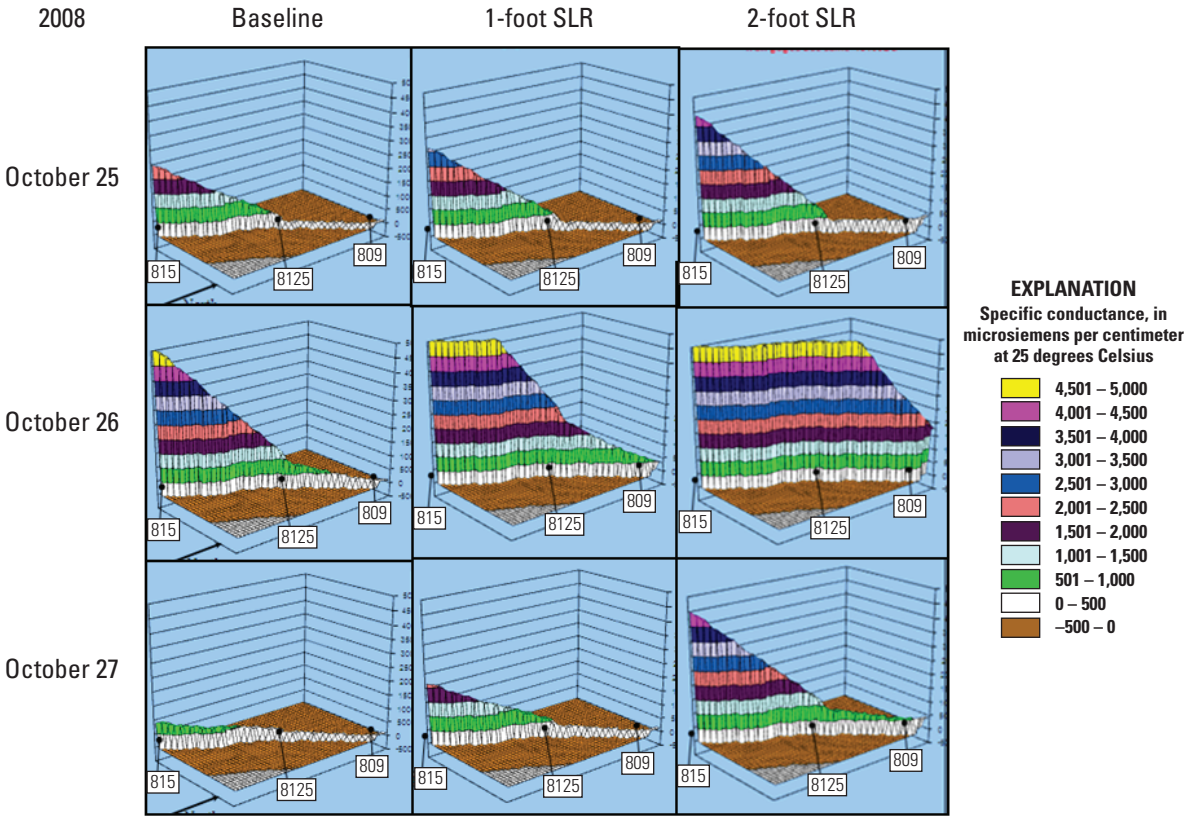

Figure 56. Screen capture of three-dimensional longitudinal plots of a salinity-intrusion event on October 25–27, 2008, at selected stations in the South End of the Waccamaw River and Atlantic Intracoastal Waterway study area, South Carolina. The plots show the specific-conductance response to historical conditions (baseline) and 1-foot and 2-foot sea-level rises (SLR) at gages along the South End. Note: The gage numbers have been shortened and distances between gage locations are approximate. Specific conductance values greater than 5,000 microsiemens per centimeter are truncated.

sea-level rises of up to 3 ft, and the number of days the predicted specific-conductance values exceeded thresholds of 1,000, 2,000, and 3,000 µS/cm for each 14-year simulation period was computed. The number of days that a specific-conductance threshold is exceeded for sea-level rises of 0 to 3 ft for the three sites on the South End and three sites on the North End are shown in figures 57 and 58, respectively. For example, under historical conditions, the simulated historical daily specific conductance at the Pawleys Island gage exceeded 2,000 µS/cm for almost 200 days during the 14-year simulation period (fig. 57*B*). Simulations of the same conditions incorporating a 1-ft sea-level rise indicate that the number of days the municipal water at the intake is unsuitable for supply would double to 400 days, and a 2-ft rise would increase the number of days when the specific conductance of water at the intake exceeded 2,000 µS/cm to 700 days.

The specific-conductance response for the North End sites differs completely from that of the South End sites. For the North End, unlike the South End, the number of days where the daily specific conductance exceeds the specified thresholds decreases with incremental increases in sea level. There is a positive net flow in the AIW from Bucksport to Little River Inlet (fig. 6) which maintains the freshwater in this reach of the AIW. The increase in sea level would also increase water levels from Little River Inlet to Winyah Bay with a larger tidal range propagating from the south (table 6). The increase in sea level would increase the gradient and net transport of freshwater along the AIW toward Little River Inlet. The effect is most pronounced at the Myrtlewood gage (fig. 58*A*) where the frequency of salinity intrusions exceeding 1,000 and 2,000 µS/cm is 30 and 180 days, respectively, during the 14-year simulation period. With a 1-ft rise in sea level,

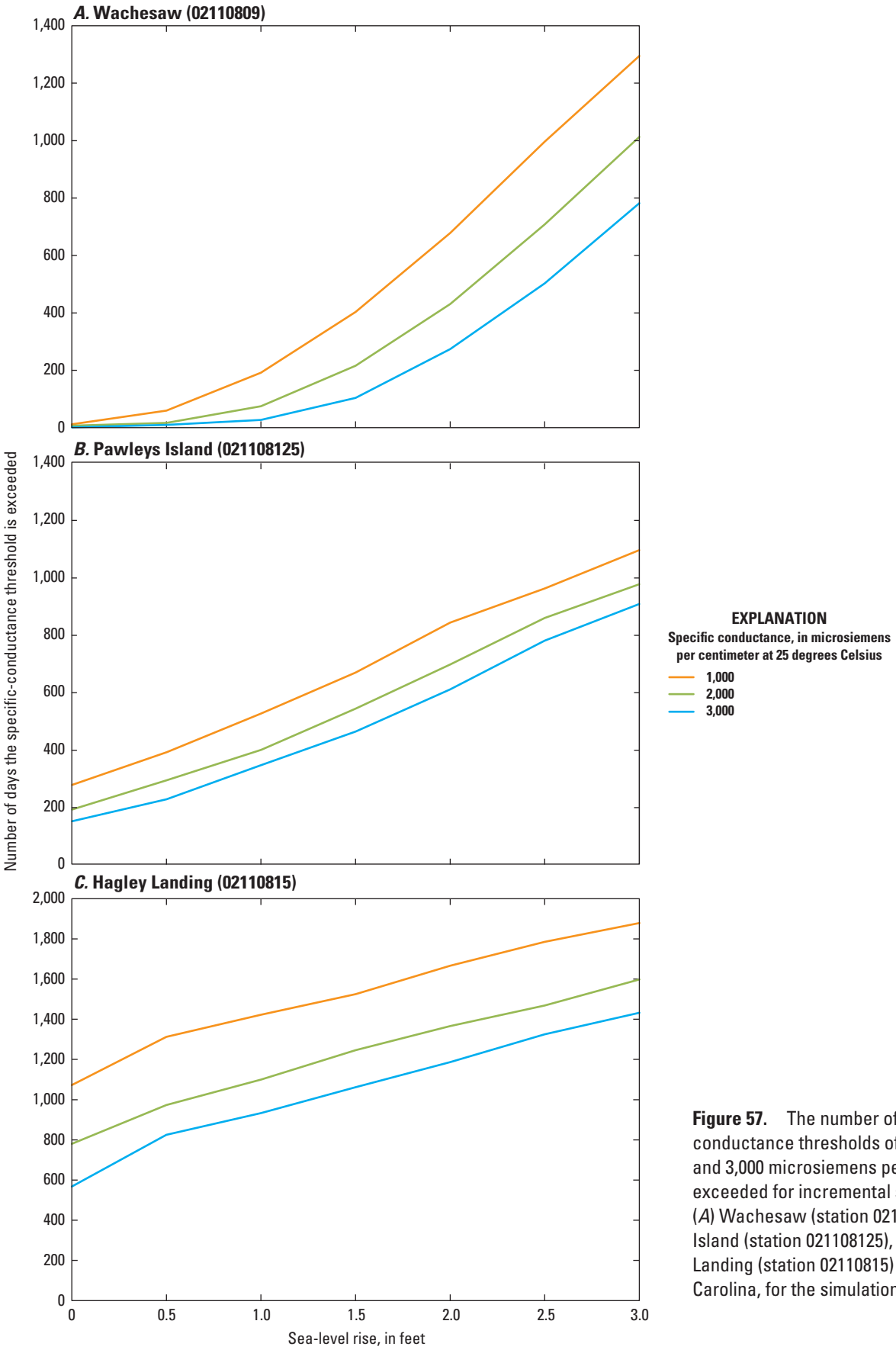

Figure 57. The number of days specific conductance thresholds of 1,000, 2,000, and 3,000 microsiemens per centimeter are exceeded for incremental sea-level rises at (*A*) Wachesaw (station 02110809), (*B*) Pawleys Island (station 021108125), and (*C*) Hagley Landing (station 02110815) gages, South Carolina, for the simulation period 1995–2009.

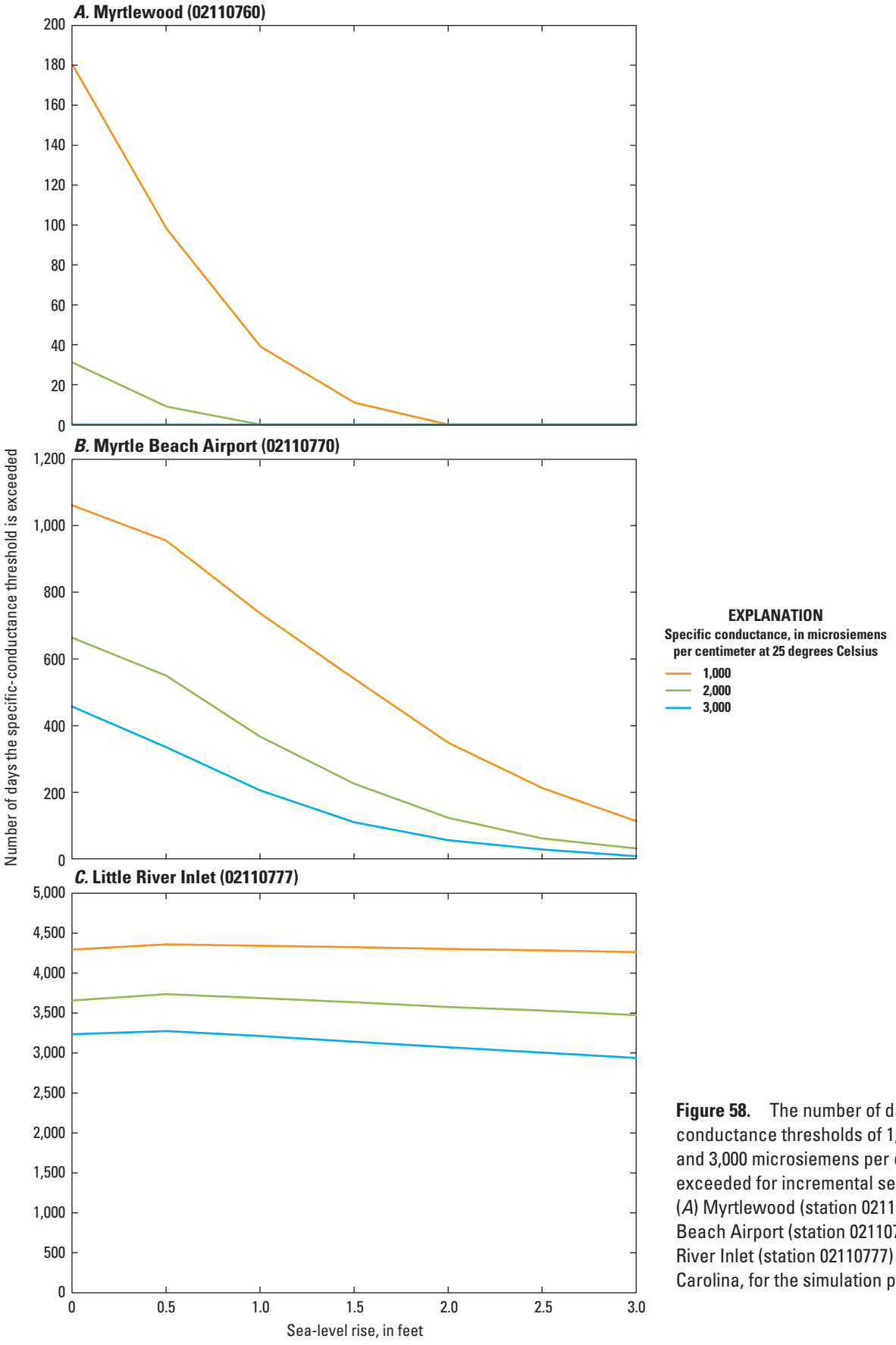

Figure 58. The number of days specific-conductance thresholds of 1,000, 2,000, and 3,000 microsiemens per centimeter are exceeded for incremental sea-level rises at (*A*) Myrtlewood (station 02110760), (*B*) Myrtle Beach Airport (station 02110770), and (*C*) Little River Inlet (station 02110777) gages, South Carolina, for the simulation period 1995–2009.

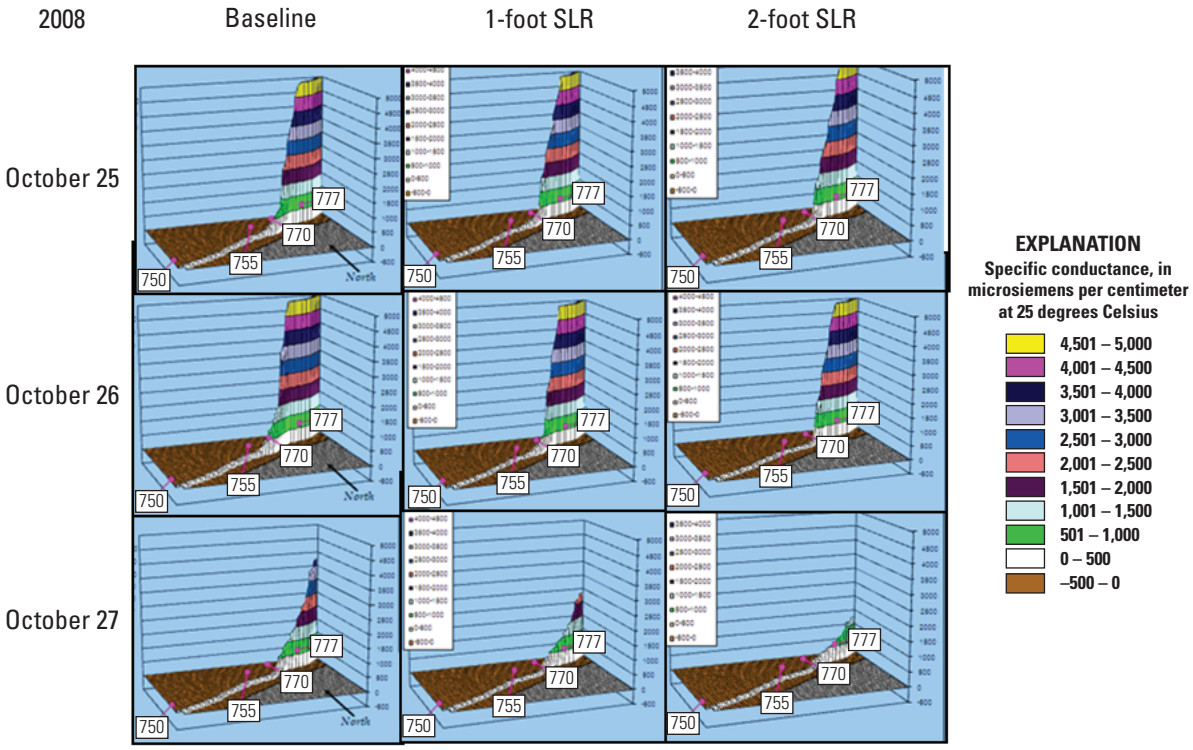

Figure 59. Screen capture of three-dimensional longitudinal plots of a salinity-intrusion event on October 25–27, 2008, at selected stations in the North End of the Waccamaw River and Atlantic Intracoastal Waterway study area, South Carolina. The plots show the specific-conductance response to historical conditions (baseline) and 1-foot and 2-foot sea-level rises (SLR) at gages along the North End. Note: The gage numbers have been shortened and distances between gage locations are approximate. Specific conductance values greater than 5,000 microsiemens per centimeter are truncated.

there are no occurrences of daily specific conductance greater than 2,000 µS/cm and only 40 days with values higher than 1,000 µS/cm. At the Little River gage, there is only a small decrease in specific conductance with sea-level rise (fig. 58*C*).

Specific conductance during the moderate intrusion event on October 25 to 27, 2008, is shown in figure 59, along with the specific-conductance response to projected 1-ft and 2-ft sea-level rises for three gaging stations along the North End of the Grand Strand. The 3D longitudinal plots in figure 59 show that the projected specific-conductance response at the North End gaging stations to a rise in sea level is smaller than that projected for the South End gaging stations (fig. 56). The longitudinal plots show limited intrusion into the AIW. A rise in sea level decreases streamflows to the south (as seen in figure 56 and the increased salinity intrusion) and increases streamflows to the north toward Little River Inlet. The effect of sea-level rise is clearly seen on the recession of the intrusion event on October 27, 2008. The simulated actual conditions (baseline) resulted in specific conductance values of 3,000 to 3,500 µS/cm, and a 2-ft sea-level rise decreased the values to 501 to 1,000 µS/cm.

Changes in Streamflow: PRISM-2

Projections of climate change for the 21st century generated by GCMs indicate changes in temperature and precipitation patterns, which will affect the timing and quantity of streamflow to the coast (Karl and others, 2009). For the southeastern United States, there is no consensus among results of the GCMs on the hydrologic response of the region. The GCMs predict that temperatures will increase. However, some models predict an overall increase in precipitation, whereas other models predict a decrease in precipitation (Karl and others, 2009). The effect of climate change projections by GCMs on salinity intrusion can be evaluated using PRISM-2 (fig. 10). The precipitation and temperature predictions of the GCM are used as inputs to the watershed model of the Yadkin-Pee Dee basin developed by the University of South Carolina [Hydrologic Simulation Program–Fortran (HSPF)]. The HSPF model simulated the streamflow for the Waccamaw, Little Pee Dee, Pee Dee, Lynches, and Black Rivers, and these data were used as defined streamflow inputs to PRISM-2. The grid scales of the GCM and Yadkin-Pee Dee basin are shown in figure 60.

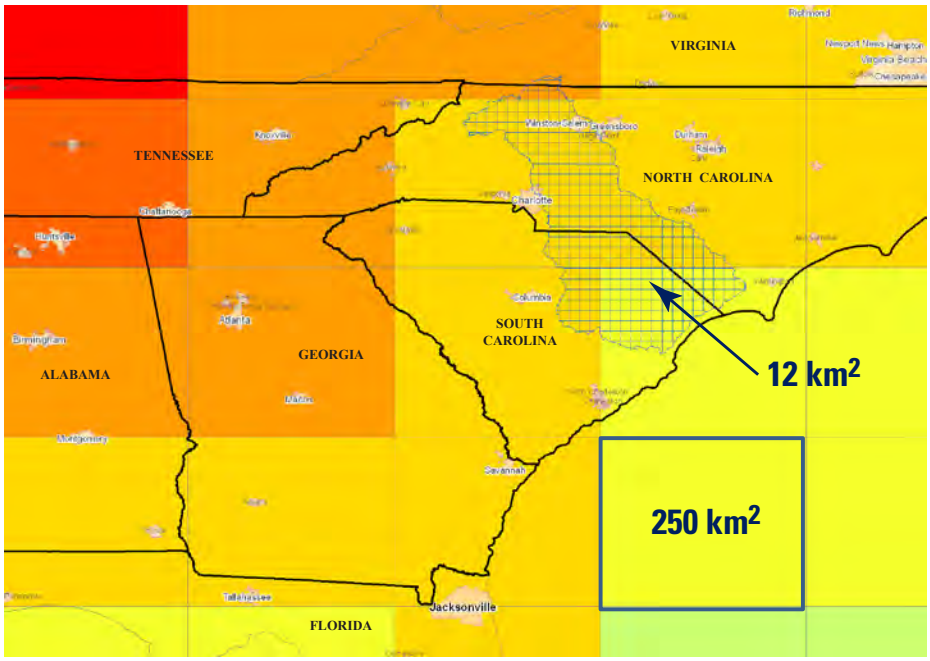

Figure 60. Example of the scale of the global circulation model (250-square-kilometer grid) and the scale of the Yadkin-Pee Dee Basin (12-square-kilometer grid), North Carolina, South Carolina, and Georgia.

User-Defined Hydrographs: PRISM-2

The downscaled temperature and precipitation data for the ECHO CGM (Legutke and Voss, 1999) for the A2 carbon emission climate scenario, which assumes that nations will continue to pursue their interests individually rather than cooperate internationally in dealing with climate change (Intergovernmental Panel on Climate Change, 2007), were used as input to the HSPF watershed model. The ECHO GCM is a hybrid coupled ocean-atmosphere GCM of the Hamburg version of the European Center atmospheric GCM (**EC**HAM) and the Hamburg Primitive Equation ocean GCM (**HO**PE). Simulations of streamflows for the Waccamaw, Little Pee Dee, Pee Dee, Lynches, and Black Rivers for 1980 to 2010 and 2040 to 2070 were obtained from the HSPF watershed model (D. Tufford, University of South Carolina Department of Biology, written commun., 2011). For the simulation period of PRISM-2 (1995–2009), single-mass curves of cumulative flow (fig. 61*A*) were generated for the total inflow (QTOTAL) for the measured and simulated data, and frequency distribution curves were generated for the ECHO-HSPF simulated total inflow for 1995 to 2009 (historical) and for total inflow projected for about 60 years in the future, 2055–2069 (fig. 61*B*). Estimates of inflow from ECHO-HSPF are fairly good, considering the number of model simulation and data processing steps needed to simulate streamflow (large scale ECHO simulation output of precipitation and temperature, statistically downscaled precipitation and temperature inputs to HSPF, and HSPF simulated streamflow output). The single mass curve (fig. 61*A*) shows that the simulated ECHO-HSPF streamflows for 1995 to 2009 are approximately the same order of magnitude as the cumulative streamflow. The ECHO-HSPF streamflow projected for 2055 to 2069 shows a decrease in the cumulative total streamflow to the coast. The shapes of the simulated frequency distributions (fig. 61*B*) for the measured and simulated streamflows are similar; however, the ECHO-HSPF simulations underestimated the frequency of streamflows below 20,000 ft^3/s and overestimated the frequency of streamflows greater than 20,000 ft^3/s.

To evaluate seasonal shifts in the projected streamflows, daily duration hydrographs were plotted using the simulated ECHO-HSPF streamflows for 1980 to 2010 and 2040 to 2070 for the total inflow to the coast (fig. 62). Although the simulated historical and simulated projected streamflows appear to be similar, there are important differences, especially with respect to potential changes in salinity intrusion. Salinity intrusion along the coast is a low-flow phenomenon; therefore, changes in the distribution of low flows are the most critical processes to be considered when assessing the potential for salinity intrusion. For the winter months (January–March), the simulated projected low flows (10th percentile) are less than the corresponding simulated historical low flows, and for the spring months (April–June), the projected low flows are only slightly less than simulated historical low flows. For the summer months (July–September), simulated projected low flows are lower than the simulated historical low flows in the beginning of July but higher than simulated historical low flows in August and September. For the fall months

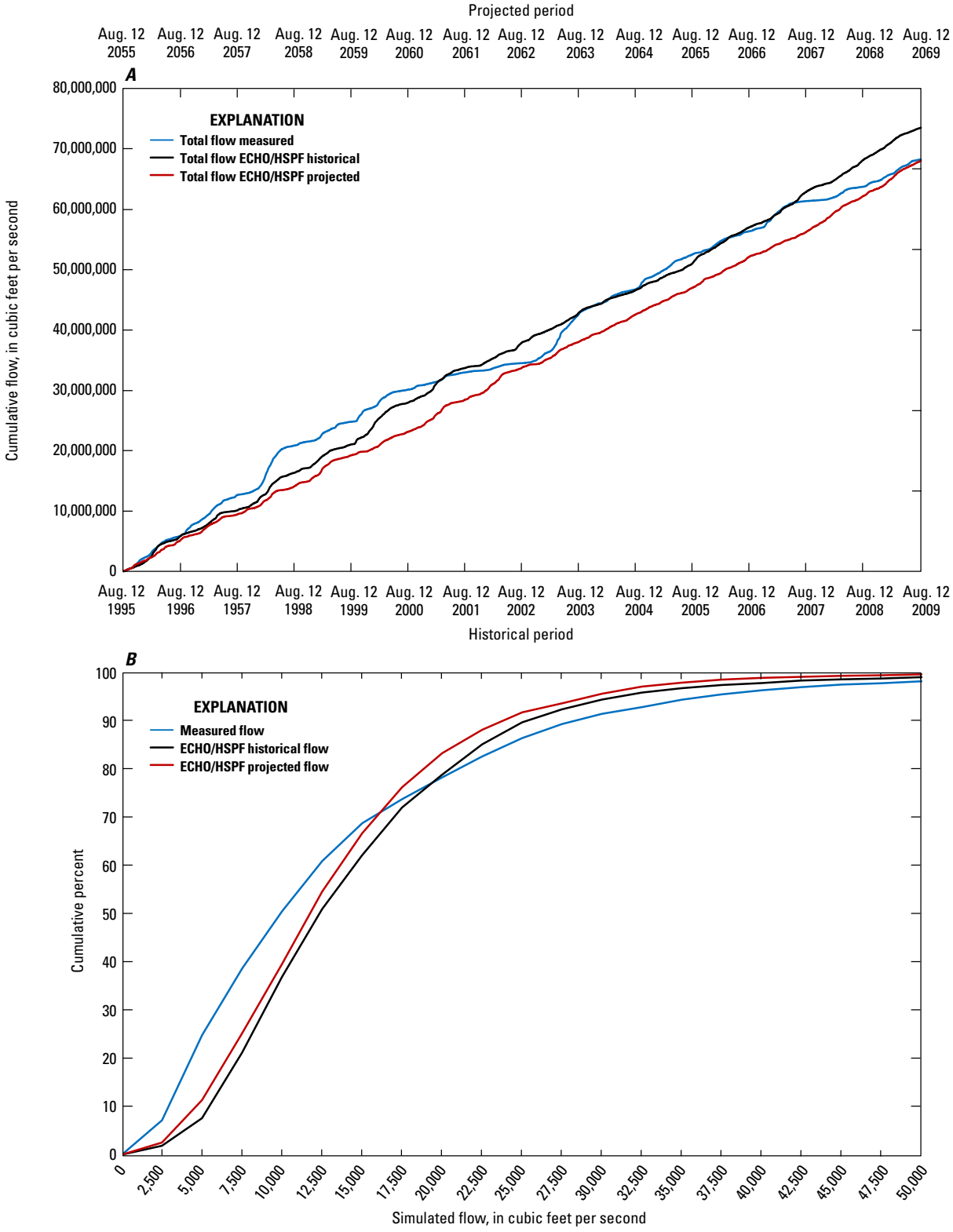

Figure 61. (*A*) The cumulative flow and (*B*) the frequency distribution for measured and simulated total flow to the Waccamaw River and Atlantic Intracoastal Waterway study area, South Carolina, for 1995–2009 and projected total flow for 2055–2069. Total flow simulated using the ECHO global circulation model and the Hydrologic Simulation Program-Fortran (HSPF) watershed model for the historical and projected periods. The ECHO GCM is a hybrid coupled ocean-atmosphere GCM of the Hamburg version of the European Center atmospheric GCM (ECHAM) and the Hamburg Primitive Equation ocean GCM (HOPE).

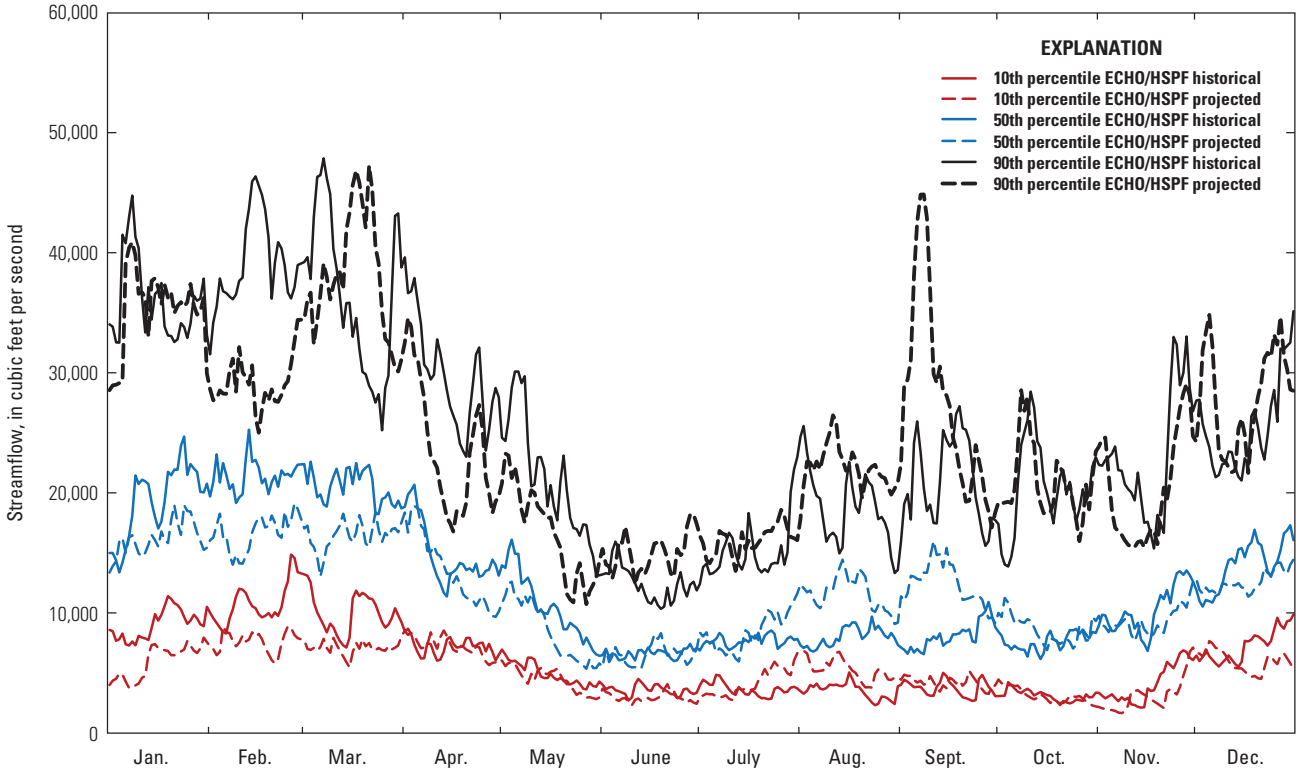

Figure 62. Daily duration hydrographs for simulated total inflow to the Waccamaw River and the Atlantic Intracoastal Waterway study area, South Carolina, for historical conditions, 1980–2010, and projected future conditions, 2040–2070. Historical and projected total flow were simulated using the ECHO global circulation model and the Hydrologic Simulation Program-Fortran watershed model. The ECHO GCM is a hybrid coupled ocean-atmosphere GCM of the Hamburg version of the European Center atmospheric GCM (ECHAM) and the Hamburg Primitive Equation ocean GCM (HOPE).

(October–December), the simulated projected low flows are less than the corresponding historical simulated low flows.

The projected ECHO-HSPF streamflows were input as user-defined hydrographs to simulate specific conductance for the 1995 to 2009 and 2055 to 2069 PRISM-2 DSS. Figure 63 shows the simulated daily specific-conductance values for the Pawleys Island gage (021108125) generated for historical and projected streamflow conditions. Substantial differences in the time series are not obvious. The future period was not selected to be meteorologically synchronized with the historical conditions of 1995 to 2009. That is to say, there is probably little value or information to be gained by noting that the intrusion event in October 2001 did not occur 60 years in the future in October 2061 or that there were large salinity intrusions in October 2003 and October 2063. The two 14-year simulations (1995–2009) do provide the data to evaluate relative changes in the timing and frequency of salinity intrusions given a particular climate-change scenario.

One approach to comparing the simulations of historical and projected specific conductance for the Pawleys Island gage (021108125) is to determine whether there are seasonal shifts in the occurrence of salinity-intrusion events that correspond to the seasonal changes in projected low flows simulated using ECHO-HSPF (fig. 62). To do this, the numbers days in which the specific conductance exceeded a threshold of 1,000 µS/cm were counted for each season (fig. 64). The simulation of the historical specific conductance shows the highest number of days with specific concentrations greater than 1,000 µS/cm occurs in the summer (July–September) with a small decrease in the number in the fall (October–December). Results of the simulation of specific conductance for the projected streamflow condition shows a change in the occurrence of intrusion events with greater than 1,000 µS/cm. The number of intrusion events increases in the spring (April–June) and decreases in the summer; most of the events occur in the fall. Under potential future climate

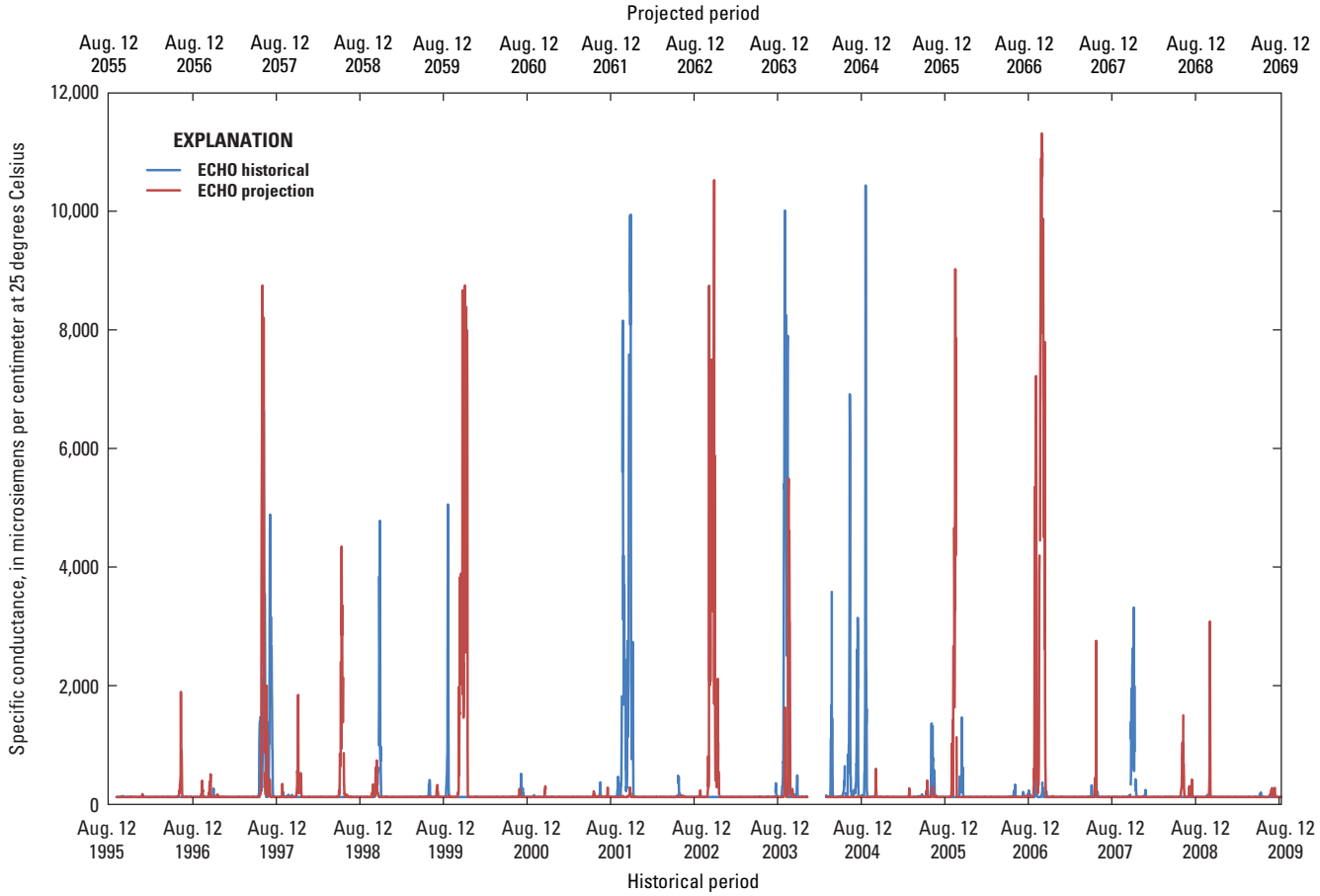

Figure 63. Simulated historical, 1995–2009, and projected, 2055–2069, daily specific-conductance values generated for Pawleys Island, South Carolina (station 021108125), using the simulated flows from the ECHO global circulation model and the Hydrologic Simulation Program-Fortran watershed model. The ECHO GCM is a hybrid coupled ocean-atmosphere GCM of the Hamburg version of the European Center atmospheric GCM (ECHAM) and the Hamburg Primitive Equation ocean GCM (HOPE).

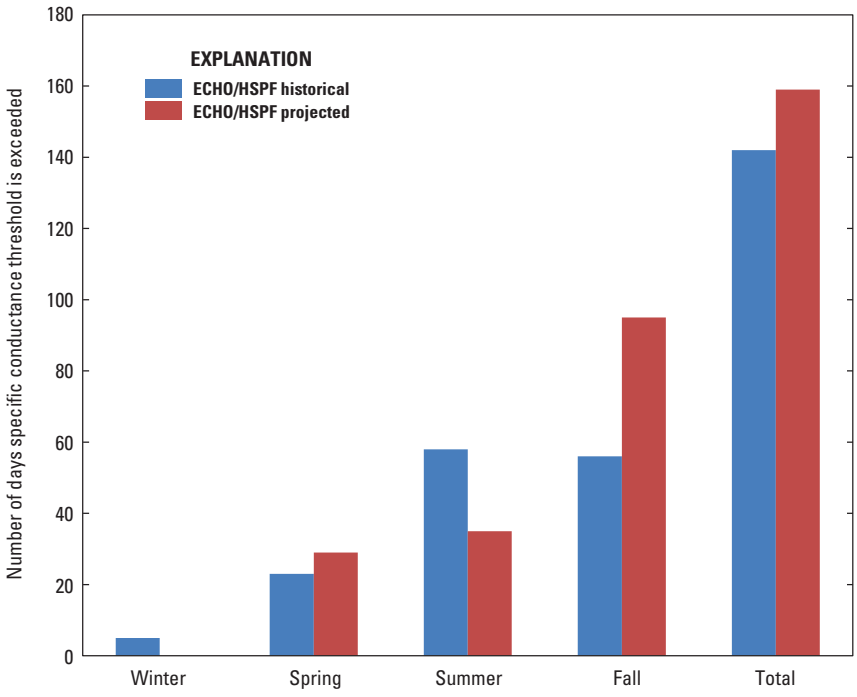

Figure 64. Number of days per season in which the daily specific conductance threshold of 1,000 microsiemens per centimeter is exceeded at the Pawleys Island gage (station 021108125), South Carolina, for the historical 1995–2009, and future, 2055–2069, simulation periods. Simulated historical and projected conditions based on total flow to the Waccamaw River and Atlantic Intracoastal Waterway study area using the ECHO global circulation model and the Hydrologic Simulation Program-Fortran (HSPF) watershed model. The ECHO GCM is a hybrid coupled ocean-atmosphere GCM of the Hamburg version of the European Center atmospheric GCM (ECHAM) and the Hamburg Primitive Equation ocean GCM (HOPE).

change, there will still be the convergence of conditions of low flow and high coastal water level to initiate an intrusion event. The decrease in the number of summer intrusion events corresponds to an increase in the 10th percentile projected streamflows seen in figure 62. Likewise, the increase in fall intrusion events corresponds to the slight decrease in the low flows in November and December. The decrease in the winter 10th percentile streamflow, although substantial, is not sufficient to cause an intrusion event.

The ECHO-HSPF streamflows also were simulated in PRISM-2 in combination with a 1-ft and 2-ft sea-level rise (fig. 65*A*). The seasonal shift in the number of days with specific conductance greater than the 1,000 µS/cm threshold from summer to fall with the projected streamflow conditions

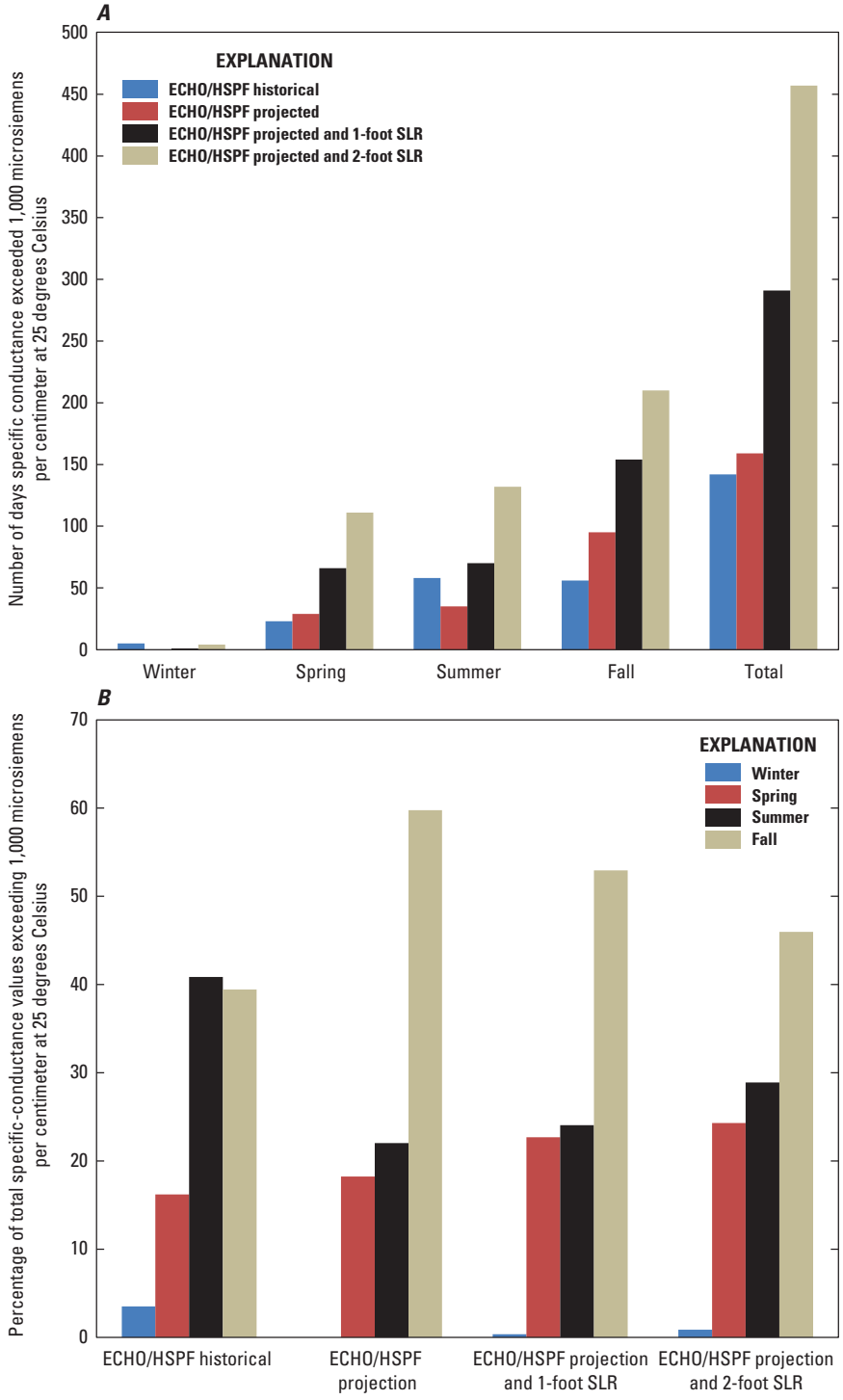

Figure 65. (*A*) The number of days in each season that the specific conductance threshold of 1,000 microsiemens per centimeter is exceeded at the Pawleys Island gage (021108125), South Carolina, for the historical, 1995–2009, projected, 2055–2069, climate changes, and projected climate changes in combination with a 1-foot sea-level rise, and a 2-foot sea-level rise, and (*B*) the percentage of simulated specific-conductance values exceeding 1,000 microsiemens per centimeter each season. Simulated historical and projected conditions are based on total flow to the Waccamaw River and Atlantic Intracoastal Waterway study area using the ECHO global circulation model and the Hydrologic Simulation Program-Fortran (HSPF) watershed model. The ECHO GCM is a hybrid coupled ocean-atmosphere GCM of the Hamburg version of the European Center atmospheric GCM (ECHAM) and the Hamburg Primitive Equation ocean GCM (HOPE).

also occurs in conjunction with 1-ft and 2-ft increases in sea level. The data in figure 65*A* are presented as the total number of days for each season and simulation. Although there is the shift in the number of days to the fall, the 1-ft and 2-ft sea-level rises show that the percentage of days in the fall decreases and the percentage of days in the winter, spring, and summer increases.

Streamflow as a Percentage of Historical Streamflow: PRISM-2

An alternative to basing future streamflow on output from GCMs is to reduce the historical streamflow by a specified percentage. As seen in the previous scenarios, decreases in streamflow increase the potential for salinity intrusion and increases in streamflow decrease the potential for salinity intrusion. As a result of the decrease in projected streamflow (fig. 61) and shifts in the timing of low flows (fig. 62), there is a wide range in the daily changes in the simulated historical and projected low flows. The daily differences between the ECHO-HSPF simulated 10th percentile historical and projected streamflows range from decreases in low flows of 60 percent to increases in low flows of 120 percent (fig. 66). Overall, the net decrease in the 10th percentile streamflows is 17.3 percent.

To evaluate net reductions in streamflows, the historical streamflow inputs used in the PRISM-2 DSS were reduced by 5, 10, 15, 20, and 25 percent. Similar to the analysis of sea-level rise (fig. 57), the numbers of days the specific conductance threshold is exceeded for each 5-percent incremental decrease in streamflow and 0-, 1-, and 2-ft sea-level rise is shown in figures, 67*A*, *B*, and *C*, respectively. A 25-percent decrease in the streamflow increased the number of days the thresholds are exceeded by approximately 45 to 90 percent for each of the three sea-level scenarios. The combined effect of a 2-ft sea-level rise and 25-percent reduction in streamflows increased the number of days the thresholds are exceed by 440 to 645 percent. For example, if the threshold is 2,000 µS/cm, then historically in the 14-year simulation there are 191 days in which the threshold is exceeded (fig. 67*A*). If the historical streamflow is reduced by 25 percent and there is a 2-ft sea-level rise, the number of days the threshold is exceeded increases to 1,067 days (fig. 67*C*), or 21 percent of the days

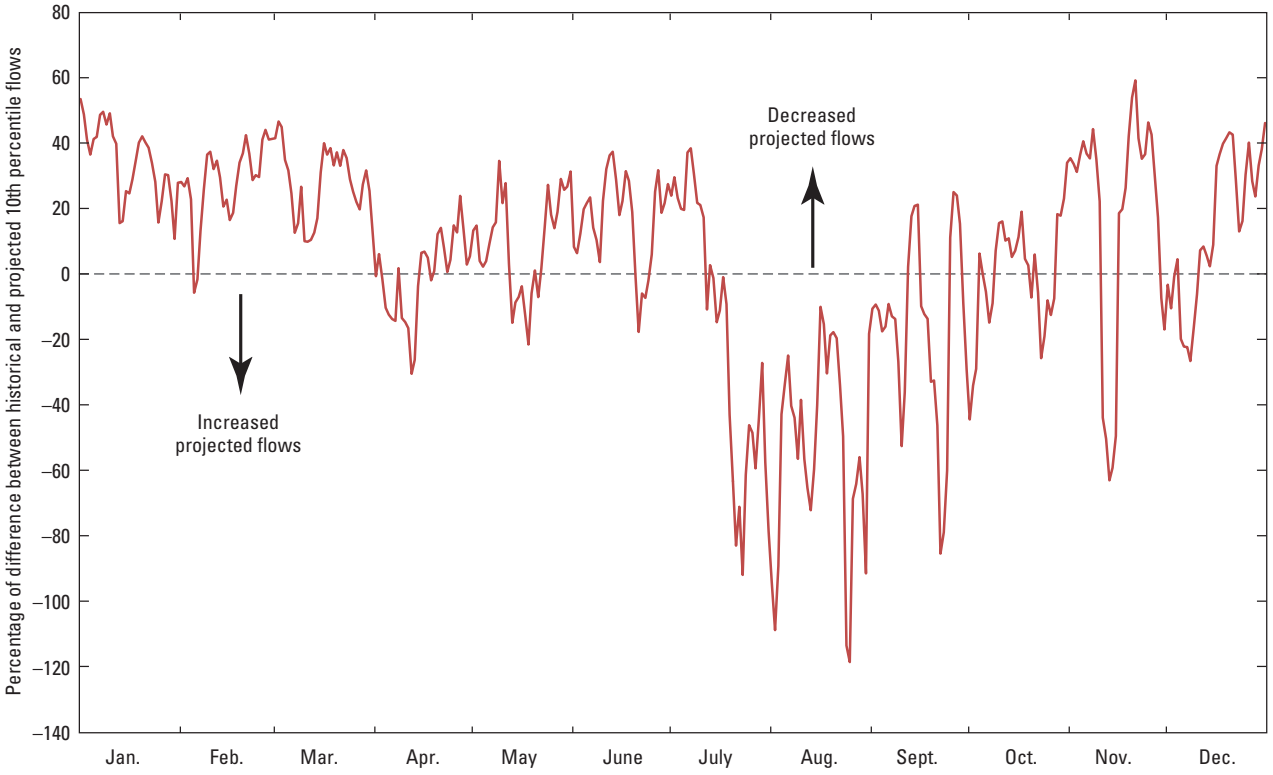

Figure 66. Effects of potential climate change on simulated flow to the Waccamaw and Atlantic Intracoastal Waterway study area, South Carolina, expressed as the difference between the daily 10th percentile of flow for future, 2040–2070, and historical, 1980–2010, periods. Positive differences represent a decrease in projected flows and negative differences represent an increase in projected flows. Simulated historical and projected conditions are based on total flow to the Waccamaw River and Atlantic Intracoastal Waterway study area using the ECHO global circulation model and the Hydrologic Simulation Program-Fortran (HSPF) watershed model. The ECHO GCM is a hybrid coupled ocean-atmosphere GCM of the Hamburg version of the European Center atmospheric GCM (ECHAM) and Hamburg Primitive Equation ocean GCM (HOPE).

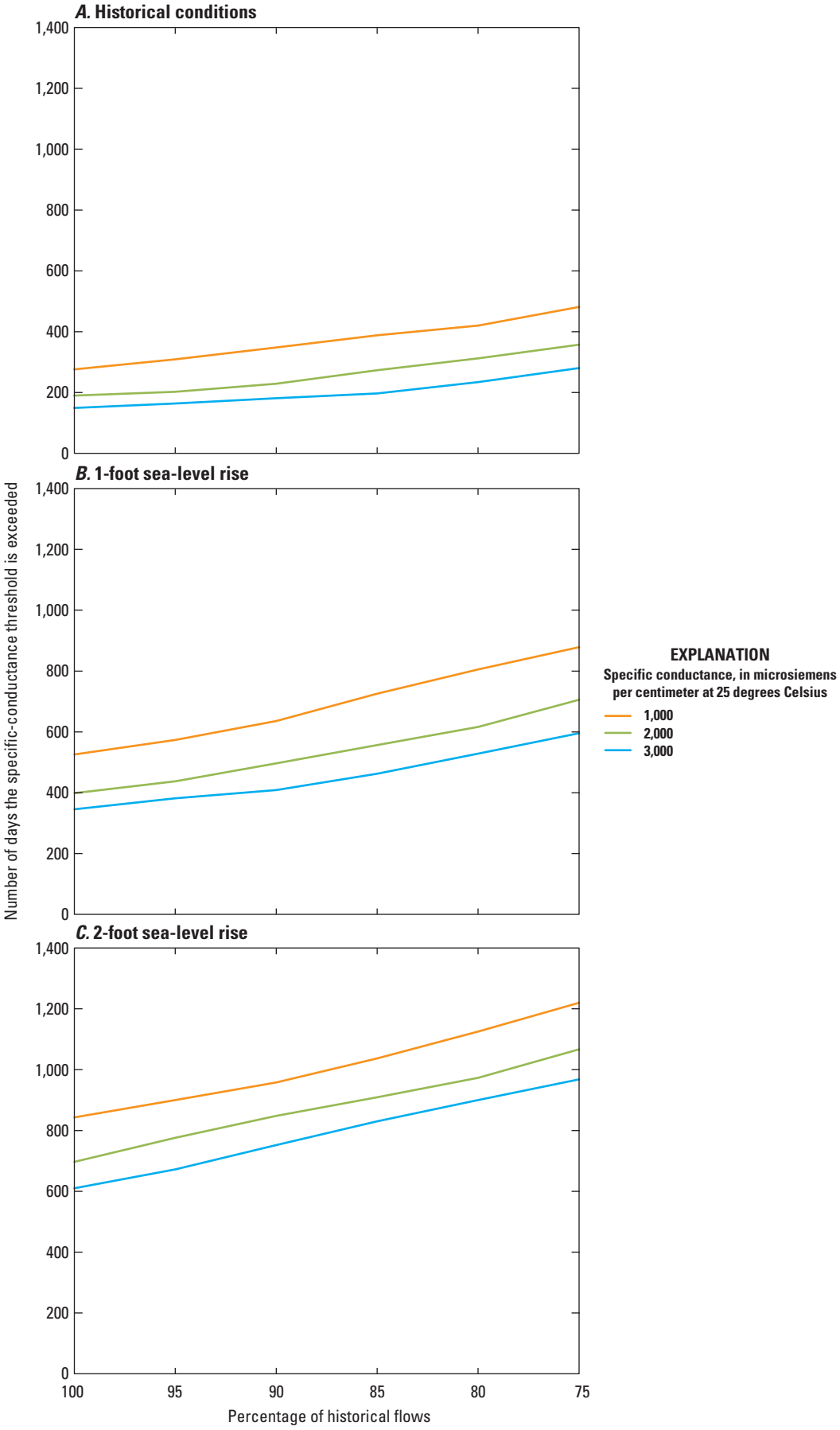

Figure 67. Number of days specific-conductance thresholds of 1,000, 2,000, and 3,000 microsiemens per centimeter are exceeded at the Pawleys Island gage (station 021108125), South Carolina, for incremental reductions of flow for (*A*) historical conditions, (*B*) a 1-foot sea-level rise, and (*C*) a 2-foot sea-level rise, during 1995–2009.

for the 14-year simulation, compared to the 4 percent of the days for the historical condition.

The results for 42 model scenarios incorporating sea-level rise and reduction in streamflows are provided in table 14. Rather than expressing the results as the number of days the threshold is exceeded for the 14-year simulation period, the results are presented as the percentage of days the threshold is exceeded for the 14-year simulation period. For example, for simulated historical conditions (no reduction in streamflow and no rise in sea level), the threshold of 1,000 µS/cm is exceeded 5.4 percent of the time for the 14-year simulation. For a reduction in streamflow of 10 percent and a rise in sea level of 1.0 ft, the percentage of time the threshold is exceeded is 13.3, or an increase of 7.9 percent. The response of specific conductance to combinations of sea-level rise and reduced streamflow also can be displayed as a 3D response surface. The percentage of time the threshold of 1,000 µS/cm is exceeded (z-axis) for 0.5-ft increments of sea-level rise up to 3 ft (x-axis) and for reductions in streamflow in increments of 5 percent (y-axis) for the Pawleys Island streamgaging station (021108125) are shown in figure 68. For no change in sea-level and no reduction in streamflow, the 1,000 µS/cm threshold is exceeded 5.4 percent of the time. For a 3-ft sea-level rise and a 25-percent reduction in streamflow, the percentage of time the threshold is exceeded increased to 32.9 percent. The 3D response surface also shows that specific conductance is much more sensitive to sea-level rise than to reductions in streamflow, as can be seen in the difference in the slope along the incremental rise in sea level axis versus the percent reduction in streamflow axis.

Table 14. Percentage of time in a 14-year simulation that the specific-conductance threshold of 1,000 microsiemens per centimeter was exceeded at the Pawleys Island gage (station 021108125), South Carolina, as a result of reductions in historical streamflow and sea-level rises.

[µS/cm, microsiemens per centimeter at 25 degrees Celsius; % flow, percent reduction in historical flows; SLR, sea-level rise; ft, feet]

% Flow/SLR	Percent of days with specific conductance greater than 1,000 µS/cm[1]						
	0 ft	0.5 ft	1 ft	1.5 ft	2 ft	2.5 ft	3 ft
0	5.4	8.3	11.0	14.0	17.6	20.1	22.8
–5	6.1	9.0	12.1	15.7	18.8	21.5	24.5
–10	7.0	10.0	13.3	17.2	20.0	23.1	26.1
–15	8.2	11.3	15.2	18.6	21.7	24.9	27.9
–20	8.9	15.1	16.8	20.0	23.5	26.6	29.8
–25	10.1	14.4	18.3	21.8	25.5	28.8	32.6

[1]The model simulation period is June 1994 to July 2008.

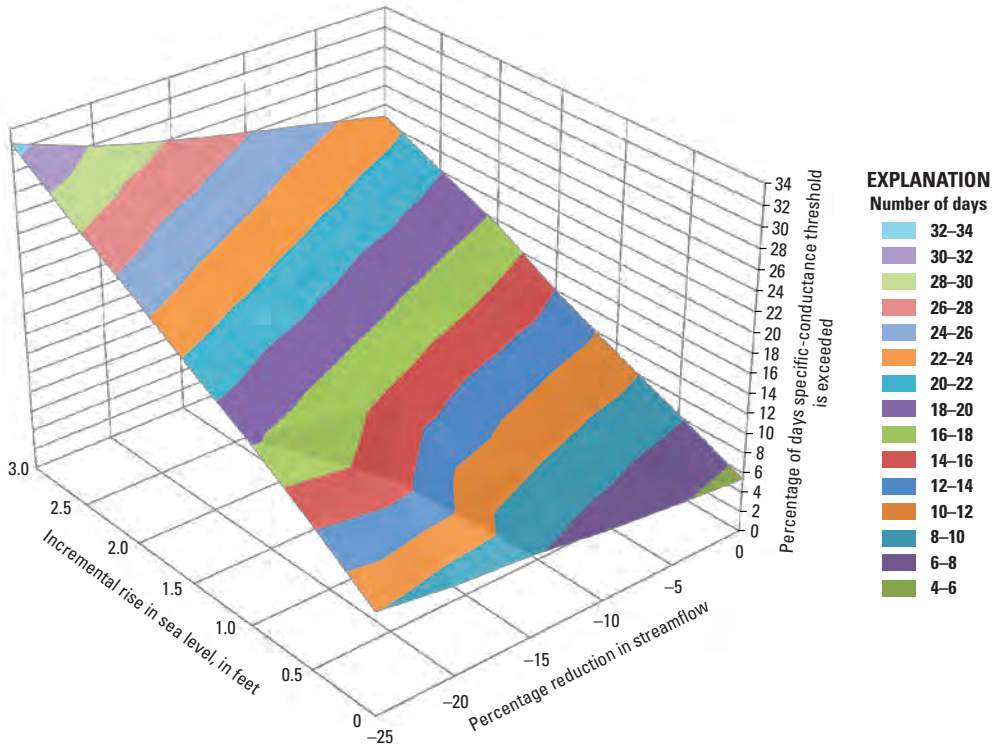

Figure 68. Three-dimensional response surface showing the percentage of days the simulated specific conductance exceeded the threshold of 1,000 microsiemens per centimeter with reductions in streamflow and incremental rises in sea level at the Pawleys Island gage (station 021108125), South Carolina, 1995–2009.

Climate-Change Scenarios Using the M2M-2 DSS

Many of the climate-change scenarios that were simulated with PRISM-2 for the Waccamaw River and AIW study area can be simulated with the M2M-2 for the lower Savannah River study area. However, there are several differences between the two DSSs. The output from the M2M-2 is expressed in salinity units (practical salinity units) rather than specific conductance, as with the PRSIM-2. A salinity value of 0.5 psu is approximately equal to 1,000 µS/cm. The M2M-2 DSS does not have the 3D longitudinal plotting utility but does have a two-dimensional (2D) visualization utility to display a plan view of the pore-water salinity in the marsh. The simulation period for the M2M-2 is 11 years, April 1994 to May 2005. Because a watershed model to simulate streamflow at the Savannah River at Clyo, Ga., (the streamflow input gage for the M2M-2) has not been developed for use with precipitation and temperature inputs, determining streamflow under future climate projections, based on downscaled precipitation and temperature data, was not feasible.

Two municipal water intakes are located in the lower Savannah River, approximately 3 miles and 15 miles upstream from Interstate 95. The scenarios presented in this section focus on the two gaging stations that are proximal to the salt-sensitive resources—the Little Back River (station 021989784; fig. 11*A*) in the Savannah National Wildlife Refuge and the Interstate 95 gage (02198840; fig. 11*A*), the streamgaging station closest to the municipal water intakes.

There is great variability in the magnitude, frequency, and duration of salinity-intrusion events in the upper reaches of the lower Savannah River estuary, as illustrated by the time series (April 1994–April 2005) for three gaging stations in the upper reaches of the river (fig. 69). The salinity was highest at the Houlihan Bridge gage (station 02198920, fig. 11*A*), often in the 4 to 8 psu range, and high salinity intrusions occurred in the 10 to 14 psu range. At the Interstate 95 gage (02198840), 6.2 miles upstream from the Houlihan Bridge gage, the salinity rarely was above the 0.5 psu level. At the Lucknow Canal gage (station 021989784; fig. 11*A*) on the Little Back River, approximately 2.2 mile to the east, salinities were often less than 0.5 psu; some salinities were as high as 2 and 3 psu.

Response of Rivers to Sea-Level Rise: M2M-2 DSS

A total of 42 scenarios encompassing reductions of streamflow in 5-percent increments, ranging from 0 to 25 percent, were evaluated in combination with increases in sea level in 0.5 ft increments, ranging from 0 to 3 ft.

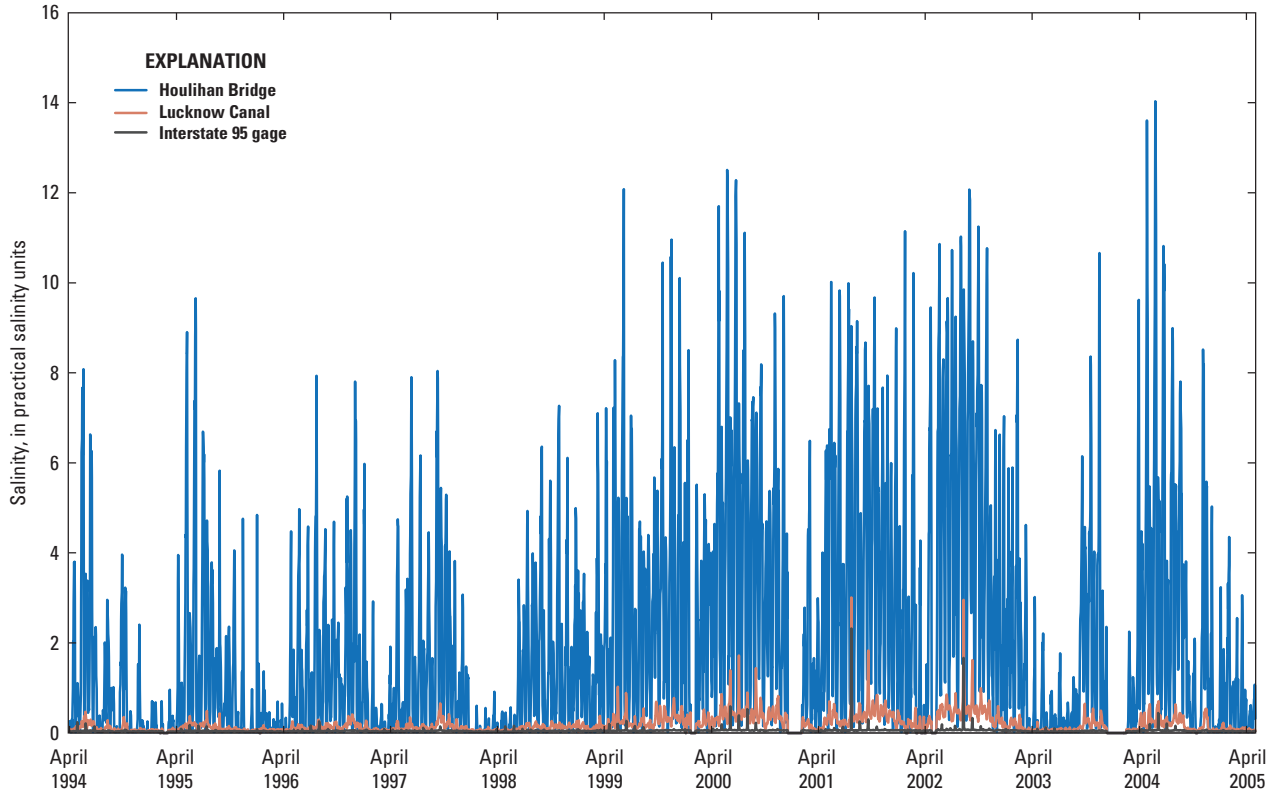

Figure 69. Measured daily salinity at the Houlihan Bridge gage (station 02198920), Lucknow Canal gage (station 021989784),and the Interstate 95 gage (station 02198840) in the vicinity of the Savannah National Wildlife Refuge, South Carolina and Georgia, April 1994–April 2005.

Simulations were run for the three upstream gaging stations in the lower Savannah River study area. The simulated salinities for the three gaging stations in response to a 1- and 2-ft rise in sea level are shown in figure 70. For the Interstate 95 gage and Lucknow Canal gage (fig. 70*A* and 70*B*), the number of salinity-intrusion events for a 1-ft sea-level rise was much greater than the number of events for historical conditions (baseline). Note that ANN models limit the extrapolation of the salinity response to a little over 6 psu at the Interstate 95 gage (fig. 70*A*). Likewise, the extrapolation of the salinity

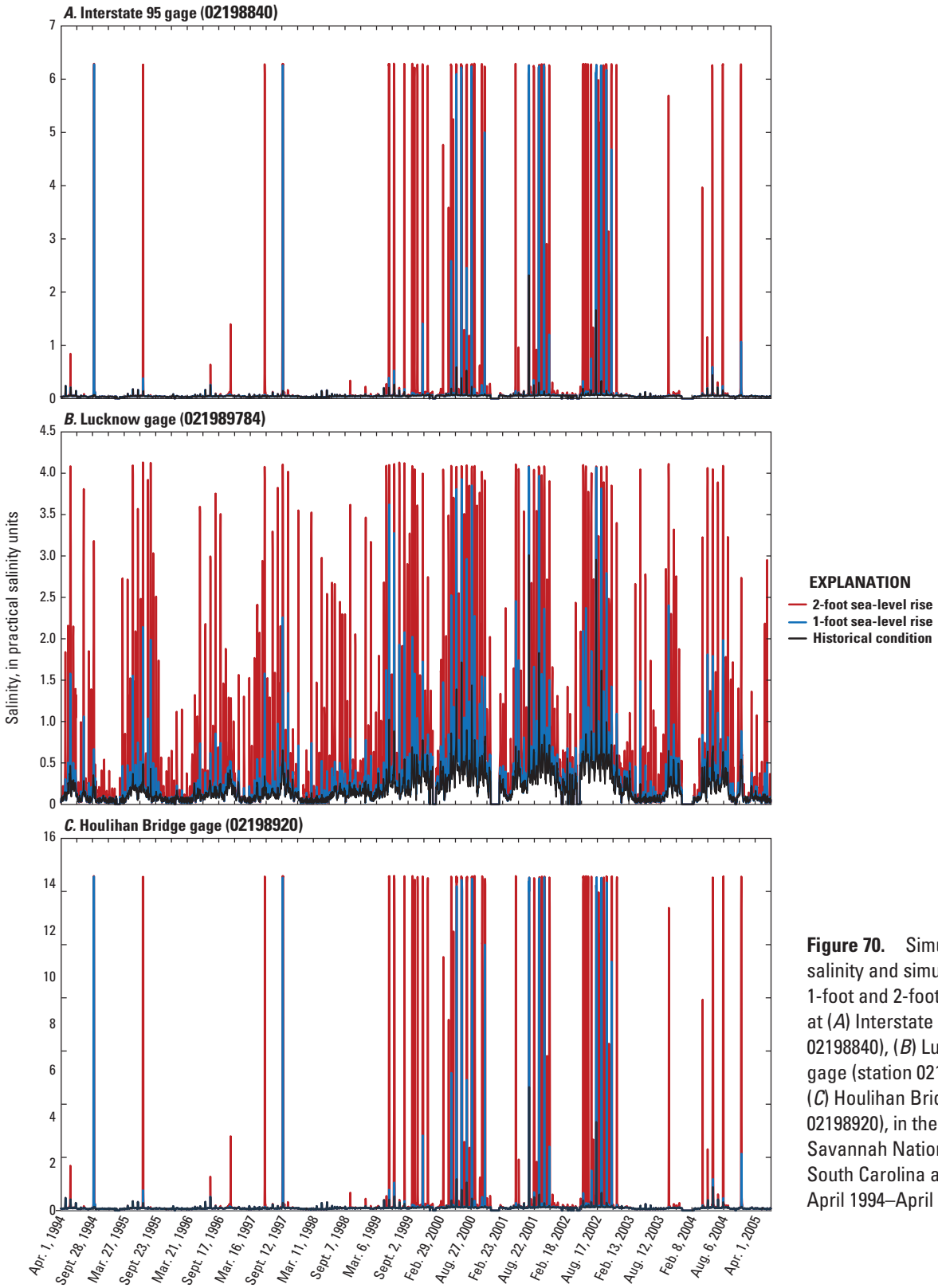

Figure 70. Simulated historical salinity and simulated salinities for 1-foot and 2-foot sea-level rises at (*A*) Interstate 95 gage (station 02198840), (*B*) Lucknow Canal gage (station 021989784), and (*C*) Houlihan Bridge gage (station 02198920), in the vicinity of the Savannah National Wildlife Refuge, South Carolina and Georgia, April 1994–April 2005.

response at the Lucknow Canal gage is limited to a little over 4 psu (fig. 70*B*). A 2-ft rise in sea level further increases the number and duration of the salinity-intrusion events at the two gaging stations and would have the effect of shifting the tidal marsh types from tidal freshwater to oligohaline (fig. 31). Salinity increased with 1- and 2-ft sea-level rises at the Houlihan Bridge gage (fig. 70*C*), but the increases in the frequency, magnitude, and duration of the salinity intrusions are not as great as at the other two gaging stations.

The time-series data also can be displayed as frequency curves with salinity values on the y-axis and the percentage ranking of the data on the x-axis (fig. 71). These plots clearly

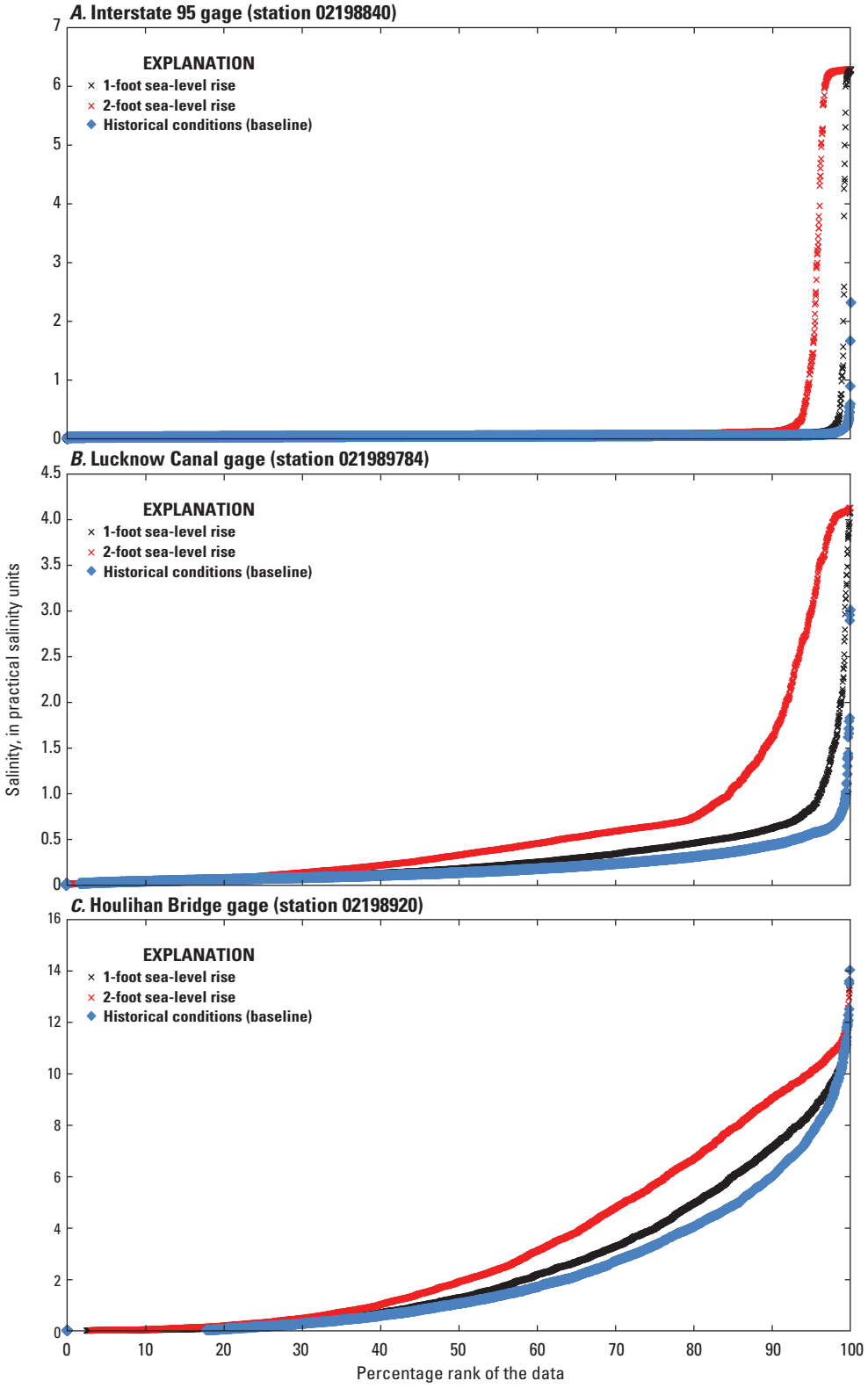

Figure 71. Frequency curves of simulated salinity conditions for historical conditions (baseline) and a 1-foot and 2-foot sea level rise at (*A*) the Interstate 95 gage (station 02198840) (*B*) Lucknow Canal gage (station 021989784), and (*C*) Houlihan Bridge gage (station 02198920), in the vicinity of Savannah National Wildlife Refuge, South Carolina and Georgia, April 1994–April 2005.

show that the salinity at all three sites increased in response to increases in sea level. For example, at the Interstate 95 gage, under the historical (baseline) conditions, there are few occurrences of salinity greater than 2 psu (fig. 71*A*). A 2-foot rise in sea level increases the occurrence of salinity to greater than 2 psu to approximately 5 percent of the time. At the Lucknow Canal gage, under historical (baseline) conditions (no rise in sea level), the salinity was 0.5 psu or less 90 percent of the time (fig. 71*B*), and the salinity was greater than 0.5 psu 10 percent of the time. A 1-ft rise in sea level shifts the frequency interval for the occurrence of events of 0.5 psu salinity by 10 percent with values greater than 0.5 psu occurring 20 percent of the time. A 2-ft rise increases the salinity at the site even more, and salinity of 0.5 psu occurred 40 percent of the time.

Effects of Decreased Streamflow and Sea-Level Rise on Simulated Salinity: M2M-2 DSS

As was done with the PRISM-2 DSS for the Waccamaw River and AIW study area, historical streamflows for the lower Savannah River study area were reduced to provide estimates of anticipated changes in streamflow associated with climate change. Frequency curves for simulated salinity are shown in figure 72 for five scenarios of sea-level rise with and without streamflow reduction at the Interstate 95 and Lucknow Canal gaging stations. The decrease in streamflow combined with the 1-ft rise in sea level increased the salinity at the sites and moved the frequency curves closer to the salinity of a 2-ft rise in sea level.

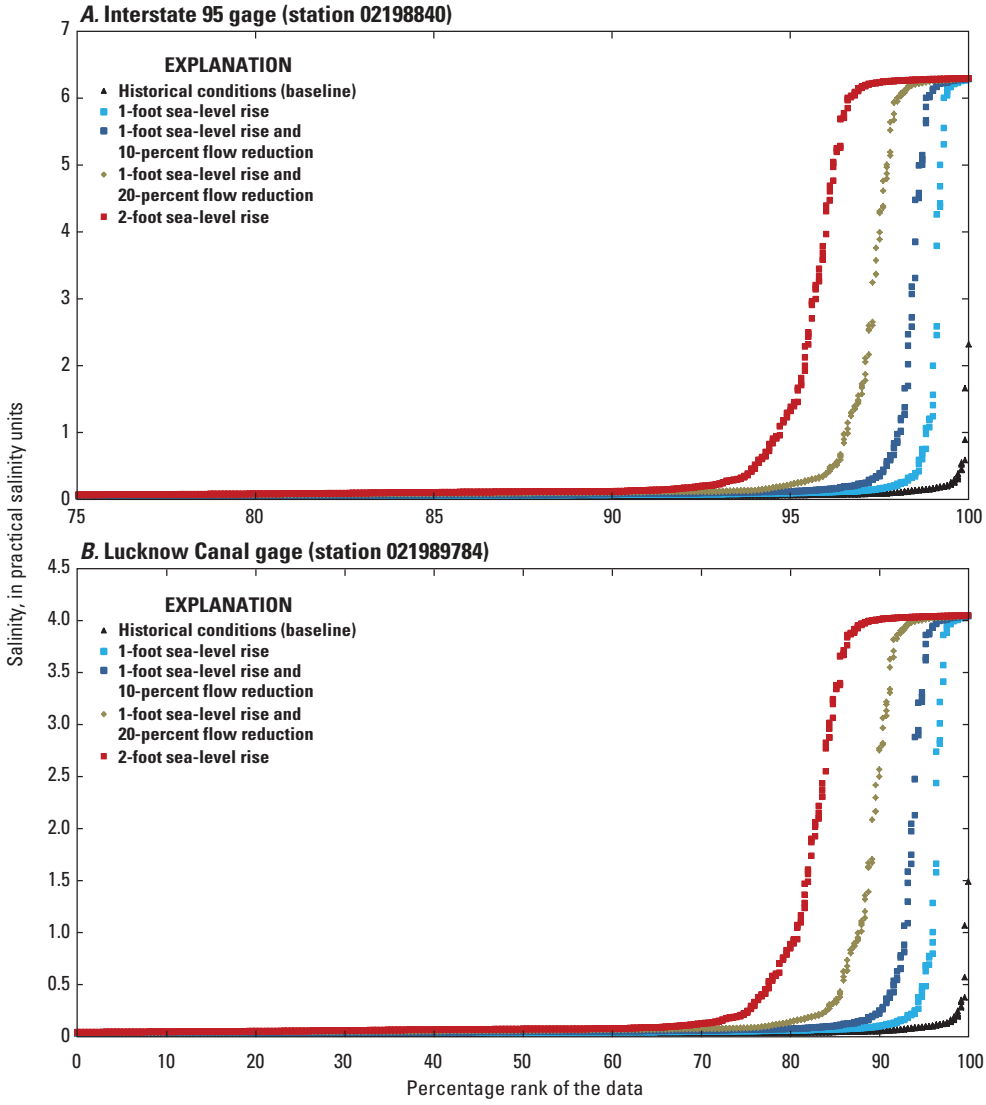

Figure 72. Frequency curves of simulated salinity for historical conditions (baseline), 1-foot and 2-foot sea level rises, and a 1-foot sea-level rise in combination with a 10- and 20- percent reductions in streamflow at (*A*) the Interstate 95 gage(station 02198840) and (*B*) Lucknow Canal gage (station 021989784) in the vicinity of Savannah National Wildlife Refuge, South Carolina and Georgia, April 1994–April 2005.

The percentages of time that simulated salinity values exceeded a 0.5 psu threshold at the Interstate 95 gage for various scenarios of sea-level rise and streamflow reduction during the 11-year simulation period are provided in table 15 and fig. 73. The greater effect of sea-level rise on salinity, as shown in the 3D response curve for the Interstate 95 gage on the Savannah River, is similar to that for the Pawleys Island gage (fig. 68). The salinity response resulting from the percent reduction in streamflow became more sensitive to the incremental rise in sea level with higher sea levels. This can be seen in the increased slope of the reduction of streamflow with the increase in sea level (fig. 73). The number of days that salinity exceeded the threshold increased by 4.7 percent for a 25-percent reduction in streamflow from the baseline conditions (table 15). For a 1-ft sea-level rise, the same reduction in streamflow increased the number of days by 7.3 percent, and a 2-ft sea-level rise increased the number of days by 7.9 percent relative to the simulated historical conditions.

Table 15. Percentage of time that the salinity threshold of 0.5 practical salinity unit is exceeded at Interstate 95 (station 02198840), Georgia, as a result of reductions in historical streamflow and sea-level rises.

[psu, practical salinity units; % flow, percent reduction in historical flows; SLR, sea-level rise; ft, foot]

% Flow/SLR	Percent of days that salinity is greater than 0.5 psu						
	0 ft	0.5 ft	1 ft	1.5 ft	2 ft	2.5 ft	3 ft
0	0.2	0.5	1.4	3.1	5.9	9.7	13.6
–5	0.3	0.7	1.8	3.9	7.0	11.2	15.4
–10	0.4	0.9	2.3	4.6	8.6	12.5	17.7
–15	0.5	1.4	3.0	5.8	10.0	14.5	20.0
–20	0.6	1.7	3.8	7.1	11.4	16.8	22.0
–25	1.0	2.2	4.7	8.7	13.3	19.3	24.1

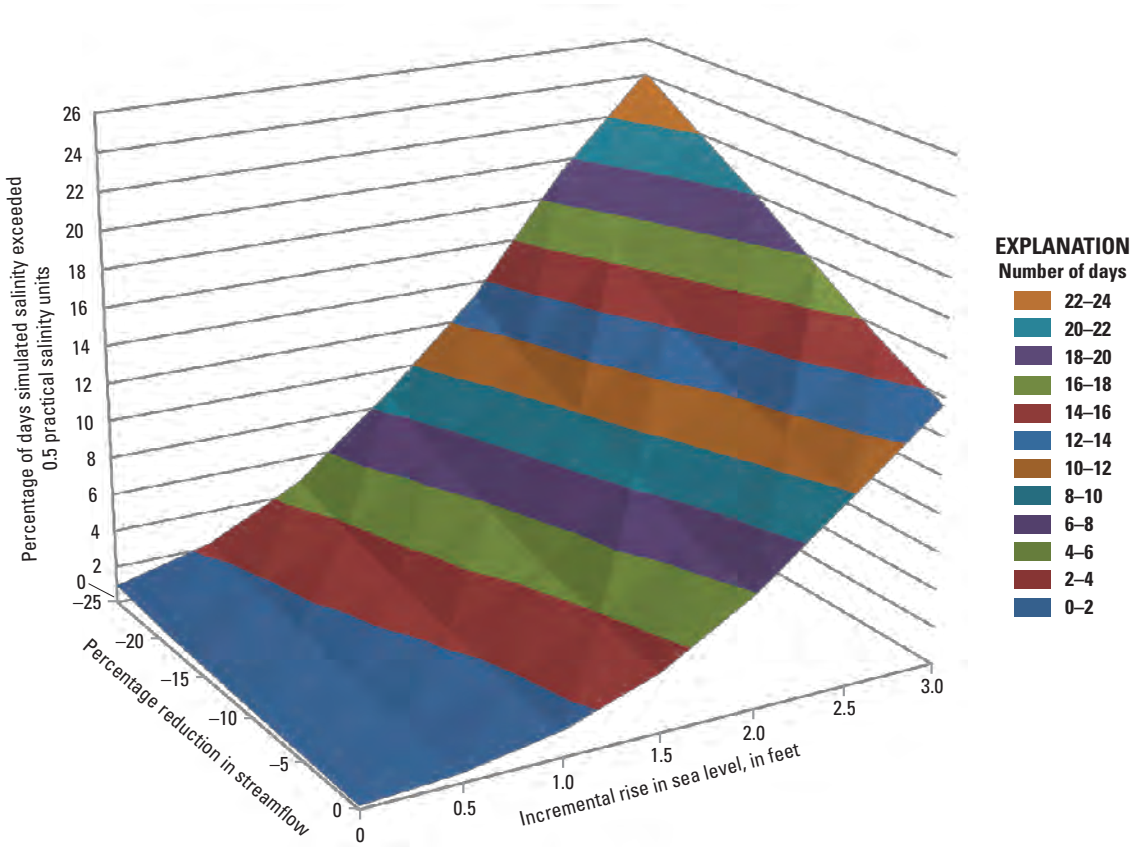

Figure 73. Three-dimensional response surface showing the percentage of days the simulated salinity exceeded the threshold of 0.5 practical salinity units is exceeded for reductions in streamflow and incremental sea-level rises at the Interstate 95 gage (station 02198840) in the vicinity of Savannah National Wildlife Refuge, South Carolina and Georgia, April 1994–April 2005.

Effects of Decreased Streamflow and Sea-Level Rise on Marsh Pore-Water Salinity: M2M-2 DSS

The M2M-2 DSS was used to evaluate a potential change in pore-water salinity with an increase in sea level and a reduction in streamflow. The M2M-2 generates an output file used for 2D visualization of the pore-water salinity response to a user scenario. Because plant communities of tidal marshes respond to long-term conditions (months to seasons) and not episodic salinity intrusion events of days, the M2M-2 visualization application computes and displays monthly (or greater) averages of salinity conditions for the marsh on the basis of simulated conditions at seven marsh pore-water sites and river conditions. The scenario of a 1-ft sea-level rise and a 20-percent reduction in streamflow was used to demonstrate the marsh visualization utility. Simulated salinity at the Lucknow Canal gage (021989784) for historical (baseline) conditions, 1-ft and 2-ft sea-level rises, and a 1-ft sea-level rise in conjunction with a 20-percent reduction in streamflow for the summer and fall 1999 are shown in figure 74. The period June 1 to December 31, 1999, represents average conditions for which the simulated historical salinity was less than 0.5 psu most of the time and occasionally exceeded 0.5 psu. The salinity time series shows the higher salinity values occurring on a 28-day tidal cycle and correspond to spring tides (fig. 74).

The simulations for summer and fall 1999 at the Lucknow Canal gage indicate that the magnitude of salinity intrusion would increase with increasing sea level and decreasing streamflow. For example, salinity simulations indicate an increase in sea level of 1 and 2 ft would result in an increase in the magnitude of the salinity-intrusion event to 2.0 and 4.0 psu, respectively, in late September 1999. Simulations incorporating a 1-ft sea-level rise with a 20-percent reduction in streamflow for the same intrusion event indicate that a salinity response intermediate to the responses for 1- and 2-ft sea-level rises would occur. The rise in sea level and reduction in streamflow increased the magnitude of the salinity-intrusion

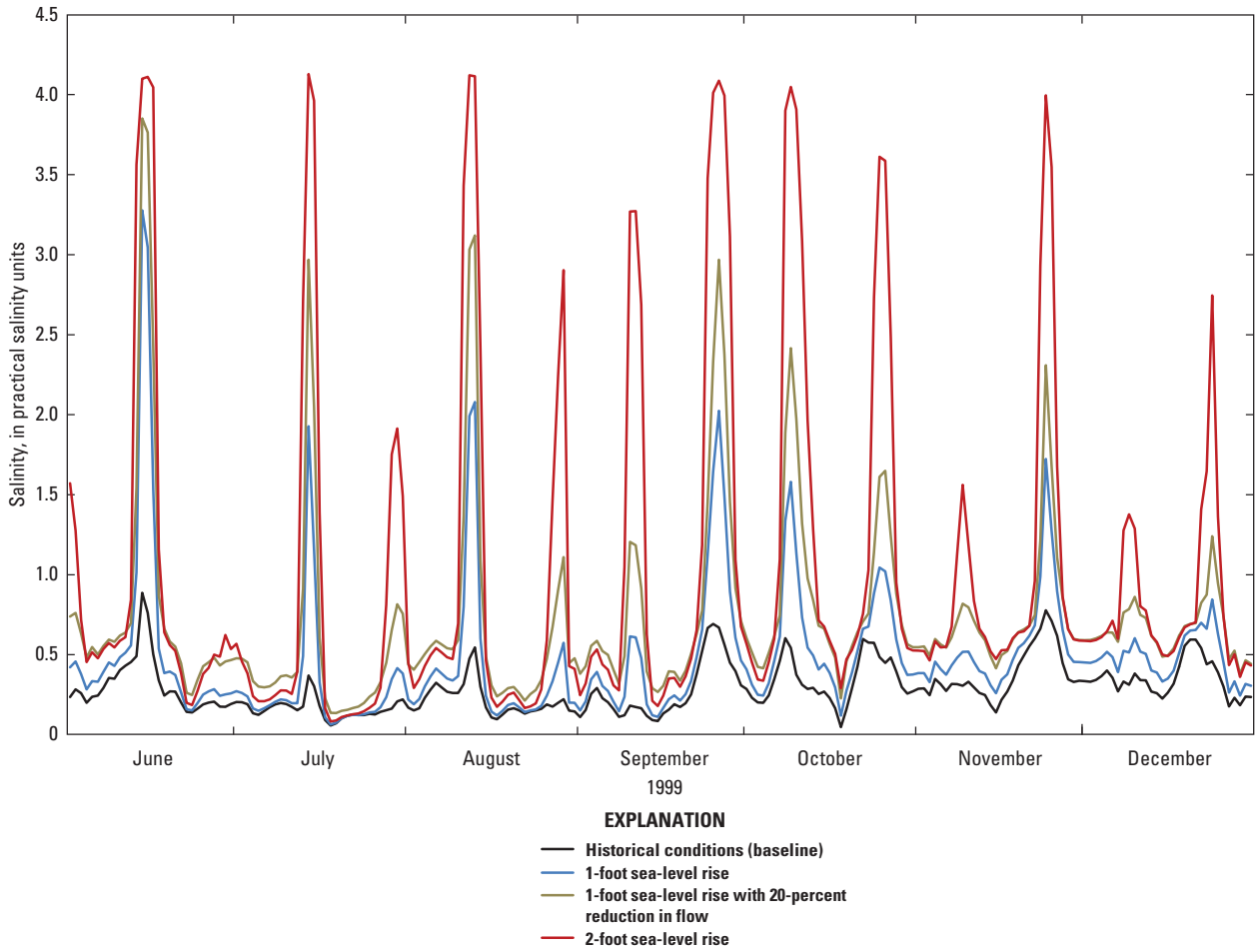

Figure 74. Simulated salinity conditions for a historical (baseline), a 1-foot and a 2-foot sea level rise, and a 1-foot sea-level rise with 20-percent reduction in streamflow at the Lucknow Canal gage (station 021989784) in the vicinity of Savannah National Wildlife Refuge, South Carolina and Georgia, June 1–December 31, 1999.

events occurring on a 14-day spring tidal cycle (fig. 74). The sea-level rise and streamflow reduction scenarios also affect the pore-water salinity in the marsh. The simulated pore-water salinity for historical conditions (baseline) and for a 1-ft sea-level rise and 20-percent reduction in streamflow at the B2 marsh site between the Middle and Little Back Rivers (fig. 11*B*) are shown in figure 75. The dynamics of salinity in the pore water is dampened in comparison to that of the Little Back River gage at Lucknow Canal. Unlike the simulated salinity response at the Little Back River gage to the scenarios, where the magnitude and duration of the salinity-intrusion event sharply increased over a period of days, the pore-water salinity in the marsh increased by 0.5 to 0.6 psu, effectively doubling the background level.

The 2D marsh Color-Gradient Visualization Program was used to display the 1-month average response to the climate-change scenario. The difference between the historical conditions (baseline) and the scenario 1-ft sea-level rise with a 20-percent reduction in streamflow was computed and averaged for a month. The 2D Color-Gradient Visualization Program interpolates and extrapolates M2M-2 output to fill and color a grid of the study area (fig. 76). The M2M-2 DSS provides a qualitative view of the large-scale, longitudinal USGS marsh network (fig. 11*B*) and river gaging stations on the Savannah River at Interstate 95 gage (02198840, fig. 11*A*) and Back River upstream from the tide gate (near station 02198977; fig. 11*A*). For the climate-change scenario 1-ft sea-level rise with a 20-percent reduction in streamflow (fig. 76), the greatest effect was in the lower reaches of the marsh and in the marsh between the Middle and Little Back Rivers.

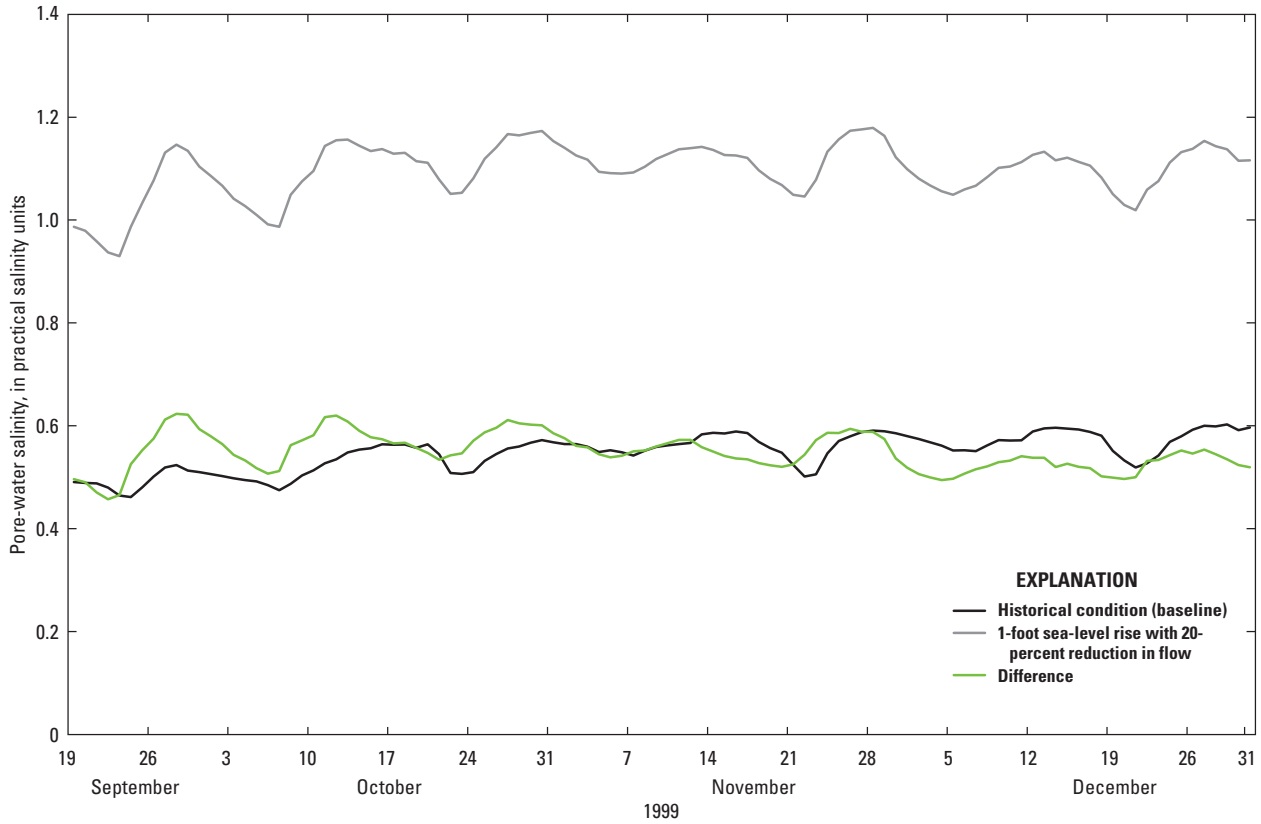

Figure 75. Simulated pore-water salinity historical conditions (baseline) and a 1-foot sea-level rise with 20-percent reduction in streamflow, and the difference between the two at the B2 marsh gage in the Savannah National Wildlife Refuge, South Carolina, September 19, 1999–December 31, 1999.

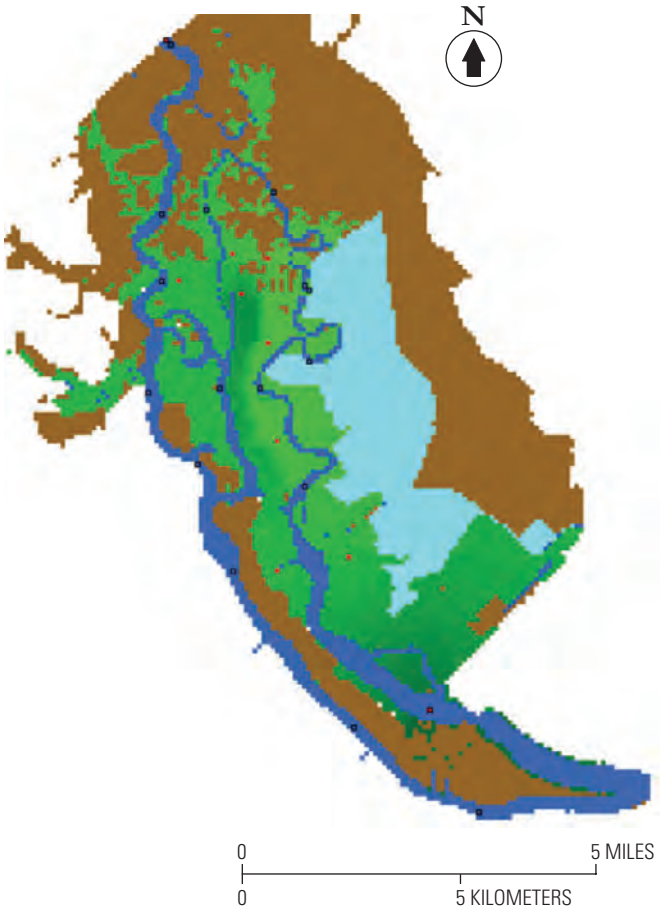

Figure 76. Two-dimensional color-gradient visualization of the tidal marshes in the vicinity of Savannah National Wildlife Refuge, South Carolina and Georgia, showing the differences in simulated average salinity of marsh pore water between historical conditions and a 1-foot sea-level rise with 20-percent reduction in streamflow, September 19 –October 19, 1999. Darker green color shades indicate greater differences between the two simulations.

Summary and Conclusions

The availability of freshwater in coastal streams is frequently affected by salinity intrusion. The balance between freshwater and saltwater in coastal streams primarily is governed by the interaction of hydrologic streamflow conditions and sea level. Changes in streamflow and sea level, anticipated as a result of potential changes in climate, could affect the frequency, duration, and magnitude of salinity intrusions in coastal areas. Evaluation of the effects of changes in salinity is particularly important for coastal areas of the southeastern United States because of the large number of municipal water-supply intakes in coastal rivers. This study addressed salinity dynamics in the vicinity of water-supply intakes in the Waccamaw River and the Atlantic Intracoastal Waterway (AIW) study area in South Carolina and in the lower Savannah River study area along the South Carolina and Georgia border.

To evaluate the effects of potential climate changes on salinity intrusions, anticipated alterations in hydrology and sea level need to be simulated separately and in combination. Global circulation, watershed, and salinity intrusion models need to be integrated to evaluate various climate-change scenarios. Salinity in the Waccamaw River and AIW, and the Savannah River, is constantly responding to changing streamflow and tidal conditions. The location of the saltwater-freshwater interface is a balance between upstream river streamflows and downstream tidal forcing. During periods of high streamflow, it is difficult for salinity to intrude upstream, and the saltwater-freshwater interface is moved downstream toward the ocean. During periods of low streamflow, salinity

is able to intrude upstream, and the saltwater-freshwater interface is moved upstream by tidal forcing, by an increase in mean water levels, a change in tidal range, or a combination of the three. The goal of this study was to develop effective models to predict salinity intrusion in the freshwater parts of the Waccamaw River and AIW, and lower Savannah River, study areas for a given set of streamflow, water-level, and tidal-range conditions. The artificial neural network (ANN) models for both study areas were able to simulate the salinity dynamics of the system and capture the long-term trends in the data with a relatively lower percent model error. For the models of the Waccamaw River and AIW, the R^2 (coefficient of determination) for the daily models ranged from 0.69 to 0.88, and the percent model error was 8.9 percent or less. For the lower Savannah River, the R^2 for the models ranged from 0.57 to 0.88, and the percent model error was 6.1 percent or less.

To facilitate the dissemination and use of the salinity-intrusion models, the **P**ee Dee **R**iver and **I**ntracoastal Waterway **S**alinity Intrusion **M**odel **D**ecision **S**upport **S**ystem **2** (PRISM-2 DSS) for Waccamaw River and AIW, and the **M**odel-**to**-**M**arsh **D**ecision **S**upport **S**ystem **2** (M2M-2 DSS) for the lower Savannah River, were developed as spreadsheet applications that provide predictive models with real-time databases for ANN model simulations, graphical user interfaces, and displays of results. These features make the DSSs easily distributable and immediately usable by all interested stakeholders. The PRISM-2 and M2M-2 DSSs were used to simulate potential climate-change scenarios of sea-level rise and changes in streamflow to the coast. To simulate the effects of sea-level rise, the mean coastal water levels were incremented by 0.5 foot to simulate sea-level rises of up to 3 feet in PRISM-2 and M2M-2. Nomographs were generated for six sea-level-rise scenario simulations that show the number of days the predicted specific conductance (or salinity) values exceeded predetermined thresholds for specific conductance or salinity for each incremental sea-level rise. For example, daily specific conductance greater than 2,000 microsiemens per centimeter (µS/cm) historically occurred on almost 200 days over the 14-year simulation period at the Pawleys Island gage. A 1-foot sea-level rise would double the number of days the municipal intake is unavailable to 400 days, and a 2-foot rise would increase the unavailability to nearly 2 years (700 days).

Projections of climate change for the 21st century by global circulation models (GCMs) indicate changes in temperature and precipitation patterns that will affect the timing and quantity of streamflow to the coast. Salinity intrusion is a low-flow phenomenon, so to evaluate net reductions in streamflows, the historical streamflow in PRISM-2 and M2M-2 was reduced by 5, 10, 15, 20, and 25 percent. To evaluate the combination of reduced streamflow and sea-level rise, the incremental reductions in streamflow were combined with sea-level rises of 0, 1, and 2 feet. Similar to the analysis of sea-level rise, the number of days the specific conductance or salinity threshold is exceeded for each 5-percent incremental decrease in streamflow for 0-, 1-, and 2-foot sea-level rises was computed. A 25-percent decrease in the streamflow increased the number of days for the three thresholds of 1,000, 2,000, and 3,000 µS/cm by approximately 45 to 90 percent for each of the three sea-level scenarios for the 14-year simulation period at the Pawleys Island gage. The combined effect of a 2-foot sea-level rise and 25-percent reduction in streamflow increased the number of days the thresholds are exceeded by 440 to 645 percent. For example, if the threshold is 2,000 µS/cm, for the historical 14-year simulation, then the threshold is exceeded on 191 days (4 percent of the days). If the streamflow is reduced to 75-percent of the historical streamflow and there is a 2-foot sea-level rise, then the number of days the threshold is exceeded increases to 1,067 days, an increase of 559 percent, or 21 percent of the days for the 14-year simulation.

The responses of specific conductance to combinations of sea-level rise and reduced streamflow at the Pawley's Island gage in the Waccamaw River and AIW study area and the Interstate 95 gage in the lower Savannah River study area were displayed as a three-dimensional (3D) response surfaces. The 3D response surfaces were generated from 42 model simulations of incremental rises in sea level (x-axis) and incremental reductions in streamflow (y-axis). The simulated percentage of days that the daily specific-conductance threshold is exceeded is shown on the z-axis. The 3D response surface showed that specific conductance is much more sensitive to sea-level rise than to reductions in streamflow for both study areas.

The effect of climate-change projections from a global circulation model (GCM) on salinity intrusion was evaluated by using PRISM-2. The precipitation and temperature predictions from the GCM were used as inputs to the watershed model of the Yadkin-Pee Dee basin developed by the University of South Carolina [Hydrologic Simulation Program-Fortran (HSPF)]. The HSPF model simulated the streamflow for the Waccamaw, Little Pee Dee, Pee Dee, Lynches, and Black Rivers, and these streamflow data were used as user-defined flow inputs to PRISM-2. The downscaled temperature and precipitation data for the ECHO CGM for the A2 carbon emission climate scenario was used as input to the HSPF model, and streamflows for the Waccamaw, Little Pee Dee, Pee Dee, Lynches, and Black Rivers were simulated for 1980 to 2010 and 2040 to 2070. The ECHO GCM is a hybrid coupled ocean-atmosphere GCM of the Hamburg version of the European Center atmospheric GCM (**EC**HAM) and the Hamburg Primitive Equation ocean GCM (**HO**PE).To evaluate seasonal shifts in the projected streamflows, daily duration hydrographs were plotted using the simulated ECHO-HSPF streamflows for 1980 to 2010 and 2040 to 2070 for the total streamflow to the coast. Although the historical and projected streamflows appear similar there are important differences, especially with respect to potential changes in salinity intrusion. Salinity intrusion along the coast is a low-flow phenomenon; therefore, changes in low flow, as represented by the 10th percentile streamflows, are the most critical for potential salinity intrusion.

Results of the specific-conductance simulation with projected streamflow conditions shows a change in the occurrence of intrusion events greater than 1,000 µS/cm at the Pawleys Island gage. The number of intrusion events increase in the spring and decrease in the summer, and most of the events occur in the fall. Under potential climate change, a salinity-intrusion event will still be initiated by the convergence of conditions of low flow and high coastal water level. The decrease in the number of summer intrusion events corresponds to an increase in the 10th percentile projected streamflows. Likewise, the increase in the number of fall intrusion events corresponds to the slight decrease in the low flows in November and December. The decrease in the winter 10th-percentile streamflow, although significant, does not decrease streamflow to the level that would cause a salinity-intrusion event.

Selected References

Abarbanel, H.D.I., 1996, Analysis of observed chaotic data: New York, Springer-Verlag, Inc., p. 4–12.

Applied Technology and Management, 1998, Hydrodynamics and water quality modeling of the Lower Savannah River estuary, engineering report prepared for Georgia Ports Authority, Savannah, Ga.: Charleston, S.C., Applied Technology and Management, Inc., May 1998 [variously paged].

Barber, H.E., and Gann, A.R., 1989, A history of the Savannah District U.S. Army Corps of Engineers, 1829–1989, Savannah District: Savannah, Ga., U.S. Army Corps of Engineers, 554 p.

Bear, Jacob, Cheng, A.H.D., Sorek, Shaul, Ouazar, Driss, and Herrera, I., eds., 1999, Seawater intrusion in coastal aquifers—Concepts, methods and practices: Dordrecht, The Netherlands, Kluwer Academic Publishers, 625 p.

Blodgett, D.L., Booth, N.L., Kunicki, T.C., Walker, J.L., and Viger, R.J., 2011, Description and testing of the Geo Data Portal: Data integration framework and Web processing services for environmental science collaboration: U.S. Geological Survey Open-File Report 2011–1157, 9 p. (Available at *http://pubs.usgs.gov/of/2011/1157/*.)

Buccola, N.L., and Wood, T.M., 2010, Empirical models of wind conditions on Upper Klamath Lake, Oregon: U.S. Geological Survey Scientific-Investigations Report 2010–5201, 26 p.

Burden, R.L., Faires, J.D., and Reynolds, A.C., 1978, Numerical analysis: Boston, Prindle, Weber, and Schmidt, p. 40.

Burkett, V.R., Taylor, I.L., Belnap, J., Cronin, T.M., Dettinger, M.D., Frazier, E.L., Haines, J.W., Kirtland, D.A., Loveland, T.R., Milly, P.C.D., O'Malley, R., and Thompson, R.S., 2011, Public review draft, USGS global change science strategy: A framework for understanding and responding to climate and land-use change: U.S. Geological Survey Open-File Report 2011–1033, 32 p.(Available at *http://pubs.usgs.gov/of/2011/1033/pdf/ofr2011-1033.pdf.)*

Carswell, W.J., Sanders, C.L, Jr., and Johnson, D.M., 1988, Freshwater supply potential of the Atlantic Intracoastal Waterway near Myrtle Beach, South Carolina: U.S. Geological Survey Water-Resources Investigations Report 88–4066, 45 p.

Collins, M.R., Post, W.C., and Russ, D.C., 2001, Distribution of shortnose sturgeon in the lower Savannah River: South Carolina Department of Natural Resources, final report to Georgia Ports Authority, accessed February, 4, 2013, at *http://sav-harbor.com/*.

Conrads, P.A., and Roehl, E.A., Jr., 1999, Comparing physics-based and neural network models for predicting salinity, water temperature, and dissolved oxygen concentration in a complex tidally affected river basin: Proceeding of the South Carolina Environmental Conference, Myrtle Beach, March 1999, 6 p.

Conrads, P.A., and Roehl, E.A., Jr., 2005, Integration of data-mining techniques with mechanistic models to determine the impacts of non-point source loading on dissolved oxygen in tidal waters: Proceeding of the South Carolina Environmental Conference, Myrtle Beach, March 2005, 6 p.

Conrads, P.A., and Roehl, E.A., Jr., 2007, Analysis of salinity intrusion in the Waccamaw River and the Atlantic Intracoastal Waterway near Myrtle Beach, South Carolina, 1995–2002: U.S. Geological Survey, Scientific Investigations Report 2007–5110, p. 41, 2 apps.

Conrads, P.A., Roehl, E.A., Jr., and Cook, J.B., 2002a, Estimation of tidal marsh loading effects in a complex estuary: Proceeding of the American Water Resources Association Annual Conference, New Orleans, May 2002, 6 p.

Conrads, P.A., Roehl, E.A., Jr., Daamen, R.C., and Kitchens, W.M., 2006, Simulation of water levels and salinity in the rivers and tidal marshes in the vicinity of the Savannah National Wildlife Refuge, Coastal South Carolina and Georgia: U.S. Geological Survey Scientific Investigations Report 2006–5187, 134 p.

Conrads, P.A., Roehl, E.A., Jr., and Martello, W.P., 2002b, Estimating point-source impacts on the Beaufort River using neural network models: Proceeding of the American Water Resources Association Annual Conference, New Orleans, May 2002, 6 p.

Conrads, P.A., Roehl, E.A., Jr., and Martello, W.P., 2003, Development of an empirical model of a complex, tidally affected river using artificial neural networks: Proceeding of the Water Environment Federation TMDL 2003 Specialty Conference, Chicago, Illinois, November 2003, 30 p.

Conrads, Paul A., Roehl, E.A., Jr., Davie, S.R., 2011, Simulation of specific conductance and chloride concentration in Abercorn Creek, Georgia, 2000–2009: U.S. Geological Survey Scientific Investigations Report 2011–5074, 46 p.

Cowardin, L.M., Carter, V.M., Golet, F.C., and LaRoe, E.T., 1979, Classification of wetlands and deepwater habitats of the United States: U.S. Fish and Wildlife Service, FWS/OBS-79/31.

Dalton, M.S., and Jones, S.A., comps., 2010, Southeast Regional Assessment Project for the National Climate Change and Wildlife Science Center: U.S. Geological Survey Open-File Report 2010–1213, 38 p.

Daly, C., Halbleib, M., Smith, J.I., Gibson, W.P., Doggett, M.K., Taylor, G.H., Curtis, J., and Pasteris, P.A., 2008, Physiographically-sensitive mapping of temperature and precipitation across the conterminous United States: International Journal of Climatology, v. 28, p. 2031–2064.

Devine, T.W., and Roehl, E.A., Jr., 2003, Virtual sensors—Cost effective monitoring: Proceeding of the Air and Waste Management Association Annual Conference, June 2003, 10 p.

Drewes, P.A., and Conrads, P.A., 1995, Assimilative capacity of the Waccamaw River and the Atlantic Intracoastal Waterway near Myrtle Beach, South Carolina, 1989–92: U.S. Geological Survey Water-Resources Investigations Report 95–4111, 58 p.

Dutta, Soumitra, Wierenga, Berend, and Dalebout, Arco, 1997, Case-based reasoning systems: From automation to decision-aiding and stimulation: IEEE Transactions on Knowledge and Data Engineering, v. 9, no. 6, p. 911–912.

Dyer, K.R., 1997, Estuaries—A physical introduction (2d ed.): New York, John Wiley and Sons, Ltd. 195 p.

Furlow, J., Scheraga, J.D., Freed, R., and Rock, K., and Joel D., 2002, The vulnerability of public water systems to sea level rise, *in* Lesnik, J.R., ed., Proceedings of the Coastal Water Resource Conference, American Water Resources Association, Middleburg, Va., TPS-02-1, p. 31–36.

Granger, M.L., 1968, History of the Savannah District, 1829–1968: Savannah, Ga., U.S. Army Corps of Engineers, Savannah District, 114 p.

Hinton, G.E., 1992, How neural networks learn from experience: Scientific American, v. 267, no. 3, p. 144–151.

Intergovernmental Panel on Climate Change (IPCC), 2007, Summary for policymakers, Contribution of working group I to the fourth assessment report of the intergovernmental panel on climate change, *in* Solomon, S., Qin, D., Manning, M., Chen, Z., Marquis, M., Tignor, K.A.M., Miller, H., eds., Climate change 2007: The physical science basis: Cambridge, United Kingdom/New York, Cambridge University Press, p. 1–18.

Jensen, B.A., 1994, Expert systems—Neural networks: Instrument Engineers' Handbook (3d ed.): Radnor, Pa., Chilton, p. 48–54.

Karl, T.R., Melillo, J.M., and Peterson, T.C., eds., 2009, Global climate change impacts in the United States: Cambridge University Press, 2009.

Lamar, W.L., 1942, Industrial quality of the public water supplies in Georgia, 1940: U.S. Geological Survey Water-Supply Paper 912, 83 p.

Latham, P.J., 1990, Plant distributions and competitive interactions along a gradient of tidal freshwater and brackish marshes: Dissertation presented to the graduate school of the University of Florida.

Legutke, S., and Voss, R., 1999, The Hamburg Atmosphere-Ocean Coupled Circulation Model ECHO-G, Technical Report No. 18: Hamburg, Germany German Climate Computer Centre (DKRZ), 62 p.

Miller, R.L., Bradford, W.L., and Peters, N.E., 1988, Specific conductance: Theoretical considerations and application to analytical quality control: U.S. Geological Survey Water-Supply Paper 2311, 16 p.

National Oceanic and Atmospheric Administration, 2010, Tide station locations and ranges, accessed August 19, 2011, at *http://tidesandcurrents.noaa.gov/tides10*.

National Oceanic and Atmospheric Administration, 2012, Incorporating sea level change scenarios at the local level: National Oceanic and Atmospheric Administration – Coastal Services Center, 13 p., 1 app.

National Research Council (NRC), 1987, Responding to changes in sea level: Engineering Implications: Washington, D.C., National Academy Press, 148 p.

North Carolina Department of Environment and Natural Resources, Division of Water Quality, 1998, Yadkin-Pee Dee River basinwide water quality management plan, Chapter 2—General basin description, 35 p., accessed May 1, 2007, at *http://h2o.enr.state.nc.us/basinwide/yadkin/yadch2.doc.*

North Carolina Department of Environment and Natural Resources, Division of Water Resources, 2001, North Carolina State Water Plan Basin 18, Yadkin-Pee Dee, 7 p., accessed on May 1, 2007, at *http://www.ncwater.org/Reports_and_Publications/swsp/swsp_jan2001/final_pdfs/B18_YadkinPeeDee.pdf*.

Odum, W.E., Smith, T.J., III, Hoover, J.K., and McIvor, C.C., 1984, The ecology of tidal freshwater marshes of the United States east coast: A community profile: U.S. Fish and Wildlife Service, FWS/OBS-83/17, 177 p.

Pearlstine, L.G., Latham, P.J., Kitchens, W.M., and Bartleson, R.D., 1990, Development and application of a habitat succession model for the wetland complex of the SNWR, volume II, final report: Gainesville, Fla., Submitted to the U.S. Fish and Wildlife Service, Savannah Coast Refuges, by the Florida Cooperative Fish and Wildlife Research Unit.

Press, W.H., Teukolsky, S.A., Vetterling, W.T., and Flannery, B.P., 1993, Numerical recipes in C: The art of scientific computing: Cambridge University Press, 1,007 p.

Risley, J.C., Roehl, E.A, Jr., and Conrads, P.A., 2003, Estimating water temperatures in small streams in Western Oregon using neural network models: U.S. Geological Survey Water-Resources Investigations Report 02–4218, 67 p.

Roehl, E.A., Jr., and Conrads, P.A., 1999, Near real-time control for matching wastewater discharges to the assimilative capacity of a complex, tidally affected river basin: Proceeding of the 1999 South Carolina Environmental Conference, Myrtle Beach, March 15–16, 1999, 6 p.

Roehl, E.A., Jr., and Conrads, P.A., 2006, Hydrologic modeling using multivariate state space reconstruction, *in* Gourbesville, Philippe, Cunge, Jean, Guinot, Vincent, and Liong, Shie-Yui, eds., Proceedings of Hydroinformatics 2006, v. 1, p. 765–772.

Roehl, E.A., Jr., Conrads, P.A., and Daamen, R.C., 2006, Features of advanced decision support systems for environmental studies, management, and regulation: Proceedings of the International Environmental Modeling and Software Society Summit, Burlington, Vt., July 2006, 8 p.

Roehl, E.A., Jr., Conrads, P.A., and Roehl, T.A.S., 2000, Real-time control of the salt front in a complex tidally affected river basin, Smart Engineering System Design, v. 10: New York, ASME Press, Proceedings of the Artificial Neural Networks in Engineering Conference, p. 947–954.

Roehl, Ed, Jr., Conrads, P.A., and Cook, J.B., 2003, Discussion of "Using complex permittivity and artificial neural networks for contaminant prediction": Journal of Environmental Engineering, v. 129, p. 1069–1071.

Rosenblatt, F., 1958, The perceptron: A probabilistic model for information storage and organization in the brain: Psychological Review, v. 65, no. 6, p. 386–408.

Rumelhart, D.E., Hinton, G.E., and Williams, R.J., 1986, Learning internal representations by error propagation, *in* Rumelhart, D.E., McClelland, J.L., and the PDP Research Group, Parallel distributed processing—Explorations in the microstructure of cognition, v 1: Cambridge Mass., MIT Press, p. 318–362.

Sanders, C.L., Kubik, H.E., Hoke, J.T., and Kirby, W.H., 1990, Flood frequency of the Savannah River at Augusta, Georgia: U.S. Geological Survey Water-Resources Investigations Report 90–4024, 87 p.

Seaber, P.R., Kapinos, F.P., and Knapp, G.L., 1994, Hydrologic unit maps: U.S. Geological Survey Water-Supply Paper 2294, 63 p.

South Carolina Department of Health and Environmental Control, 1998, Total maximum daily load determination for the Waccamaw River and the Atlantic Intracoastal Water Way near Myrtle Beach, S.C.: State of South Carolina Administrative Record TMDL Submittal for the Waccamaw River and Atlantic Intracoastal Water Biochemical Oxygen Demand, 64 p.

South Carolina Water Resources Commission, 1983, South Carolina State Water Assessment, Report No. 140, 367 p.

Stringfield, W.J., 1995, Bathymetry of Stevens Creek and Neal Shoals Reservoirs, South Carolina, 1990: U.S. Geological Survey Water-Resources Investigation Report 94–4232, 3 sheets.

Tetra Tech, 2005, Development of the EFDC hydrodynamic model for the Savannah Harbor: Prepared for the U.S. Army Corps of Engineers, Savannah District: Atlanta, Ga., Tetra Tech, Inc., [variously paged].

Tetra Tech, 2006, Development of the hydrodynamic and water quality models for the Savannah Harbor Expansion Project: Prepared for U.S. Army Corps of Engineers, Savannah District: Contract No: DACA65-99-D-0065, [variously paged].

U.S. Army Corps of Engineers, 2011, Water resource policies and authorities—Incorporating sea-level change consideration in civil works program: Circular No. 1165-2-211, July 1, 2009, 31 p.

U.S. Army Corps of Engineers, 2012, Final environmental impact statement, Savannah Harbor Expansion Project, Chatham County, Georgia and Jasper County, South Carolina: U.S. Army Corps of Engineers, Savannah District, South Atlantic Division, accessed November 6, 2012, at *http://sav-harbor.com/*.

U.S. Geological Survey, 1986, National water summary 1985—Hydrologic events and surface-water resources: U.S. Geological Survey Water-Supply Paper 2300, 506 p.

U.S. Geological Survey, 2012, Water-resources data for the United States, Water Year 2011: U.S. Geological Survey Water-Data Report WDR-US-2011, site 02198500, accessed February, 4, 2013, at *http://wdr.water.usgs.gov/wy2011/pdfs/02198500.2011.pdf*.

Weiss, S.M., and Indurkhya, Nitin, 1998, Predictive data mining—A practical guide: San Francisco, Morgan Kaufmann Publishers, Inc., p. 1.

Welch, Z.C., and Kitchens, W.M., 2006, Predicting freshwater and oligohaline tidal marsh vegetation communities: Florida Cooperative Fish and Wildlife Research Unit, University of Florida, Report Submitted to U.S. Army Corps of Engineers, Solicitation: W91278-06-T-0012 (Available at *http://sav-harbor.com/*.)

Whitehead, J., Tufford, D., Dow, K., and Carbone, G., 2011, Assessing the impact of salt-water intrusion in the Carolinas under future climatic and sea-level conditions, Charleston, S.C., SC Sea Grant Consortium/NC Sea Grant, Final project report NOAA Grant No. NA08OAR4310715, 23 p.

Will, T.A., and Jennings, C.A., 2001, Assessment of spawning sites and reproductive status of striped bass, *Morone saxatilis*, in the Savannah River estuary: Georgia Cooperative Fish and Wildlife Research Unit, University of Georgia, Final Report for Project 10-21-RR251-144 prepared for The Georgia Ports Authority, accessed May 9, 2011, at *http://sav-harbor.com/*.

Wood, A.W., Leung, L.R., Sridhar, V., and Lettenmaier, D.P., 2004, Hydrologic implications of dynamical and statistical approaches to downscaling climate model surface temperature and precipitation fields: Climatic Change, v. 62, p. 189–216.

Prepared by:
USGS Science Publishing Network
Raleigh Publishing Service Center
3916 Sunset Ridge Road
Raleigh, NC 27607

Manuscript approved for publication on February 23, 2013
Editorial review by Ruth Larkins
Illustrations prepared by Jeff Corbett
Layout by Kay Naugle
Cover design by Ray Douglas

For additional information regarding this publication, contact:
Director
USGS South Carolina Water Science Center
720 Gracern Road, Suite 129
Columbia, SC 29210
phone: 803–750–6100
e-mail: dc_sc@usgs.gov

Or visit the South Carolina Water Science Center Web site at:
http://sc.water.usgs.gov